

NASA SP-7037 (318)

June 1995

p. 93

AERONAUTICAL ENGINEERING

A CONTINUING BIBLIOGRAPHY WITH INDEXES

(NASA-SP-7037(318)) AERONAUTICAL
ENGINEERING: A CONTINUING
BIBLIOGRAPHY WITH INDEXES
(SUPPLEMENT 318) (NASA) 93 p

N95-27543

Unclass

00/01 0050085



National Aeronautics and
Space Administration

Scientific and Technical
Information Office

The NASA STI Office ... in Profile

Since its founding, NASA has been dedicated to the advancement of aeronautics and space science. The NASA Scientific and Technical Information (STI) Office plays a key part in helping NASA maintain this important role.

The NASA STI Office provides access to the NASA STI Database, the largest collection of aeronautical and space science STI in the world. The Office is also NASA's institutional mechanism for disseminating the results of its research and development activities.

Specialized services that help round out the Office's diverse offerings include creating custom thesauri, translating material to or from 34 foreign languages, building customized databases, organizing and publishing research results ... even providing videos.

For more information about the NASA STI Office, you can:

- **Phone** the NASA Access Help Desk at (301) 621-0390
- **Fax** your question to the NASA Access Help Desk at (301) 621-0134
- **E-mail** your question via the **Internet** to help@sti.nasa.gov
- **Write** to:

NASA Access Help Desk
NASA Center for AeroSpace Information
800 Elkridge Landing Road
Linthicum Heights, MD 21090-2934

NASA SP-7037 (318)

June 1995

AERONAUTICAL ENGINEERING

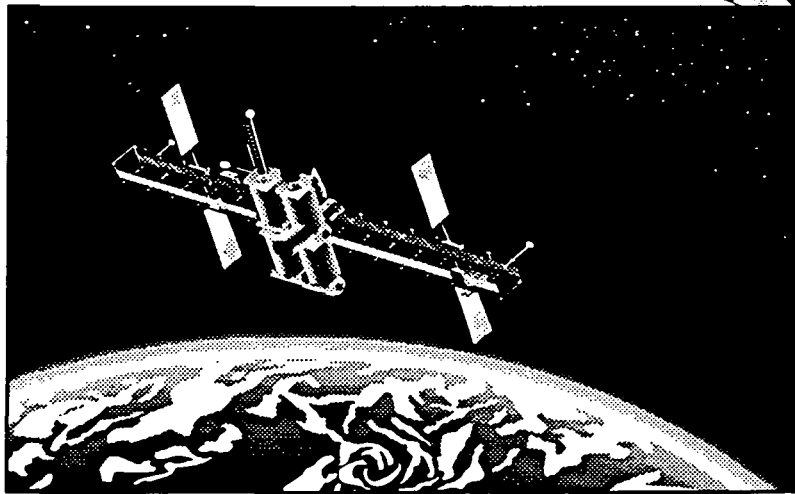
A CONTINUING BIBLIOGRAPHY WITH INDEXES



National Aeronautics and Space Administration
Scientific and Technical Information Office
Washington, DC

1995

The New NASA Video Catalog is Here



Free!

To order your free copy call
the NASA Access Help Desk at
(301) 621-0390 or
fax to (301) 621-0134 or
e-mail to helpdesk@sti.nasa.gov

EXPLORE THE UNIVERSE

This publication was prepared by the NASA Center for Aerospace Information,
800 Elkridge Landing Road, Linthicum Heights, MD 21090-2934, (301) 621-0390.

INTRODUCTION

This issue of *Aeronautical Engineering — A Continuing Bibliography with Indexes* (NASA SP-7037) lists 217 reports, journal articles, and other documents recently announced in the NASA STI Database.

Accession numbers cited in this issue include:

Scientific and Technical Aerospace Reports (STAR) (N-10000 Series)
Open Literature (A-60000 Series)

N95-19883 — N95-19882
A95-669894 — A95-73326

The coverage includes documents on the engineering and theoretical aspects of design, construction, evaluation, testing, operation, and performance of aircraft (including aircraft engines) and associated components, equipment, and systems. It also includes research and development in aerodynamics, aeronautics, and ground support equipment for aeronautical vehicles.

Each entry in the publication consists of a standard bibliographic citation accompanied, in most cases, by an abstract. The listing of the entries is arranged by the first nine *STAR* specific categories and the remaining *STAR* major categories. This arrangement offers the user the most advantageous breakdown for individual objectives. The citations include the original accession numbers from the respective announcement journals.

Seven indexes—subject, personal author, corporate source, foreign technology, contract number, report number, and accession number—are included.

A cumulative index for 1995 will be published in early 1996.

The NASA CASI price code table, addresses of organizations, and document availability information are located at the back of this issue.



SCAN Goes Electronic!

If you have NASA Mail or if you can access the Internet, you can get biweekly issues of *SCAN* delivered to your desk—top absolutely free!

Electronic SCAN takes advantage of computer technology to alert you to the latest aerospace-related, worldwide scientific and technical information that has been published.

No more waiting while the paper copy is printed and mailed to you. You can review *Electronic SCAN* the same day it is released! And you get all 191—or any combination of—subject areas of announcements with abstracts to browse at your leisure. When you locate a publication of interest, you can print the announcement or electronically add it to your publication order list.

Electronic SCAN
Timely
Flexible
Complete
Free!

Start your free access to *Electronic SCAN* today. Over 1,000 announcements of new reports, books, conference proceedings, journal articles . . . and more—delivered to your computer every two weeks.

For instant access via Internet:

[ftp.sti.nasa.gov](ftp://ftp.sti.nasa.gov)
[gopher.sti.nasa.gov](ftp://gopher.sti.nasa.gov)
listserv@sti.nasa.gov

For additional information:

e-mail: help@sti.nasa.gov
scan@sti.nasa.gov

(Enter this address on the "To" line. Leave the subject line blank and send. You will receive an automatic reply with instructions in minutes.)

Phone: (301) 621-0390 Fax: (301) 621-0134

Write: NASA Access Help Desk
NASA STI Office
NASA Center for AeroSpace Information
800 Elkridge Landing Road
Linthicum Heights, MD 21090-2934



National Aeronautics and
Space Administration
Scientific and Technical
Information Office

TABLE OF CONTENTS

Category 01	Aeronautics	219
Category 02	Aerodynamics Includes aerodynamics of bodies, combinations, wings, rotors, and control surfaces; and internal flow in ducts and turbomachinery.	220
Category 03	Air Transportation and Safety Includes passenger and cargo air transport operations; and aircraft accidents.	225
Category 04	Aircraft Communications and Navigation Includes digital and voice communication with aircraft; air navigation systems (satellite and ground based); and air traffic control.	227
Category 05	Aircraft Design, Testing and Performance Includes aircraft simulation technology.	229
Category 06	Aircraft Instrumentation Includes cockpit and cabin display devices; and flight instruments.	232
Category 07	Aircraft Propulsion and Power Includes prime propulsion systems and systems components, e.g., gas turbine engines and compressors; and onboard auxiliary power plants for aircraft.	235
Category 08	Aircraft Stability and Control Includes aircraft handling qualities; piloting; flight controls; and autopilots.	236
Category 09	Research and Support Facilities (Air) Includes airports, hangars and runways; aircraft repair and overhaul facilities; wind tunnels; shock tubes; and aircraft engine test stands.	237
Category 10	Astronautics Includes astronautics (general); astrodynamics; ground support systems and facilities (space); launch vehicles and space vehicles; space transportation; space communications, spacecraft communications, command and tracking; spacecraft design, testing and performance; spacecraft instrumentation; and spacecraft propulsion and power.	239
Category 11	Chemistry and Materials Includes chemistry and materials (general); composite materials; inorganic and physical chemistry; metallic materials; nonmetallic materials; propellants and fuels; and materials processing.	240
Category 12	Engineering Includes engineering (general); communications and radar; electronics and electri- cal engineering; fluid mechanics and heat transfer; instrumentation and photogra- phy; lasers and masers; mechanical engineering; quality assurance and reliability; and structural mechanics.	242

Category 13	Geosciences	251
	Includes geosciences (general); earth resources and remote sensing; energy production and conversion; environment pollution; geophysics; meteorology and climatology; and oceanography.	
Category 14	Life Sciences	N.A.
	Includes life sciences (general); aerospace medicine; behavioral sciences; man/system technology and life support; and space biology.	
Category 15	Mathematical and Computer Sciences	256
	Includes mathematical and computer sciences (general); computer operations and hardware; computer programming and software; computer systems; cybernetics; numerical analysis; statistics and probability; systems analysis; and theoretical mathematics.	
Category 16	Physics	257
	Includes physics (general); acoustics; atomic and molecular physics; nuclear and high-energy; optics; plasma physics; solid-state physics; and thermodynamics and statistical physics.	
Category 17	Social Sciences	N.A.
	Includes social sciences (general); administration and management; documentation and information science; economics and cost analysis; law, political science, and space policy; and urban technology and transportation.	
Category 18	Space Sciences	N.A.
	Includes space sciences (general); astronomy; astrophysics; lunar and planetary exploration; solar physics; and space radiation.	
Category 19	General	N.A.
Subject Index		A-1
Personal Author Index		B-1
Corporate Source Index		C-1
Foreign Technology Index		D-1
Contract Number Index		E-1
Report Number Index		F-1
Accession Number Index		G-1
Appendix		APP-1

TYPICAL REPORT CITATION AND ABSTRACT

NASA SPONSORED

↓
ON MICROFICHE

ACCESSION NUMBER → N95-10318*# Dow Chemical Co., Midland, MI. ← **CORPORATE SOURCE**

TITLE → **NOVEL MATRIX RESINS FOR COMPOSITES FOR AIRCRAFT PRIMARY STRUCTURES, PHASE 1** Final Report, Apr. 1989 - Mar. 1992

AUTHORS → EDMUND P. WOO, P. M. PUCKETT, S. MAYNARD, M. T. BISHOP, K. J. BRUZA, J. P. GODSCHALX, AND M. J. MULLINS Aug. 1992 ← **PUBLICATION DATE**
164 p

CONTRACT NUMBERS → (Contracts NAS1-18841; RTOP 510-02-11-02)

REPORT NUMBERS → (NASA-CR-189657; NAS 1.26:189657) Avail: CASI HC A08/MFA02 ← **AVAILABILITY AND PRICE CODE**

The objective of the contract is the development of matrix resins with improved processability and properties for composites for primarily aircraft structures. To this end, several resins/systems were identified for subsonic and supersonic applications. For subsonic aircraft, a series of epoxy resins suitable for RTM and powder prepreg was shown to give composites with about 40 ksi compressive strength after impact (CAI) and 200 F/wet mechanical performance. For supersonic applications, a thermoplastic toughened cyanate prepreg system has demonstrated excellent resistance to heat aging at 360 F for 4000 hours, 40 ksi CAI and useful mechanical properties at greater than or equal to 310 F. An AB-BCB-maleimide resin was identified as a leading candidate for the HSCT. Composite panels fabricated by RTM show CAI of approximately 50 ksi, 350 F/wet performance and excellent retention of mechanical properties after aging at 400 F for 4000 hours. Author

TYPICAL JOURNAL ARTICLE CITATION AND ABSTRACT

NASA SPONSORED

↓

ACCESSION NUMBER → A95-60192* National Aeronautics and Space Administration. Ames. ← **CORPORATE SOURCE**
Research Center, Moffett Field, CA.

TITLE → **AERODYNAMIC INTERACTIONS BETWEEN A ROTOR AND WING IN HOVER**

AUTHORS → FORT F. FELKER NASA. Ames Research Center, Moffett Field, ← **AUTHOR'S AFFILIATION**
CA, US and JEFFREY S. LIGHT NASA. Ames Research Center,
Moffett Field, CA, US Journal of the American Helicopter Society ← **JOURNAL TITLE**

PUBLICATION DATE → 2 Jun. 1986 p. 53-61

REPORT NUMBER → (HTN-94-00714) Copyright

An experimental investigation of rotor/wing aerodynamic interactions in hover is described. The investigation consisted of both a large-scale and a small-scale test. A 0.658-scale V-22 rotor and wing was used in the large-scale test. Wing download, wing surface pressure, rotor performance, and rotor downwash data from the large-scale test are presented. A small-scale experiment was conducted to determine how changes in the rotor/wing geometry affected the aerodynamic interactions. These geometry variations included the distance between the rotor and wing, wing incidence angle, wing flap angle, rotor rotation direction, and configurations both with the rotor axis at the tip of the wing (tilt rotor configuration) and with the rotor axis at the center of the wing (compound helicopter configuration). Author (Herner)

AERONAUTICAL ENGINEERING

A Continuing Bibliography (Suppl. 318)

June 1995

01

AERONAUTICS (GENERAL)

A95-69967

COMPARISON OF PARAMETER IDENTIFICATION ALGORITHMS FOR FLIGHT VEHICLES

DAL HO LEE Kyungwon Univ, Kyunggi, Korea, Republic of and JANG GYU LEE Transactions of the Japan Society for Aeronautical and Space Sciences (ISSN 0549-3811) vol. 36, no. 114 February 1994 p. 249-256 refs (BTN-94-EIX94371347708) Copyright

The extended Kalman filter (EKF), maximum likelihood (ML), and nonlinear recursive prediction error (NRPE) methods are employed to identify the aerodynamic coefficients of flight vehicles which are modeled by nonlinear equations of motion in state space. The three methods are compared using simulated flight test data. A six-degree-of-freedom airframe model for an autonomously piloted vehicle (APV) is first constructed containing twenty five aerodynamic coefficients. The coefficients are then identified from noise corrupted flight test data using the above three methods. The results show that all the three methods are capable of identifying the APV aerodynamic coefficients, and they exhibit similarly satisfactory results. Considering all the aspects related to the parameter identification of flight vehicle, such as accuracy, convergence, and computational burden, it can be said that the EKF is superior to the other methods. Author (EI)

A95-69968

AERODYNAMIC MECHANISM OF GALLOPING

YASUHARU NAKAMURA Kyushu Univ, Kasuga, Japan and KATSUYA HIRATA Transactions of the Japan Society for Aeronautical and Space Sciences (ISSN 0549-3811) vol. 36, no. 114 February 1994 p. 257-269 refs (BTN-94-EIX94371347709) Copyright

A unified account of the aerodynamic excitation mechanism of high- and low-speed galloping of bluff cylinders with or without a downstream splitter plate is presented in this paper. This report is mainly based on recent experimental findings on the galloping of rectangular cylinders. In particular, it is shown that the shear-layer/edge direct interaction is closely related to both the onset and the subsiding of the galloping, depending on the situation. Author (EI)

A95-69969

GROUND EFFECT CALCULATION OF TWO-DIMENSIONAL AIRFOIL

ETSUO MORISHITA Univ of Tokyo, Tokyo, Japan and KAORU TEZUKA Transactions of the Japan Society for Aeronautical and Space Sciences (ISSN 0549-3811) vol. 36, no. 114 February 1994 p. 270-280 refs (BTN-94-EIX94371347710) Copyright

The ground effect of a two-dimensional airfoil is calculated by the Euler equations. Both the composite grid system and the forced solution technique are found to be effective in the calculation. The Euler solutions give almost the same results as those by the panel methods

with the compressible correction except when the critical Mach number is reached. Author (EI)

N95-19967# Transportation Research Board, Washington, DC. PUBLIC-SECTOR AVIATION ISSUES: GRADUATE RESEARCH AWARD PAPERS, 1992-1993 Transportation Research Record

1994 44 p See also PB93-206258 (PB94-217478; TRB/TRR-1428; ISBN-0-309-05506-7) Avail: CASI HC A03/MF A01

The papers in this document reports on research topics chosen by graduate students selected for awards from a nationwide competition under Seventh Graduate Research Award Program on Public-Sector Aviation issues (1992-1993). It has the following contents: Dynamic Analysis of Oligopolistic Behavior in the U.S. Airline Industry; Movements of Domestic Airline Technical Efficiency Scores over Time; Implications for Future Industry Structure; Evaluating Self-Analysis as a Strategy for Learning Crew Resource Management in Undergraduate Flight Training; and Airfoil Performance in Heavy Rain. NTIS

N95-20091 Federal Aviation Administration, Washington, DC. Office of Aviation Policy and Plans.

CENSUS US CIVIL AIRCRAFT CALENDAR YEAR 1993 Annual Report 31 Dec. 1993

444 p Limited Reproducibility: More than 20% of this document may be affected by microfiche quality (AD-A286309; FAA-APO-94-10) Avail: CASI HC A19

This report presents information about the U.S. civil aircraft fleet. It includes detailed tables of air carrier aircraft and an inventory of registered aircraft by manufacturer and model, and general aviation aircraft by state and county of the owner. DTIC

N95-21640* National Aeronautics and Space Administration, Washington, DC.

AERONAUTICAL ENGINEERING: A CONTINUING BIBLIOGRAPHY WITH INDEXES (SUPPLEMENT 315)

Mar. 1995 84 p (NASA-SP-7037(315); NAS 1.21:7037(315)) Avail: CASI HC A05

This bibliography lists 217 reports, articles, and other documents introduced into the NASA scientific and technical information system in Mar. 1995. Subject coverage includes: design, construction and testing of aircraft and aircraft engines; aircraft components, equipment, and systems; ground support systems; and theoretical and applied aspects of aerodynamics and general fluid dynamics. Author

N95-22046# Wright Lab., Wright-Patterson AFB, OH.

DAMAGE TOLERANT REPAIR TECHNIQUES FOR PRESSURIZED AIRCRAFT FUSELAGES Final Report, 15 Jun. 1991 - 15 Nov. 1993

ROBERT S. FREDELL 6 Jun. 1994 281 p

(Contract(s)/Grant(s): AF PROJ. 2401)

(AD-A286298; WL-TR-94-3134) Avail: CASI HC A13/MF A03

Concerns over the safety of the continued use of aging transport aircraft have been voiced in the industry. A key component in the structural integrity of aging aircraft is the damage tolerance of fuselage structural repairs. The investigation focuses on the analysis and

A
B
S
T
R
A
C
T
S

02 AERODYNAMICS

testing of contemporary repair methods and develops two improvements. The first technique, known as soft patching, is appropriate for damage tolerant riveted repairs to incidental fuselage damage. Soft patching involves the use of high strength, moderate elastic modulus GLARE 3 fiber metal laminate patches. They extend the fatigue life of riveted repairs to monolithic aluminum fuselages while reducing life cycle costs. The second technique involves bonded crack patching of intact fatigue cracks in fuselage skins. An easy to use analysis program is presented along with analytical and test results of a low cost, high performance patch material known as GLARE 2. The findings demonstrate that GLARE 2 can replace the expensive boron/epoxy composites used in fuselage crack patching applications. DTIC

02 AERODYNAMICS

Includes aerodynamics of bodies, combinations, wings, rotors, and control surfaces; and internal flow in ducts and turbomachinery.

A95-70136* National Aeronautics and Space Administration. Ames Research Center, Moffett Field, CA.

FLOW RESOLUTION AND DOMAIN INFLUENCE IN RAREFIED HYPERSONIC BLUNT-BODY FLOWS

BRIAN L. HAAS National Aeronautics and Space Administration. Ames Research Center, Moffett Field, CA and MICHAEL A. FALLAVOLLITA Journal of Thermophysics and Heat Transfer (ISSN 0887-8722) vol. 8, no. 4 October-December 1994 p. 751-757 refs

(BTN-95-EIX95082502729) Copyright

This parametric study assesses the influence of upstream domain size and grid resolution upon flowfield properties and body aerodynamics computed for rarefield flows over cold blunt bodies with a direct simulation Monte Carlo (DSMC) particle method. Empirical correlations are suggested for aerodynamic coefficients for two-dimensional flows past a perpendicular flat plate. Freestream parameters that were varied in the study include the Mach number, Knudsen number, surface temperature, and intermolecular potential. Insufficient grid resolution leads to overprediction of aerodynamic heating and forces in the DSMC method. Molecular diffusion from the body surface results in greater far-field domain influence as flow rarefaction increases. As a result, insufficient upstream domain size in the DSMC method leads to overprediction of heating and drag. Simulation of a hard sphere gas is more sensitive to grid resolution, whereas simulation of a Maxwell gas is more sensitive to upstream domain size. Finally, a simple study of normal shock waves indicates that a grid cell dimension less than one-third of the upstream mean free path is required to capture shock profiles accurately. Author (EI)

A95-71029 TIME-RESOLVED SURFACE HEAT FLUX MEASUREMENTS IN THE WING/BODY JUNCTION VORTEX

D. J. LEWIS Virginia Polytechnic Inst and State Univ, Blacksburg, VA, R. L. SIMPSON, and T. E. DILLER Journal of Thermophysics and Heat Transfer (ISSN 0887-8722) vol. 8, no. 4 October-December 1994 p. 656-663 refs
(BTN-95-EIX95082502716) Copyright

Time- and spatially-resolved heat flux measurements are reported for the endwall surface in the turbulent, incompressible flow in the nose region of a wing-body junction formed by a wing and a flat plate. Both the wing and the flat plate were heated and held at a constant and uniform temperature. The effects of cylindrical wing geometry on heat flux were investigated by taking heat flux measurements in the nose regions of a 3:2 elliptic nose/NACA 0020 tail shape, a circular cylinder with a wedge tail, and an NACA 0015. Heat flux rates were increased up to a factor of 3 over the heat flux rates in the approach boundary layer. The rms of the heat flux fluctuations were as high as 25% of the mean heat flux in the vortex-dominated nose region. Away from the wing, upstream of the time-averaged vortex center, augmentation in the heat flux is due to increased turbulent mixing caused by large-scale

unsteadiness of the vortex. A new three-dimensional extension of an existing correlation is proposed to account for the effects of the horseshoe vortex on heat transfer in this region. Adjacent to the wing the augmentation in heat flux is due to a change in the mean velocity field. Author (EI)

A95-71177 MEASUREMENT AROUND A ROTOR BLADE EXCITED IN PITCH. PART 1: DYNAMIC INFLOW

SHIUH-GUANG LIOU Georgia Inst. of Technology, Atlanta, GA, US, N. M. KOMERATH Georgia Inst. of Technology, Atlanta, GA, US, and MIHIR KUMAR LAL Georgia Inst. of Technology, Atlanta, GA, US American Helicopter Society, Journal (ISSN 0002-8711) vol. 39, no. 2 April 1994 p. 4-12 Research sponsored by US Army Research Office
(HTN-95-31007) Copyright

This is the first of two papers describing experiments on a two-blade rotor in hover, under controlled pitch excitation. Measurements of the inflow to the rotor are described, first under steady conditions, and then under prescribed 4-per-rev pitch excitation. The high data rates, data acquisition techniques and data quality required for this experiment are demonstrated, including 4-per-rev velocity variations due to 1-degree pitch oscillation, extracted over a single period of rotor revolution at 600 rpm. The steady case results agree with lifting-line-based analytical predictions except in the tip region, as expected. The excited-blade case shows the 4-per-rev velocity perturbation, and the dependence on the phase of the excitation. Spectral analysis of the Laser Doppler Velocimeter (LDV) data shows multiple harmonics of the excitation frequency. The rate of pitch change is seen to be high enough to produce substantial hysteresis effects, whose variation with radial position is measured. The hysteresis is seen to arise from the inboard shed vorticity, and to decay towards the tip. Author (Hermer)

A95-71178 MEASUREMENT AROUND A ROTOR BLADE EXCITED IN PITCH. PART 2: UNSTEADY SURFACE PRESSURE

MIHIR KUMAR LAL Georgia Inst. of Technology, Atlanta, GA, US, SHIUH-GUANG LIOU Georgia Inst. of Technology, Atlanta, GA, US, G. A. PIERCE Georgia Inst. of Technology, Atlanta, GA, US, and N. M. KOMERATH Georgia Inst. of Technology, Atlanta, GA, US American Helicopter Society, Journal (ISSN 0002-8711) vol. 39, no. 2 April 1994 p. 13-20 Research sponsored by US Army Research Office
(HTN-95-31008) Copyright

This paper describes measurements of chordwise distributions of unsteady pressure at three radial locations on a stiff two-bladed teetering helicopter rotor in hover, with the blades executing simple harmonic pitch oscillations about the quarter-chord pitch axis. The effect of dynamic inflow on rotor unsteady surface pressure has been extensively documented. Two means of changing dynamic inflow have been employed, first by varying rotor speed and forcing frequency, and second by changing the mean pitch angle. The effects of wake dynamics are seen through the phase difference between vorticity shed by previous blades and by previous revolutions of the reference blade, and through wake spacing. This phase depends on the ratio of excitation frequency to blade passage frequency, the number of blades in the rotor, and on the type of excitation applied. The reduced frequency effect and the tip effect on the lifting perturbation pressure have been demonstrated. Author (Hermer)

A95-71179 AERODYNAMIC AND WAKE METHODOLOGY EVALUATION USING MODEL UH-60A EXPERIMENTAL DATA

MICHAEL S. TOROK United Technologies Corporation, Stratford, CT, US and CHARLES R. BEREZIN United Technologies Corporation, Stratford, CT, US American Helicopter Society, Journal (ISSN 0002-8711) vol. 39, no. 2 April 1994 p. 21-29
(HTN-95-31009) Copyright

An evaluation of several aerodynamic methodologies; lifting line, lifting surface and Computational Fluid Dynamics (CFD), and wake methodologies; vortex lattice and constant vorticity contour

models, is made to determine their applicability and validity in the prediction of helicopter airloads. Integrated blade loads, blade pressures and blade strain data taken on a model UH-60A BLACK HAWK rotor are utilized to assess the capabilities of the aerodynamic analyses. Prescribed torsional deformations, derived from test data, are used to create a uniform basis from which to compare the methods. Test conditions chosen for this study include a high-speed transonic flow condition, a low speed, highly distorted wake condition, and a descending flight, blade-vortex interaction (BVI) condition. Results, in general, show good agreement between predicted and measured blade loads. Both 2-dimensional and 3-dimensional unsteady aerodynamic models show improvement over a quasi-steady model, with the 3-dimensional Full Potential Rotor (FPR) method yielding the best predictions in the blade tip region. Three wake models, United Technologies Research Center's (UTRC's) FREEWAKE, Continuum Dynamics Inc.'s (CDI's) RotorCRAFT, and Johnson's dual-peak, modified Scully model perform comparably, all having difficulties in predicting the complex vortex flow in the first quadrant. The FPR analysis yields good predictions of chordwise pressure distributions. For the blade-vortex interaction (BVI) condition, the inclusion of a discrete vortex segment within the computational domain of FPR yields a significantly improved BVI pulse prediction. This translates to a largely improved BVI acoustic prediction.

Author (Hemer)

A95-71180
VORTICITY CONCENTRATION AT THE EDGE OF THE
INBOARD VORTEX SHEET

J. M. KIM Georgia Inst. of Technology, Atlanta, GA, US, N. M. KOMERATH Georgia Inst. of Technology, Atlanta, GA, US, and S. G. LIOU Georgia Inst. of Technology, Atlanta, GA, US American Helicopter Society, Journal (ISSN 0002-8711) vol. 39, no. 2 April 1994 p. 30-34

(HTN-95-31010) Copyright

Flow visualization and velocity measurements are used to show that the outer edge of the trailing vortex sheet from an untwisted rotor blade rolls up into a discrete vortical structure which is opposite in sense and approximately one-half the strength of the tip vortex. This occurs both in hover and low-speed forward flight of a two-bladed teetering rotor, and at both upstream and downstream edges of the wake in forward flight. The roll-up process and the trajectories of the tip vortex and the counter-rotating vortex are examined using digitized laser sheet video images. Azimuth-resolved velocity data are used to quantify vortex strengths.

Author (Hemer)

A95-71181* National Aeronautics and Space Administration, Langley Research Center, Hampton, VA.

EFFECTS OF LEADING AND TRAILING EDGE FLAPS ON
THE AERODYNAMICS OF AIRFOIL/VORTEX
INTERACTIONS

AHMED A. HASSAN McDonnell Douglas Helicopter Company, Mesa, AZ, US, L. N. SANKAR Georgia Inst. of Technology, Atlanta, GA, US, and H. TADGHIGHI McDonnell Douglas Helicopter Company, Mesa, AZ, US American Helicopter Society, Journal (ISSN 0002-8711) vol. 39, no. 2 April 1994 p. 35-46

(Contract(s)/Grant(s): NAS1-19136)

(HTN-95-31011) Copyright

A numerical procedure has been developed for predicting the two-dimensional parallel interaction between a free convecting vortex and a NACA 0012 airfoil having leading and trailing edge integral-type flaps. Special emphasis is placed on the unsteady flap motion effects which result in alleviating the interaction at subcritical and supercritical onset flows. The numerical procedure described here is based on the implicit finite-difference solutions to the unsteady two-dimensional full potential equation. Vortex-induced effects are computed using the Biot-Savart Law with allowance for a finite core radius. The vortex-induced velocities at the surface of the airfoil are incorporated into the potential flow model via the use of the velocity transpiration approach. Flap motion effects are also modeled using the transpiration approach. For subcritical interactions, our results indicate that trailing edge flaps can be used to alleviate the impulsive loads experienced by the airfoil. For supercritical interactions, our results demonstrate the necessity of using a leading

edge flap, rather than a trailing edge flap, to alleviate the interaction. Results for various time-dependent flap motions and their effect on the predicted temporal sectional loads, differential pressures, and the free vortex trajectories are presented

Author (Hemer)

A95-71183 National Aeronautics and Space Administration, Ames Research Center, Moffett Field, CA.

ADVANCE FINITE ELEMENT MODELING OF ROTOR BLADE
AEROELASTICITY

F. K. STRAUB McDonnell Douglas Helicopter Systems, Mesa, AZ, US, K. B. SANGHA Lockheed Aeronautical Systems Co., Marietta, GA, US, and B. PANDA Boeing Defense & Space Group, Helicopter Division, Philadelphia, PA, US American Helicopter Society, Journal (ISSN 0002-8711) vol. 39, no. 2 April 1994 p. 56-68 Research supported by McDonnell Douglas Helicopter Company (Contract(s)/Grant(s): NAS2-12343)

(HTN-95-31013) Copyright

An advanced beam finite element has been developed for modeling rotor blade dynamics and aeroelasticity. This element is part of the Element Library of the Second Generation Comprehensive Helicopter Analysis System (2GCHAS). The element allows modeling of arbitrary rotor systems, including bearingless rotors. It accounts for moderately large elastic deflections, anisotropic properties, large frame motion for maneuver simulation, and allows for variable order shape functions. The effects of gravity, mechanically applied and aerodynamic loads are included. All kinematic quantities required to compute airloads are provided. In this paper, the fundamental assumptions and derivation of the element matrices are presented. Numerical results are shown to verify the formulation and illustrate several features of the element.

Author (Hemer)

A95-72566
ON THE CHOICE OF APPROPRIATE BASES FOR
NONLINEAR DYNAMIC MODAL ANALYSIS

O. A. BAUCHAU Rensselaer Polytechnic Inst., Troy, NY, US and D. GUERNSEY Rensselaer Polytechnic Inst., Troy, NY, US American Helicopter Society, Journal (ISSN 0002-8711) vol. 38, no. 4 October 1993 p. 28-36

(Contract(s)/Grant(s): DAAL03-88-C-0004)

(HTN-95-A0495) Copyright

This paper focuses on assessing the accuracy of various modal bases in nonlinear dynamic modal analysis of helicopter rotor blades by comparing their prediction with a reference solution obtained by integrating in time the full finite element equations. Both the full finite element and the modal models are based on the same discretization of the physical problem, and are derived from a mixed variational principle. This variational statement is a purely algebraic, fourth order expression that is ideally suited for modal reduction. Perturbation modes, which extract information about the nonlinear behavior of the structure from higher order derivatives of the variational principle, are shown to provide an excellent basis for the modal analysis, as they accurately capture the nonlinear kinematic couplings. Perturbation modes provide a more accurate model than that based on natural vibration mode shapes, which are very poor at synthesizing these nonlinear kinematic couplings. However, in the presence of nonlinearities associated with rotational dynamic effects, both natural vibration and perturbation mode shapes fail to accurately represent the dynamic behavior of the blade.

Author (Hemer)

A95-72567* National Aeronautics and Space Administration, Ames Research Center, Moffett Field, CA.

FLAP-LAG DAMPING IN HOVER AND FORWARD FLIGHT
WITH A THREE-DIMENSIONAL WAKE

A. R. MANJUNATH Indian Inst. of Science, Bangalore, India, J. NAGABHUSHANAM Indian Inst. of Science, Bangalore, India, GOPAL H. GAONKAR Florida Atlantic Univ., Boca Raton, FL, US, DAVID A. PETERS Washington Univ., Saint Louis, MO, US, and AY SU Yuan-Ze Inst. of Tech., Chungli, Taiwan American Helicopter Society, Journal (ISSN 0002-8711) vol. 38, no. 4 October 1993 p. 37-49

02 AERODYNAMICS

(Contract(s)/Grant(s): NAG2-462; DAAL03-91-G-0007)
(HTN-95-A0496) Copyright

Prediction of lag damping is difficult owing to the delicate balance of drag, induced drag and Coriolis forces in the in-plane direction. Moreover, induced drag is sensitive to dynamic wake, both shed and trailing components, and thus its prediction requires adequate unsteady-wake representation. Accordingly, rigid-blade flap-lag equations are coupled with a three-dimensional finite-state wake model; three isolated rotor configurations with three, four and five blades are treated over a range of thrust levels, Lock numbers, lag frequencies and advance ratios. The investigation includes convergence characteristics of damping with respect to the number of radial shape functions and harmonics of the wake model for multiblade modes of low frequency (less than 1/rev.) to high frequency (greater than 1/rev.). Predicted flap and lag damping levels are then compared with similar predictions with (1) rigid wake (no unsteady induced flow), (2) Loewy lift deficiency and (3) dynamic inflow. The coverage also includes correlations with the measured lag regressive-mode damping in hover and forward flight and comparisons with similar correlations with dynamic wake model are consistently higher than the predictions with the dynamic inflow model; even for the low frequency lag regressive mode, the number of wake harmonics should at least be equal to twice the number of blades.

Author (Hemer)

A95-72568* National Aeronautics and Space Administration. Langley Research Center, Hampton, VA.

AIR AND GROUND RESONANCE OF HELICOPTERS WITH ELASTICALLY TAILORED COMPOSITE ROTOR BLADES

EDWARD C. SMITH Pennsylvania State Univ., State College, PA, US and INDERJIT CHOPRA Maryland Univ., College Park, MD, US American Helicopter Society, Journal (ISSN 0002-8711) vol. 38, no. 4 October 1993 p. 50-61

(Contract(s)/Grant(s): NAG1-1253; DAAL03-88-C-0002)
(HTN-95-A0497) Copyright

The aeromechanical stability, including air resonance in hover, air resonance in forward flight, and ground resonance, of a helicopter with elastically tailored composite rotor blades is investigated. Five soft-inplane hingeless rotor configurations, featuring elastic pitch-lag, pitch-flap and extension-torsion couplings, are analyzed. Elastic couplings introduced through tailored composite blade spars can have a powerful effect on both air and ground resonance behavior. Elastic pitch-flap couplings (positive and negative) strongly affect body, rotor and dynamic inflow modes. Air resonance stability is diminished by elastic pitch-flap couplings in hover and forward flight. Negative pitch-lag elastic coupling has a stabilizing effect on the regressive lag mode in hover and forward flight. The negative pitch-lag coupling has a detrimental effect on ground resonance stability. Extension-torsion elastic coupling (blade pitch decreases due to tension) decreases regressive lag mode stability in both airborne and ground contact conditions. Increasing thrust levels has a beneficial influence on ground resonance stability for rotors with pitch-flap and extension-torsion coupling and is only marginally effective in improving stability of rotors with pitch-lag coupling.

Author (Hemer)

A95-72570

PARAMETRIC STUDIES FOR TILTROTOR AEROELASTIC STABILITY IN HIGHSPEED FLIGHT

MARK W. NIXON Army Vehicle Structures Directorate, Hampton, VA, US American Helicopter Society, Journal (ISSN 0002-8711) vol. 38, no. 4 October 1993 p. 71-79

(HTN-95-A0499) Copyright

The influence of several system design parameters on tiltrotor aeroelastic stability is examined for the highspeed (axial) flight mode. The results are based on a math model in which the wing is assumed to be cantilevered and is represented by beam finite elements having vertical bending, chordwise bending and torsional degrees of freedom. A quasi-steady aerodynamic model is used for both the wing and rotor system. Coupling of the rotor flapping modes with the wing elastic modes produces a whirl motion, typical of

tiltrotors, that can become unstable at high speeds. The sensitivity of this instability with respect to rotor frequencies, wing stiffness and forward wing sweep is examined. Some important new trends are identified regarding the role of blade lag dynamics and forward wing sweep in tiltrotor aeroelastic stability. Two important conclusions based on these trend studies are that the blade lag frequency may be tuned to improve tiltrotor stability, and forward wing sweep is destabilizing because of changes in rotor force components associated with the sweep.

Author (Hemer)

N95-19913* National Aeronautics and Space Administration. Langley Research Center, Hampton, VA.

STATIC INVESTIGATION OF TWO FLUIDIC THRUST-VECTORING CONCEPTS ON A TWO-DIMENSIONAL CONVERGENT-DIVERGENT NOZZLE

DAVID J. WING Dec. 1994 203 p

(Contract(s)/Grant(s): RTOP 505-62-30-01)

(NASA-TM-4574; L-17350; NAS 1.15:4574) Avail: CASI HC A10/MF A03

A static investigation was conducted in the static test facility of the Langley 16-Foot Transonic Tunnel of two thrust-vectoring concepts which utilize fluidic mechanisms for deflecting the jet of a two-dimensional convergent divergent nozzle. One concept involved using the Coanda effect to turn a sheet of injected secondary air along a curved sidewall flap and, through entrainment, draw the primary jet in the same direction to produce yaw thrust vectoring. The other concept involved deflecting the primary jet to produce pitch thrust vectoring by injecting secondary air through a transverse slot in the divergent flap, creating an oblique shock in the divergent channel. Utilizing the Coanda effect to produce yaw thrust vectoring was largely unsuccessful. Small vector angles were produced at low primary nozzle pressure ratios, probably because the momentum of the primary jet was low. Significant pitch thrust vector angles were produced by injecting secondary flow through a slot in the divergent flap. Thrust vector angle decreased with increasing nozzle pressure ratio but moderate levels were maintained at the highest nozzle pressure ratio tested. Thrust performance generally increased at low nozzle pressure ratios and decreased near the design pressure ratio with the addition of secondary flow.

Author

N95-19946# Aircraft Research Association Ltd., Bedford (England). INVESTIGATION OF A THERMAL BUOYANCY EFFECT ON THE DRAG OF HALF MODELS TESTED IN THE ARA TRANSONIC WIND TUNNEL

DENNIS R. STANNILAND, IAN F. BURNS, and JOHN E. GREEN May 1994 12 p Presented at the 19th Congress of the International Council of the Aeronautical Sciences, Anaheim, CA, Sep. 1994 (ARA-MEMO-407) Avail: CASI HC A03/MF A01

The demand for improved drag repeatability from wind tunnel measurements, together with the increasing size of models (driven by the requirement for accurate representation of small components), has led to the need for a greater understanding of the flow near the porous walls of the ARA Transonic Wind Tunnel and the implications of very small changes in this flow on the model force measurements. A detailed investigation of the variability of drag measurements on a half model identified a diurnal variation which could be attributed to the small changes in temperature difference between the tunnel shell and the freestream. This paper describes measurements which have been made in the tunnel to identify the cause of this non-repeatability. The results show a variation in the boundary layer development on the tunnel walls caused by differences in the heat transfer in the plenum chamber. This can change the Mach number in the vicinity of a half model afterbody by approximately 0.002 for a temperature increment of 5 deg K, implying a change in drag coefficient of 0.0002 for a typical civil aircraft model. An extension to the test section has been designed, which was successful in removing the thermal influence on the boundary layer thickness and centerline Mach number in the empty tunnel. However, some thermal buoyancy remains when a half model is tested in the redesigned section, although this is significantly reduced for a large model. A correction procedure has been

developed which has virtually eliminated thermal buoyancy as a source of error, resulting in a drag repeatability of better than 1 count.
Author

N95-19991# Aeronautical Systems Div., Wright-Patterson AFB, OH.

OPEN SKIES PROJECT COMPUTATIONAL FLUID DYNAMIC ANALYSIS Final Report, Nov. 1992 - May 1993

JAMES C. SLAVEY, MARK S. JURKOVICH, ROBERT M. WEYER, and JOSEPH C. ZUPPARDO Mar. 1994 130 p
(AD-A285928; ASC-TR-94-5027) Avail: CASI HC A07/MF A02

A Computational Fluid Dynamic (CFD) analysis has been performed on a WC-135B aircraft that has been modified at Wright-Patterson AFB (WPAFB) forming the first Open Skies aircraft designated OC-135B. The studies included the use of panel method, full potential, and Navier-Stokes methods utilizing 2-D/axisymmetric, and 3-D. While providing information useful to the Open Skies program, the studies also provide a good example of how lower order and higher order computational aerodynamic methods can be used together to obtain the maximum benefit from CFD at a minimum cost. Flight test tufting and accelerometer data confirmed the results of the 3-D Full Navier-Stokes results.
DTIC

N95-19996* National Aeronautics and Space Administration. Hugh L. Dryden Flight Research Center, Edwards, CA.

F-16XL INTERVIEW WITH MARTA BOHN-MEYER

(Videotape)

27 Jul. 1992 Videotape: 30 min. playing time, in color, with sound
(NASA-TM-110505; NONP-NASA-VT-95-41117) Avail: CASI VHS A02/BETA A22

Marta Bohn-Meyer discusses the cooperative research between Rockwell Industries and NASA research facilities in their effort to optimize and maintain the supersonic laminar flow on the F-16XL aircraft. Research on the airfoil design, chord optimization, introduction of a suction feature to maintain pressure distribution, and CFD, both theoretical and actual phenomena, are discussed. Bohn-Meyer discusses the difference between supersonic and subsonic laminar flow, cross flow, reasons behind using this particular F-16 aircraft for this research, and the future of this ongoing research, including the data base that investigators are building from wind tunnel data and in-flight validation.
DFRC

N95-20177 California Inst. of Tech., Pasadena, CA. Graduate Aeronautical Labs.

RESEARCH ON BLUFF BODY VORTEX WAKES

ANATOL ROSHKO, ANTHONY LEONARD, and MORTEZA GHARIB 1994 8 p Limited Reproducibility: More than 20% of this document may be affected by microfiche quality
(Contract(s)/Grant(s): N00014-94-1-0793)
(AD-A286319) Avail: CASI HC A02

The basic approach is to obtain measurements in correlated laboratory experiments and numerical simulations of flows past bluff bodies, especially circular cylinders. Laboratory measurements include flow visualization and digital particle image velocimetry (DPIV). Numerical simulations are based on vortex methods. Interpretation of relations between velocity/vorticity fields and body forces is sought through the generalized Biot-Savart law. The role of Reynolds number, effects of three dimensionality, and effects of body motion are investigated. Relations to the mean near-wake flow and mean force (drag) are also studied, for their basic technological importance and also for insights into the unsteady motion.
DTIC

N95-20248# Arnold Engineering Development Center, Arnold AFS, TN.

DESCRIPTION AND FLOW CHARACTERIZATION OF HYPERSONIC FACILITIES Final Report, Jul. 1992 - Jul. 1993

A. ANDERSON, R. K. MATTHEWS, J. R. MAUS, and R. A. CRAWFORD Aug. 1994 59 p
(AD-A284291; AEDC-TR-94-8) Avail: CASI HC A04/MF A01

Hypersonic test facilities will continue to play a major role in the development of hypersonic vehicles. In the past, ground test facilities were often used to perform configuration parametric studies and/or to develop large databases. Future testing will emphasize understanding of fluid physics and validation of codes. Computational fluid dynamics (CFD) has made great progress in the past two decades, but the marriage of CFD and ground testing is clearly a reality today, and will become even more important in the future. One of the challenges for the experimentalist is to develop and utilize facilities that simulate hypersonic flight, and to provide the required data precision to validate CFD codes. This provides a brief review of facility fundamental considerations and simulation issues. It is clear that no one facility will meet the wide variety of test objectives; therefore, the test facilities span a range of size, run time, complexity, and operating cost. Representative facilities are described, as well as their test capabilities, and shortfalls.
DTIC

N95-20688*# National Aeronautics and Space Administration. Langley Research Center, Hampton, VA.

THE PERSONAL AIRCRAFT: STATUS AND ISSUES

SCOTT G. ANDERS, SCOTT C. ASBURY, KENNETH S. BRENTNER, DENNIS M. BUSHNELL, CHRISTOPHER E. GLASS, WILLIAM T. HODGES, SHELBY J. MORRIS, JR., and MICHAEL A. SCOTT Dec. 1994 126 p

(Contract(s)/Grant(s): RTOP 232-01-04-01)

(NASA-TM-109174; NAS 1.15:109174) Avail: CASI HC A07/MF A02

Paper summarizes the status of personal air transportation with emphasis upon VTOL and converticair capability. The former obviates the need for airport operations for personal aircraft whereas the latter provides both ground and air capability in the same vehicle. Fully automatic operation, ATC and navigation is stressed along with consideration of acoustic, environmental and cost issues.
Author

N95-20758# Aircraft Research Association Ltd., Bedford (England).

THE DYNAMIC APPROACH TO ROTOR BLADE RESEARCH:

ARA'S OSCILLATORY TEST FACILITY

CAROLINE M. HUMPHREYS Sep. 1994 12 p Presented at the ICAS 1994, Anaheim, CA, Sep. 1994 Original contains color illustrations

(ARA-MEMO-405) Avail: CASI HC A03/MF A01 color page

Helicopters' forward flight performance is limited by the rapid build up in blade and control loads which occur when rotor blades enter stall conditions. Due to a combination of the helicopter forward speed and the rotor rotational velocity the rotor sections experience a wide range of local onset conditions, this leads to vastly different flow characteristics across the span and through the rotational cycle. A great deal of time and effort has been devoted to studying this flow phenomena. Consequently, information covering all aspects of unsteady aerodynamics is easily available. However, one area that needs up-dating is the description of the experimental test facilities that are able to simulate these flow conditions. The dynamic rig at the Aircraft Research Association was designed and built in the 1970's. Since then, as new technology became available, the rig's capabilities have been steadily improved. The paper reports on these amendments.
Author

N95-20794*# National Aeronautics and Space Administration. Lewis Research Center, Cleveland, OH.

APPLICATION OF PRESSURE SENSITIVE PAINT IN HYPERSONIC FLOWS

KENOL JULES, MARIO CARBONARO (Von Hoerner und Sulger Electronic G.m.b.H., Schwetzingen, Germany.), and STEPHAN ZEMSCH (Von Hoerner und Sulger Electronic G.m.b.H., Schwetzingen, Germany.) Feb. 1995 17 p Sponsored by Von Karman fellowship and AF

(Contract(s)/Grant(s): RTOP 466-05-02)

(NASA-TM-106824; E-9373; NAS 1.15:106824) Avail: CASI HC A03/MF A01

It is well known in the aerodynamic field that pressure distribution measurement over the surface of an aircraft model is a problem

02 AERODYNAMICS

in experimental aerodynamics. For one thing, a continuous pressure map can not be obtained with the current experimental methods since they are discrete. Therefore, interpolation or CFD methods must be used for a more complete picture of the phenomenon under study. For this study, a new technique was investigated which would provide a continuous pressure distribution over the surface under consideration. The new method is pressure sensitive paint. When pressure sensitive paint is applied to an aerodynamic surface and placed in an operating wind-tunnel under appropriate lighting, the molecules luminesce as a function of the local pressure of oxygen over the surface of interest during aerodynamic flow. The resulting image will be brightest in the areas of low pressure (low oxygen concentration), and less intense in the areas of high pressure (where oxygen is most abundant on the surface). The objective of this investigation was to use pressure sensitive paint samples from McDonnell Douglas (MDD) for calibration purpose in order to assess the response of the paint under appropriate lighting and to use the samples over a flat plate/conical fin mounted at 75 degrees from the center of the plate in order to study the shock/boundary layer interaction at Mach 6 in the Von Karman wind-tunnel. From the result obtained it was concluded that temperature significantly affects the response of the paint and should be given the uppermost attention in the case of hypersonic flows. Also, it was found that past a certain temperature threshold, the paint intensity degradation became irreversible. The comparison between the pressure tap measurement and the pressure sensitive paint showed the right trend. However, there exists a shift when it comes to the actual value. Therefore, further investigation is under way to find the cause of the shift. Author

N95-21031* Purdue Univ., West Lafayette, IN. Dept. of Aeronautics and Astronautics.

WAKE MEASUREMENTS IN A STRONG ADVERSE PRESSURE GRADIENT

R. HOFFENBERG, JOHN P. SULLIVAN, and S. P. SCHNEIDER
1994 13 p

(Contract(s)/Grant(s): NAG2-854)

(NASA-CR-197272; NAS 1.26:197272; AIAA PAPER 94-2613) Avail: CASI HC A03/MF A01

The behavior of wakes in adverse pressure gradients is critical to the performance of high-lift systems for transport aircraft. Wake deceleration is known to lead to sudden thickening and the onset of reversed flow; this 'wake bursting' phenomenon can occur while surface flows remain attached. Although 'wake bursting' is known to be important for high-lift systems, no detailed measurements of 'burst' wakes have ever been reported. Wake bursting has been successfully achieved in the wake of a flat plate as it decelerated in a two-dimensional diffuser, whose sidewalls were forced to remain attached by use of slot blowing. Pilot probe surveys, L.D.V. measurements, and flow visualization have been used to investigate the physics of this decelerated wake, through the onset of reversed flow. Author

N95-21338* National Aeronautics and Space Administration. Langley Research Center, Hampton, VA.

APPLICATION OF NAVIER-STOKES CODE PAB3D WITH KAPPA-EPSILON TURBULENCE MODEL TO ATTACHED AND SEPARATED FLOWS

KHALED S. ABDOL-HAMID (Analytical Services and Materials, Inc., Hampton, VA.), B. LAKSHMANAN (Old Dominion Univ., Norfolk, VA.), and JOHN R. CARLSON Jan. 1995 43 p
(Contract(s)/Grant(s): RTOP 505-59-10-20)

(NASA-TP-3480; L-17354; NAS 1.60:3480) Avail: CASI HC A03/MF A01

A three-dimensional Navier-Stokes solver was used to determine how accurately computations can predict local and average skin friction coefficients for attached and separated flows for simple experimental geometries. Algebraic and transport equation closures were used to model turbulence. To simulate anisotropic turbulence, the standard two-equation turbulence model was modified by adding nonlinear terms. The effects of both grid density and the turbulence

model on the computed flow fields were also investigated and compared with available experimental data for subsonic and supersonic free-stream conditions. Author

N95-21343* Notre Dame Univ., IN. Dept. of Aerospace and Mechanical Engineering.

EXPERIMENTS ON THE FLOW FIELD PHYSICS OF CONFLUENT BOUNDARY LAYERS FOR HIGH-LIFT SYSTEMS Progress Report

ROBERT C. NELSON, F. O. THOMAS, and H. C. CHU 1994

18 p Original contains color illustrations

(Contract(s)/Grant(s): NAG2-905)

(NASA-CR-197318; NAS 1.26:197318) Avail: CASI HC A03/MF A01; 3 functional color pages

The use of sub-scale wind tunnel test data to predict the behavior of commercial transport high lift systems at in-flight Reynolds number is limited by the so-called 'inverse Reynolds number effect'. This involves an actual deterioration in the performance of a high lift device with increasing Reynolds number. A lack of understanding of the relevant flow field physics associated with numerous complicated viscous flow interactions that characterize flow over high-lift devices prohibits computational fluid dynamics from addressing Reynolds number effects. Clearly there is a need for research that has as its objective the clarification of the fundamental flow field physics associated with viscous effects in high lift systems. In this investigation, a detailed experimental investigation is being performed to study the interaction between the slat wake and the boundary layer on the primary airfoil which is known as a confluent boundary layer. This little-studied aspect of the multi-element airfoil problem deserves special attention due to its importance in the lift augmentation process. The goal of this research is to provide an improved understanding of the flow physics associated with high lift generation. This process report will discuss the status of the research being conducted at the Hessert Center for Aerospace Research at the University of Notre Dame. The research is sponsored by NASA Ames Research Center under NASA grant NAG2-905. The report will include a discussion of the models that have been built or that are under construction, a description of the planned experiments, a description of a flow visualization apparatus that has been developed for generating colored smoke for confluent boundary layer studies and some preliminary measurements made using our new 3-component fiber optic LDV system. Author

N95-21659 Defence Science and Technology Organization, Melbourne (Australia). Aeronautical and Maritime Research Lab. A PRELIMINARY STUDY OF THE AIRWAKE MODEL USED IN AN EXISTING SH-60B/FFG-7 HELICOPTER/SHIP SIMULATION PROGRAM

LINCOLN P. ERM May 1994 44 p

(DSTO-TR-0015; AR-008-644) Copyright Avail: Issuing Activity (DSTO Aeronautical and Maritime Research Lab., GPO Box 4331, Melbourne, Victoria 3001, Australia)

The ship airwake model in a SH-60B/FFG-7 helicopter/ship simulation program is studied in detail. The airwake model is based on wind tunnel measurements obtained for another ship type, with geometric scaling applied to make it suitable for an FFG-7 frigate. Velocities over the flight deck of an FFG-7, predicted using the program, are compared with those obtained from full-scale tests on HMAS Darwin. Differences between predicted and measured velocities are often found to occur, indicating that the model used for prediction should be based on measurements for an FFG-7. Author

N95-21864 Department of the Navy, Washington, DC.

LIFT ENHANCEMENT DEVICE Patent

SAMUEL GREENHALGH, inventor (to Navy) 9 Aug. 1994 11 p
Filed 26 May 1993 Supersedes AD-D016196

(AD-D016522; US-PATENT-5,335,886; US-PATENT-APPL-SN-067763; US-PATENT-CLASS-244-21) Avail: US Patent and Trademark Office

A lift enhancing device for a solid wing is disclosed. A solid wing

with a swept leading edge and unswept trailing edge has a rectangular flap attached along the trailing edge. The flap can be a single segment or can be a plurality of segments joined at contiguous edges. The flap oscillates during air movement and enhances the lift produced. DTIC

N95-21877 Wright Lab., Wright-Patterson AFB, OH.
PRESSURE MEASUREMENTS ON AN F/A-18 TWIN VERTICAL TAIL IN BUFFETING FLOW. VOLUME 1: WIND TUNNEL TEST SUMMARY Final Report, Apr. 1993 - Aug. 1994

CHRIS PETTIT, MICHAEL BANFORD, DANSEN BROWN, and ED PENDLETON 31 Aug. 1994 105 p Limited Reproducibility: More than 20% of this document may be affected by microfiche quality (AD-A279126; WL-TM-94-3039-VOL-1) Avail: Issuing Activity (Defense Technical Information Center (DTIC))

Buffeting pressure measurements were made on the vertical tail surface of a full scale F/A-18 aircraft model in the National Full Scale Aerodynamics Complex at NASA Ames Research Center. Test variables included aircraft angle-of-attack, aircraft sideslip angle, and dynamic pressure. Accelerometers were used to obtain vertical tail accelerations. Pressure transducers were mounted on the starboard vertical tail. Steady and unsteady pressures were obtained. Unsteady pressure data were reduced to power spectral density (PSD) and cross spectral density (CSD) forms. Both steady and unsteady RMS pressure coefficients are also presented. Volume 1 contains the general description of the model, the test program, and highlights of the reduced data. DTIC

N95-21892 Aeronautical Research Labs., Melbourne (Australia).
DERIVED GUST SPECTRA FOR THE MACCHI MB326H
P. PIPERIAS Feb. 1993 41 p
(ARL-TN-3; AR-007-124) Copyright Avail: Issuing Activity (Director, Aeronautical Research Lab., 506 Lorimer St., Fishermens Bend, Victoria 3207, Australia)

Gust spectra for the RAAF Macchi MB326H aircraft fleet have been derived. In-house software has been used with current mission profiles to determine load-exceedence diagrams. Missions exhibiting high exceedences have been identified. Author

N95-22448* Stanford Univ., CA. Center for Turbulence Research.
UNSTRUCTURED-GRID LARGE-EDDY SIMULATION OF FLOW OVER AN AIRFOIL
KENNETH JANSEN *In its* Annual Research Briefs, 1994 p 161-173 Dec. 1994
Avail: CASI HC A03/MF A04

Historically, large-eddy simulations (LES) have been restricted to simple geometries where spectral or finite difference methods have dominated due to their efficient use of structured grids. Structured grids, however, not only difficulty representing complex domains and adapting to complicated flow features, but also are rather inefficient for simulating flows at high Reynolds numbers. The lack of efficiency stems from the need to resolve the viscous sublayer, which requires very fine resolution in all three directions near the wall. Structured grids make use of a stretching to reduce the normal grid spacing but must carry the fine resolution in the streamwise and spanwise directions throughout the domain. The unnecessarily fine grid for much of the domain leads to disturbingly high grid estimates. Chapman (1979), and later Moin & Jimenez (1993), pointed out that, in order to advance the technology to airfoils at flight Reynolds numbers, structured grids must be abandoned in lieu of what are known as nested or unstructured grids. The finite element method can efficiently solve the Navier-Stokes equations on unstructured grids. Although the CPU cost per time step per element is somewhat higher than structured grid methods, this effect is more than offset by the reduction in the number of elements. The use of unstructured grids, coupled with the advances in dynamic subgrid-scale modeling such as those made by Germano et al. (1991) and Ghosal et al. (1994), make LES of an airfoil tractable. We have chosen the NACA 4412 airfoil at maximum lift as the first simulation

since this flow has not been successfully simulated with the Reynolds-averaged Navier-Stokes equations. Author

03

AIR TRANSPORTATION AND SAFETY

Includes passenger and cargo air transport operations; and aircraft accidents.

A95-71021**ICE ACCRETION ON AIRCRAFT WINGS**

P. TRAN Ecole Polytechnique de Montreal, Montreal (Quebec), M. T. BRAHIMI, and I. PARASCHIVOIU Canadian Aeronautics and Space Journal (ISSN 0008-2821) vol. 40, no. 3 September 1994 p. 91-98 refs
(BTN-95-EIX95082502224) Copyright

A numerical method has been developed to calculate ice accretion on three-dimensional wings of any cross-section using the viscous-inviscid interaction technique. This technique matches a panel method for external potential flow calculation with a boundary layer correction. The resulting velocity field is subsequently used to compute water droplet trajectories and their impact points on the wing to obtain the quantity of accumulated ice. Results using this method to simulate rime ice accretion on a NACA 0012 airfoil yield ice shapes that are in good agreement with numerical and experimental data. Author (EI)

N95-20071# Naval Research Lab., Washington, DC.**A REVIEW OF WATER MIST TECHNOLOGY FOR FIRE SUPPRESSION Memorandum Report**

P. A. TATUM, C. L. BEYLER (Hughes Associates, Inc., Columbia, MD.), P. J. DINENNO (Hughes Associates, Inc., Columbia, MD.), E. K. BUDNICK (Hughes Associates, Inc., Columbia, MD.), and G. G. BACK (Hughes Associates, Inc., Columbia, MD.) 30 Sep. 1994 93 p
(Contract(s)/Grant(s): NR PROJ. RH2-1-S-22)
(AD-A285738; NRL/MR/6180-94-7624) Avail: CASI HC A05/MF A01

The potential efficacy of water mist fire suppression systems has been demonstrated in a wide range of applications and by numerous experimental programs. These applications have included Class B spray and pool fires, aircraft cabins, shipboard machinery and engine room spaces, shipboard accommodation spaces, and computer and electronics applications. To summarize these experimental efforts, the efficacy of a particular water mist system is strongly dependent on the ability to not only generate sufficiently small droplet sizes but also distribute sufficient mist concentrations throughout the compartment. A widely accepted critical concentration of water droplets required to extinguish a fire is yet to be determined. Factors that contribute to the success or failure of a water mist system for a particular application include droplet size, velocity, the spray pattern geometry as well as the momentum and mixing characteristics of the spray jet, and the geometry and other characteristics of the protected area. At this time, the effect of these factors on system effectiveness is not well known. This will necessitate evaluation of water mist in context of a specific system for unique applications for the reasonable future unless breakthroughs in understanding of mist distribution and flame interaction occur through research. DTIC

N95-20093 Galaxy Scientific Corp., Pleasantville, NJ.**TEST AND EVALUATION REPORT FOR THE MANUAL DOMESTIC PASSIVE PROFILING SYSTEM (MDPPS) Final Report**

J. L. FOBES, RONALD J. LOFARO, J. P. BERKOWITZ, N. J. DOLAN, and D. S. FISCHER Sep. 1994 55 p Limited Reproducibility: More than 20% of this document may be affected by microfiche quality

03 AIR TRANSPORTATION AND SAFETY

(Contract(s)/Grant(s): DTFA03-92-C-0035)

(AD-A286312; DOT/FAA/CT-94/86) Avail: CASI HC A04

Presented are a compilation of data collected at Northwest Airlines terminal, General Mitchell International Airport, Milwaukee, Wisconsin, from February 22-24, 1994. The study was conducted in support of the Aviation Security Human Factors Research Program located at the Federal Aviation Administration Technical Center (FAATC), Atlantic City International Airport, New Jersey. Real-time (e.g., at the ticket counter and gate) passenger profiling was conducted February 22-24, 1994 in Milwaukee, Wisconsin. Passengers on twenty-one Northwest Airline flights were profiled according to parameters set forth by the Passenger Profiling Subject Matter Expert panel. One hundred ten passengers (82.7%) were cleared by the profile; twenty-three (17.3%) were not cleared. The mean time to profile was 1 minute 23 seconds. An analysis of variance (ANOVA) and a subsequent least square difference (LSD) multiple comparison showed it took significantly longer to profile passengers who were not cleared (mean = 1 minute 27 seconds) than to profile passengers who were cleared (mean = 1 minute 9 seconds) ($F(131, 1) = 36.87, p = .000$). Interview and anecdotal data are also summarized. DTIC

N95-20174# Galaxy Scientific Corp., Pleasantville, NJ. COMMUTER AIRPLANE ACCIDENT DATA ANALYSIS Final Report

G. WITTLIN Aug. 1994 34 p

(Contract(s)/Grant(s): DTFA03-89-C-00043)

(AD-A286315; DOT/FAA/CT-94/75) Avail: CASI HC A03/MF A01

This report presents the results of a review of data from 120 commuter and air taxi airplane accidents that occurred from 1978 through 1986. The main objectives of this study are (1) to present the severe, but survivable impact condition data from the accident database and (2) to formulate appropriate crash design impact parameters. In 1980 the Federal Aviation Administration Technical Center (FAATC) initiated the Aircraft Crashworthiness Program, which resulted in a compilation of commuter airplane accident data. The program's objectives were (1) to define potentially survivable commuter airplane crash scenarios and (2) to provide impact parameters associated with the appropriate crash scenarios. Based on the data that was received, a crash survivable design envelope was defined for commuter airplanes. DTIC

N95-20275# Galaxy Scientific Corp., Pleasantville, NJ. COMMUTER/AIR TAXI DITCHINGS AND WATER-RELATED IMPACTS THAT OCCURRED FROM 1979 TO 1989 Final Report, Jun. 1990 - Dec. 1992

CHARLES C. CHEN and MARK MULLER Jul. 1994 105 p

(Contract(s)/Grant(s): DTFA03-89-C-00043)

(AD-A285691; DOT/FAA/CT-92/4) Avail: CASI HC A06/MF A01

This report documents an investigation of ditchings and water-related impacts for commuter-category aircraft that occurred during the years 1979 through 1989. The main source of accident data was the National Transportation Safety Board (NTSB). Data were also sought from the International Civil Aviation Organization and the U.S. Navy Safety Center. A total of 46 accidents was obtained and examined for this study. Of these, 40 cases satisfied the criteria for inclusion into the database. Impact and post-impact conditions were categorized to assess aircraft behavior and occupant survivability. Two impact scenarios and two post-impact scenarios were established. Special emphasis was placed on examining aircraft flotation behavior and post-impact survivability. In addition, five representative case studies are presented to demonstrate aspects peculiar to the commuter-category aircraft water impact and post-impact sequence that could not be adequately covered by the statistical categorizations alone. DTIC

N95-20706*# National Aeronautics and Space Administration. Langley Research Center, Hampton, VA. WHY DO AIRLINES WANT AND USE THRUST REVERSERS? A COMPILATION OF AIRLINE INDUSTRY RESPONSES TO

A SURVEY REGARDING THE USE OF THRUST REVERSERS ON COMMERCIAL TRANSPORT AIRPLANES
JEFFREY A. YETTER Jan. 1995 65 p
(Contract(s)/Grant(s): RTOP 538-05-13-01)
(NASA-TM-109158; NAS 1.15:109158) Avail: CASI HC A04/MF A01

Although thrust reversers are used for only a fraction of the airplane operating time, their impact on nacelle design, weight, airplane cruise performance, and overall airplane operating and maintenance expenses is significant. Why then do the airlines want and use thrust reversers? In an effort to understand the airlines need for thrust reversers, a survey of the airline industry was made to determine why and under what situations thrust reversers are currently used or thought to be needed. The survey was intended to help establish the cost/benefits trades for the use of thrust reversers and airline opinion regarding alternative deceleration devices. A compilation and summary of the responses given to the survey questionnaire is presented. Author

N95-21518# Eagle Ventures, Rockville, MD. INDEPENDENT REVIEW OF AVIATION TECHNOLOGY AND RESEARCH INFORMATION ANALYSIS SYSTEM (ATRIAS) DATABASE Final Report

RONALD J. LOFARO, L. HITCHCOCK, S. L. BOGGS, and J. E. MATESKI Feb. 1994 92 p

(Contract(s)/Grant(s): DTFA01-93-P-02265)

(AD-A284049; DOT/FAA/CT-94/12) Avail: CASI HC A05/MF A01

This technical report presents the findings of a critical review of the Aviation Technology and Research Information Analysis System (ATRIAS) for its capability to support the Federal Aviation Administration (FAA)/Aviation Security Research and Development Service's (ACA) Explosive Detection Systems (EDS) programs and Aviation Security Human Factors Program (ASHFP). This review was conducted by an independent consultant selected by the FAA. Section 1 of the report gives a descriptive overview of the ATRIAS analysis and reporting system. The findings of the independent review are contained in sections 2 and 3 of the report. Overall, ATRIAS was found to address many technology application areas relevant to the FAA's aviation security programs. However, the findings did recommend specific modifications to ATRIAS that will provide enhanced information collection and analysis for six topic areas of prime relevance to the FAA's EDS and ASHFP programs. DTIC

N95-21831# Hughes STX, Inc., Lexington, MA. RADAR STUDIES OF AVIATION HAZARDS

F. I. HARRIS, RALPH S. DONALDSON, JR., DAVID J. SMALLEY, and SHU-LIN TUNG 31 May 1994 94 p

(Contract(s)/Grant(s): F19628-93-C-0054)

(AD-A285845; PL-TR-94-2146; SR-1) Avail: CASI HC A05/MF A01

During the first year of this contract, research was directed toward the development of new techniques to monitor and forecast weather related aviation hazards with Doppler weather radar. Focus was on the characterization of the structure of severe convective storms and of synoptic scale baroclinic fronts. One aspect that was examined is the detection and quantization of the weak echo region usually seen in severe convective storms. Another has been the search for lightning precursors. Finally, considerable effort has been expended on the automated depiction of the wind and precipitation structure associated with baroclinic fronts. DTIC

N95-22318# Federal Aviation Administration, Atlanta, GA. FUSELAGE BURNTHROUGH FROM LARGE EXTERIOR FUEL FIRES Final Report

HARRY WEBSTER Jul. 1994 128 p

(AD-A286295; DOT/FAA/CT-90-10) Avail: CASI HC A07/MF A02

The burnthrough resistance of aircraft fuselages to external fuel fire was investigated in this test series. Three tests were conducted in a wheels-up mode and three in the wheels-down configuration. A comprehensive data base was developed documenting fire entry paths, burnthrough time, and cabin environmental

conditions. The overall resistance of the two test intact aircraft fuselages to fire penetration was documented. DTIC

N95-22319# Galaxy Scientific Corp., Pleasantville, NJ.
TEST AND EVALUATION PLAN (TEP) FOR IMPROVISED EXPLOSIVE DEVICE SCREENING SYSTEMS (IEDSS)
 JAMES L. FOBES, RONALD J. LOFARO, ROBERT L. MALONE, DOUGLAS S. FISCHER, and JACK BERKOWITZ 14 Aug. 1994
 54 p

(Contract(s)/Grant(s): DTFA03-89-C-00043)
 (AD-A286382; DOT/FAA/CT-94/87) Avail: CASI HC A04/MF A01
 This document is the Operational Test and Evaluation Plan (OT&E) to evaluate the effectiveness of X-ray baggage screening equipment for Improvised Explosive Devices (IED's) in cluttered baggage. The Improvised Explosive Device Screening Systems (IEDSS) to be tested during the OT&E consist of standard (black and white) and enhanced (color) display X ray equipment and their operators. The X ray equipment will be used to scan for simulated IEDs in both checked (C) and carry-on (CO) cluttered baggage. The OT&E will be conducted at San Francisco International Airport (SFO). The results will be analyzed and become part of a later document. DTIC

N95-22352# Hughes Associates, Inc., Columbia, MD.
ANALYSIS OF TEST CRITERIA FOR SPECIFYING FOAM FIREFIGHTING AGENTS FOR AIRCRAFT RESCUE AND FIREFIGHTING Final Report
 JOSEPH L. SCHEFFEY and JOSEPH A. WRIGHT Aug. 1994
 96 p Sponsored by FAA
 (AD-A286381; DOT/FAA/CT-94/04) Avail: CASI HC A05/MF A01

Foam agent quantities and application rates for FAA certified airports are based on large-scale fire test data of Aqueous Film-Forming Foam (AFFF) and protein-based foams. The philosophy is to control aircraft fuel fires in sixty seconds. Foam agents which are used for aviation applications should demonstrate this level of performance, including a safety factor which assures adequate performance under less than optimum conditions. A review of standard test methods and performance criteria indicates a wide range of requirements. The U.S. Military Specification (MIL SPEC) for AFFF, on which the original agent criteria was developed, is the most stringent in terms of extinguishment application density. However, no direct correlation has been demonstrated between many of the required physical/chemical properties tests and fire extinguishment/burnback performance. It was demonstrated, using comparative data from numerous small and large-scale fire tests, that the small-scale MIL SPEC fire tests correlate with large-scale test results. MIL SPEC agents, which provide a safety factor over minimum FAA requirements, also are formulated to have proportioning, storage, stability, and shelf-life attributes appropriate for crash rescue firefighting applications. Adoption of the MIL SPEC for AFFF agents is recommended. Future work related to foam testing should focus on the use of first principles to establish fundamental foam extinguishment mechanisms. DTIC

N95-22417# Naval Postgraduate School, Monterey, CA.
FORECASTING AIRCRAFT MISHAPS USING MONTHLY MAINTENANCE REPORTS M.S. Thesis
 JOHN S. VANHOUTEN Sep. 1994 73 p
 (AD-A286049) Avail: CASI HC A04/MF A01

Naval Aviation aircraft mishaps continue to be of great concern due to the high cost of loss of life and aircraft. The goal of this thesis is to develop a predictive statistical model that accurately forecasts Marine Corps AV-8B Harrier aircraft mishaps based on existing monthly maintenance reports. Monthly maintenance reports provide numerous independent variables based on personnel levels and maintenance hours that could possibly be used to forecast aircraft mishaps. These variables were graphically analyzed to determine any relationships that could be exploited in developing the model. Higher order relationships were investigated by the method of principal components and logistic regression. After a thorough

analysis, there appears to be no combination of variables in this particular data that could be used to forecast aircraft mishaps. The overall result of the thesis is that there is no relationship between monthly maintenance reports and aircraft mishaps that can be exploited to develop a predictive statistical model. DTIC

04

AIRCRAFT COMMUNICATIONS AND NAVIGATION

Includes digital and voice communication with aircraft; air navigation systems (satellite and ground based); and air traffic control.

A95-70671
COMMENTS ON 'CORRECTION OF INERTIAL NAVIGATION WITH LORAN C ON NOAA'S P-3 AIRCRAFT'
 BARRIE W. LEACH Institute for Aerospace Research, Ottawa, Ontario, Canada and J. IAN MACPHERSON Institute for Aerospace Research, Ottawa, Ontario, Canada Journal of Atmospheric and Oceanic Technology (ISSN 0739-0572) vol. 11, no. 4, pt. 1 August 1994 p. 1048-1053
 (HTN-95-70149) Copyright

A recent paper by Masters and Leise that addresses the problem of correcting inertial navigation data using Loran C describes another variation on the traditional approach that has been used by researchers in the airborne science community for many years. Somewhat disturbing are several inaccurate statements in their paper concerning possible problems in the use of modern Kalman filtering-smoothing techniques in this context. This correspondence attempts to clarify some of the misconceptions and errors expressed in their paper, based on the authors' own positive experiences with applying Kalman filter-smoother algorithms to correct inertial navigation data being supplied by a modern strapdown navigation system. Author (Hermer)

A95-72885
COMMENTS ON EFFECT OF WET SNOW ON THE NULL-REFERENCE ILS SYSTEM
 ALFRED R. LOPEZ ARL Associates Inc, Commack, NY, United States IEEE Transactions on Aerospace and Electronic Systems (ISSN 0018-9251) vol. 30, no. 4 October 1994 p. 1086-1090 refs
 (BTN-95-EIX95142555488) Copyright

The subject paper has raised some issues regarding the probability of the Instrument Landing System (ILS) radiating out-of-tolerance vertical guidance signals. An independent study has substantiated the findings of that paper and adds further concern regarding some FAA ILS snow procedures. The principal conclusions of this paper are: (1) an analysis, based on Walton's discovery of rare snow conditions that cause the null-reference ILS antenna image to disappear, indicates that these conditions can cause out-of-tolerance guidance signals; (2) operation without a monitor of the image radiation can result in signal-in-space guidance signal errors that are significantly beyond the intended limit values; and (3) the integrity of image glide path equipment in snow environments does not satisfy the ILS integrity requirements. Author (EI)

A95-72888
PRECISE NAVIGATION USING ADAPTIVE FIR FILTERING AND TIME DOMAIN SPECTRAL ESTIMATION
 JOE M. TOTH, RALPH MASON, and KEN J. RUNTZ IEEE Transactions on Aerospace and Electronic Systems (ISSN 0018-9251) vol. 30, no. 4 October 1994 p. 1071-1076 refs
 (BTN-95-EIX95142555485) Copyright

This paper introduces a new low cost, short range, positioning system based on adaptive finite impulse response (FIR) filtering and time domain spectral estimation. The system can determine absolute positions with a high degree of accuracy and is well suited for

04 AIRCRAFT COMMUNICATIONS AND NAVIGATION

real time navigation. The approach is based upon signal processing techniques and a priori knowledge of the system transfer function. The first step is to measure the phase response of the linear transfer function and then using a FIR filter the time response of the system can be determined. The FIR filter computes the time response by performing a deconvolution between the measured phase response, and the complex conjugate of the transfer function. By correlating the known input impulse response with the output of the FIR filter, an error term is generated. The time delay of the system is determined by adjusting the FIR filter coefficients to minimize the error term. Simulated analysis of the system indicates a worst case error of +/- 16 cm. Author (EI)

A95-72891

ATTITUDE DETERMINATION USING DEDICATED AND NONDEDICATED MULTIANTENA GPS SENSORS

G. LU, M. E. CANNON, G. LACHAPPELLE, and P. KIELLAND IEEE Transactions on Aerospace and Electronic Systems (ISSN 0018-9251) vol. 30, no. 4 October 1994 p. 1053-1059 refs (BTN-95-EIX95142555482) Copyright

We show that the use of nondedicated Global Positioning System (GPS) sensors to determine the attitude parameters of a vessel yields the same level of performance as the use of a dedicated multiantenna receiver, namely an agreement of the order of 0.1 deg (1 sigma). The test platform is a survey launch operating at cruising speeds of 10 to 15 kt. The dedicated multiantenna receiver is a four-antenna Ashtech 3DF unit, while the nondedicated sensor array consists of three NovAtel GPSCard(sup TM) receivers. The approach used to resolve the relative carrier phase integer ambiguities between the antennas is discussed and the use of antenna baseline constraints is analyzed. A least-squares procedure which utilizes all the position information from the antennas for the estimation of the attitude parameters and their accuracy is presented. The attitude determination results from the two configurations tested are intercompared. Author (EI)

N95-19950*# McDonnell-Douglas Aerospace, Long Beach, CA. CREW AIDING AND AUTOMATION: A SYSTEM CONCEPT FOR TERMINAL AREA OPERATIONS, AND GUIDELINES FOR AUTOMATION DESIGN Final Report

JOHN P. DWYER Dec. 1994 216 p (Contract(s)/Grant(s): NAS1-18028; RTOP 505-64-13-22) (NASA-CR-4631; NAS 1.26:4631; CRAD-9206-TR-8940) Avail: CASI HC A10/MF A03

This research and development program comprised two efforts: the development of guidelines for the design of automated systems, with particular emphasis on automation design that takes advantage of contextual information, and the concept-level design of a crew aiding system, the Terminal Area Navigation Decision Aiding Mediator (TANDAM). This concept outlines a system capable of organizing navigation and communication information and assisting the crew in executing the operations required in descent and approach. In service of this endeavor, problem definition activities were conducted that identified terminal area navigation and operational familiarization exercises addressing the terminal area navigation problem. Both airborne and ground-based (ATC) elements of aircraft control were extensively researched. The TANDAM system concept was then specified, and the crew interface and associated systems described. Additionally, three descent and approach scenarios were devised in order to illustrate the principal functions of the TANDAM system concept in relation to the crew, the aircraft, and ATC. A plan for the evaluation of the TANDAM system was established. The guidelines were developed based on reviews of relevant literature, and on experience gained in the design effort. Author

N95-20195# Sandia National Labs., Albuquerque, NM. SAR IMAGE REGISTRATION IN ABSOLUTE COORDINATES USING GPS CARRIER PHASE POSITION AND VELOCITY INFORMATION

S. BURGETT and M. MEINDL 1994 5 p Presented at the

International Symposium on Kinematic Systems in Geodesy, Geomatics, and Navigation, Banff, Alberta, 30 Aug. - 2 Sep. 1994 (Contract(s)/Grant(s): DE-AC04-94AL-85000) (DE94-018738; SAND-94-1417C; CONF-9408163-1) Avail: CASI HC A01/MF A01

It is useful in a variety of military and commercial application to accurately register the position of synthetic aperture radar (SAR) imagery in absolute coordinates. The two basic SAR measurements, range and Doppler, can be used to solve for the position of the SAR image. Imprecise knowledge of the SAR collection platform's position and velocity vectors introduce errors in the range and Doppler measurements and can cause the apparent location of the SAR image on the ground to be in error by tens of meters. Recent advances in carrier phase GPS techniques can provide an accurate description of the collection vehicle's trajectory during the image formation process. In this paper, highly accurate carrier phase GPS trajectory information is used in conjunction with SAR imagery to demonstrate a technique for accurate registration of SAR images in WGS-84 coordinates. Flight test data will be presented that demonstrates SAR image registration errors of less than 4 meters. DOE

N95-21020 Federal Aviation Administration, Atlantic City, NJ. AN EVALUATION OF AUTOMATIC TERMINAL INFORMATION SERVICE (ATIS) FLIGHT DECK DISPLAY PRESENTATION OPTIONS Technical Report, period ending Dec. 1992

ALBERT REHMANN Mar. 1994 62 p Limited Reproducibility: More than 20% of this document may be affected by microfiche quality (AD-A280100; DOT/FAA/CT-TN93/25) Avail: Issuing Activity (Defense Technical Information Center (DTIC))

This document describes the first of three studies relating to human factors aspects in the flight deck display of Automatic Terminal Information Service (ATIS). This research is being conducted by the Federal Aviation Administration (FAA) Technical Center. The first part-task study examined basic format design variables. Its purpose was to begin addressing flight deck design issues pertinent to the design of the tower ATIS workstation and, collect data relevant to standard and certification groups within the FAA. Future studies in an FAA Technical Center high-fidelity mock-up and various aircraft simulators will examine full mission issues, such as procedures, equipment mechanization, and automation. Avionics data link human factors, Automatic Terminal Information Service (ATIS), Aircraft Communications Addressing and Reporting System (ACARS). DTIC

N95-21148# Federal Aviation Administration, Atlantic City, NJ. MINIMA REDUCTION SIMULATION TEST RESULTS BARRY BILLMANN, EDWARD PUGACZ, and CARL EVERBERG Jul. 1994 73 p (AD-A285626; DOT/FAA/CT-TN92/47) Avail: CASI HC A04/MF A01

This report presents the results of tests conducted in a Beech-200 (B-200) simulator located at the Beech Learning Center in Wichita, Kansas, and operated by Flight-Safety International (FSI). The testing was conducted to examine the feasibility of reducing approach minimums below Category I by utilizing a highly accurate navigation signal, such as the Microwave Landing System (MLS), when standard Category II approach and runway lighting are not available. Results are presented which indicate that properly trained crews using flight director-equipped aircraft can operate to lower approach minima than standard Category I without full Category II approach and runway lighting. Performance in the visual segment and touchdown performance is shown to be equivalent regardless of the availability of touchdown zone or runway centerline lighting. The benefits of a Category II approach lighting system (ALSF-2) are mitigated by the fact that when the aircraft breaks out of weather at the lower decision heights (DH's), i.e., 150 feet above ground level (AGL), most of the approach light system is already behind the aircraft. Recommendations are made for further testing in actual aircraft. DTIC

N95-21369 Eurocontrol Experimental Centre, Bretigny (France).
DATA LINK TERMINAL DLT DOCUMENT
 P. RUAULT and A. PHILIPPART Mar. 1994 164 p
 (P895-110805; EEC/NOTE-12/94) Avail: Issuing Activity (National
 Technical Information Service (NTIS))

This note describes the Mode-S Data Link Terminal (DLT) which was developed and assembled by the EUROCONTROL Experimental Center. The DLT is a simplified Multi purpose Control and Display Unit (MCDU). It replaces the aircraft MCDU in the on-board experimental Mode-S installation. Based on the ARINC characteristic 739 the terminal is connected to the Data Link Processor Unit DLPU-C2 via the ARINC 429 bus. The DLT gives the aircrew access to data bases via the Mode-S data link. NTIS

N95-21520# Sandia National Labs., Albuquerque, NM.
ASSESSMENT OF A NON-DEDICATED GPS RECEIVER SYSTEM FOR PRECISE AIRBORNE ATTITUDE DETERMINATION

M. E. CANNON (Calgary Univ., Alberta.), H. SUN, T. E. OWEN, and M. A. MEINDL 1994 10 p Presented at the Ion-GPS 1994, Salt Lake City, UT, 21 Sep. 1994
 (Contract(s)/Grant(s): DE-AC04-94AL-85000)
 (DE94-019309; SAND-94-1136C; CONF-9409185-2) Avail: CASI HC A02/MF A01

The use of a non-dedicated GPS receiver system for attitude determination was assessed in airborne mode through a test conducted at Sandia National Laboratories. Four independent NovAtel GPSCard(trademark) receivers were installed in Sandia's Twin Engine Otter with two antennas mounted on the fuselage and two on the wing tips at separations of 6 to 18 m. A strapdown INS (Inertial Navigation System) was also on board the aircraft in order to provide an independent attitude reference at rates between 4 and 10 Hz. During the multi-day test, GPS measurements were recorded between 1 and 10 Hz. Carrier phase measurements were post-processed using a double difference approach developed at The University of Calgary in which integer ambiguities were resolved in seconds using the known antenna separations as constraints. The tracking capability of the system is demonstrated under dynamics consisting of roll and pitch angles up to 45 and 12 degrees, respectively. Comparisons between the GPS and INS attitude angles are presented for two of the test days and show agreement at the several arcminute level. Conclusions are made with respect to system accuracy and performance in an operational airborne environment. DOE

N95-21891# California Polytechnic State Univ., San Luis Obispo, CA. Dept. of Aeronautical Engineering.

A REAL-TIME ALGORITHM FOR INTEGRATING DIFFERENTIAL SATELLITE AND INERTIAL NAVIGATION INFORMATION DURING HELICOPTER APPROACH M.S. Thesis

TY HOANG Apr. 1994 67 p
 (Contract(s)/Grant(s): NCC2-775)
 (NASA-CR-197409; NAS 1.26:197409) Avail: CASI HC A04/MF A01

A real-time, high-rate precision navigation Kalman filter algorithm is developed and analyzed. This Navigation algorithm blends various navigation data collected during terminal area approach of an instrumented helicopter. Navigation data collected include helicopter position and velocity from a global position system in differential mode (DGPS) as well as helicopter velocity and attitude from an inertial navigation system (INS). The goal of the Navigation algorithm is to increase the DGPS accuracy while producing navigational data at the 64 Hertz INS update rate. It is important to note that while the data was post flight processed, the Navigation algorithm was designed for real-time analysis. The design of the Navigation algorithm resulted in a nine-state Kalman filter. The Kalman filter's state matrix contains position, velocity, and velocity bias components. The filter updates positional readings with DGPS position, INS velocity, and velocity bias information. In addition, the filter incorporates a sporadic data rejection scheme. This relatively

simple model met and exceeded the ten meter absolute positional requirement. The Navigation algorithm results were compared with truth data derived from a laser tracker. The helicopter flight profile included terminal glideslope angles of 3, 6, and 9 degrees. Two flight segments extracted during each terminal approach were used to evaluate the Navigation algorithm. The first segment recorded small dynamic maneuver in the lateral plane while motion in the vertical plane was recorded by the second segment. The longitudinal, lateral, and vertical averaged positional accuracies for all three glideslope approaches are as follows (mean plus or minus two standard deviations in meters): longitudinal (-0.03 plus or minus 1.41), lateral (-1.29 plus or minus 2.36), and vertical (-0.76 plus or minus 2.05). Author

N95-22161*# Rockwell Space Operations Co., Houston, TX. Flight Design and Dynamics Dept.

THE NAVIGATION TOOLKIT

WILLIAM F. RICH and STEPHEN W. STROM Oct. 1994 7 p
 Presented at OOPSLA 1994, Portland, OR, 23-27 Oct. 1994
 (Contract(s)/Grant(s): NAS9-18000)
 (NASA-CR-197290; NAS 1.26:197290) Avail: CASI HC A02/MF A01

This report summarizes the experience of the authors in managing, designing, and implementing an object-oriented applications framework for orbital navigation analysis for the Flight Design and Dynamics Department of the Rockwell Space Operations Company in Houston, in support of the Mission Operations Directorate of NASA's Johnson Space Center. The 8 person year project spanned 1.5 years and produced 30,000 lines of C++ code, replacing 150,000 lines of Fortran/C. We believe that our experience is important because it represents a 'second project' experience and generated real production-quality code - it was not a pilot. The project successfully demonstrated the use of 'continuous development' or rapid prototyping techniques. Use of formal methods and executable models contributed to the quality of the code. Keys to the success of the project were a strong architectural vision and highly skilled workers. This report focuses on process and methodology, and not on a detailed design description of the product. But the true importance of the object-oriented paradigm is its liberation of the developer to focus on the problem rather than the means used to solve the problem. Author

05

AIRCRAFT DESIGN, TESTING AND PERFORMANCE

Includes aircraft simulation technology.

A95-72569

DESIGN OPTIMIZATION OF ROTOR BLADES FOR IMPROVED PERFORMANCE AND VIBRATION

CYNTHIA B. CALLAHAN McDonnell Douglas Helicopter Co., Mesa, AZ, US and FREDRICH K. STRAUB McDonnell Douglas Helicopter Co., Mesa, AZ, US American Helicopter Society, Journal (ISSN 0002-8711) vol. 38, no. 4 October 1993 p. 62-70 (HTN-95-A0498) Copyright

A multidisciplinary optimization tool for helicopter rotor blade design has been developed which efficiently and effectively determines blade aerodynamic and structural designs for improved performance and reduced fuselage vibrations. The comprehensive analysis code, CAMRAD/JA, forms the analysis core of the program while CONMIN's method of feasible directions provides the optimization algorithm. Blade aerodynamic and structural properties are used as design variables while rotor power required, dynamic hub loads and/or fuselage vibrations may be minimized as the objective function. The present paper describes a comprehensive application of the optimization tool to the McDonnell Douglas Helicopter Company AH-64A helicopter, including the introduction of additional design variables and objective function options. Results are presented for forward flight performance improvement, fuselage vibra-

05 AIRCRAFT DESIGN, TESTING AND PERFORMANCE

tion reduction, and combined performance/vibration optimization. The optimized designs are shown to provide significant improvements in the design objectives. The mechanisms for the improvements and the practical suitability of the designs are evaluated.

Author (Herner)

A95-72571

PREDICTION OF ENERGY ABSORPTION CAPABILITY OF COMPOSITE STIFFENERS

AKIF O. BOLUKBASI McDonnell Douglas Helicopter Co., Mesa, AZ, US and DAVID H. LAANANEN Arizona State Univ., Tempe, AZ, US American Helicopter Society, Journal (ISSN 0002-8711) vol. 38, no. 4 October 1993 p. 80-84

(HTN-95-A0500) Copyright

An analytical methodology for predicting energy absorption capability of composite open-section stiffeners is presented. The methodology is based on composite laminate and elastic stability theories and on nondimensional crippling data. Applications of this methodology to graphite/epoxy channel and hat stiffeners are presented. The graphite/epoxy stiffener designs that were studied utilized ply drop-offs to initiate crushing and to maintain elastic stability. The analytical results for the energy-absorbing capability of the stiffeners are compared with test results. The energy absorption characteristics associated with different laminate designs are identified, and their significance to the design of energy-absorbing stiffeners is discussed.

Author (Herner)

A95-72580* National Aeronautics and Space Administration, Washington, DC.

BUCKLING AND VIBRATION ANALYSIS OF LAMINATED PANELS USING VICONOPT

DAVID KENNEDY Wales Univ. Coll. of Cardiff, Cardiff, UK, FRED W. WILLIAMS Wales Univ. Coll. of Cardiff, Cardiff, UK, and MELVIN S. ANDERSON Old Dominion Univ., Norfolk, VA, US Journal of Aerospace Engineering (ISSN 0893-1321) vol. 7, no. 3 July 1994 p. 245-262 Research sponsored by British Aerospace (Contract(s)/Grant(s): NCCW-2; NAS1-18584)

(PAPER-1746; HTN-95-A0509) Copyright

The analysis aspects of the 23,000-line FORTRAN program VIPASA with constraints and optimization (VICONOPT) are described. Overall stiffness matrices assembled from the earlier exact vibration and instability of plate assemblies including shear and anisotropy (VIPASA) flat plate stiffnesses are optionally coupled by Langrangian multipliers to find critical buckling loads, or natural frequencies of undamped vibration, of prismatic assemblies of anisotropic flat plates with arbitrarily located point supports or simple transverse supporting frames. The longitudinal continuity of typical wing and fuselage panels is closely approximated because the solutions are for the infinitely long structure obtained by repeating a bay and its supports longitudinally. Any longitudinally invariant in-plane plate stresses are permitted, and very rapid solutions are guaranteed by numerous refinements, including multilevel substructuring and a method for repetitive cross sections that is exact for regular polygons used to represent cylinders. Modal displacements and stresses in or between plies of laminated plates are calculated and plotted, with values being recovered at all nodes of substructures. Comparison with usual approximate finite-element methods confirms that, for comparably converged solutions, VICONOPT is typically between 100 and 10(exp 4) times faster.

Author (Herner)

A95-72585

NEW AIRFOIL-DESIGN CONCEPT WITH IMPROVED AERODYNAMIC CHARACTERISTICS

DEMETER G. FERTIS Akron Univ., Akron, OH, US Journal of Aerospace Engineering (ISSN 0893-1321) vol. 7, no. 3 July 1994 p. 328-339

(PAPER-4384; HTN-95-A0514) Copyright

The research in this paper is the result of an experimental study regarding a new airfoil-design concept, which is developed to produce greater lift coefficients over a much broader range of

operational angles of attack, to improve or eliminate stall at virtually all operational airspeeds, to increase functional lift-to-drag ratios over a greater range of operational angles of attack, and to be adaptable for aircraft of both the fixed-wing and the rotary-wing types. The writer has combined his effort with L. L. Smith, and a U.S. Patent, entitled 'Airfoil', Patent No. 4,606,519, was obtained on August 19, 1986. Patents were also obtained or are pending in other countries. The experimental results, obtained by using the new airfoil-design concept, have been compared with experimental results obtained from a conventional NACA 23012 airfoil. Flight performance tests by using a 2.134-m (7.0 ft) model and remote-control devices, as well as flow-separation studies, were also performed. The results were compared with the ones obtained by using the NACA 23012 airfoil.

Author (Herner)

N95-19963# Defence Science and Technology Organization, Melbourne (Australia). Aeronautical and Maritime Research Lab. VARIATIONS OBSERVED IN THE AC GENERATOR SIGNAL PERIOD OF A SEA KING HELICOPTER

D. M. BLUNT Jun. 1994 25 p

(AD-A284280; DSTO-GD-0004; DODA-AR-008-545) Avail: CASI HC A03/MF A01

The AC generator in the Sea King helicopter can be used as a convenient source of a tachometer signal from the main rotor gearbox, thus enabling synchronous vibration signal averages to be calculated for every shaft in the gearbox. The signal averaging software developed by ARL determines the shaft speeds by measuring the tachometer signal period. Variations in the tachometer signal period not caused by changes in gearbox speed will affect the accuracy of the vibration signal averages. An examination has been made of the AC generator signal of a Sea King helicopter recorded on a Bruel & Kjaer 4 channel FM tape recorder (model 7003). The results show that the signal averaging software measures short term period variations (from one period to the next) in the AC generator signal of up to approximately 2% of the mean period. It was found that while most of this variation probably arises from noise present in the recording environment, a considerable proportion comes from noise introduced through the tape recording and filtering processes.

DTIC

N95-19994* National Aeronautics and Space Administration. Hugh L. Dryden Flight Research Center, Edwards, CA.

F-15 RESOURCE TAPE (Videotape) 1994

Videotape: 9 min. 25 sec. playing time, in color, with sound (NASA-TM-110502; NONP-NASA-VT-95-41114) Avail: CASI VHS A02/BETA A22

An F-15 fighter aircraft is portrayed in resource video. A flight test is shown with take-off, touch and go landings, some flight maneuvers, and pilot to control tower communication with references to drag vectors.

CASI

N95-20155* National Aeronautics and Space Administration. Hugh L. Dryden Flight Research Center, Edwards, CA.

ACOUSTIC CLIMB TO CRUISE TEST (Videotape)

27 Nov. 1991 Videotape: 9 min. 30 sec. playing time, in color, with sound (NASA-TM-110504; NONP-NASA-VT-95-41116) Avail: CASI VHS A02/BETA A22

Flight test film footage of three different aircraft testing the acoustical noise levels during take-off, climb, maneuvers, and touch and go landings are described. These sound tests were conducted on two fighter aircraft and one cargo aircraft. Results from mobile test vehicle are shown.

DFRC

N95-20181 Naval War Coll., Newport, RI. Dept. of Operations. **BOMBER FORCE 2000: OPERATIONAL CONCEPTS FOR LONG-RANGE COMBAT AIRCRAFT Final Report**

JEFFREY K. BEENE 8 Feb. 1994 61 p Limited Reproducibility: More than 20% of this document may be affected by microfiche quality

(AD-A279378) Avail: Issuing Activity (Defense Technical Informa-

tion Center (DTIC)

This research paper seeks to synthesize analyses of air power theory and doctrine, historical insights from major operations, current thinking, and the emerging strategic environment to detail concepts for improved planning and execution of future air operations. These operations would fully integrate bombers as long-range combat aviation assets. The search for a type of aircraft to fit the doctrine derived from early interpretations of air power theory has hindered development of bomber potential. The use of atomic weapons at the end of World War 2 and the ensuing Cold War further obscured understanding of bombers, their real contribution hinging on viewing them as long-range combat aircraft. Today, the bomber is not obsolete, but its traditional nuclear paradigm is. The emergence of regional threats combined with a shrinking defense establishment and the global compression of time and space demand full integration of bomber aircraft into the U.S. air power arsenal. These aircraft provide a theater commander with a unique capability to respond rapidly across the spectrum of conflict from a peacetime show of force to major nuclear or nonnuclear conflict. However, for the operational commander to employ bomber assets effectively requires a full recognition of bomber attributes and a thorough understanding of their capabilities. DTIC

N95-20212# General Accounting Office, Washington, DC. National Security and International Affairs Div.

NAVAL AVIATION: F-14 UPGRADES ARE NOT ADEQUATELY JUSTIFIED. REPORT TO CONGRESSIONAL COMMITTEES

Oct. 1994 12 p

(AD-A286338; GAO/NSIAD-95-12; B-257718) Avail: CASI HC A03/MF A01; GAO, PO Box 6015, Gaithersburg, MD 20884-6015 HC

The implications of the Navy's decision to spend about \$2.5 billion between fiscal years 1994 and 2003 for a limited ground attack upgrade and other modifications to about 200 F-14 Tomcat fighters was evaluated. This upgrade was included to add limited ground attack capability and other improvements to 210 F-14 Tomcat fighter aircraft. According to the Navy, the ground attack capabilities were required to partially compensate for the loss in combat capabilities during the period starting in 1997, when all of its A-6E Intruder attack aircraft are scheduled to be retired, to the turn of the century when the F/A-18E/F, the next generation strike fighter, is scheduled to arrive. Although the Navy justified F-14 attack upgrades as necessary to replace some capability that will be lost when it retires all A-6E attack aircraft by fiscal year 1998, planned upgrades will not include an air-to-ground radar for precision ground mapping that would permit crews to locate, identify, and attack targets in adverse weather and poor visibility. In addition, no F-14 will be able to launch current or planned precision munitions or stand-off weapons, except for LGBs. Upgraded F-14's generally have greater range than the F/A-18C and could possibly reach targets beyond the Hornet's range. However, this capability may not be needed with the Navy's shift to a littoral warfare strategy. If greater range is needed, the Navy's Tomahawk cruise missile can attack targets up to a range of about 700 miles, and Air Force bombers have even greater range. Both supplement and complement carrier aviation in striking deep within enemy territory. The Navy has not made a compelling case to proceed with its \$2.5 billion plan. DTIC

N95-20329 Department of Defense, Washington, DC.

UNMANNED AERIAL VEHICLES

31 May 1994 135 p Limited Reproducibility: More than 20% of this document may be affected by microfiche quality

(AD-A286190) Avail: CASI HC A07

The Unmanned Aerial Vehicle (UAV) Joint Project Office was officially established in response to Congressional direction by a charter signed by the Director of Defense Research and Engineering on 16 October 1989. This master plan is structured into three parts: an executive summary; a main body providing extensive detail on management, supporting the user, programs, commonality and interoperability, technology, analysis and simulation, integrated logistics support, training, human systems integration, test and

evaluation, international programs, and resources; and an appendix of supporting material including discussions of dual uses of UAV's and UAV civil airspace management issues. CASI

N95-20370*# National Aeronautics and Space Administration. Langley Research Center, Hampton, VA.

PARALLEL CALCULATION OF SENSITIVITY DERIVATIVES FOR AIRCRAFT DESIGN USING AUTOMATIC DIFFERENTIATION

C. H. BISCHOF (Argonne National Lab., IL.), T. L. KNAUFF, JR. (Argonne National Lab., IL.), L. L. GREEN, and K. J. HAIGLER Jan. 1994 24 p Presented at the 5th AIAA/NASA/USAF/SSMO Symposium on Multidisciplinary Analysis and Optimization Conference, Panama City, FL, 7-9 Sep. 1994

(Contract(s)/Grant(s): W-31-109-ENG-38)

(NASA-TM-110103; NAS 1.15:110103; DE94-016894; ANL/MCS/CP-82870; CONF-9409187-1) Avail: CASI HC A03/MF A01

Realistic multidisciplinary design optimization (MDO) of advanced aircraft using state-of-the-art computers is an extremely challenging problem from both the physical modelling and computer science points of view. In order to produce an efficient aircraft design, many trade-offs must be made among the various physical design variables. Similarly, in order to produce an efficient design scheme, many trade-offs must be made among the various MDO implementation options. In this paper, we examine the effects of vectorization and coarse-grained parallelization on the SD calculation using a representative example taken from a transonic transport design problem. DOE

N95-20466 Naval Test Pilot School, Patuxent River, MD. **T-45A HIGH ANGLE OF ATTACK TESTING: US NAVAL TEST PILOT SCHOOL 46TH ANNUAL REUNION AND SYMPOSIUM**

MAX ROGERS and PATRICK PERUSSE 29 Apr. 1994 17 p Symposium was held Limited Reproducibility: More than 20% of this document may be affected by microfiche quality (AD-A284000) Avail: CASI HC A03

The Symposium provides a forum for the evaluation of high angle of attack (haoa) flying qualities and propulsion system characteristics. Its purpose is to also determine the suitability of T-45A aircraft to perform air combat maneuvering and out-of-control flight training missions. Derived from text

N95-20772# Kaman Sciences Corp., Albuquerque, NM. **TIM-SCT CABLE TESTING PROTOCOL Final Report, 24 Aug. 1992 - 24 Aug. 1993**

KURT H. COONROD, KARL R. JURISSON, J. T. HENDRICKSON, and DONALD P. MCLEMORE Sep. 1994 40 p (Contract(s)/Grant(s): F29601-92-C-0109) (AD-A286633; PL-TR-93-1110) Avail: CASI HC A03/MF A01

This document presents a standardized approach for measuring transfer impedance of shielded aircraft cables in-situ. The approach is based on the present Shielded Cable Tester (SCT) and Transfer Impedance Meter (TIM) instruments. DTIC

N95-20860# Technische Hochschule, Aachen (Germany). Inst. fuer Mechanik.

PREDICTION OF ROTOR-BLADE DEFORMATIONS DUE TO UNSTEADY AIRLOADS Interim Report No. 2

STEFAN SCHLECHTRIEM and JOSEF BALLMANN 31 Jul. 1994 5 p

(Contract(s)/Grant(s): N68171-94-C-9068)

(AD-A286593; R/D-7213-AN-01) Avail: CASI HC A01/MF A01

SOFIA, a computer code for aeroelastic computations, was applied to predict the rotor blade deformations due to unsteady airloads caused by BVI and to investigate appropriate control movements to minimize vibration and noise. The computation of the unsteady, compressible, inviscid flow about rotor-blades uses an Euler CFD code, while a quasi one-dimensional structural solver is used to compute the deformation of the rotor blades. DTIC

05 AIRCRAFT DESIGN, TESTING AND PERFORMANCE

N95-21186* National Aeronautics and Space Administration. Ames Research Center, Moffett Field, CA.
SIMULATION OF ROTOR BLADE ELEMENT TURBULENCE
R. E. MCFARLAND and KEN DUISENBERG (Systems Consultants, Inc., Falls Church, VA.) Jan. 1995 17 p
(Contract(s)/Grant(s): RTOP 505-64-29)
(NASA-TM-108862; A-95028; NAS 1.15:108862) Avail: CASI HC A03/MF A01

A piloted, motion-based simulation of Sikorsky's Black Hawk helicopter was used as a platform for the investigation of rotorcraft responses to vertical turbulence. By using an innovative temporal and geometrical distribution algorithm that preserved the statistical characteristics of the turbulence over the rotor disc, stochastic velocity components were applied at each of twenty blade-element stations. This model was implemented on NASA Ames' Vertical Motion Simulator (VMS), and ten test pilots were used to establish that the model created realistic cues. The objectives of this research included the establishment of a simulation-technology basis for future investigation into real-time turbulence modeling. This goal was achieved; our extensive additions to the rotor model added less than a 10 percent computational overhead. Using a VAX 9000 computer the entire simulation required a cycle time of less than 12 msec. Pilot opinion during this simulation was generally quite favorable. For low speed flight the consensus was that SORBET (acronym for title) was better than the conventional body-fixed model, which was used for comparison purposes, and was determined to be too violent (like a washboard). For high speed flight the pilots could not identify differences between these models. These opinions were something of a surprise because only the vertical turbulence component on the rotor system was implemented in SORBET. Because of the finite-element distribution of the inputs, induced outputs were observed in all translational and rotational axes. Extensive post-simulation spectral analyses of the SORBET model suggest that proper rotorcraft turbulence modeling requires that vertical atmospheric disturbances not be superimposed at the vehicle center of gravity but, rather, be input into the rotor system, where the rotor-to-body transfer function severely attenuates high frequency rotorcraft responses. Author

N95-21425 National Physical Lab., Teddington (England). Div. of Radiation Science and Acoustics.
EFFECT OF ATMOSPHERIC PRESSURE ON MEASURED AIRCRAFT NOISE LEVELS
R. C. PAYNE Mar. 1994 58 p
(PB95-130423; NPL-RSA(EXT)0048) Copyright Avail: Issuing Activity (National Technical Information Service (NTIS))

Noise certification of subsonic jet airplanes, heavy propeller-driven airplane and helicopters is carried out using the procedures described in the International Civil Aviation Organization (ICAO) document Annex 16. Measured noise levels are corrected to reference atmospheric conditions to allow for differences in air attenuation resulting from variations in ambient temperature and relative humidity. The attenuation is calculated using the Society of Automotive Engineers standard ARP 866A. The procedure does not include the effect of ambient atmospheric pressure. The report discusses the influence of atmospheric pressure on the attenuation of sound transmitted to the ground during noise certification tests carried out using airfields at altitude. ARP 866A and three alternative procedures that include the effect of atmospheric pressure are assessed, and calculations are made of air attenuation rates based on reference atmospheric pressure and pressures that are representative of those that occur at airfields located at altitudes of up to 10000 feet (3048 m). Comparison of these attenuation rates shows differences that are dependent on temperature, relative humidity, frequency and altitude. The effect of these differences on EPNL evaluation is difficult to assess as it is dependent not only on meteorological conditions, but also on spectral shape and propagation distance. NTIS

N95-21730* Sandia National Labs., Albuquerque, NM.
A USER'S GUIDE TO LUGSAN 1.1: A COMPUTER

PROGRAM TO CALCULATE AND ARCHIVE LUG AND SWAY BRACE LOADS FOR AIRCRAFT-CARRIED STORES
W. N. DUNN Jul. 1994 202 p
(Contract(s)/Grant(s): DE-AC04-94AL-85000)
(DE95-001919; SAND-94-1826) Avail: CASI HC A10/MF A03

LUGSAN (LUG and Sway brace ANalysis) is an analysis and database computer program designed to calculate store lug and sway brace loads from aircraft captive carriage. LUGSAN combines the rigid body dynamics code, SWAY85 and the maneuver calculation code, MILGEN, with an INGRES database to function both as an analysis and archival system. This report describes the operation of the LUGSAN application program, including function description, layout examples, and sample sessions. This report is intended to be a user's manual for version 1.1 of LUGSAN operating on the VAX/VMS system. The report is not intended to be a programmer or developer's manual. DOE

N95-22039 Naval Postgraduate School, Monterey, CA.
EFFECT OF JUNCTURE FILLETS ON DOUBLE-DELTA WINGS UNDERGOING SIDESLIP AT HIGH ANGLES OF ATTACK M.S. Thesis
WEN-HUAN CHANG Sep. 1994 216 p Limited Reproducibility: More than 20% of this document may be affected by microfiche quality
(AD-A286165) Avail: CASI HC A10

A flow visualization study of the vortical flow over a baseline double-delta wing model and a diamond-fillet double-delta wing model both with sharp leading edges was conducted in the Naval Postgraduate School water tunnel using the dye-injection technique. The main focus of this study was to observe the effect of juncture fillet on the vortex core trajectory, and vortex burst location on the wing surface at high angles of attack with sideslip angles. The results indicate that the strake vortex burst point moves upstream with increasing angle of attack at zero sideslip angle; but at constant angle of attack the windward side strake vortex burst location moves upstream and inboard while the leeward side vortex burst point moves downstream and outboard with increasing sideslip angle. Comparison of test results between the baseline model and the diamond-fillet model indicates a clear delay for the latter model in terms of both vortex core trajectory and breakdown location at high angles of attack with and without sideslip angle. The vortex breakdown data for the diamond-fillet model implies lift augmentation during sideslip motion, thus supporting the concept of flow control using fillets. DTIC

06

AIRCRAFT INSTRUMENTATION

Includes cockpit and cabin display devices; and flight instruments.

N95-20032* Federal Aviation Administration, Atlantic City, NJ.
INVESTIGATION OF FLIGHT DATA RECORDER FIRE TEST REQUIREMENTS
LAWRENCE J. CURRAN, JR. Oct. 1994 27 p
(AD-A285832; DOT/FAA/CT-TN94/23) Avail: CASI HC A03/MF A01

This report evaluates fire test methodologies for aircraft flight data and cockpit voice recorders. The current fire test requirement consists of a 30-minute exposure to a propane burner calibrated to the heating conditions created by a jet fuel fire. A comparison was made of the internal temperature of flight recorder models subjected to the propane burner standard and a jet fuel fire. The internal temperature was approximately 40 percent higher during the fuel fire tests which were 6-8 minutes in duration. Although the fuel fire duration was limited, it appears that a 60-minute propane burner test exposure is a feasible and conservative means of evaluating the thermal resistance of a flight recorder subjected to a 30-minute fuel fire. An additional fire test condition (500 F/10 hours) has been proposed to simulate a smoldering fire which may persist for a long

period of time at a remote site. A state-of-the-art magnetic tape of the cockpit voice recorder was subjected to this condition in an oven and failed the test, demonstrating the severity of this exposure environment. DTIC

N95-20631# Advisory Group for Aerospace Research and Development, Neuilly-Sur-Seine (France). Avionics Panel.
ADVANCED PACKAGING CONCEPTS FOR DIGITAL AVIONICS [LES TECHNIQUES AVANCEES DE MISE SOUS BOITIER]
 Oct. 1994 287 p In ENGLISH and FRENCH Symposium held in San Diego, CA, 6-9 Jun. 1994
 (AGARD-CP-562; ISBN-92-836-0004-5) Copyright Avail: CASI HC A13/MF A03

A critical impediment to significantly improving the performance of digital airborne electronics or avionics is the limitation posed by current electronics packaging concepts. This symposium brought together experts from seemingly diverse, but interlocking disciplines ranging from logisticians to digital designers to mechanical engineers to establish the current baseline in digital packaging, failure modes of the electronics and support problems. Trends in both supportability and processing were described for early 21st century application. Along with the projections of asymptotic increase in signal, image and data processing, dramatic increases in thermal densities, chip interconnects, correctors and backplane traffic were described. For individual titles, see N95-20632 through N95-20659.

N95-20632# Wright Lab., Wright-Patterson AFB, OH. Avionics Directorate.
THE IMPACT OF ADVANCED PACKAGING TECHNOLOGY ON MODULAR AVIONICS ARCHITECTURES
 REED MORGAN and JOHN OSTGAARD In AGARD, Advanced Packaging Concepts for Digital Avionics 12 p Oct. 1994
 Copyright Avail: CASI HC A03/MF A03

This paper explores how advances in digital packaging will impact network requirements at the system level. Two main issues connected with modular digital packaging for avionics were investigated: (1) Can conventional electrical designs continue to handle the information network speed and wirability requirements needed at the backplane to efficiently utilize advanced modular data and signal processors? (2) Considering projected network requirements for future sensors, displays, etc., (which are made possible because of digital packaging advances), what type of system architecture will be needed? The paper concludes that: (1) Beyond the module (PCB) interface, a new type of backplane implementation will eventually be needed to support the flexibility and growth needs of modular processing. Several new approaches other than a passive electrical backplane could be employed; however, a switched, photonic-based approach is proposed for information distribution between digital processing modules as well as for interconnection between peripherals. Digital packaging advances will result in I/O speeds of about 2 Gigabits/sec, and (2) advanced integrated RF and EO sensors and display technologies will require network data rates in the range of 2 Gigabits/sec in order to communicate in real time with the high speed signal and graphics processor modules in the common integrated processor racks. Many of these 'peripheral' functions will require virtual point-point links because continuous, streaming data is involved. This resulting system architecture recommended is a switched optical network which interconnects sources and sinks of information to the modular processing assets, as well as providing a network for intermodule intercommunication within the rack. Issues of protocol control of this network remain. Further, several advances in photonic packaging and connectors will be required to make this new architectural approach a reality. Although photonics offers the best long-range solution, significant technology difficulties must be overcome. Author

N95-20633# Naval Air Warfare Center, Indianapolis, IN. Aircraft Div.
STANDARD HARDWARE ACQUISITION AND RELIABILITY PROGRAM (SHARP) ADVANCED SEM-E PACKAGING

MARY H. MOSIER and ANTHONY HAWKINS In AGARD, Advanced Packaging Concepts for Digital Avionics 10 p Oct. 1994
 Copyright Avail: CASI HC A02/MF A03

The objective of the 'Advanced SEM-E Packaging' is 'to identify existing SEM-E and modular avionics characteristics; delineate where they are not defined; and document consensual requirements and guidance for military and commercial applications to provide a framework for open systems architecture implementation'. SHARP has teamed with the Air Force Modular Avionics Systems Architecture (MASA) Program to bridge Industry and government agencies in defining and documenting Standard Electronic Module (SEM) format E advanced packaging requirements. The baseline for the working group has been identified, but SHARP and MASA are soliciting participation and input from industry, other agencies, and NATO. Author

N95-20634# Dassault Aviation, Saint-Cloud (France).
FASTPACK: OPTIMIZED SOLUTIONS FOR MODULAR AVIONICS DERIVED FROM A PARAMETRIC STUDY. PART 1: PLATFORM FEATURES [FASTPACK: SOLUTIONS OPTIMISEES POUR LE CONDITIONNEMENT DE L'AVIONIQUE MODULAIRE ISSUES D'UNE ETUDE PARAMETRIQUE. PART 1: ASPECTS PORTEUR]
 G. VEBER, S. BARBAGELETA (Eurocopter France, Marignane, France.), and P. HELIE In AGARD, Advanced Packaging Concepts for Digital Avionics 11 p Oct. 1994 In FRENCH
 Copyright Avail: CASI HC A03/MF A03

Modular avionics is one of the major concepts to be applied to future avionics systems with the objective of cost (LCC - Life Cycle Cost) containment and improvement of operational performance. The objectives associated with such a concept are numerous: improvement of reliability, standardization, interchangeability, interoperability, etc. To obtain these objectives it is necessary to define characteristics standards for modules (LRM - Line Replaceable Module). The definition of these standards for LRM has a direct impact on the modules and their integration. The choice of the best concept takes place through a careful study of the repercussions of each solution on all levels (racks, bays and platforms), in all the technical fields (thermal, electric, mechanical, electromagnetic protection, connectors). This article presents the results of a parametric platform/system-avionics study and more particularly the possible choices for orientation of the platform on aircraft or helicopters. The method used defines the platform constraints to be parameterized and their interactions. The effects are initially integrated in a model representative of standard missions. Thus the results, field by field, show the importance of the effects of constraints on the platform system. Finally, a process of complete dimensioning of the platform, including the functional reliability aspects leads to the synthesis. This allows both a quantitative and qualitative check of the robustness of the compromises carried out. In conclusion, the control of the platform/avionics-system compromise, by an approach of simultaneous engineering, makes it possible to justify a solution of conditioning of the modular avionics in the optics of a future system.

Transl. by CASI

N95-20635# Thomson-CSF, Paris (France).
FASTPACK: OPTIMIZED SOLUTIONS FOR MODULAR AVIONICS DERIVED FROM A PARAMETRIC STUDY. PART 2: AVIONICS
 M. CAPLOT, G. LABAUNE, C. CAPOGNA, C. SARNO (Sextant Avionique, Valence, France.), J. HERREWYN (Dassault Electronique, Saint-Cloud, France.), J. C. DHAUSSY (Dassault Electronique, Saint-Cloud, France.), and P. BLEICHER (Dassault Electronique, Saint-Cloud, France.) In AGARD, Advanced Packaging Concepts for Digital Avionics 13 p Oct. 1994 Sponsored by Ministry of Defence Copyright
 Avail: CASI HC A03/MF A03

The main requirements for modular avionics have a strong influence on the Packaging solutions for the Line Replaceable Modules (LRM's) and the rack. Packaging is here including: mechanical concepts, cooling, power supplies, interconnections and

06 AIRCRAFT INSTRUMENTATION

electromagnetic compatibility. To define the packaging solutions for the next generation of avionics, a parametric study, FASTPACK, has been performed at the platform and avionics levels. The present paper deals with the avionics part and shows how the FASTPACK parametric study has been conducted in order to define a synthesis in each domain, used to derive Packaging concepts. The main results include the choice of a LRM format, called FAST, a distributed power supply network within the rack, conduction and liquid flow through cooling, shielding on the rack against external electromagnetic threats and shielding on the LRM for rack internal interferences and, finally, the first definition of the LRM connector. Author

N95-20636# Naval Air Warfare Center, Warminster, PA. Aircraft Div.

THE ADVANCED AVIONICS SUBSYSTEM TECHNOLOGY DEMONSTRATION PROGRAM

TIMMONAGHAN, GHANIKANAWATI, JACOB ABRAHAM, DANIEL OLSON, and RAVI IYER *In* AGARD, Advanced Packaging Concepts for Digital Avionics 13 p Oct. 1994
Copyright Avail: CASI HC A03/MF A03

The Navy's Advanced Avionics Subsystem Technology (AASST) Fault Tolerant program is clarifying the Navy's fault tolerant avionics specifications methods and acceptance tests. The goal of the program will be to clarify the Specification and Statement of Work language needed in future procurements and to demonstrate fault tolerant validation tools on the avionics design. A set of tool features will then be developed that spans the needs of fault tolerant computer system design from early concept studies to full scale production and operational support, both hardware and software. The paper will give an overview of the AASST Fault Tolerant Demonstration and focus on two tools that are being used in the demonstration: FERRARI - a software fault injector that will be used to validate the fault tolerance of the Common Integrated Processor (CIP), the F-22 Mission Processor, and GRIND - a concept evaluation tool that will be used to evaluate the overall CIP architecture. Author

N95-20641# GEC-Marconi Research Centre, Great Baddow (England).

MCMS FOR AVIONICS: TECHNOLOGY SELECTION AND INTERMODULE INTERCONNECTION

N. CHANDLER, I. R. CROSTON, S. G. TYLER, T. G. HAMILL (GEC-Marconi Avionics Ltd., Rochester, England.), and P. E. HOLBOURN (GEC-Marconi Avionics Ltd., Edinburgh, Scotland.) *In* AGARD, Advanced Packaging Concepts for Digital Avionics 15 p Oct. 1994 Sponsored by European Commission
Copyright Avail: CASI HC A03/MF A03

There are already several Multi Chip Module (MCM) technologies suitable for avionics applications, and new variations and updates are continually being added. The optimum technology choice for each avionics application will depend on many factors, including the electrical and thermal requirements, the operating environment, size, weight, quantity, cost, etc. This paper will compare the attributes of the various MCM technologies, both at present and future trends, including 3D assembly/packaging and the use of active substrates for MCM-D's. The means of mounting MCM's and interconnecting them into the system using electrical or optical interconnection will also be compared. Some of the methods used to remove very high levels of power dissipation will also be discussed, in relation to the different technologies. The requirements of electronic modules in different parts of avionics systems may be sufficiently different that alternative solutions are optimal for the various parts. The paper will briefly review the range of requirements across military (and comparable civil) avionics systems and, by considering the technology options, indicate how the optimum choice can be decided, both for the MCM's themselves and for the means of interconnection between MCM's and from MCM's to other parts of the system. Author

N95-20650# Naval Air Warfare Center, Warminster, PA. Aircraft Div.

THE IEEE SCALABLE COHERENT INTERFACE: AN APPROACH FOR A UNIFIED AVIONICS NETWORK

RALPH LACHENMAIER and THOMAS STRETCH (AMPAC, Inc., Norristown, PA.) *In* AGARD, Advanced Packaging Concepts for Digital Avionics 10 p Oct. 1994 Copyright Avail: CASI HC A02/MF A03

The U.S. Navy Next Generation Computer Resources (NGCR) High Speed Data Transfer Network (HSDTN) program has chosen the IEEE Scalable Coherent Interface (SCI) as one of its baseline standards. This paper proposes to use SCI as a unified avionics network and describes SCI and extensions to it — particularly an extension known as SCI/ Real Time (SCI/RT). Because SCI can be used in a serial configuration, such a network provides an alternative to the need for ever denser and ever more reliable backplane connectors by reducing the number and size of interconnects and, hence, the need for large numbers of pins. In addition, SCI reduces packaging problems by using a small amount of board real estate and by using distance insensitive links which can extend board to board or box to box, thus facilitating a distributed backplane approach for retrofit aircraft applications. SCI is currently being applied to both parallel and to serial implementations, to both message passing and shared memory computing paradigms, and to both electrical and optical physical layers. SCI/RT is a set of proposed enhancements, developed initially by the Canadian Navy and now being evaluated by the NGCR HSDTN and IEEE working groups, to make SCI more fault tolerant and to provide the determinism and priorities necessary to support Rate Monotonic Scheduling. Addition of these features will allow SCI to perform in a unified and seamless manner, the functions of command and control interconnect, data flow network and sensor/video network. Electrical and optical, and serial and parallel links can be intermixed for the most cost effective solution. As an added benefit, SCI has potential for use interconnecting multiple processing chips on the same board. Author

N95-20657# Thomson-CSF, Paris (France). Div. Radars et Contre-Mesures.

MODULAR SUPPLIES FOR A DISTRIBUTED ARCHITECTURE [ALIMENTATIONS MODULAIRES POUR UNE ARCHITECTURE DISTRIBUEE]

A. MOREAU, J. M. REY, M. CAPLOT, and J. P. DELVINQUIER *In* AGARD, Advanced Packaging Concepts for Digital Avionics 12 p Oct. 1994 *In* FRENCH
Copyright Avail: CASI HC A03/MF A03

Future avionics systems will be based on a modular architecture in which each elementary function will correspond to a line replaceable module (LRM). Parametric studies, such as FASTPACK, showed that the optimal solution for the supply systems was an architecture distributed on only one level of energy transformation, i.e., a modular supply on each LRM able to deliver 50 W with 100 W directly starting from the main supply system (270 V(dc) or three-phase network 200 V/400 rectified Hz). In order to obtain a coherent level of integration of the digital circuits, it was necessary to develop such modular supplies with a power density of about 1500 W/dm³ (sup 3) per unit of volume. In addition, so that these supplies can be established directly on a LRM simple face, their thickness had to be limited to 6.8 mm (case included/understood). To achieve this goal, a total integration that guaranteed the performances of the electric supplies, high frequency hybrid converters (of the order of MHz) were developed. After a presentation of the advantages of an architecture of distributed supply and a review of the main technical aims, this article describes the techniques and technologies implemented to achieve these goals. A thorough description of the developed modular supplies is given for delivered powers ranging between 50 W and 100 W and for various output voltages. Finally, the future developments planned to reach a power density of 4000 W/dm³ (sup 3) per unit of volume are reviewed. Transl. by CASI

N95-20659# Rohde and Schwartz, Munich (Germany).

MODULAR CNI AVIONICS SYSTEM

P. H. REITBERGER and G. MEY (Ministry of Defence, Bonn, Germany.) *In* AGARD, Advanced Packaging Concepts for Digital Avionics 11 p Oct. 1994

Copyright Avail: CASI HC A03/MF A03

Today's aircraft contain a multitude of different radio functions

for communications, navigation and identification. The individual radio functions, like VHF/UHF, JTIDS/MIDS, GPS or NIS, are each handled by an individual piece of equipment consisting of several LRU. In the absence of built-in redundancy, the failure of a single LRU can result in a failure of a radio function. In the future, individual radio functions need to be integrated in a modular system concept, the modular CNI system (communication - navigation - identification). Author

N95-22024# Science Applications International Corp., Dayton, OH. **SYSTEMS ENGINEERING DESIGN AND TECHNICAL ANALYSES FOR STRATEGIC AVIONICS CREW-STATION DESIGN EVALUATION FACILITY (SACDEF) Final Report, 15 Jan. 1988 - 14 May 1993**

JOHN D. STENGEL, HARRY HEATON, STEVE FINCH, JAMES HOPPER, and TERESA MCKELVEY May 1994 71 p
(Contract(s)/Grant(s): F33615-87-C-0531)
(AD-A286239; AL/CF-TR-1994-0074) Avail: CASI HC A04/MF A01

This report summarizes all work efforts completed under Contract F33615-87-C-0531, systems engineering design and technical analysis (SEDATA) for the Strategic Avionics Crew Station Design Evaluation Facility (SACDEF). This report consists of four main sections. Section 1 is an overview of SACDEF contract. Section 2 contains descriptions of specific tasks completed under the SEDATA for SACDEF contract. Section 3 contains conclusions and recommendations. Section 4 contains references, which includes reports and documentation produced under specific tasks of the contract. The Armstrong Laboratory has been involved in supporting the development and refinement of Strategic Bomber Crew Systems for almost 25 years. The SACDEF of the CFHI branch within the Human Engineering Division is responsible for research addressing crew station design and areas currently include aircrew workload evaluations, new control/display concepts, display device image quality, and electrophysiological correlates of crew performance. Specific emphasis is directed toward the development of advanced controls and displays for bomber aircraft, employing state-of-the-art, multi-functional display devices and computer programming techniques. An ongoing requirement has been to maintain the SACDEF B-52G Defensive Simulator and the B-1B Engineering Research Simulator (ERS) as designed, developed, tested, and delivered to Armstrong Laboratory under a previous contract. This report documents the work activities completed by Science Applications International Corporation for the SEDATA for SACDEF over the period 15 January 1988 through 14 May 1993. DTIC

N95-22036# PDA Engineering, Costa Mesa, CA. **RESPONSE OF THE B-1B AIR DATA SENSOR TO SIMULATED DUST CLOUD ENVIRONMENTS Technical Report, 17 Sep. 1992 - 15 Aug. 1993**

ROBERT G. OEDING 1 Nov. 1994 106 p
(Contract(s)/Grant(s): DNA001-91-C-0021)
(AD-A286134; PDA-TR-1754-02-01; DNA-TR-93-164) Avail: CASI HC A06/MF A02

This report describes an experimental evaluation of the effects of dusty flow environments on the performance of the B-1B air data sensor (ADS). The evaluations were conducted in the DNA dust erosion facility which is located at PDA Engineering laboratories in Santa Ana, CA. The dust erosion facility was modified to provide a high speed dust jet with controlled moisture addition. Full-scale ADS probes were submerged in the dust flow and probe performance was monitored. Performance measurements included total, static, and angle-of-attack pressure outputs. Also pre- and post-test weights of the probes and pressure line dust filters were obtained in order to determine ingested particle mass. Both dry and wet flows included two levels of water addition to simulate cloud precipitation/moisture. The test configurations, procedures, and results are described. DTIC

N95-22232# Naval Postgraduate School, Monterey, CA. **EVALUATION OF THE HAWORTH-NEWMAN AVIONICS DISPLAY READABILITY SCALE M.S. Thesis**
CHARLES F. CHIAPPETTI Sep. 1994 63 p

(AD-A286127) Avail: CASI HC A04/MF A01

This study investigates the suitability of the Haworth-Newman Display Readability Rating Scale as a performance-based test and evaluation tool. This evaluation has been necessary to determine if the scale actually measures display readability, and if consistent, reproducible results are attainable. Background information on the scale's development is presented along with a brief description of display readability characteristics. A technique for systematic degradation of display readability and a method of displaying degraded symbology sets is introduced. A flight simulation experiment was conducted to obtain performance data, Haworth-Newman readability ratings, and participants' written comments for each of the degraded symbology set levels. Five Naval test pilots attempted to maintain specified heading, altitude, and airspeed while utilizing the ten levels of symbology sets and then used the Haworth-Newman scale to rate the display readability for each. Experimental results are discussed and recommendations presented. DTIC

07

AIRCRAFT PROPULSION AND POWER

Includes prime propulsion systems and systems components, e.g., gas turbine engines and compressors; and on-board auxiliary power plants for aircraft.

A95-70133

ENGINE LIFE MEASUREMENT AND DIAGNOSTICS

CHRIS J. POMFRET Wright-Patterson AFB Aerospace Engineering (Warrendale, Pennsylvania) (ISSN 0736-2536) vol. 14, no. 6 June 1994 p. 11-14

(BTN-95-EIX95041505024) Copyright

Advances in artificial intelligence particularly neural network technology may provide an opportunity to enhance trending and diagnostic facilities for the gas-turbine engine of aircrafts. Current monitoring systems are labor-intensive, costly, provide limited and slow diagnosis of engine faults, and have an inadequate recording system. To address these issues, the US Air Force, for example, has launched the Integrated High Performance Turbine Engine Technology project. It is expected to sense more parameters but with minimal intrusion, weight addition, and system complexity, thereby improving the comprehensiveness and value of engine health monitoring. EI

N95-21243# General Electric Co., Schenectady, NY. Composite and Structural Ceramics Program.

TOUGHENED SILCOMP COMPOSITES FOR GAS TURBINE ENGINE APPLICATIONS Final Report, Apr. 1992 - Jun. 1994
G. S. CORMAN, K. L. LUTHRA, M. K. BRUN, and P. J. MESCHTER
Jul. 1994 115 p

(Contract(s)/Grant(s): DE-FC02-92CE-41000)
(DE95-002851; DOE/CE-41000/2) Avail: CASI HC A06/MF A02

The two main factors driving the development of new industrial gas turbine engine systems are fuel efficiency and reduced emissions. One method of providing improvements in both areas is to reduce the cooling air requirements of the hot gas path components. For this reason ceramic components are becoming increasingly attractive for gas turbine applications because of their greater refractoriness and oxidation resistance. Among the ceramics being considered, continuous fiber ceramic composites (CFCC's) are leading candidates because they combine the high temperature stability of ceramics with the toughness and damage tolerance of composites. The purpose of this program, which is part of DOE's CFCC initiative, is to evaluate the use of CFCC materials as gas turbine engine components, and to demonstrate the feasibility of producing such components from Toughened Silcomp composites. Toughened silcomp is a CFCC material made by a reactive melt infiltration process, and consists of continuous SiC reinforcing fibers, with an appropriate fiber coating, in a fully dense matrix of SiC and Si. Based on the material physical properties, the material/

07 AIRCRAFT PROPULSION AND POWER

process improvements realized in Phase 1, and the preliminary design analyses from Task 1, they feel the feasibility of fabricating Toughened Silcomp with the requisite physical and mechanical properties for the intended applications has been demonstrated. Remaining work for Phase 2 is to further improve the system for enhanced oxidation resistance, incorporate additional process controls to enhance the reproducibility of the material, transition the fabrication process to the selected vendors for scale-up, develop a more complete material property data base, including long-term mechanical behavior, and fabricate and test preliminary 'representative part' specimens. DOE

N95-21383*# National Aeronautics and Space Administration, Lewis Research Center, Cleveland, OH.

TWO-DIMENSIONAL IMAGING OF OH IN A LEAN BURNING HIGH PRESSURE COMBUSTOR

R. J. LOCKE (NYMA, Inc., Brook Park, OH.), Y. R. HICKS, R. C. ANDERSON, K. A. OCKUNZZI (Ohio Aerospace Inst., Cleveland, OH.), and G. L. NORTH (Army Research Lab., Cleveland, OH.) Feb. 1995 16 p Presented at the 33rd Aerospace Sciences Meeting and Exhibit, Reno, NV, 9-12 Jan. 1995; sponsored by AIAA Original contains color illustrations (Contract(s)/Grant(s): NAS3-27186; RTOP 537-02-21) (NASA-TM-106854; E-9444; NAS 1.15:106854; AIAA PAPER 95-0173) Avail: CASI HC A03/MF A01; 5 functional color pages

Planar laser-induced fluorescence (PLIF) images of OH have been obtained from an optically accessible, lean burning high pressure combustor burning Jet-A fuel. These images were obtained using various laser excitation lines of the OH A (reverse arrow) X (1,0) band for several fuel injector configurations with pressures ranging from 1013 kPa (10 atm) to 1419 kPa (14 atm). Non-uniformities in the combustor flow, attributed to differences in fuel injector configuration, are revealed by these images. Contributions attributable to fluorescent aromatic hydrocarbons and complex fuel chemistries are also not evident. Author

N95-22341*# National Aeronautics and Space Administration, Washington, DC.

TURBINE DESIGN AND APPLICATION

ARTHUR J. GLASSMAN, ed. (National Aeronautics and Space Administration, Lewis Research Center, Cleveland, OH.) Cleveland, OH Jun. 1994 390 p (NASA-SP-290; E-5666; NAS 1.21:290; LC-94-67487) Avail: CASI HC A17/MF A04

NASA has an interest in turbines related primarily to aeronautics and space applications. Airbreathing turbine engines provide jet and turboshaft propulsion, as well as auxiliary power for aircraft. Propellant-driven turbines provide rocket propulsion and auxiliary power for spacecraft. Closed-cycle turbine engines using inert gases, organic fluids, and metal fluids have been studied for providing long-duration electric power for spacecraft. Other applications of interest for turbine engines include land-vehicle (cars, trucks, buses, trains, etc.) propulsion power and ground-based electrical power. In view of the turbine-system interest and efforts at Lewis Research Center, a course entitled 'Turbine Design and Application' was presented during 1968-69 as part of the In-house Graduate Study Program. The course was somewhat revised and again presented in 1972-73. Various aspects of turbine technology were covered including thermodynamic and fluid-dynamic concepts, fundamental turbine concepts, velocity diagrams, losses, blade aerodynamic design, blade cooling, mechanical design, operation, and performance. The notes written and used for the course have been revised and edited for publication. Such a publication can serve as a foundation for an introductory turbine course, a means for self-study, or a reference for selected topics. Any consistent set of units will satisfy the equations presented. Two commonly used consistent sets of units and constant values are given after the symbol definitions. These are the SI units and the U.S. customary units. A single set of equations covers both sets of units by including all constants required for the U.S. customary units and defining as unity those not required for the SI units. Author

08

AIRCRAFT STABILITY AND CONTROL

Includes aircraft handling qualities; piloting; flight controls; and autopilots.

A95-71182* National Aeronautics and Space Administration, Ames Research Center, Moffett Field, CA.

ROTORCRAFT CONTROL SYSTEM DESIGN FOR UNCERTAIN VEHICLE DYNAMICS USING QUANTITATIVE FEEDBACK THEORY

R. A. HESS Univ. of California, Davis, CA, US American Helicopter Society, Journal (ISSN 0002-8711) vol. 39, no. 2 April 1994 p. 47-55

(Contract(s)/Grant(s): NCC2-624)

(HTN-95-31012) Copyright

Quantitative Feedback Theory describes a frequency-domain technique for the design of multi-input, multi-output control systems which must meet time or frequency domain performance criteria when specified uncertainty exists in the linear description of the vehicle dynamics. This theory is applied to the design of the longitudinal flight control system for a linear model of the BO-105C rotorcraft. Uncertainty in the vehicle model is due to the variation in the vehicle dynamics over a range of airspeeds from 0-100 kts. For purposes of exposition, the vehicle description contains no rotor or actuator dynamics. The design example indicates the manner in which significant uncertainty exists in the vehicle model. The advantage of using a sequential loop closure technique to reduce the cost of feedback is demonstrated by example. Author (Hemer)

A95-71184

SMART STRUCTURES IN THE CONTROL OF AIRFRAME VIBRATIONS

S. HANAGUD Georgia Inst. of Technology, Atlanta, GA, US and G. L. NAGESH BABU Georgia Inst. of Technology, Atlanta, GA, US American Helicopter Society, Journal (ISSN 0002-8711) vol. 39, no. 2 April 1994 p. 69-72

(Contract(s)/Grant(s): DAAL03-88-C-0003)

(HTN-95-31014) Copyright

The feasibility of using piezoelectric sensors and actuators to actively control vibrations at selected locations of an airframe is analytically studied. The airframe is assumed to experience oscillatory loads at multiples of 'n per revolution' in an n-bladed helicopter. The control system is designed using principles of H(sub infinity) control. Author (Hemer)

A95-72564

A GENERALIZED ALGORITHM FOR INVERSE SIMULATION APPLIED TO HELICOPTER MANEUVERING FLIGHT

R. A. HESS California Univ., Davis, CA, US and C. GAO Chung Shien Inst. of Science and Technology, Taiwan American Helicopter Society, Journal (ISSN 0002-8711) vol. 38, no. 4 October 1993 p. 3-15

(HTN-95-A0493) Copyright

The inverse simulation problem is discussed in which control inputs that will enable a vehicle to follow a specified trajectory are determined by a numerical technique. The particular technique for inverse simulation which is proposed alleviates some of the problems associated with algorithms which require numerical differentiation of vehicle states in the solution process. The proposed technique emphasizes integration and is presented as a generalized approach to the inverse simulation problem. The algorithm can be applied to problems in which the number of controls exceeds the number of constrained variables. Using a readily available model of a BO-105 rotorcraft, with linear aerodynamics but with nonlinear inertial cross-coupling and kinematics, the algorithm is exercised by obtaining the control inputs necessary to enable the rotorcraft to complete a series

of discrete maneuvering tasks involving side-steps, bob-ups, hurdle-hops and level turns, each performed with and without a stability augmentation system in operation. A potential application of inverse simulation is the formulation of task-driven bandwidth requirements for stability augmentation system design. Author (Hemer)

A95-72565* National Aeronautics and Space Administration. Ames Research Center, Moffett Field, CA.

HIGH-ORDER STATE SPACE SIMULATION MODELS OF HELICOPTER FLIGHT MECHANICS

FREDERICK D. KIM NASA. Ames Research Center, Moffett Field, CA, US, ROBERTO CELI Maryland Univ., College Park, MD, US, and MARK B. TISCHLER Army Aviation Systems Command, Moffett Field, CA, US American Helicopter Society, Journal (ISSN 0002-8711) vol. 38, no. 4 October 1993 p. 16-27

(Contract(s)/Grant(s): NCA2-S11)

(HTN-95-A0494) Copyright

This paper describes the formulation and validation of a high-order linearized mathematical model of helicopter flight mechanics, which includes rotor flap and lag degrees of freedom as well as inflow dynamics. The model is extracted numerically from an existing nonlinear, blade element, real-time simulation model. Extensive modifications in the formulation and solution process of the nonlinear model, required for a theoretically rigorous linearization, are described in detail. The validation results show that the linearized model successfully captures the coupled rotor-fuselage dynamics in the frequency band most critical for the design of advanced flight control systems. Additional results quantify the extent to which the order of the model can be reduced without loss of fidelity.

Author (Hemer)

N95-20004# Wright Lab., Wright-Patterson AFB, OH.
SUMMARY OF A JOINT PROGRAM OF RESEARCH INTO AIRCRAFT FLIGHT CONTROL CONCEPTS Final Report, 1983 - 1992

KNUT WILHELM, ROBERT W. WOODCOCK, and DAVID B. LEGGETT May 1993 83 p

(Contract(s)/Grant(s): AF PROJ. 2403)

(AD-A280012; WL-TR-94-3039) Avail: CASI HC A05/MF A01

The report summarizes the research work into aircraft flight control concepts carried out by WL and DLR under the MoU. Addressed are the methods and scientific approaches used for two subtasks as Pilot vehicle integration and In-Flight Simulation Methodologies. Main emphasis from WL is laid on the different projects performed on the NT-33 and TIFS In-Flight Simulators in order to identify the influence of various system related parameters on longitudinal and lateral handling qualities. The work done by DLR describes the specific technique to be used for ground attack tasks (GRATE) for handling quality research and the development and system identification of DLR's new In Flight Simulator ATTAS.

DTIC

N95-21122 Charles River Analytics, Inc., Cambridge, MA.
A NEURAL EXPERT APPROACH TO SELF DESIGNING FLIGHT CONTROL SYSTEMS Final Report, 15 Jul. 1993 - 14 Jan. 1994

SHERIF M. BOTROS, ALPER K. CAGLAYAN, and GREG L. ZACHARIAS 21 Apr. 1994 70 p Limited Reproducibility: More than 20% of this document may be affected by microfiche quality (Contract(s)/Grant(s): F49620-93-C-0050)

(AD-A279965; R93081; AFOSR-94-0310TR) Avail: CASI HC A04

Based on the simulations performed in this phase 1 study, we show that Hopfield and RBF feedforward network architectures may have a great potential in the control of nonlinear systems. In particular, Hopfield implementation of Lagrange multiplier method is suitable for real-time adaptive optimal control. Similarly, RBF feedforward neural network architectures are suitable for learning inverse dynamics and inverse trim in aircraft FCS applications. In addition, RBF feedforward are easier to train than backpropagation sigmoid networks since RBF formulation results in linear param-

eters. The initial simulations we performed show very promising results as exemplified by the small control errors in closed-loop Simulations using the nonlinear /A-18 longitudinal dynamics. Further studies are needed to test the applicability of the techniques to real world problems and to study the robustness, stability and general reliability of the proposed neural techniques. Neural networks by themselves cannot be the panacea to all the nonlinear control problems. An effort has to be made to incorporate all the available knowledge about the dynamics system to achieve good performance. DTIC

N95-21214# Wright Lab., Wright-Patterson AFB, OH.
PRESSURE MEASUREMENTS ON AN F/A-18 TWIN VERTICAL TAIL IN BUFFETING FLOW. VOLUME 4, PART 1: BUFFET CROSS SPECTRAL DENSITIES Final Report, 15 Apr. 1993 - 15 Aug. 1994

CHRIS PETTIT, DANSEN BROWN, MICHAEL BANFORD, and ED PENDLETON Aug. 1994 695 p See also AD-A285555

(Contract(s)/Grant(s): AF PROJ. 2401)

(AD-A285593; WL-TM-94-3112-VOL-4-PT-1) Avail: CASI HC A99/MF A06

Buffeting pressure measurements were made on the vertical tail surface of a full scale F/A-18 aircraft model in the National Full Scale Aerodynamics Complex at NASA Ames Research Center. Test variables included aircraft angle-of-attack, aircraft sideslip angle, and dynamic pressure. Accelerometers were used to obtain vertical tail accelerations. Pressure transducers were mounted on the starboard vertical tail. Steady and unsteady pressures were obtained. Unsteady pressure data were reduced to PSD and CSD forms. Both steady and unsteady RMS pressure coefficients are also presented. Volume 1 contains the general description of the model, the test program, and highlights of the reduced data. Volume 2 contains steady and unsteady RMS data. Volume 3 contains unsteady PSD results. Volume 4 contains unsteady CSD results. DTIC

09

RESEARCH AND SUPPORT FACILITIES (AIR)

Includes airports, hangars and runways; aircraft repair and overhaul facilities; wind tunnels; shock tube facilities; and engine test blocks.

A95-71656* National Aeronautics and Space Administration. Goddard Space Flight Center, Greenbelt, MD.

A SURVEY OF BIDIRECTIONAL GREATER THAN OR EQUAL TO MEV ION FLOWS DURING THE HELIOS 1 AND HELIOS 2 MISSION: OBSERVATIONS FROM THE GODDARD SPACE FLIGHT CENTER INSTRUMENTS

I. G. RICHARDSON NASA. Goddard Space Flight Center, Greenbelt, MD, US The Astrophysical Journal, Part 1 (ISSN 0004-637X) vol. 420, no. 2 January 10, 1994 p. 926-942

(HTN-95-70542) Copyright

A survey is made of 1.1-2.1 MeV and 3-21 MeV bidirectional ion flows (BIFs) in the solar wind at 0.3-1.0 AU observed by the Goddard Space Flight Center instruments on the Helios 1 and Helios 2 spacecraft during the spacecraft mission in 1974-1984 and 1979-1980, respectively. Some 774 events have been identified Helios 1, and 223 at Helios 2, with mean durations of approximately 2.5 hr at each spacecraft. BIFs were observed for approximately 1%-3% of the observation time during solar minimum conditions in 1975-1977 and for approximately 10%-14% in 1980-1981 around solar maximum. These occurrence rates are similar to those of approximately 1 MeV BIFs observed at the Interplanetary Monitoring Platform 8 and International Sun Earth Explorers (ISEE) 3 spacecraft, and of bidirectional electron heat fluxes at ISEE 3. Solar wind plasma parameters during BIFs were similar to those found generally during the Helios missions, though BIFs have a greater tendency to be associated with cool, low-beta plasma, moderately enhanced and low-variance magnetic fields, both less than 300 km/s and greater than 750 km/s solar wind. Solar wind features associated with the

09 RESEARCH AND SUPPORT FACILITIES (AIR)

greater than 4 hr duration BIFs include clear plasma shock-driver signatures: approximately 36% of the events; postshock plasma, not associated with shock-driver signatures: approximately 13%; noncompressive density enhancements: approximately 22% (half associated with plasma proton temperature depression); high-speed streams not associated with shocks: approximately 10%; corotating interaction regions: approximately 5%; immediately upstream of shocks: approximately 5%. Around 8% were associated with other solar wind structures, while approximately 4% showed no associated structure. BIFs were present in several of the shock drivers associated with coronal mass ejections (CMEs) observed by the Solwind coronagraph during intervals when Helios 1 was off the limbs of the Sun, showing directly the association of some BIFs with CMEs. some BIFs with CMEs. Author (Herner)

N95-19931# Army Research Inst. for the Behavioral and Social Sciences, Alexandria, VA.

USING THE BACKWARD TRANSFER PARADIGM TO VALIDATE THE AH-64 SIMULATOR TRAINING RESEARCH ADVANCED TESTBED FOR AVIATION Final Report, Jan. 1993 - Oct. 1993

JOHN E. STEWART, II Sep. 1994 44 p
(AD-A285758; ARI-RR-1666) Avail: CASI HC A03/MF A01

The Simulator Training Research Advanced Testbed for Aviation (STRATA) is a modular simulation system for the AH-64 helicopter. The Adams and McAbee backward transfer of training paradigm was used to determine if AH-64 piloting skills transfer to STRATA. Ten AH-64 pilots participated in the experiment. They were asked to fly a mission scenario consisting of 13 single-pilot aircrew training manual (ATM) tasks. No orientation or practice sessions were given. Most participants rated STRATA as highly similar to the AH-64 in handling, but believed the visual display system had limitations for extremely low-altitude tasks like hovering. Performance ratings during the experiment by a senior instructor pilot (IP) indicated that of the total 130 task events, 88.5% were performed to ATM standards. After the experiment, four independent judges, all aviators, rank-ordered participant performance on the stationary hover task using output from STRATA's automated performance measurement system. Rankings showed agreement between judges and high correlation with IP ratings made during the experiment. DTIC

N95-19955# Army Engineer Waterways Experiment Station, Vicksburg, MS. Geotechnical Lab.

SUPER-HEAVY AIRCRAFT STUDY Final Report WALTER R. BARKER and CARLOS R. GONZALEZ Apr. 1994 73 p

(AD-A279602; WES/TR/GL-94-12) Avail: CASI HC A04/MF A01

The test data for performance of flexible pavements were collected, sorted, and tabularized. The test data were analyzed using Boussinesq and layered elastic pavement models. To assist in the analysis, two computer programs were developed. The first program used the Boussinesq model to compute equivalent single-wheel loads. This program will compute the equivalent single-wheel load considering any selected cutoff distance. The second program used layered elastic theory for the analysis of pavements structures. The program has the capability of determining maximum pavement response for several response parameters, determining allowable loads for selected performance criteria, and computing a new layered elastic aircraft classification number. Several different performance criteria were developed including deflection criteria employing different cutoff distances, and strain criteria determined from the layered elastic pavement model. It was shown that deflection and strain criteria could be developed for the design of heavy multiwheel aircraft which would be independent of the number of tires in the aircraft gear. Performance criteria based on deflection, vertical strain, horizontal shear strain, maximum shear strain, and octahedral strain were incorporated into the layered elastic computer program to give predictions for pavement performance. Comparisons of the strain criteria were made with the current design criteria. DTIC

N95-20080*# National Aeronautics and Space Administration, Langley Research Center, Hampton, VA.

VAPOR GENERATOR WAND Patent Application

DAVID B. ROBELEN, inventor (to NASA) 28 Nov. 1994 12 p
(NASA-CASE-LAR-15058-1; NAS 1.71:LAR-15058-1; US-PATENT-APPL-SN-359320) Avail: CASI HC A03/MF A01

In low speed wind tunnels it is often desirable to visualize airflow to augment observations made with instruments such as strain and pressure gages. Current technology devices for delivery of a vapor are bulky and thus disrupt local airflow. It is the object of this invention to provide a device capable of delivering a stream of vapor with a minimal effect on local airflow. The present invention achieves this object by utilizing a narrow tube as a heating device for producing the vapor. Running an electrical current through the tube provides resistive heating to a liquid which produces a vapor when boiled. As the entire heating and delivery portion of the device is simply a small cylinder the disruption to airflow within the tunnel is minimized. This allows an experimenter to place the source of vapor fairly close to a model without causing too much change to the model data. The novelty of the present invention lies in reducing the bulk of current technology devices by combining the acts of heating and delivery. Author

N95-20624 Carnegie-Mellon Univ., Pittsburgh, PA. School of Computer Science.

COLLECTED PAPERS OF THE SOAR/IFOR PROJECT, SPRING 1994 Technical Report

W. L. JOHNSON, RANDOLPH M. JONES, DAVID KEIRSEY, FRANK V. KOSS, and JOHN E. LAIRD 25 Apr. 1994 105 p Limited Reproducibility: More than 20% of this document may be affected by microfiche quality

(Contract(s)/Grant(s): N00014-92-K-2015)
(AD-A280063; CMU-CS-94-134; CSE-TR-207-94; ISI/SR-94-379)
Avail: CASI HC A06

Since the summer of 1992, the Soar/IFOR research group has been building intelligent automated agents for tactical air simulation. The ultimate goal of this project is to develop automated pilots whose behavior in simulated engagements is indistinguishable from that of human pilots. This technical report is a collection of the research papers that have been generated from this project as of Spring 1994. The research covered in these papers spans a wide spectrum of issues in agent development such as explanation, managing situational awareness, managing multiple interacting goals, coordination between multiple agents, natural language processing, developing believable agents, event tracking, and the infrastructure to support agent development, including knowledge acquisition and use, interfacing to simulation environments, and developing low cost simulators. DTIC

N95-20669*# National Aeronautics and Space Administration, Langley Research Center, Hampton, VA.

16-FOOT TRANSONIC TUNNEL TEST SECTION FLOWFIELD SURVEY

J. A. YETTER and W. K. ABEYOUNIS Dec. 1994 92 p
(Contract(s)/Grant(s): RTOP 538-05-13-01)
(NASA-TM-109157; NAS 1.15:109157) Avail: CASI HC A05/MF A01

A flow survey has been made of the test section of the NASA Langley Research Center 16-Foot Transonic Tunnel at subsonic and supersonic speeds. The survey was performed using five five-hole pyramid-head probes mounted at 14 inch intervals on a survey rake. Probes were calibrated at freestream Mach numbers from 0.50 to 0.95 and from 1.18 to 1.23. Flowfield surveys were made at Mach numbers from 0.50 to 0.90 and at Mach 1.20. The surveys were made at tunnel stations 130.6, 133.6, and 136.0. By rotating the survey rake through 180 degrees, a cylindrical volume of the test section 4.7 feet in diameter and 5.4 feet long centered about the tunnel centerline was surveyed. Survey results showing the measured test section upflow and sidewall characteristics and local Mach number distributions are presented. The report documents the survey probe calibration techniques used, summarizes the proce-

dural problems encountered during testing, and identifies the data discrepancies observed during the post-test data analysis. Author

N95-20799# Aircraft Research Association Ltd., Bedford (England). **TESTING IN THE ARA TRANSONIC WIND TUNNEL**
DICK JORDAN Mar. 1994 48 p Original contains color illustrations
 (ARA-MEMO-395) Avail: CASI HC A03/MF A01

This note is an overview of the ARA 2.74 x 2.44m Transonic Wind Tunnel facility which covers the full Mach number range $M = 0$ to 1.4. A description of the main features of the tunnel circuit is given together with operational details. The test capabilities encompass a wide variety of model configurations which can be mounted on interchangeable full or half-span model carts. Load measurements are made using strain-gauge balances in conjunction with an appropriate sting or support strut. Several standard model support arrangements are provided but specialized rigs are frequently developed for particular requirements. High pressure air is available for tests involving propulsion simulation. An advanced data acquisition and data reduction system produces on-line corrected results which are presented on inter-active color graphic displays. Emphasis is placed on the consistently good flow quality in the working section, the high accuracy and repeatability of the aerodynamic measurements, the routine corrections incorporated in the data reduction, and the high productivity of testing in this tunnel.

Author

N95-20992 Dayton Univ. Research Inst., OH. **COLOR CONTROL IN A MULTICHANNEL SIMULATOR DISPLAY: THE DISPLAY FOR ADVANCED RESEARCH AND TRAINING** Final Report, Jun. 1990 - Jul. 1993
CELESTE M. HOWARD Mar. 1994 35 p Limited Reproducibility: More than 20% of this document may be affected by microfiche quality
 (Contract(s)/Grant(s): F33615-90-C-0005)
 (AD-A279717; AL/HR-TR-1994-0024) Avail: Issuing Activity (Defense Technical Information Center (DTIC))

This report outlines the principles for color-matching of computer-generated imagery in displays made up of sectors served by several display devices. These principles are discussed with reference to a particular multichannel simulator display for which the display devices are projection cathode ray tubes. DTIC

N95-21436# Purdue Univ., West Lafayette, IN. Aerospace Sciences Lab. **DEVELOPMENT OF QUIET-FLOW SUPERSONIC WIND TUNNELS FOR LAMINAR-TURBULENT TRANSITION RESEARCH** Final Report, May 1990 - Dec. 1994
STEVEN P. SCHNEIDER Dec. 1994 55 p
 (Contract(s)/Grant(s): NAG1-1133)
 (NASA-CR-197286; NAS 1.26:197286) Avail: CASI HC A04/MF A01

This grant supported research into quiet-flow supersonic wind-tunnels, between May 1990 and December 1994. Quiet-flow nozzles operate with laminar nozzle-wall boundary layers, in order to provide low-disturbance flow for studies of laminar-turbulent transition under conditions comparable to flight. Major accomplishments include: (1) the design, fabrication, and performance-evaluation of a new kind of quiet tunnel, a quiet-flow Ludweig tube; (2) the integration of pre-existing codes for nozzle design, 2D boundary-layer computation, and transition-estimation into a single user-friendly package for quiet-nozzle design; and (3) the design and preliminary evaluation of supersonic nozzles with square cross-section, as an alternative to conventional quiet-flow nozzles. After a brief summary of (1), a description of (2) is presented. Published work describing (3) is then summarized. The report concludes with a description of recent results for the Tollmien-Schlichting and Gortler instability in one of the square nozzles previously analyzed. Author

N95-21719# Test Devices, Inc., Hudson, MA. **PORTABLE STATIC TEST FACILITY FOR SMALL, EXPENDABLE, TURBOJET ENGINES, PHASE 1** Final Report

BORISLAV MILATOVIC 28 Oct. 1994 127 p
 (Contract(s)/Grant(s): DAAH01-94-C-RO32)
 (AD-A286337) Avail: CASI HC A07/MF A02

Test Devices, Inc. has completed the preliminary design for the Portable Static Test Facility (PSTF) for small, expendable, turbojet engines (50 - 1000 lb thrust) as part of the Phase 1 effort under SBIR contract DAAH01-94-C-RO32. The goal of providing a preliminary design for a development and test facility at a reasonable cost, assembled from standard, transportable modules and requiring minimum setup was achieved. During the Phase 1 activities a detailed analysis was performed that covered the description of engines to be tested, engine test procedures, general test specifications, test facility requirements and design considerations, installation, and engine control and test data requirements. From this a preliminary design for the portable test facility was prepared, plus a conceptual installation design and a preliminary design for the engine control and data system. DTIC

10

ASTRONAUTICS

Includes astronautics (general); astrodynamics; ground support systems and facilities (space); launch vehicles and space vehicles; space transportation; spacecraft communications, command and tracking; spacecraft design, testing and performance; spacecraft instrumentation; and spacecraft propulsion and power.

A95-70124
ASCENT WIND MODEL FOR LAUNCH VEHICLE DESIGN
S. I. ADELFRANG New Technology, Inc, Huntsville, AL, United States, **O. E. SMITH, and G. W. BATTS** Journal of Spacecraft and Rockets (ISSN 0022-4650) vol. 31, no. 3 May-June 1994 p. 502-508
 (BTN-95-EIX95041503799) Copyright

A vector wind model has been developed for launch vehicle design. The model produces wind profiles for evaluation of vehicle control and trajectory variables required for assessment of proposed designs for new NASA launch vehicles. The wind model is based on the concept that the wind components of vectors at two altitudes have a probability distribution function that is quadrivariate normal. Given a wind vector at one altitude, the conditional distribution of the wind components at any other altitude is bivariate normal. A process is described for derivation of vector wind profiles based on the statistical model. The process produces wind profiles that are a reasonable substitute for measured wind profile samples. The model wind profiles produce dispersions in aerodynamic load indicators (ALI) that cover the dispersion range of ALI calculated from an extensive sample of Jimsphere wind profiles; this is accomplished at a selected altitude with only 12 model wind profiles compared to 1800 measured Jimsphere profiles. This represents an opportunity for a considerable reduction of computational effort during design phases that require many iterations to establish a launch vehicle design philosophy. Author (EI)

A95-70139
THERMOCHEMICAL NONEQUILIBRIUM VISCOUS SHOCK-LAYER ANALYSIS FOR A MARS AEROCAPTURE VEHICLE
KOJIRO SUZUKI Inst for Space and Astronautical Science, Kanagawa, Japan and **TAKASHI ABE** Journal of Thermophysics and Heat Transfer (ISSN 0887-8722) vol. 8, no. 4 October-December 1994 p. 773-780 refs
 (BTN-95-EIX95082502732) Copyright

The effects of thermal and chemical nonequilibrium on the aerothermodynamic environment over a Mars aerocapture vehicle are studied. In order to understand the characteristics of the flow at

10 ASTRONAUTICS

aerobraking, the classification of the stagnation region flow has been carried out from a viewpoint of the extent of the thermal and chemical nonequilibrium in the shock layer. The numerical analysis of the forebody flowfield over a spacecraft has been made by using the viscous shock-layer equations, including the thermal and chemical nonequilibrium effects of carbon dioxide. The influences of the thermal nonequilibrium on the flow properties in the shock layer become significant at an altitude above 60 km. As for the wall heating rate, however, its influence is not as strong as the influence of the wall catalyticity. The sensitivities of the wall heating rate to the uncertainties in the real gas effect models are investigated parametrically. The wall heating rate is strongly affected by the wall catalyticity. Consequently, a chemical nonequilibrium flow analysis is necessary for the analysis of the aerothermodynamic environment of a Mars aerocapture vehicle. Author (EI)

A95-70543

PRECISE ORBIT DETERMINATION WITH A SHORT-ARC TECHNIQUE

P. BONNEFOND Observatoire de la Cote d'Azur, Grasse, France and P. EXERTIER Observatoire de la Cote d'Azur, Grasse, France In *Interactions between physics and dynamics of solar system bodies; International Astronomical Symposium, Pleneuf-Val-Andre, France, Jun. 21-28, 1992.* A95-70509 Celestial Mechanics and Dynamical Astronomy (ISSN 0923-2958) vol. 57, no. 1-2 October 1993 p. 405

Copyright

Satellites carrying altimeters can measure the height of the satellite above the ocean surface with an accuracy of about 2 cm to 10 cm. In order to use fully these data, for studies of ocean topography, it is necessary to determine the height of the satellite above a reference surface with a similar accuracy; it is also necessary to calibrate the altimetric measurements. These points require a precise orbit determination in order to obtain an absolute satellite position with an accuracy of a few centimeters, at least locally, and essentially for the radial component. Considering the value of the expected accuracy of the radar altimeters, the use of a short-arc technique based on a geometric approach should permit us to take into account local errors in limited geographical regions which can not be considered in a global orbit computation by a dynamical approach. Our method consists in fitting the geometrical positions of the satellite over a short period of time with the tracking measurements from a ground station network and considering a simplified orbital error model. We correct the reference orbit by applying along-track, across-track and radial displacements, that are represented as simple constants, or with a linear or quadratic variation in time. The ability of the short-arc technique to reach the required accuracy on the radial orbit component is shown. Author (revised by Hemer)

N95-20646# Westinghouse Electric Corp., Baltimore, MD.

HIGH DENSITY MONOLITHIC PACKAGING TECHNOLOGY FOR DIGITAL/MICROWAVE AVIONICS

TIMOTHY FERTIG, THERESA WALTER, ERIC GAVER, and KEVIN LEAHY In AGARD, *Advanced Packaging Concepts for Digital Avionics* 12 p Oct. 1994

Copyright Avail: CASI HC A03/MF A03

There has been a need for generic technologies and common approaches in design, development, and manufacturing of military and commercial products. This need is more pronounced and pressing today than ever before. With the objective to dramatically enhance avionics reliability, maintainability and availability (RM&A), an integrated, generic technology for packaging, cooling, and interconnection of high density and high performance circuits was developed. It is named High Density Monolithic Packaging (HDMP). Under the sponsorship of Wright Laboratory, a two-part complementary program (1990-1994), named Advanced Radio-Frequency Packaging/ARFP was contracted to Westinghouse. Under the ARFP program, the HDMP technology is being applied and its promising capability is being assessed for its ability to reduce the low power RF avionics life-cycle cost. Being better than half way through the

program, the results and projections have been extremely promising. The technology assessment is approximately 50 percent complete and initial results have been extremely successful. Although the focus of the development effort has been on RF subsystems, the basic elements of HDMP technology have applications beyond RF/microwave subsystems. As digital processing speeds increase, RF/microwave design techniques must be applied to maintain high speed digital signal integrity. The basic elements of the HDMP technology are: low temperature co-fired ceramic (LTCC), solderless interconnects, multichip modules (MCM's), and composite heatsink materials. The key technology element, in this avionics availability enabling technology, is LTCC. LTCC material technology is a monolithic multilayered ceramic and conductor/metalization structure used as a substrate to support dense co-habitation of high density electronic circuits, their interconnections, and the electro-mechanical integrity of the integrated constituents. Author

N95-20906# Prins Maurits Lab. TNO, Rijswijk (Netherlands).

INTEGRAL ROCKET RAMJETS

R. F. CALZONE Mar. 1994 49 p

(AD-A285135; PML-1994-B29; TDCK-93-2570) Avail: CASI HC A03/MF A01

A rough overview of the important aspects and problem areas associated with the development of Integral Rocket Ramjet (IRR) technology is given in this report. The IRR is a supersonic air-breathing concept in which the gas generator produces fuel-rich gases. These fuel-rich gases are burnt in the secondary combustion chamber with ambient air captured and decelerated in the inlet. During the boost phase, a solid propellant booster provides the thrust necessary to achieve the velocity at which the ramjet may be operated (about $M = 2$). The booster is integrated in the secondary combustion chamber. DTIC

11

CHEMISTRY AND MATERIALS

Includes chemistry and materials (general); composite materials; inorganic and physical chemistry; metallic materials; nonmetallic materials; and propellants and fuels.

A95-71022

NUMERICAL MODELLING OF TRANSVERSE IMPACT ON COMPOSITE COUPONS

O. MAJEED Carleton Univ., Ottawa (Ontario), M. J. WORSWICK, P. V. STRAZNICKY, and C. POON Canadian Aeronautics and Space Journal (ISSN 0008-2821) vol. 40, no. 3 September 1994 p. 99-106 refs

(BTN-95-EIX95082502225) Copyright

Results from low- and high-energy impact simulations of composite coupons using the LS-DYNA3D finite element code are presented. The numerically-derived force and strain history data were compared with experimental data. The low-energy simulations were largely elastic, and the impact force and strain history results showed satisfactory agreement with the experimental data. The high-energy models generated significant damage, and the impact force history results were found to be highly dependent on the mesh discretization used for the composite coupon. Author (EI)

A95-71024

MODELLING OF PILLOWING DUE TO CORROSION IN FUSELAGE LAP JOINTS

N. C. BELLINGER Institute for Aerospace Research, Ottawa (Ontario), S. KRISHNAKUMAR, and J. P. KOMOROWSKI Canadian Aeronautics and Space Journal (ISSN 0008-2821) vol. 40, no. 3 September 1994 p. 125-130 refs

(BTN-95-EIX95082502227) Copyright

A mathematical model was developed to correlate the amplitude of the pillowing deformation of lap joints to the degree of

corrosion inside the joint. The model is expected to be capable of predicting the extent of the corrosion within a joint in terms of thickness loss at the internal surfaces from the amplitude of the pilling of the outer skin. The resulting out-of-plane displacements obtained from the model will be used to generate simulated D Sight images. D Sight is a simple optical non-destructive surface inspection technique that is capable of detecting changes in out-of-plane displacements greater than 10 micrometers. The model indicated that the pilling ratio (central deflection to thickness loss) caused by the corrosion products was independent of the modulus of rigidity and thickness of the skin. Finite element techniques in conjunction with the mathematical model were used to determine the amplitude of the pilling in a simple lap joint. Author (EI)

N95-20299# Lynntech, Inc., College Station, TX.
CORROSION OF AIRCRAFT MATERIALS: CORRELATION BETWEEN NANOMETER SCALE AND MACROSCOPIC STRUCTURAL DAMAGE PARAMETERS Annual Report
 A. GONZALES-MARTIN, D. HODKO, C. ANDREWS, and O. J. MURPHY 15 Aug. 1994 8 p
 (Contract(s)/Grant(s): F49620-94-C-0040)
 (AD-A285930; AFOSR-94-0674TR) Avail: CASI HC A02/MF A01

The following work has been carried out during the reporting period: (1) imaging of pitting corrosion initiation in aluminum at the nanometer scale; (2) study of the effects of main atmospheric pollutants on the initiation of the corrosion process; (3) identification of surface regions at an aluminum sample where corrosion is most likely to occur; (4) measurements of the electrochemical impedance spectra on Al sample before and during the pitting process in NaCl; and (5) identification of the impedance parameters characteristic for the pitting the corrosion of the aluminum sample. DTIC

N95-20481 Eltron Research, Inc., Boulder, CO.
ELECTROCHEMICAL IMPEDANCE PATTERN RECOGNITION FOR DETECTION OF HIDDEN CHEMICAL CORROSION ON AIRCRAFT COMPONENTS Annual Report,
 15 Jun. - 14 Aug. 1994
 ANTHONY F. SAMMELLS and JAMES S. BOWERS Aug. 1994
 4 p Limited Reproducibility: More than 20% of this document may be affected by microfiche quality
 (Contract(s)/Grant(s): F49620-94-C-0043)
 (AD-A284998; AFOSR-94-0608TR) Avail: CASI HC A01

This program is addressing the need for diagnostic instrumentation to detect the presence of hidden chemical corrosion occurring at aircraft titanium and aluminum alloys. The approach is being directed towards development of pattern recognition schemes based upon the initial on-line acquisition of electrochemical impedance spectra using Fast Fourier Transform Electrochemical Impedance Spectroscopy (FFTEIS) instrumentation from the suspect corrosion site. Author (DTIC)

N95-20655# Thomson-CSF, Paris (France). Div. Radars et Contre-Mesures.

COMPOSITE CASES FOR AIRBORNE ELECTRONIC EQUIPMENT: A TECHNOLOGY STUDY AND EMC [BOITIERS COMPOSITES POUR EQUIPEMENTS ELECTRONIQUES AEROPORTES: UNE ETUDE TECHNOLOGIQUE ET CEM]

B. DUMONT, J. LECUELLET, S. LAFORET, G. LABAUNE, and M. CAPLOT In AGARD, Advanced Packaging Concepts for Digital Avionics 12 p Oct. 1994 In FRENCH
 Copyright Avail: CASI HC A03/MF A03

The goal of this paper is to present work related to the development (study, fabrication, qualification) of a box and a bonnet cover out of composite materials intended for airborne electronic equipment on fighter aircraft. Work was undertaken with a double objective: assess mass characteristics compared to a metal case and obtain equivalent electromagnetic shielding performance. The technological step is presented: choice of materials and the processes of fabrication, mechanical and electromagnetic dimension-

ing. The methods of manufacture are described; they made it possible to obtain the desired characteristics. The metal composite material elements are currently being used on fighter aircraft.

Transl. by CASI

N95-20656# Sextant Avionique, Valence (France).
LIGHTWEIGHT ELECTRONIC ENCLOSURES USING COMPOSITE MATERIALS

C. SARNO In AGARD, Advanced Packaging Concepts for Digital Avionics 12 p Oct. 1994 Sponsored by Ministry of Defence
 Copyright Avail: CASI HC A03/MF A03

The ever increasing demand in technical and economical performances improvement of aircrafts has a direct incidence for avionics. Except microelectronic integration, the enclosures have a high potential of evolution. The main advantages of composite materials over metals in forming electronic enclosure are: reduction of weight (minimum 30 percent), better resistance to corrosion, improved fatigue and impact resistance, achievement of complex shapes, and low coefficient of thermal expansion. The main problems to be solved in extending the application of the use of composite materials to the field of airborne electronic equipments are to: provide adequate electromagnetic shielding, ensure survival in harsh thermal and mechanical environments, and achieve global competitiveness of the final products. Different technologies have been considered: injection molding of short fibers reinforced thermoplastic for small sized equipments (V less than 21), pressure molding of graphite and glass reinforced thermosets for ATR case families, and metal matrix composites. This paper will address the main investigations that have been undertaken in France since 1986 in the first two fields covering both manufacturing and evaluation results. Author

N95-20716# Eltron Research, Inc., Boulder, CO.
ELECTROCHEMICAL IMPEDANCE PATTERN RECOGNITION FOR DETECTION OF HIDDEN CHEMICAL CORROSION ON AIRCRAFT COMPONENTS Annual Report,
 15 Aug. - 14 Oct. 1994
 ANTHONY F. SAMMELLS and JAMES S. BOWERS 14 Oct. 1994
 4 p

(Contract(s)/Grant(s): F49620-94-C-0043)
 (AD-A285998; AFOSR-94-0673TR) Avail: CASI HC A01/MF A01
 Progress is presented for the program goal of developing diagnostic instrumentation for both detecting the presence and degree of hidden chemical corrosion on aircraft titanium and aluminum alloy components. DTIC

N95-21687 Battelle Columbus Labs., OH.
AIRCRAFT CORROSION STUDY Final Report
 J. T. STROPKI and R. D. SMITH Dec. 1993 62 p Limited Reproducibility: More than 20% of this document may be affected by microfiche quality
 (Contract(s)/Grant(s): F09603-90-D-2217)
 (AD-A279527; CGR/DC-01/94; USCG-D-05-94) Avail: Issuing Activity (Defense Technical Information Center (DTIC))

A comparison of the test results obtained for the unaged French and 2024-T3 (bare and hard anodized) alloys suggests that the resistance of all materials to raindrop erosion is identical. Superior performance of the hard anodized Alloy 2024-T3 sample was not observed during the erosion testing. Post-test examinations of the hard anodized 2024-T3 sample indicate that the performance of the coating was limited by spalling of the coating from the substrate. A review of the literature suggests that this condition is due to abnormal surface roughness of the anodic coating. This condition, which can be minimized with the application of silicone waxes (or similar surface treatments) to the coated surfaces, does contribute to poor chemical and impact resistance. No pretest surface characterizations were performed on this material. In summary, the results of this program suggest that Alloy 2024-T3 be considered as a candidate replacement material for the French alloy that is currently being used on the outer wing slats of the HU-25A aircraft. DTIC

11 CHEMISTRY AND MATERIALS

N95-21969 Dayton Univ., OH.

LUBRICANT EVALUATION AND PERFORMANCE, 2 Final Technical Report, 1 Jan. 1991 - 12 Jul. 1993

COSTANDY S. SABA, MICHAEL A. KELLER, KENNETH K. CHAO, DOUGLAS K. TOTH, MARY F. BORCHERS, and HOOVER A. SMITH Feb. 1994 475 p Limited Reproducibility: More than 20% of this document may be affected by microfiche quality (Contract(s)/Grant(s): F33615-88-C-2817)

(AD-A279144; UDR-TR-93-81-2; WL-TR-93-2126-2) Avail: Issuing Activity (Defense Technical Information Center (DTIC))

Thermal and oxidative stability, deposition and foaming techniques were developed for predicting the performance of candidate 4 cSt lubricants, polyphenyl ether (PPE), C-ether and other experimental fluids for use in advanced aircraft turbine engines. A novel sealed tube test was developed to study the rate of reaction in both liquid and vapor phase using only microliter quantities of the lubricants. Blending agents and/or diluents were used to improve the low temperature properties and high temperature oxidative stability of PPE. In-line magnetic wear sensors were evaluated as condition monitoring devices for oil systems with sensitivity well below 5 micrometers. Microfiltration effect on wear was investigated with the results showing effective reduction in secondary wear. HP-DSC analysis technique was limited as an oxidative stability screening device for PPE but was effective in demonstrating differences among various PPE formulations. The tribological behavior of high temperature fluids was evaluated and compared in the boundary lubrication regime using various steel and ceramic specimens. A sliding three-ball-on-disk wear test device was developed for reducing sample size, controlling scar geometry and determining lubricant consumption rate and tribochemistry. The effect of soft and hard solid particulates on the fatigue and wear lives of rolling elements was investigated using a recently developed three-ball rolling test. DTIC

N95-22132# Naval Air Warfare Center, Warminster, PA. Air Vehicle and Crew Systems Technology Dept.

CORROSION BEHAVIOR OF LANDING GEAR STEELS

EUN U. LEE 29 Oct. 1993 24 p (AD-A285862; NAWCADWAR-94001-60) Avail: CASI HC A03/MF A01

A study was conducted on the corrosion behavior of an AerMet 100 steel and a 300M steel. This study included investigations of stress corrosion cracking (SCC), immersion corrosion, salt spray corrosion, and humidity corrosion of both steels. For the SCC investigation, double cantilever beam (DCB) specimens were employed, and for the immersion, salt spray, and humidity corrosion investigations, sheet specimens were used. The SCC rate is less and the threshold stress intensity for stress corrosion (K_{ISCC}) is greater in the AerMet 100 steel (33 ksi*in(exp 1/2)) than in the 300M steel (19 ksi*in(exp 1/2)), indicating better SCC resistance of the AerMet 100 steel. In the AerMet 100 steel, the stress corrosion crack grows along an intergranular and transgranular path in the direction of forging deformation. The immersion corrosion and salt spray corrosion rates of the AerMet 100 steel is 33 - 40% and 13 - 20% of those for the 300M steel, respectively. Evidence of humidity corrosion is not detectable in the AerMet 100 steel within the employed test period 110 days, whereas it is substantial (2.0413 mpy or 0.0447 mdd) in the 300M steel. The overall results indicate that the AerMet 100 steel is superior to the 300M steel with respect to the corrosion resistance as well as the mechanical properties. DTIC

12

ENGINEERING

Includes engineering (general); communications; electronics and electrical engineering; fluid mechanics and heat transfer; instrumentation and photography; lasers and masers; mechanical engineering; quality assurance and reliability; and structural mechanics.

A95-69976

RCS MEASUREMENTS, TRANSFORMATIONS, AND COMPARISONS UNDER CYLINDRICAL AND PLANE WAVE

ILLUMINATION

V. J. VOKURA Arizona State Univ, Tempe, AZ, United States, **CONSTANTINE A. BALANIS, and CRAIG R. BIRTCHE** IEEE Transactions on Antennas and Propagation (ISSN 0018-926X) vol. 42, no. 3 March 1994 p. 329-334 refs (BTN-94-EIX94371347126) Copyright

Monostatic RCS measurements of a long bar (at X-band) and of a scale model aircraft (at C-band) were performed under the quasi-plane wave illumination produced by a dual parabolic-cylinder CATR. At Arizona State University's ElectroMagnetic Anechoic Chamber (EMAC) facility, these measurements were repeated under the cylindrical wave illumination produced by a March Microwave Single-Plane Collimating Range (SPCR). The SPCR measurements were corrected using the 'reference target method.' The corrected SPCR measurements are in good agreement with the CATR measurements. Author (EI)

A95-70131

CERCIGNANI-LAMPIS-LORD GAS-SURFACE INTERACTION MODEL: COMPARISONS BETWEEN THEORY AND SIMULATION

M. S. WORONOWICZ ViGYAN, Inc, Hampton, VA, United States and **D. F. G. RAULT** Journal of Spacecraft and Rockets (ISSN 0022-4650) vol. 31, no. 3 May-June 1994

p. 532-534

(BTN-95-EIX95041503806) Copyright

The article presents a study on the phenomenon of gas surface interaction using Cercigni Lampis Lord gas surface interaction model. The C-L model is incorporated into a free molecule theory to create complex expressions describing lift and drag coefficients. The experiment was done on flow over a single sided plate with freestream speed and direct simulation Monte Carlo (DSMC) estimates were studied for lift and drag coefficients. EI

A95-70132

INTEGRATED IR SENSORS

MICHAEL TOM Hughes Aircraft Co and **EDWARD TRUJILLO** Aerospace Engineering (Warrendale, Pennsylvania) (ISSN 0736-2536) vol. 14, no. 6 June 1994 p. 7-10

(BTN-95-EIX95041505023) Copyright

Integrated infrared (IR) sensors which exploit modular avionics concepts can provide features such as operational flexibility, enhanced stealthiness, and ease of maintenance to meet the demands of tactical, airborne sensor systems. On-board, tactical airborne sensor systems perform target acquisition, tracking, identification, threat warning, missile launch detection, and ground mapping in support of situation awareness, self-defense, navigation, target attack, weapon support, and reconnaissance activities. The use of sensor suites for future tactical aircraft such as US Air Force's multirole fighter require a blend of sensor inputs and outputs that may vary over time. It is expected that special-role units of these tactical aircraft will be formed to conduct tasks and missions such as anti-shiping, reconnaissance, or suppression of enemy air defenses. EI

A95-70844

MODELING RESONANCE IN WAVEGUIDE-TO-MICROSTRIP JUNCTIONS BY UNILATERAL FIN LINE RESONATORS

TAHAR KEZAI Univ Catholique de Louvain, Louvain-La-Neuve, Belgium and **ANDRE VANDERVORST** IEEE Transactions on Microwave Theory and Techniques (ISSN 0018-9480) vol. 42, no. 2 February 1994 p. 223-226 refs (BTN-94-EIX94381323445) Copyright

A method for the rigorous calculation of the resonant frequencies observed in waveguide-to-microstrip transitions is developed.

The method is general and includes all types of waveguide-to-microstrip junctions. The resonant parts are modeled as unilateral fin line resonators with similar shapes. The resonance frequencies are determined by using the spectral domain approach with appropriate basis functions. Measurements were made they are in good agreement with the data computed from the model. Author (EI)

A95-71033

ADAPTIVE REMESHING FOR CONVECTIVE HEAT TRANSFER WITH VARIABLE FLUID PROPERTIES

DOMINIQUE PELLETIER Ecole Polytechnique de Montreal, Montreal (Quebec), FLORIN ILINCA, and JEAN-FRANCOIS HETU Journal of Thermophysics and Heat Transfer (ISSN 0887-8722) vol. 8, no. 4 October-December 1994 p. 687-694 refs (BTN-95-EIX95082502720) Copyright

This article presents an adaptive finite element method based on remeshing to solve incompressible viscous flow problems for which fluid properties present a strong temperature dependence. Solutions are obtained in primitive variables using a highly accurate finite element approximation on unstructured grids. Two general purpose error estimators are presented, which take into account the temperature dependence of fluid properties. The methodology is applied to a problem of practical interest: the thermal convection of corn syrup in an enclosure with localized heating. Predictions are in good agreement with experimental measurements. The method leads to improved accuracy and reliability of finite element predictions. Author (EI)

A95-71040* National Aeronautics and Space Administration. Ames Research Center, Moffett Field, CA.

MEASUREMENT AND ANALYSIS OF NITRIC OXIDE RADIATION IN AN ARCJET FLOW

DIKRAN S. BABIKIAN, NIGEL K. J. M. GOPAUL, and CHUL PARK Journal of Thermophysics and Heat Transfer (ISSN 0887-8722) vol. 8, no. 4 October-December 1994 p. 737-743 refs (BTN-95-EIX95082502727) Copyright

Radiation from the nitric oxide (NO) band systems emitted by the flow in the test section of a 20-MW arcjet wind tunnel was measured and compared with the computed values for the purpose of testing the validity of an existing thermochemical model. The settling chamber pressure and enthalpy were 2.4 atm and 28 +/- 10 MJ/kg, respectively. The measurements were made using photographic films in the wavelength region from 225 to 305 nm. Of the four band systems of NO (beta, gamma, delta, and epsilon), vibrational transitions were observed from only the upper $v' = 0$ levels. Excitation temperatures were deduced by comparing the experimental spectrum with those calculated using the nonequilibrium radiation code NEQAIR. The rotational, vibrational, and electronic excitation temperatures deduced from the data were $T(\text{sub } r) = 560 \pm 50 \text{ K}$, $T(\text{sub } v) \text{ less than or } = 950 \pm 50 \text{ K}$, and $T(\text{sub } ex) = 11,500 \pm 520 \text{ K}$, respectively. A multitemperature nonequilibrium nozzle flow code NOZNT was used to calculate the nozzle flow. The calculated temperatures were $T(\text{sub } r) = 560 \text{ K}$, $T(\text{sub } v) = 950 \text{ K}$, and electron thermal temperature $T(\text{sub } e) = 6100 \text{ K}$, respectively at 30 MJ/kg. The presented results show that by using the centerline enthalpy value deduced from heat transfer measurement and the NOZNT code, one can predict the freestream conditions in an arcjet wind-tunnel flow fairly well. Author (EI)

A95-71744

LARGE-SCALE COMPUTATIONAL FLUID DYNAMICS BY THE FINITE ELEMENT METHOD

W. G. HABASHI Concordia Univ, Montreal, Que, Canada, M. ROBICHAUD, V.-N. NGUYEN, W. S. GHALY, M. FORTIN, and J. W. H. LIU International Journal for Numerical Methods in Fluids (ISSN 0271-2091) vol. 18, no. 11 June 15, 1994 p. 1083-1105 refs (BTN-94-EIX94381359154) Copyright

Solution methods are presented for the large systems of linear equations resulting from the implicit, coupled solution of the Navier-Stokes equations in three dimensions. Two classes of methods for such solution have been studied: direct and iterative methods. For direct methods, sparse matrix algorithms have been investigated and a Gauss elimination, optimized for vector-parallel processing, has been developed. Sparse matrix results indicate that reordering algorithms deteriorate for rectangular, i.e. $M \times M \times N$, grids in three dimensions as N gets larger than M . A new local nested dissection reordering scheme that does not suffer from these difficulties, at least in two dimensions, is presented. The vector-parallel Gauss elimination is very efficient for processing on today's supercomputers, achieving execution rates exceeding 2 center-dot 3 Gflops the Cray YMP-8 and 9 center-dot 2 Gflops on the NEC on SX3. For iterative methods, two approaches are developed. First, conjugate-gradient-like methods are studied and good results are achieved with a preconditioned conjugate gradient squared algorithm. Convergence of such a method being sensitive to the preconditioning, a hybrid viscosity method is adopted whereby the preconditioner has an artificial viscosity that is gradually lowered, but frozen at a level higher than the dissipation introduced in the physical equations. The second approach is a domain decomposition one in which overlapping domain and side-by-side methods are tested. For the latter, a Lagrange multiplier technique achieves reasonable rates of convergence. Author (EI)

A95-71867

BONDED COMPOSITE REPAIR OF CRACKED LOAD-BEARING HOLES

J. PAUL Aeronautical Research Lab, Melbourne, Australia, R. A. BARTHOLOMEUSZ, R. JONES, and M. EKSTROM Engineering Fracture Mechanics (ISSN 0013-7944) vol. 48, no. 3 June 1994 p. 455-461 refs (BTN-94-EIX94401360553) Copyright

Externally bonded composite repairs have recently been shown to be an effective technique for repairing a range of structural problems associated with cracked or damaged aircraft components, including multi-site damage in cracked fuselage lap-joints. This paper attempts to further clarify the mechanisms by which these repairs work. The results are presented of a combined numerical and experimental investigation into the use of bonded repairs for a load-bearing hole containing a single 'through-thickness' crack. The specimen was repaired with bonded boron/epoxy doublers and a steel sleeve insert. Constant amplitude fatigue tests were performed, on both the repaired and unrepaired specimens, and the resultant fatigue-crack-growth data are presented. This crack-growth data is then correlated with the stress intensity factors obtained from a three-dimensional finite element analysis. Author (EI)

A95-72648

ELECTROMAGNETIC BACKSCATTERING FROM A HELICOPTER ROTOR IN THE DECA-METRIC WAVE BAND REGIME

HARRY E. GREEN Univ of Adelaide, Adelaide, Australia IEEE Transactions on Antennas and Propagation (ISSN 0018-926X) vol. 42, no. 4 April 1994 p. 501-509 refs (BTN-94-EIX94381353130) Copyright

This paper gives a theoretical solution to the problem of determining the radar cross section and doppler spectrum of a helicopter rotor as presented to a radar operating in the decametric wave band (3-30 MHz). At such frequencies for all practical rotors the scattering regime is either Rayleighian or resonant. The solution proceeds by modeling the rotor as an equivalent set of radial wires on which the incident wave is assumed to excite sinusoidally distributed currents. It is shown that, subject to certain simplifying assumptions, the doppler spectrum has a form similar to that associated with tone modulation of a frequency modulated bearer. The theoretical work is confirmed by experiment. Author (EI)

12 ENGINEERING

N95-19912*# Detroit Diesel Allison, Indianapolis, IN.
EXPERIMENTAL STUDY OF VANE HEAT TRANSFER AND AERODYNAMICS AT ELEVATED LEVELS OF TURBULENCE Final Report
FORREST E. AMES Cleveland, OH NASA Nov. 1994 125 p
(Contract(s)/Grant(s): NAS3-25950; RTOP 505-62-10)
(NASA-CR-4633; E-9203; NAS 1.26:4633) Avail: CASI HC A06/MF A02

A four vane subsonic cascade was used to investigate how free stream turbulence influences pressure surface heat transfer. A simulated combustor turbulence generator was built to generate high level (13 percent) large scale (Lu approximately 44 percent inlet span) turbulence. The mock combustor was also moved upstream to generate a moderate level (8.3 percent) of turbulence for comparison to smaller scale grid generated turbulence (7.8 percent). The high level combustor turbulence caused an average pressure surface heat transfer augmentation of 56 percent above the low turbulence baseline. The smaller scale grid turbulence produced the next greatest effect on heat transfer and demonstrated the importance of scale on heat transfer augmentation. In general, the heat transfer scaling parameter $U(\text{sub infinity}) TU(\text{sub infinity}) LU(\text{sub infinity})(\text{exp } -1/3)$ was found to hold for the turbulence. Heat transfer augmentation was also found to scale approximately on $Re(\text{sub ex})(\text{exp } 1/3)$ at constant turbulence conditions. Some evidence of turbulence intensification in terms of elevated dissipation rates was found along the pressure surface outside the boundary layer. However, based on the level of dissipation and the resulting heat transfer augmentation, the amplification of turbulence has only a moderate effect on pressure surface heat transfer. The flow field turbulence does drive turbulent production within the boundary layer which in turn causes the high levels of heat transfer augmentation. Unlike heat transfer, the flow field straining was found to have a significant effect on turbulence isotropy. On examination of the one dimensional spectra for u' and v' , the effect to isotropy was largely limited to lower wavenumber spectra. The higher wavenumber spectra showed little or no change. The high level large scale turbulence was found to have a strong influence on wake development. The free stream turbulence significantly enhanced mixing resulting in broader and shallower wakes than the baseline case. High levels of flow field turbulence were found to correlate with a significant increase in total pressure loss in the core of the flow. Documenting the wake growth and characteristics provides boundary conditions for the downstream rotor. Author

N95-19953*# National Aeronautics and Space Administration, Lewis Research Center, Cleveland, OH.
FLOW COEFFICIENT BEHAVIOR FOR BOUNDARY LAYER BLEED HOLES AND SLOTS
B. P. WILLIS, D. O. DAVIS, and W. R. HINGST Jan. 1995 16 p
Presented at the 33rd Aerospace Sciences Meeting and Exhibit, Reno, NV, 9-12 Jan. 1995; sponsored by AIAA
(Contract(s)/Grant(s): RTOP 505-62-52)
(NASA-TM-106846; E-9420; NAS 1.15:106846; AIAA PAPER 95-0031) Avail: CASI HC A03/MF A01

An experimental investigation into the flow coefficient behavior for nine boundary layer bleed orifice configurations is reported. This test was conducted for the purposes of exploring boundary layer control through mass flow removal and does not address issues of stability bleed. Parametric data consist of bleed region flow coefficient as a function of Mach number, bleed plenum pressure, and bleed orifice geometry. Seven multiple hole configurations and two single slot configurations were tested over a supersonic Mach number range of 1.3 to 2.5 (nominal). Advantages gained by using multiple holes in a bleed region instead of a single spanwise slot are discussed and the issue of modeling an entire array of bleed orifices based on the performance of a single orifice is addressed. Preconditioning the flow approaching a 90 degree inclined (normal) hole configuration resulted in a significant improvement in the performance of the configuration. The same preconditioning caused only subtle changes in performance for a 20 degree inclined (slanted) configuration. Author

N95-20191# National Inst. of Standards and Technology, Boulder, CO. Electronics and Electrical Engineering Lab.
MEASUREMENTS OF SHIELDING EFFECTIVENESS AND CAVITY CHARACTERISTICS OF AIRPLANES
D. A. HILL, M. L. CRAWFORD, R. T. JOHNK, A. R. ONDREJKA, and D. G. CAMELL Jul. 1994 63 p
(PB94-210051; NISTIR-5023) Avail: CASI HC A04/MF A01

We present measured data for shielding effectiveness, cavity Q, and cavity time constant of three small (twin-engine) airplanes for frequencies from 400 MHz to 18 GHz. Both CW and time-domain measurement methods were used, and the time-domain method yields higher values of cavity Q. Both methods yield Q values below a theoretical upper bound determined by window leakage losses. The measured shielding effectiveness is quite variable, but averages about 15 dB. The measured time constants are also variable and average about 15 ns. This short time constant is a result of the low Q of the aircraft cavities. NTIS

N95-20295 Department of the Navy, Washington, DC.
MALONE-BRAYTON CYCLE ENGINE/HEAT PUMP Patent
THOMAS A. GILMOUR, inventor (to Navy) 12 Jul. 1994 9 p
Filed 28 Sep. 1993
(AD-D016573; US-PATENT-5,327,745; US-PATENT-APPL-SN-127567; US-PATENT-CLASS-62-467) Avail: US Patent and Trademark Office

A machine, such as a heat pump, and having an all liquid heat exchange fluid, operates over a more nearly ideal thermodynamic cycle by adjustment of the proportionality of the volumetric capacities of a compressor and an expander to approximate the proportionality of the densities of the liquid heat exchange fluid at the chosen working pressures. Preferred forms of a unit including both the compressor and the expander on a common shaft employs difference in axial lengths of rotary pumps of the gear or vane type to achieve the adjustment of volumetric capacity. Adjustment of the heat pump system for differing heat sink conditions preferably employs variable compression ratio pumps. DTIC

N95-20414 Southwest Research Inst., San Antonio, TX.
EDDY CURRENT FOR DETECTING SECOND-LAYER CRACKS UNDER INSTALLED FASTENERS Final Report, 30 Sep. 1991 - 31 Oct. 1993
GARY L. BUCKHARDT, ROBERT E. BEISSNER, EDITH A. CREEK, and JAY L. FISHER Feb. 1994 110 p Limited Reproducibility: More than 20% of this document may be affected by microfiche quality
(Contract(s)/Grant(s): F33615-91-C-5661)
(AD-A279871; SWRI-17-4665; WL-TR-93-4125) Avail: Issuing Activity (Defense Technical Information Center (DTIC))

Southwest Research Institute developed an eddy current (EC) laboratory breadboard inspection system to detect second-layer cracks around installed fasteners in two-layer airframe structures with the probe positioned on the first layer (outside surface). Probe design considered both cup and segment-core configurations as exciter coils and various orientations and positions of sensor coils. Highest sensitivity was obtained with a segment-core exciter covering an 85 degree segment with the sensor oriented normal to the specimen surface and placed near the core outer leg. EC data were presented in two-dimensional color images. The goal of detecting a 2.5mm second-layer flaw through a first-layer thickness of 6.4mm was achieved in eight of nine specimen configurations which contained simulated cracks. The specimens included structure geometries containing second-layer edges, first-layer edges, adjacent fasteners, different fastener sizes, different flaw orientations around the hole, and fasteners of different materials (titanium and steel). In fatigue crack specimens supplied by WL/MLLP, where adjacent fasteners were spaced more closely and caused interfering signals, flaw detection was more difficult; however, a 2.5mm flaw was detected through a 4.5mm first layer by comparing the signal patterns from adjacent holes. DTIC

N95-20484# Colorado Univ., Boulder, CO. Dept. of Chemistry and Biochemistry.

STATE-TO-STATE COLLISIONAL DYNAMICS OF ATMOSPHERIC SPECIES Technical Report, 1 Aug. 1993 - 31 Jul. 1994

DAVID J. NESBITT 30 Aug. 1994 6 p
(Contract(s)/Grant(s): F49620-93-1-0444; AF-AFOSR-0231-93) (AD-A285053; JILA-153-1236; AFOSR-94-0559TR) Avail: CASI HC A02/MF A01

The AFOSR/AASERT research efforts over this past year have been toward the following two thrusts: (1) state-to-state collisional energy transfer in H₂O, HF and CH₄ in crossed molecular beams via high sensitivity, direct absorption of a single mode IR probe laser, and (2) development and testing of high resolution IR laser Dopplerimetry methods for measuring velocity and quantum-state resolved Cl + HCl scattering in open shell collision systems. DTIC

N95-20530*# Air Force Systems Command, Wright-Patterson AFB, OH.

PHOTOVOLTAIC ELECTRIC POWER APPLIED TO UNMANNED AERIAL VEHICLES (UAV)

JACK GEIS and JACK H. ARNOLD (Rockwell International Corp., Canoga Park, CA.) In NASA. Lewis Research Center, Proceedings of the 13th Space Photovoltaic Research and Technology Conference (SPRAT 13) p 257-268 Sep. 1994
Avail: CASI HC A03/MF A04

Photovoltaic electric-powered flight is receiving a great deal of attention in the context of the United States' Unmanned Aerial Vehicle (UAV) program. This paper addresses some of the enabling technical areas and their potential solutions. Of particular interest are the long-duration, high-altitude class of UAV's whose mission it is to achieve altitudes between 60,000 and 100,000 feet, and to remain at those altitudes for prolonged periods performing various mapping and surveillance activities. Addressed herein are studies which reveal the need for extremely light-weight and efficient solar cells, high-efficiency electric motor-driven propeller modules, and power management and distribution control elements. Since the potential payloads vary dramatically in their power consumption and duty cycles, a typical load profile has been selected to provide commonality for the propulsion power comparisons. Since missions vary widely with respect to ground coverage requirements, from repeated orbiting over a localized target to long-distance routes over irregular terrain, we have also averaged the power requirements for on-board guidance and control power, as well as ground control and communication link utilization. In the context of the national technology reinvestment program, wherever possible we modeled components and materials which have been qualified for space and defense applications, yet are compatible with civilian UAV activities. These include, but are not limited to, solar cell developments, electric storage technology for diurnal operation, local and ground communications, power management and distribution, and control servo design. And finally, the results of tests conducted by Wright Laboratory on ultralight, highly efficient MOCVD GaAs solar cells purchased from EPI Materials Ltd. (EML) of the UK are presented. These cells were also used for modeling the flight characteristics of UAV aircraft. Author (revised)

N95-20599 Massachusetts Inst. of Tech., Lexington, MA. Lincoln Lab.

GPS-SQUITTER CAPACITY ANALYSIS

VINCENT A. ORLANDO and WILLIAM H. HARMAN 20 May 1994 46 p Limited Reproducibility: More than 20% of this document may be affected by microfiche quality
(Contract(s)/Grant(s): DTFA01-93-Z-02012; F19628-90-C-0002) (AD-A280037; ATC-214) Avail: Issuing Activity (Defense Technical Information Center (DTIC))

GPS-Squitter is a system concept that merges the capabilities of Automatic Dependent Surveillance (ADS) and the Mode S beacon radar. The result is an integrated concept for seamless surveillance and data link that permits equipped aircraft to participate in ADS and/or beacon ground environments. This concept offers many possibilities for transition from a beacon to an ADS-based environment. This report provides the details of the techniques used to estimate GPS-Squitter surveillance

and data link capacity. Surveillance capacity of airborne aircraft is calculated for the omni and six-sector ground stations. Next, the capacity of GPS-Squitter for surface traffic is estimated. The interaction between airborne and surface operations is addressed to show the independence of these systems. Air ground data link capacity for GPS-Squitter is estimated, together with an estimate of the use of the Mode S link to support other ground surveillance and data link activities as well as TCAS operation. The analysis indicates the low transponder occupancy resulting from the total effect of these activities. Low occupancy is a key requirement in avoiding interference with the operation of the current ATCRBS and future Mode S interrogators. DTIC

N95-20638# Texas Instruments, Inc., Dallas, TX. Defense Systems and Electronics Group.

ULTRA-RELIABLE DIGITAL AVIONICS (URDA) PROCESSOR

REAGAN BRANSTETTER, WILLIAM RUSZCZYK, and FRANK MIVILLE In AGARD, Advanced Packaging Concepts for Digital Avionics 10 p Oct. 1994

Copyright Avail: CASI HC A02/MF A03

Texas Instruments Incorporated (TI) developed the URDA processor design under contract with the U.S. Air Force Wright Laboratory and the U.S. Army Night Vision and Electro-Sensors Directorate. TI's approach couples advanced packaging solutions with advanced integrated circuit (IC) technology to provide a high-performance (200 MIPS/800 MFLOPS) modular avionics processor module for a wide range of avionics applications. TI's processor design integrates two Ada-programmable, URDA basic processor modules (BPM's) with a JIAWG-compatible PiBus and TMBus on a single F-22 common integrated processor-compatible form-factor SEM-E avionics card. A separate, high-speed (25-MWord/second 32-bit word) input/output bus is provided for sensor data. Each BPM provides a peak throughput of 100 MIPS scalar concurrent with 400-MFLOPS vector processing in a removable multichip module (MCM) mounted to a liquid-flowthrough (LFT) core and interfacing to a processor interface module printed wiring board (PWB). Commercial RISC technology coupled with TI's advanced bipolar complementary metal oxide semiconductor (BiCMOS) application specific integrated circuit (ASIC) and silicon-on-silicon packaging technologies are used to achieve the high performance in a miniaturized package. A Mips R4000-family reduced instruction set computer (RISC) processor and a TI 100-MHz BiCMOS vector coprocessor (VCP) ASIC provide, respectively, the 100 MIPS of a scalar processor throughput and 400 MFLOPS of vector processing throughput for each BPM. The TI Aladdin ASIC chipset was developed on the TI Aladdin Program under contract with the U.S. Army Communications and Electronics Command and was sponsored by the Advanced Research Projects Agency with technical direction from the U.S. Army Night Vision and Electro-Sensors Directorate. Author

N95-20643# Rome Lab., Griffiss AFB, NY.

RELIABILITY ASSESSMENT OF MULTICHIP MODULE TECHNOLOGIES VIA THE TRISERVICE/NASA RELTECH PROGRAM

DANIEL F. FAYETTE In AGARD, Advanced Packaging Concepts for Digital Avionics 9 p Oct. 1994
Copyright Avail: CASI HC A02/MF A03

Multichip Module (MCM) packaging/interconnect technologies have seen increased emphasis from both the commercial and military communities as a means of increasing capability and performance while providing a vehicle for reducing cost, power and weight of the end item electronic application. This is accomplished through three basic Multichip module technologies, MCM-L that are laminates, MCM-C that are ceramic type substrates and MCM-D that are deposited substrates (e.g., polymer dielectric with thin film metals). Three types of interconnect structures are also used with these substrates and include, wire bond, Tape Automated Bonds (TAB) and flip chip ball bonds. Application, cost, producibility and reliability are the drivers that will determine which MCM technology will best fit a respective need or requirement. With all the benefits and technologies cited, it would be expected that the use of, or the planned use of, MCM's would be more extensive in both military and commercial

applications. However, two significant roadblocks exist to implementation of these new technologies: the absence of reliability data and a single national standard for the procurement of reliable/quality MCM's. To address the preceding issues, the Reliability Technology to Achieve Insertion of Advanced Packaging (RELTECH) program has been established. This program, which began in May 1992, has endeavored to evaluate a cross section of MCM technologies covering all classes of MCM's previously cited. NASA and the Tri-Services (Air Force Rome Laboratory, Naval Surface Warfare Center, Crane IN and Army Research Laboratory) have teamed together with sponsorship from ARPA to evaluate the performance, reliability and producibility of MCM's for both military and commercial usage. This is done in close cooperation with our industry partners whose support is critical to the goals of the program. Several tasks are being performed by the RELTECH program and data from this effort, in conjunction with information from our industry partners, as well as discussions with industry organizations (IPC, EIA, ISHM, etc.) are being used to develop the qualification and screening requirements for MCM's. Specific tasks being performed by the RELTECH program include technical assessments, product evaluations, reliability modeling, environmental testing, and failure analysis. This paper will describe the various tasks associated with the RELTECH program, status, progress and a description of the national dual use specification being developed for MCM technologies. Author

N95-20644# Rome Lab., Griffiss AFB, NY.
ASSURING KNOWN GOOD DIE (KGD) FOR RELIABLE, COST EFFECTIVE MCMS
 DANIEL E. DASKIEWICH In AGARD, Advanced Packaging Concepts for Digital Avionics 7 p Oct. 1994
 Copyright Avail: CASI HC A02/MF A03

A key requirement for achieving high yield multichip modules (MCM's) is assuring that the individual dice are known good devices (KGD). A KGD is defined as a bare die available at the same quality and reliability as the equivalent single chip packaged parts. Integrated circuits (IC's) that are Known Good will function over a specified temperature range, are compatible with the MCM approach utilized, and contain no short-term or long-term reliability hazards. The application of reliability and testability techniques at all levels of MCM development, particularly at the chip level, will maximize MCM yield. Today's testing and qualification requirements, defined by MIL-STD-883 Methods 5008 and 2010, are not capable of assuring KGD as defined above. The development of cost effective requirements for achieving 99.9 percent yields poses a challenge which requires new and novel approaches and better methods for bare die testing, wafer level burn-in, tape automated bonding (TAB), temporary packaging, at-speed device testing at the wafer, die, and MCM level. Also of great importance are the methods for built-in self test (BIST), built-in test (BIT), and boundary scan. New standards in very large scale integration (VLSI) device testing must be developed in order for MCM's to be reliable and economical. Rome Laboratory (RL) has funded a program to address and develop these requirements. The objectives of the RL program are to: research and evaluate current and proposed burn-in, electrical and interconnect test techniques for assuring known good VLSI circuits at wafer and die level; and evaluate various methods of incorporating testability features which will decrease test time and cost. In addition, MCM-level reliability and performance assessment procedures will be evaluated to determine appropriate testing concepts and procedures that will assure the procurement of reliable, cost effective MCM's for DOD/NASA applications. The program consists of two phases: Phase One will be a study phase to evaluate, analyze, trade-off, and select best techniques for test and burn-in of wafers, bare die and MCM's. Phase Two will be a demonstration of a cost effective procedure for assuring high quality/reliable production of MCM's based on the KGD methods developed in Phase One. Author

N95-20647# Maryland Univ., College Park, MD. CALCE Electronic Packaging Research Center.
LIQUID FLOW-THROUGH COOLING OF ELECTRONIC

MODULES

S. SRIDHAR, M. D. OSTERMAN, J. M. CARBONELL (Wright Lab., Wright-Patterson AFB, OH.), and K. E. HEROLD In AGARD, Advanced Packaging Concepts for Digital Avionics 6 p Oct. 1994
 Sponsored by Westinghouse Electric Corp. and AMRL
 Copyright Avail: CASI HC A02/MF A03

Thermal management of future avionics modules will be a critical design issue. New advances in integrated circuit technology and electronic packaging will allow the design of densely populated electronics modules with potential power dissipation levels in excess of 1.0 W/cm² (exp 2). While the module power level trend will be to increase, the maximum allowable junction temperature for integrated circuits may be lowered to provide more benign thermal environment for electronics. This negates the use of conventional thermal management techniques in new avionics applications. A number of trade studies were performed to determine which cooling technique would be best suited to meet the anticipated reliability and performance requirements for the year 2005 and beyond. The approaches to module cooling technologies considered were: edge cooled conduction, immersion, and hollow core flow-through. The technology selected was the hollow core flow-through. This paper discusses the results of flow-through cooling investigations on both single-pass cold plates and SEM-E modules. Author

N95-20648# Naval Air Warfare Center, Indianapolis, IN. Aircraft Div.

IMMERSION/TWO PHASE COOLING
 JACK JONES and EMMETT PERKOSKI In AGARD, Advanced Packaging Concepts for Digital Avionics 11 p Oct. 1994
 Copyright Avail: CASI HC A03/MF A03

Due to increasing heat dissipation requirements, the need for an advanced cooling technique in current military avionics has been recognized. Immersion cooling with phase change has been demonstrated in a Format E clamshell module as an alternative. This module is capable of dissipating more than 700 Watts. From the development of the Format E clamshell module the AAS&T (Advanced Avionics Subsystems and Technology) Program has begun an effort to utilize the clamshell module in the development of a 3/4 ATR Format E Standard Avionics Enclosure utilizing immersion/change of phase cooling. The power dissipation requirement for the enclosure is 6500 Watts minimum. The cooling medium for both efforts is a Fluorinert (FS-72). The FS-72 is an environmentally safe coolant. As the need for greater heat removal and reliability increases, cooling technology must become more advanced to meet the needs of next generation aircraft. Author

N95-20649# Deutsche Aerospace A.G., Munich (Germany). Military Aircraft Div.

MICROCHANNEL HEAT PIPE COOLING OF MODULES
 G. MOSER In AGARD, Advanced Packaging Concepts for Digital Avionics 12 p Oct. 1994
 Copyright Avail: CASI HC A03/MF A03

The purpose of this presentation is the proposal of a novel, highly sophisticated cooling technique with a promising performance, but with a very early status of development - the microchannel heat pipe cooling. This technique can be directly adapted to the basic idea of Modular Avionics resulting on the hardware side in a modular packaging design with interchangeable modules. Due to the early status of the development and of the basic research some of the very stringent requirements for military airborne equipment are not met yet (or information is missing) like the impact of acceleration and orientation; nevertheless, the normal performance capability is highly compliant with the dramatically increasing local maximum heat densities and total maximum heat dissipations, which are forecast for future avionic applications. The presentation shall highlight the status of the development and the benefits of this technique; the latter is done by a comparison to the well established cooling methods for the module like Liquid Flow Through (LFT) and conduction cooling, in order to provide a clear impression of the cooling capabilities. Especially if the microchannel heat pipe is combined with a micro heat exchanger for the heat transfer off the

module, the performance with respect to the maximum local heat density, the most challenging requirement for the future, is high in excess of the LFT method. Author

N95-20653# GEC-Marconi Materials Technology, Towcester (England).

HIGH PERFORMANCE BACKPLANE COMPONENTS FOR MODULAR AVIONICS

C. J. GROVES-KIRKBY, M. J. GOODWIN, J. P. HALL, G. GLYNN, J. HANKEY, M. D. SALIK, R. C. GOODFELLOW, and D. J. JIBB (GEC-Marconi Avionics Ltd., Chelmsford, England.) In AGARD, Advanced Packaging Concepts for Digital Avionics 6 p Oct. 1994 (Contract(s)/Grant(s): ESPRIT 3 PROJ. 6276) Copyright Avail: CASI HC A02/MF A03

The design and development of optoelectronic transceiver and optical pathway components for application in a modular avionics backplane demonstrator system are described and initial performance results are presented. Author

N95-20658# Alenia, Turin (Italy). Div. Avionica Apparat Speciali. **ELECTROMAGNETIC COMPATIBILITY EFFECTS OF ADVANCED PACKAGING CONFIGURATIONS**

B. AUDONE, L. BOLLA, and D. TARDUCCI In AGARD, Advanced Packaging Concepts for Digital Avionics 5 p Oct. 1994 Copyright Avail: CASI HC A01/MF A03

The Electromagnetic Compatibility (EMC) of digital avionic equipments assumes ever larger dimensions especially in the light of the tendency of modern technology aimed at higher data transmission rates and therefore higher clock frequencies and, at the same time, higher component density with reduced consumption. The emission and susceptibility problems commonly encountered in digital circuits are examined indicating critical areas and practicable suggestions to improve design techniques. Author

N95-20771# Kaman Sciences Corp., Albuquerque, NM. **FAULT DETECTION TECHNIQUES FOR COMPLEX CABLE SHIELD TOPOLOGIES** Final Report, 24 Aug. 1992 - 24 Aug. 1993

KURT H. COONROD, STUART L. DAVIS, and DONALD P. MCLEMORE Sep. 1994 65 p (Contract(s)/Grant(s): F29601-92-C-0109) (AD-A286632; PL-TR-93-1111) Avail: CASI HC A04/MF A01

This document presents the results of a basic principles study which investigated technical approaches for developing fault detection techniques for use on cables with complex shielding topologies. The study was limited to those approaches which could realistically be implemented on a fielded cable, i.e., approaches which would require partial disassembly of a cable were not pursued. The general approach used was to start with present transfer impedance measurement techniques and modify their use to achieve the best possible measurement range. An alternative test approach, similar to a sniffer type test, was also investigated. DTIC

N95-20781# Oak Ridge National Lab., TN. **SCALE-UP AND MODELING OF FORCED CHEMICAL VAPOR INFILTRATION**

T. M. BESMANN, J. C. MCLAUGHLIN, and T. L. STARR (Georgia Tech Research Inst., Atlanta, GA.) 1994 11 p Presented at the 18th Annual Conference on Composites and Advanced Ceramics, Cocoa Beach, FL, 9-14 Jan. 1994 (Contract(s)/Grant(s): DE-AC05-84OR-21400) (DE94-017769; CONF-940135-9) Avail: CASI HC A03/MF A01

The forced flow-thermal gradient chemical vapor infiltration (FCVI) process has been scaled-up from a maximum of 7.6 cm dia. disk to fabrication of 24 cm dia. disks, 1.6 cm in thickness. The components are turbine rotor subelements produced from polar

weave Tyranno fibers preforms. The disks were subjected to non-destructive testing and spin-tested to high rpm. The processing conditions were modeled with the GTCVI code to aid in optimization. DOE

N95-20849# Catholic Univ. of America, Washington, DC. Dept. of Mechanical Engineering.

APPLICATION OF WAVELET-FILTERING TECHNIQUES TO INTERMITTENT TURBULENT AND WALL PRESSURE EVENTS. PART 1: EXPLORATORY RESULTS Progress Report, Oct. 1993 - Oct. 1994

PABLO B. PENAFIEL, MARIO J. CASARELLA, and MARK KAMMEYER 25 Oct. 1994 43 p (Contract(s)/Grant(s): N00014-88-K-0141) (AD-A286077) Avail: CASI HC A03/MF A01

Large amplitude wall-pressure events, observed beneath a turbulent boundary layer, appear to be the signatures of intermittent organized motions within the turbulent flow. The temporal localization of these events could be applied to the active control of turbulent wall flows. This report presents preliminary results on utilizing time-frequency localization techniques (wavelet transforms) for the detection of these events. The advantage of these methods is that they do not require a priori assumptions regarding the features of the signal. A tutorial overview of these techniques is first presented. This is followed by a discussion of some exploratory results obtained from the application of wavelet filtering to wall pressure and turbulent temporal records acquired from wind tunnel experiments. DTIC

N95-20945# Centre de Recherches en Physique de l'Environnement, Velizy (France).

EXPERIMENTAL STUDY OF THE HELICOPTER-MOBILE RADIOELECTRICAL CHANNEL AND POSSIBLE EXTENSION TO THE SATELLITE-MOBILE CHANNEL

V. BLANCHETIERE-CIARLETTI, M. SYLVAIN, and P. LEMENN In AGARD, Multiple Mechanism Propagation Paths (MMPPs): Their Characterisation and Influence on System Design 12 p Jul. 1994 Copyright Avail: CASI HC A03/MF A04

The use of satellite seems to be an answer to the radioelectrical covering problem for the mobile communications, particularly in the low populated areas. Frequency bands at 1.5 and 2.5 GHz have been dedicated to these future services. Satellite-mobile links will be much more affected by propagation phenomena than the existing links between satellites and fixed stations. The reasons for that are twofold: The probable use of LEO (Low-Earth-Orbit) satellites instead of GEO; such satellites will have to be received at relatively low elevation to limit their number; the use of mobile communication terminals with small and non directive antennas that must work in various environments instead of terrestrial stations located at carefully chosen places and equipped with large diameter parabolics. These propagation phenomena mainly consist in the fading of the signal level (shadowing of the link), and a frequency selective fading due to multipath propagation. The experience run by C.R.P.E. is aimed at a better understanding of the satellite-mobile propagation channel at fixed frequency as well as on a large band. In this paper, we discuss preliminary results from a series of propagation measurements performed (by lack of any experimental satellite) on an experimental radio link at 1.45 GHz on a of 20 MHz bandwidth between a helicopter flying at a height of 2 km and a mobile receiver. The whole experiment has been run in a rural environment in Brittany (France). In a first part, we illustrate the quality of the data collected during the experiment on a typical case study and give a possible physical interpretation of the observed phenomena. Then we present statistical results concerning the various characteristics (attenuation and delay spreads) of the propagation channel. Finally, we discuss the problem of using a helicopter (flying at a height of 2 km) as a substitute for a satellite at about 1000 km and try to estimate to what extent it is possible to use the data collected during this experiment to characterize the satellite-mobile channel. To do that,

both the helicopter-mobile and the satellite-mobile propagation channels are simulated under the same environmental conditions.

Author

N95-20966 Institute for Defense Analyses, Alexandria, VA.
**THE OPPORTUNITIES FOR AND CHALLENGES OF
COMMON INTEGRATED ELECTRONICS Final Report, Jul. -
Dec. 1993**

J. R. NELSON, BERNARD L. RETTERER, and HARLEY A. CLOUD
Feb. 1994 40 p Limited Reproducibility: More than 20% of this
document may be affected by microfiche quality
(Contract(s)/Grant(s): MDA903-89-C-0003)
(AD-A279991; IDA-D-1490; IDA/HQ-93-44599; AD-E501787) Avail:
CASI HC A03

This document summarizes a portion of IDA's work concerning
common integrated electronics and the potential cost savings of using
common electronic hardware and software. It addresses trends in
avionics costs and recent experiences in applying common electronic
standards to weapon programs as a way to reduce costs. The following
essential elements of a program to acquire common integrated elec-
tronics are explored: (1) integrated system architecture; (2) advanced
technology programs; (3) open system standards; (4) standard com-
mon modules; and (5) associated management and policies. The
principal recommendation is that OSD support and coordinate such a
program by taking a strong leadership role and setting standards policy.

DTIC

N95-20998# Army Research Lab., Aberdeen Proving Ground, MD.
**STATISTICAL ANALYSIS OF TURBINE ENGINE
DIAGNOSTIC (TED) FIELD TEST DATA Final Report, Aug.
1993 - Jun. 1994**

MALCOLM S. TAYLOR and JOHN T. MONYAK Nov. 1994 23 p
(AD-A286032; ARL-TR-614) Avail: CASI HC A03/MF A01

During the summer of 1993, a field test of turbine engine diagnos-
tic (TED) software, developed jointly by U.S. Army Research Labora-
tory and the U.S. Army Ordnance Center and School, was conducted
at Fort Stuart, GA. The data were collected in conformance with a cross-
over design, some of whose considerations are detailed. The initial
analysis of the field test data was exploratory, followed by a more formal
investigation. Technical aspects of the data analysis insights that were
elicited are reported.

DTIC

N95-21001# Naval Postgraduate School, Monterey, CA.
**A COMPUTER CODE (SKINTEMP) FOR PREDICTING
TRANSIENT MISSILE AND AIRCRAFT HEAT TRANSFER
CHARACTERISTICS M.S. Thesis**

MARY L. CUMMINGS Sep. 1994 64 p
(AD-A286044) Avail: CASI HC A04/MF A01

A FORTRAN computer code (SKINTEMP) has been developed
to calculate transient missile/aircraft aerodynamic heating param-
eters utilizing basic flight parameters such as altitude, Mach number,
and angle of attack. The insulated skin temperature of a vehicle
surface on either the fuselage (axisymmetric body) or wing (two-
dimensional body) is computed from a basic heat balance relationship
throughout the entire spectrum (subsonic, transonic, supersonic,
hypersonic) of flight. This calculation method employs a simple finite
difference procedure which considers radiation, forced convection,
and non-reactive chemistry. Surface pressure estimates are based on
a modified Newtonian flow model. Eckert's reference temperature
method is used as the forced convection heat transfer model. SKINTEMP
predictions are compared with a limited number of test
cases. SKINTEMP was developed as a tool to enhance the concep-
tual design process of high speed missiles and aircraft. Recommen-
dations are made for possible future development of SKINTEMP to
further support the design process.

DTIC

N95-21061# Advisory Group for Aerospace Research and Devel-
opment, Neuilly-Sur-Seine (France). Fluid Dynamics Panel.
**APPLICATION OF DIRECT AND LARGE EDDY SIMULATION
TO TRANSITION AND TURBULENCE [L'APPLICATION DE
LA SIMULATION DIRECTE ET DE LA SIMULATION DES**

**GROS TOURBILLONS A LA TRANSITION ET A LA
TURBULENCE]**

Dec. 1994 400 p In ENGLISH and FRENCH The 74th symposium
was held in Chania, Greece, 18-21 Apr. 1994 Original contains
color illustrations
(AGARD-CP-551; ISBN-92-836-0006-1) Copyright Avail: CASI HC
A17/MF A04

The papers prepared for the AGARD Fluid Dynamics Panel (FDP)
Symposium on 'Application of Direct and Large Eddy Simulation to
Transition and Turbulence', which was held April 1994 in Greece are
contained in this report. In addition, a Technical Evaluator's Report
assessing the success of the Symposium objectives, and an edited
transcript of the General Discussion are also included. In the past two
decades significant progress has been made in the numerical simula-
tion of turbulent flows. Vast improvements in speed and memory size
of modern supercomputers, and recent progress in simulation algo-
rithms and parallel computation have put us on the threshold of being
able to simulate flows in configurations of engineering interest. For
individual titles, see N95-21062 through N95-21098.

N95-21096# Hellenic Air Force Academy, Athens (Greece). Dept.
of Aerodynamics.

**INVESTIGATION OF SHEAR LAYER TRANSITION USING
VARIOUS TURBULENCE MODELS**

J. K. KALDELLIS and G. A. GEORGANTOPOULOS In AGARD,
Application of Direct and Large Eddy Simulation to Transition and
Turbulence 11 p Dec. 1994

Copyright Avail: CASI HC A03/MF A04

The accurate prediction of shear layer transition plays an impor-
tant role in the performance amelioration of modern aero-mechanical
devices, since transitional shear layers are frequently observed on axial
turbomachine blades and other low Reynolds number airfoils. In the
present work some of the most famous existing turbulence models are
used in order to analyze a large variety of well documented experimen-
tal transitional shear flows. Particular attention is paid to the estimation
of the transition length and to the calculation of loss evolution inside the
transition area. Finally interesting conclusions of the proposed analysis
are summarized in the last part of the paper, where the behavior of
several transitional blade shear layers is examined, applying the most
reliable of the above tested turbulence models.

Author

N95-21132# National Defence Research Establishment, Stockholm
(Sweden). Dept. of Weapon Systems, Effects and Protection.
**COMPUTATION OF TRANSONIC FLOW ON COMPOSITE
OVERLAPPING GRIDS IN 2 D**

BRODD LEIF ANDERSSON Apr. 1994 134 p
(ISSN 0347-3694)

(PB95-131348; FOA-C-20972-2.5) Avail: CASI HC A07/MF A02

We study the composite overlapping grid technique by applying it
to two cases of transonic flow past an airfoil in two dimensions. A second
order accurate explicit time marching finite difference scheme for the
pseudo-unsteady Euler equations together with first order
nonconservative interpolation at the component grid interfaces has
been used. The numerical results indicate that the technique of
overlapping grids is very useful if the decomposition of the domain is
made carefully. A substantial improvement of the resolution in particular
parts of the domain is easily obtained by the use of refined subgrids.

NTIS

N95-21146# High Technology Corp., Hampton, VA.
**COMPUTATIONAL STUDIES OF LAMINAR TO
TURBULENCE TRANSITION Final Report, 15 Dec. 1990 - 14
May 1994**

MUJEEB R. MALIK and FEI LI 14 Jul. 1994 132 p
(Contract(s)/Grant(s): F49620-91-C-0014)

(AD-A285622; AFOSR-94-0488TR) Avail: CASI HC A07/MF A02

Nonlinear evolution of Goertier and crossflow vortices is investi-
gated. The associated secondary instabilities of these streamwise
vortices are also studied. The Goertier vortex is found to be subject to
two types of secondary modes: a sinuous mode and a varicose
mode similar to that observed in the experiments. The growth rate

of the sinuous mode is higher initially but the varicose mode becomes more unstable in the downstream. It is also found that crossflow vortices are subject to a high frequency secondary instability prior to breakdown, as found in experiments performed on swept wings. In agreement with the experiments, our calculations show that the frequency of this secondary instability, which resides on top of the crossflow vortex, is an order of magnitude higher than the frequency of the most amplified traveling crossflow disturbances. The interaction of stationary and traveling disturbances is also considered. These studies have been carried out by using parabolized stability equations (PSE) and a two-dimensional (2D) eigenvalue approach. The mathematical nature of PSE approximation is also discussed. DTIC

N95-21258*# National Aeronautics and Space Administration. Langley Research Center, Hampton, VA.

ACOUSTIC RECEPTIVITY DUE TO WEAK SURFACE INHOMOGENEITIES IN ADVERSE PRESSURE GRADIENT BOUNDARY LAYERS

MEELAN CHOUDHARI (High Technology Corp., Hampton, VA.), LIAN NG (Analytical Services and Materials, Inc., Hampton, VA.), and CRAIG STREETT Feb. 1995 39 p
(Contract(s)/Grant(s): NAS1-18240; NAS1-18599; RTOP 537-03-23-03)
(NASA-TM-4577; L-17162; NAS 1.15:4577) Avail: CASI HC A03/MF A01

The boundary layer receptivity to free-stream acoustic waves in the presence of localized surface disturbances is studied for the case of incompressible Falkner-Skan flows with adverse pressure gradients. These boundary layers are unstable to both viscous and inviscid (i.e., inflectional) modes, and the finite Reynolds number extension of the Goldstein-Ruban theory provides a convenient method to compare the efficiency of the localized receptivity processes in these two cases. The value of the efficiency function related to the receptivity caused by localized distortions in surface geometry is relatively insensitive to the type of instability mechanism, provided that the same reference length scale is used to normalize the efficiency function for each type of instability. In contrast, when the receptivity is induced by variations in wall suction velocity or in wall admittance distribution, the magnitudes of the related efficiency functions, as well as the resulting coupling coefficients, are smaller for inflectional (i.e., Rayleigh) modes than for the viscous Tollmien-Schlichting waves. The reduced levels of receptivity can be attributed mainly to the shorter wavelengths and higher frequencies of the inflectional modes. Because the most critical band of frequencies shifts toward higher values, the overall efficiency of the wall suction- and the wall admittance-induced receptivity decreases with an increase in the adverse pressure gradient. Author

N95-21323*# National Aeronautics and Space Administration. Ames Research Center, Moffett Field, CA.

A THREE-DIMENSIONAL ORTHOGONAL LASER VELOCIMETER FOR THE NASA AMES 7- BY 10-FOOT WIND TUNNEL

STEPHEN E. DUNAGAN and DONALD L. COOPER Feb. 1995 23 p Original contains color illustrations
(Contract(s)/Grant(s): RTOP 505-59-54)
(NASA-TM-108864; A-95032; NAS 1.15:108864) Avail: CASI HC A03/MF A01; 1 functional color page

A three-component dual-beam laser-velocimeter system has been designed, fabricated, and implemented in the 7-by 10-Foot Wind Tunnel at NASA Ames Research Center. The instrument utilizes optical access from both sides and the top of the test section, and is configured for uncoupled orthogonal measurements of the three Cartesian coordinates of velocity. Bragg cell optics are used to provide fringe velocity bias. Modular system design provides great flexibility in the location of sending and receiving optics to adapt to specific experimental requirements. Near-focus Schmidt-Cassegrain optic modules may be positioned for collection of forward or backward scattered light over a large solid angle, and may be clustered to further increase collection solid angle. Multimode fiber optics transmit collected light to the photomultiplier tubes for processing. Counters are used to process the photomultiplier signals and transfer the processed data digitally via buffered

interface controller to the host MS-DOS computer. Considerable data reduction and graphical display programming permit on-line control of data acquisition and evaluation of the incoming data. This paper describes this system in detail and presents sample data illustrating the system's capability. Author

N95-21340*# Tennessee Univ. Space Inst., Tullahoma, TN. **SUPERSONIC LAMINAR FLOW CONTROL RESEARCH** Semiannual Report No. 2, Jul. - Dec. 1994

CHING F. LO Dec. 1994 65 p
(Contract(s)/Grant(s): NAG2-881)
(NASA-CR-196049; NAS 1.26:196049) Avail: CASI HC A04/MF A01

The objective of the research is to understand supersonic laminar flow stability, transition, and active control. Some prediction techniques will be developed or modified to analyze laminar flow stability. The effects of supersonic laminar flow with distributed heating and cooling on active control will be studied. The primary tasks of the research applying to the NASA/Ames Proof of Concept (POC) Supersonic Wind Tunnel and Laminar Flow Supersonic Wind Tunnel (LFSWT) nozzle design with laminar flow control are as follows: (1) predictions of supersonic laminar boundary layer stability and transition, (2) effects of wall heating and cooling for supersonic laminar flow control, and (3) performance evaluation of POC and LFSWT nozzles design with wall heating and cooling effects applying at different locations and various lengths. Author

N95-21478# Lawrence Livermore National Lab., Livermore, CA. **AN ECHELLE GRATING SPECTROMETER (EGS) FOR MID-IR REMOTE CHEMICAL DETECTION**

C. G. STEVENS, N. THOMAS, P. KUZMENKO, and T. ALGER Jul. 1994 11 p Presented at the Annual Meeting of the Society of Photo-Optical Instrumentation Engineers, San Diego, CA, 24-29 Jul. 1994
(Contract(s)/Grant(s): W-7405-ENG-48)
(DE94-019310; UCRL-JC-118226; CONF-940723-28) Avail: CASI HC A03/MF A01

The availability of high performance two-dimensional InSb detectors enables the design and construction of mid-infrared spectrographs capable of obtaining high resolution spectra over extended spectral regions without moving components. Rugged, stable, cryo-cooled spectrographs suitable for remote field operation are now possible using prism-echelle cross dispersion designs. The authors discuss the design, fabrication, and performance of a high resolution mid-IR field spectrograph designed specifically for the detection of atmospheric-borne chemicals from airborne platforms. The instrument design provides maximum optical throughput covering the two atmospheric windows at 2.0-2.5 micron and 3.0-4.2 micron. DOE

N95-22005# Federal Aviation Administration, Cambridge, MA. National Transportation Systems Center.

RECOMMENDATION ON TRANSITION FROM PRIMARY/SECONDARY RADAR TO SECONDARY-ONLY RADAR CAPABILITY Final Report, Sep. 1993 - Mar. 1994

JANIS VILCANS and RICHARD J. LAY Oct. 1994 137 p
(AD-A286279; DOT-VNTSC-FAA-94-10; DOT/FAA/NR-94-1) Avail: CASI HC A07/MF A02

This recommendation has been prepared to support the FAA decision to deactivate primary long-range radars (LRR) and presents transition strategy and implementation plan for the transformation of the existing primary/secondary en route radar system to a beacon-only system by the year 2002. The estimated cost associated with this transition is \$2.1 billion, but the cost directly related to the decision is approximately \$138.6 million. Thus, the potential saving of approximately \$1.4 billion associated with LRR replacement results in a benefit-to-cost ratio greater than 10. It is therefore recommended that the decision to deactivate the LRR be implemented as rapidly as possible in order to minimize costs necessary to sustain and maintain the existing system; that an orderly transition be accomplished; and that the transition to the beacon-only capability be adopted on a center-by-center basis. It is also recommended that the goal of an en route beacon system, comprising stand-alone beacon radars and backed up with

12 ENGINEERING

an automatic dependent surveillance (ADS) system be established, but achievement of this goal should not delay implementation of the deactivation decision. DTIC

N95-22109*# National Aeronautics and Space Administration. Langley Research Center, Hampton, VA.

EFFECTS OF YAW AND PITCH MOTION ON MODEL ATTITUDE MEASUREMENTS

PING TCHENG, JOHN S. TRIPP, and TOM D. FINLEY Feb. 1995 11 p

(Contract(s)/Grant(s): RTOP 505-59-54-02)
(NASA-TM-4641; L-17381; NAS 1.15:4641) Avail: CASI HC A03/MF A01

This report presents a theoretical analysis of the dynamic effects of angular motion in yaw and pitch on model attitude measurements in which inertial sensors were used during wind tunnel tests. A technique is developed to reduce the error caused by these effects. The analysis shows that a 20-to-1 reduction in model attitude measurement error caused by angular motion is possible with this technique. Author

N95-22212# California Inst. of Tech., Pasadena, CA.

SHOCK WAVE INTERACTIONS IN HYPERVELOCITY FLOW

S. R. SANDERSON and B. STURTEVANT Aug. 1994 10 p

(Contract(s)/Grant(s): F49620-93-1-0338)
(AD-A286507; AFOSR-94-0727TR) Avail: CASI HC A02/MF A01

The impingement of shock waves on blunt bodies in steady supersonic flow is known to cause extremely high local heat transfer rates and surface pressures. Although these problems have been studied in cold hypersonic flow, the effects of dissociative relaxation processes are unknown. In this paper we report a model aimed at determining the boundaries of the possible interaction regimes for an ideal dissociating gas. Local analysis about shock wave intersection points in the pressure-flow deflection angle plane with continuation of singular solutions is the fundamental tool employed. Further, we discuss an experimental investigation of the nominally two-dimensional mean flow that results from the impingement of an oblique shock wave on the leading edge of a cylinder. The effects of variations in shock impingement geometry were visualized using differential interferometry. Generally, real gas effects are seen to increase the range of shock impingement points for which enhanced heating occurs. They also reduce the type 4 interaction supersonic jet width and influence the type 2-3 transition process. DTIC

N95-22299# Lawrence Livermore National Lab., Livermore, CA.
CALIOPE AND TAISIR AIRBORNE EXPERIMENT PLATFORM

C. J. CHOCOL Jul. 1994 11 p Presented at the 1994 Chemical Analysis by Laser Interrogation of Proliferation Effluents (CALIOPE ITR) Interim Technical Review, Livermore, CA, 26-28 Apr. 1994
(Contract(s)/Grant(s): W-7405-ENG-48)
(DE94-018328; UCRL-JC-118289; CONF-9404162-10) Avail: CASI HC A03/MF A01

Between 1950 and 1970, scientific ballooning achieved many new objectives and made a substantial contribution to understanding near-earth and space environments. In 1986, the Lawrence Livermore National Laboratory (LLNL) began development of ballooning technology capable of addressing issues associated with precision tracking of ballistic missiles. In 1993, the Radar Ocean Imaging Project identified the need for a low altitude (1 km) airborne platform for its Radar system. These two technologies and experience base have been merged with the acquisition of government surplus Aerostats by Lawrence Livermore National Laboratory. The CALIOPE and TAISIR Programs can benefit directly from this technology by using the Aerostat as an experiment platform for measurements of the spill facility at NTS. DOE

N95-22449*# Stanford Univ., CA. Center for Turbulence Research.
LARGE-EDDY SIMULATION OF FLOW THROUGH A PLANE, ASYMMETRIC DIFFUSER

HANS-JAKOB KALTENBACH *In its Annual Research Briefs*, 1994 p 175-184 Dec. 1994

Avail: CASI HC A02/MF A04

A challenge for traditional turbulence modeling, based on the Reynolds averaged Navier-Stokes equations, remains the accurate prediction of 'mild', adverse pressure-gradient driven separation from a smooth surface. With this study we want to explore the capability of large-eddy simulation to predict the separation which occurs on the deflected wall of an asymmetric, plane diffuser with opening angle of 10 deg. The flow through the plane diffuser exhibits some additional interesting physical phenomena which make it a challenging test case. In addition to 'mild' separation about halfway down the deflected ramp, the flow is characterized by a small backflow zone with stalled fluid in the rear part of the expanding section. The turbulent flow entering the diffuser is subject to combined adverse and radial pressure gradients stemming from the convex curvature. Finally the flow recovers into a developed, turbulent channel flow in the outlet section. Obi et al. provide measurements of mean flow, Reynolds stresses, and pressure recovery, which were obtained by means of LDV in a wind tunnel. The objective of this study is to investigate whether LES with the standard dynamic model is able to accurately predict the flow in the one-sided diffuser and to explore the resolution requirements and associated costs. Author

N95-22451*# Stanford Univ., CA. Center for Turbulence Research.

EXPERIMENTAL INVESTIGATIONS OF ON-DEMAND VORTEX GENERATORS

SEYED G. SADDUGHI *In its Annual Research Briefs*, 1994 p 197-203 Dec. 1994

Avail: CASI HC A02/MF A04

Conventional vortex generators as found on many civil aircrafts are mainly for off-design conditions - e.g. suppression of separation or loss of aileron power when the Mach number accidentally rises above the design (cruise) value. In normal conditions they perform no useful function and exert a significant drag penalty. Recently there have been advances in new designs for passive vortex generators and boundary layer control. While traditionally the generators heights were of the order of the boundary layer thickness (δ), recent advances have been made where generators of the order of $\delta/4$ have been shown to be effective. The advancement of Micro-Electro-Mechanical (MEM) devices has prompted several efforts in exploring the possibility of using such devices in turbulence control. These new devices offer the possibility of boundary layer manipulation through the production of vortices, momentum jets, or other features in the flow. However, the energy output of each device is low in general, but they can be used in large numbers. Therefore, the possibility of moving from passive vortex generators to active (on-demand) devices becomes of interest. Replacement of fixed rectangular or delta-wing generators by devices that could be activated when needed would produce substantial economies. Our proposed application is not strictly 'active' control: the vortex generators would simply be switched on, all together, when needed (e.g. when the aircraft Mach number exceeded a certain limit). To this extent our scheme is simpler; however, to promote mixing and suppress separation we desire to deposit longitudinal vortices into the outer layer of the boundary layer as in conventional vortex generators. This requires a larger device although an alternative might be an array of smaller devices, for example, a longitudinal row with phase differences in the modulation signals so that the periodic vortices join up. The vortex pair with common flow up has the advantage that it will naturally drift away from the surface, but the disadvantage is that the net vorticity is zero so that the pair is eventually obliterated by turbulent mixing, rather than simply being diffused as in the case of a single vortex. It should be possible to devise alternative shapes of cavity wall so that the jet emerges obliquely and produces net longitudinal vorticity. Author

N95-22452*# Stanford Univ., CA. Center for Turbulence Research. **DIRECT NUMERICAL SIMULATIONS OF ON-DEMAND VORTEX GENERATORS: MATHEMATICAL FORMULATION** PETROS KOUMOUTSAKOS *In its Annual Research Briefs*, 1994 p 205-214 Dec. 1994
 Avail: CASI HC A02/MF A04

The objective of the present research is the development and application of efficient adaptive numerical algorithms for the study, via direct numerical simulations, of active vortex generators. We are using innovative computational schemes to investigate flows past complex configurations undergoing arbitrary motions. Some of the questions we try to answer are: Can and how may we control the dynamics of the wake? What is the importance of body shape and motion in the active control of the flow? What is the effect of three-dimensionality in laboratory experiments? We are interested not only in coupling our results to ongoing, related experimental work, but furthermore to develop an extensive database relating the above mechanisms to the vortical wake structures with the long-range objective of developing feedback control mechanisms. This technology is very important to aircraft, ship, automotive, and other industries that require predictive capability for fluid mechanical problems. The results would have an impact in high angle of attack aerodynamics and help design ways to improve the efficiency of ships and submarines (maneuverability, vortex induced vibration, and noise).

Author

N95-22455*# Stanford Univ., CA. Center for Turbulence Research. **ACOUSTICS OF LAMINAR BOUNDARY LAYERS BREAKDOWN** MENG WANG *In its Annual Research Briefs*, 1994 p 225-242 Dec. 1994
 Avail: CASI HC A03/MF A04

Boundary layer flow transition has long been suggested as a potential noise source in both marine (sonar-dome self noise) and aeronautical (aircraft cabin noise) applications, owing to the highly transient nature of process. The design of effective noise control strategies relies upon a clear understanding of the source mechanisms associated with the unsteady flow dynamics during transition. Due to formidable mathematical difficulties, theoretical predictions either are limited to early linear and weakly nonlinear stages of transition, or employ acoustic analogy theories based on approximate source field data, often in the form of empirical correlation. In the present work, an approach which combines direct numerical simulation of the source field with the Lighthill acoustic analogy is utilized. This approach takes advantage of the recent advancement in computational capabilities to obtain detailed information about the flow-induced acoustic sources. The transitional boundary layer flow is computed by solving the incompressible Navier-Stokes equations without model assumptions, thus allowing a direct evaluation of the pseudosound as well as source functions, including the Lighthill stress tensor and the wall shear stress. The latter are used for calculating the radiated pressure field based on the Curle-Powell solution of the Lighthill equation. This procedure allows a quantitative assessment of noise source mechanisms and the associated radiation characteristics during transition from primary instability up to the laminar breakdown stage. In particular, one is interested in comparing the roles played by the fluctuating volume Reynolds stress and the wall-shear-stresses, and in identifying specific flow processes and structures that are effective noise generators.

Derived from text

N95-22457*# McDonnell-Douglas Aerospace, Saint Louis, MO. **TRANSVERSE VORTICITY MEASUREMENTS IN THE NASA AMES 80 X 120 WIND TUNNEL BOUNDARY LAYER** JOHN F. FOSS, D. G. BHOL, F. D. BRAMKAMP (Technische Hochschule, Aachen, Germany.), and J. G. KLEWICKI (Utah Univ., Salt Lake City, UT.) *In Stanford Univ. Annual Research Briefs*, 1994 p 263-268 Dec. 1994
 Avail: CASI HC A02/MF A04

The MSU compact four-wire transverse vorticity probe permits $\omega_z(\text{sub } z)(t)$ measurements in a nominally 1 sq mm domain.

Note that a conventional coordinate system is used with x and y in the streamwise and normal directions respectively. The purpose of this investigation was to acquire time series data in the same access port at the ceiling of the 80 ft x 120 ft wind tunnel (NASA Ames Research Center) as earlier used by the Wallace group from the University of Maryland and to compare the present results with those of the three-component vorticity probe used in that earlier study.

Derived from text

13
GEOSCIENCES

Includes geosciences (general); earth resources; energy production and conversion; environment pollution; geophysics; meteorology and climatology; and oceanography.

A95-70297* National Aeronautics and Space Administration. Langley Research Center, Hampton, VA. **SUBSIDENCE OF AIRCRAFT ENGINE EXHAUST IN THE STRATOSPHERE: IMPLICATIONS FOR CALCULATED OZONE DEPLETIONS**

J. M. RODRIGUEZ Atmospheric Environmental Research, Inc., Cambridge, MA, US, R.-L. SHIA Atmospheric Environmental Research, Inc., Cambridge, MA, US, M. K. W. KO Atmospheric Environmental Research, Inc., Cambridge, MA, US, C. W. HEISEY Atmospheric Environmental Research, Inc., Cambridge, MA, US, D. K. WEISTENSTEIN Atmospheric Environmental Research, Inc., Cambridge, MA, US, R. C. MIAKE-LYE Aerodyne Research, Inc., Billerica, MA, US, and C. E. KOLB Aerodyne Research, Inc., Billerica, MA, US *Geophysical Research Letters* (ISSN 0094-8276) vol. 21, no. 1 January 1, 1994 p. 69-72 (Contract(s)/Grant(s): NAS1-19161) (PAPER-93GL03426; HTN-95-A0330) Copyright

The deposition altitude of nitrogen oxides and other exhaust species emitted by stratospheric aircraft is a crucial parameter in determining the impact of these emissions on stratospheric ozone. We have utilized a model for the wake of a High-Speed Civil Transport (HSCT) to estimate the enhancements in water and reductions in ozone in these wakes as a function of time. Radiative calculations indicate differential cooling rates as large as -5K/day at the beginning of the far-wake regime, mostly due to the enhanced water abundance. These cooling rates would imply a net sinking of the wakes of about 1.2 km after three days in the limit of no mixing. Calculated mid-latitude column ozone reductions due to emissions from a Mach 2.4 HSCT would then change from about -1% to -06%. However, more realistic calculations adopting moderate mixing for the wake reduce the net sinking to less than 0.2 km, making the impact of radiative subsidence negligible.

Author (Herner)

A95-70473 National Aeronautics and Space Administration. John C. Stennis Space Center, Bay Saint Louis, MS. **EVALUATION OF THE SPARTON TIGHT-TOLERANCE AXBT** JANICE D. BOYD NASA, Stennis Space Center, Bay St. Louis, MS, US and ROBERT S. LINZELL Neptune Sciences, Inc., Slidell, LA, US *Journal of Atmospheric and Oceanic Technology* (ISSN 0739-0572) vol. 10, no. 6 December 1993 p. 892-899 Research sponsored by the Office of Naval Technology (HTN-95-40728) Copyright

Forty-six near-simultaneous pairs of conductivity - temperature - depth (CTD) and Sparton 'tight tolerance' air expendable bathythermograph (AXBT) temperature profiles were obtained in summer 1991 from a location in the Sargasso Sea. The data were analyzed to assess the temperature and depth accuracies of the Sparton AXBTs. The tight-tolerance criterion was not achieved using the manufacturer's equations but may have been achieved using customized equations computed from the CTD data. The temperature data from the customized equations had a one standard deviation error of 0.13 C. A customized elapsed fall time-to-depth conversion equation was found to be $z = 1.620t - 2.2384 x$

13 GEOSCIENCES

$10(\exp -4) t(\exp 2) + 1.291 \times 10(\exp -7) t(\exp 3)$, with z the depth in meters and t the elapsed fall time after probe release in seconds. The standard deviation of the depth error was about 5 m; a rule of thumb for estimating maximum bounds on the depth error below 100 m could be expressed as $\pm 2\%$ of depth or ± 10 m, whichever is greater. This equation gave greater depth accuracy than either the manufacturer's supplied equation or the navy standard equation.

Author (Herner)

A95-70655* National Aeronautics and Space Administration. Marshall Space Flight Center, Huntsville, AL.

HIGH-RESOLUTION IMAGING OF RAIN SYSTEMS WITH THE ADVANCED MICROWAVE PRECIPITATION RADIOMETER

ROY W. SPENCER NASA. Marshall Space Flight Center, Huntsville, AL, US, ROBBIE E. HOOD NASA. Marshall Space Flight Center, Huntsville, AL, US, FRANK J. LAFONTAINE NASA. Marshall Space Flight Center, Huntsville, AL, US, ERIC A. SMITH Florida State Univ., Tallahassee, FL, US, ROBERT PLATT Georgia Institute of Technology, Atlanta, GA, US, JOE GALLIANO Galliano and Associates, Roswell, GA, US, VANESSA L. GRIFFIN NASA. Marshall Space Flight Center, Huntsville, AL, US, and ELENA LOBL NASA. Marshall Space Flight Center, Huntsville, AL, US *Journal of Atmospheric and Oceanic Technology* (ISSN 0739-0572) vol. 11, no. 4, pt. 1 August 1994 p. 849-857 (HTN-95-70133) Copyright

An advanced Microwave Precipitation Radiometer (AMPR) has been developed and flown in the NASA ER-2-high-altitude aircraft for imaging various atmospheric and surface processes, primarily the internal structure of rain clouds. The AMPR is a scanning four-frequency total power microwave radiometer that is externally calibrated with high-emissivity warm and cold loads. Separate antenna systems allow the sampling of the 10.7- and 19.35-GHz channels at the same spatial resolution, while the 37.1- and 85.5-GHz channels utilize the same multifrequency feedhorn as the 19.35-GHz channel. Spatial resolutions from an aircraft altitude of 20-km range from 0.6 km at 85.5 GHz to 2.8 km at 19.35 and 10.7 GHz. All channels are sampled every 0.6 km in both along-track and cross-track directions, leading to a contiguous sampling pattern of the 85.5-GHz 3-dB beamwidth footprints, 2.3X oversampling of the 37.1-GHz data, and 4.4X oversampling of the 19.35- and 10.7-GHz data. Radiometer temperature sensitivities range from 0.2 to 0.5 C. Details of the system are described, including two different calibration systems and their effect on the data collected. Examples of oceanic rain systems are presented from Florida and the tropical west Pacific that illustrate the wide variety of cloud water, rainwater, and precipitation-size ice combinations that are observable from aircraft altitudes.

Author (Herner)

A95-70656* National Aeronautics and Space Administration. Marshall Space Flight Center, Huntsville, AL.

BEHAVIOR OF AN INVERSION-BASED PRECIPITATION RETRIEVAL ALGORITHM WITH HIGH-RESOLUTION AMPR MEASUREMENTS INCLUDING A LOW-FREQUENCY 10.7-GHZ CHANNEL

E. A. SMITH Florida State Univ., Tallahassee, FL, US, X. XIANG Florida State Univ., Tallahassee, FL, US, A. MUGNAI Istituto di Fisica dell' Atmosfera, Frascati, Italy, R. E. HOOD NASA. Marshall Space Flight Center, Huntsville, AL, US, and R. W. SPENCER NASA. Marshall Space Flight Center, Huntsville, AL, US *Journal of Atmospheric and Oceanic Technology* (ISSN 0739-0572) vol. 11, no. 4, pt. 1 August 1994 p. 858-873 Research sponsored by NASA, Gruppo Nazionale per la Difesa dalle Catastrofi Idrogeologiche of Italy

(Contract(s)/Grant(s): NAG5-1602; NAG-991; NATO-CG-890894; DE-FC05-85ER-250000) (HTN-95-70134) Copyright

A microwave-based, profile-type precipitation retrieval algorithm has been used to analyze high-resolution passive microwave measurements over an ocean background, obtained by the Advanced Microwave Precipitation Radiometer (AMPR) flown on a NASA ER-2 aircraft. The analysis is designed to first determine the

improvements that can be gained by adding brightness temperature information from the AMPR low-frequency channel (10.7 GHz) to a multispectral retrieval algorithm nominally run with satellite information at 19, 37, and 85 GHz. The impact of spatial resolution degradation of the high-resolution brightness temperature information on the retrieved rain/cloud liquid water contents and ice water contents is then quantified in order to assess the possible biases inherent to satellite-based retrieval. Careful inspection of the high-resolution aircraft dataset reveals five distinctive brightness temperature features associated with cloud structure and scattering effects that are not generally detectable in current passive microwave satellite measurements. Results suggest that the inclusion of 10.7-GHz information overcomes two basic problems associated with three-channel retrieval. Intercomparisons of retrievals carried out at high-resolution and then averaged to a characteristic satellite scale to the corresponding retrievals in which the brightness temperatures are first convolved down to the satellite scale suggest that with the addition of the 10.7-GHz channel, the rain liquid water contents will not be negatively impacted by special resolution degradation. That is not the case with the ice water contents as they appear to be quite sensitive to the imposed scale, the implication being that as spatial resolution is reduced, ice water contents will become increasingly underestimated.

Author (Herner)

A95-70950

FOLIAGE TRANSMISSION MEASUREMENTS USING A GROUND-BASED ULTRAWIDE BAND (300-1300 MHz) SAR SYSTEM

D. R. SHEEN Environmental Research Inst of Michigan, Ann Arbor, MI, United States, N. P. MALINAS, D. W. KLETZLI, JR., T. B. LEWIS, and JUAN F. ROMAN *IEEE Transactions on Geoscience and Remote Sensing* (ISSN 0196-2892) vol. 32, no. 1 January 1994 p. 118-130 refs (BTN-94-EIX94381351617) Copyright

The attenuation of a forest clearly impacts the ability of airborne SAR systems to image objects within the forest. The level of this attenuation is a function of tree characteristics over the frequency band used in the radar. To experimentally measure the transmission properties of foliage, a bistatic (line-of-site) wide-band system has been built by the Environmental Research Institute of Michigan (ERIM), sponsored by the Air Force's Wright Laboratory, Avionics directorate. This system is polarimetric and can operate coherently over the band from 300 to 1300 MHz. The variation in foliage transmission over the frequency band is important because an imaging radar typically operates coherently over a bandwidth. The system can scan foliage in angle to determine spatial variations in the foliage attenuation. This angular variation in foliage attenuation is quite important because imaging radars typically synthesize an aperture by scanning over a range of angles. The ERIM Wide-Band System is ground-based, with one antenna attached to a carriage which can move 10 m horizontally along an elevated rigid track and the other antenna attached to a fixed tripod. Measurements with the system were conducted during July 1991 at the University of Michigan Biological Field Station in Pellston, MI. The measurements of the mean attenuation as a function of depression angle (15-45 deg) and frequency (300-1300 MHz) of four different forest types are presented. In addition to mean attenuation, the variance in attenuation and the autocorrelation of the attenuation (in angle) are presented. These results imply that the variation of the foliage properties over the bandwidth and scan geometry (or angular variation) will degrade the ability of a radar to focus a foliage-obscured object.

Author (EI)

A95-71186

WATER VAPOR CONTINUUM ABSORPTION IN MID-LATITUDES: AIRCRAFT MEASUREMENTS AND MODEL COMPARISONS

S. D. RUDMAN Meteorological Office, UK, R. W. SAUNDERS Meteorological Office, UK, C. G. KILSBY Meteorological Office, UK, and P. J. MINNETT Brookhaven National Laboratory, US Royal Meteorology Society, *Quarterly Journal* (ISSN 0035-9009) vol. 120, no. 518 July 1994 p. 795-807

(Contract(s)/Grant(s): DE-AC02-76CH-00016)
(HTN-95-40756) Copyright

Recently reported measurements by the Meteorological Research Flight C-130 aircraft over the tropical Atlantic have shown that existing models of infrared water vapor continuum absorption underestimate its magnitude by up to 30%. This paper presents additional results from more recent measurements made close to the south-west approaches of the British Isles and over the eastern Mediterranean Sea. These measurements are compared with two models: GENLN2, a line-by-line model, and the widely used band model LOWTRAN7. The measured radiances suggest a consistent underestimate in both models of the water vapor continuum absorption. The modified parametrization for the water vapor continuum absorption, inferred from the tropical results, was also used here to check its validity for lower water vapor amounts and lower temperatures. As with the tropical results, increasing the self-broadening coefficient by a constant factor, or increasing the temperature dependence, improves the agreement between the measurements and the model predictions. Author (Hemer)

**A95-71908
AIRCRAFT-BORNE, LASER-INDUCED FLUORESCENCE
INSTRUMENT FOR THE IN SITU DETECTION OF
HYDROXYL AND HYDROPEROXYL RADICALS**

P. O. WENNERGREN Harvard Univ, Cambridge, MA, United States, R. C. COHEN, N. L. HAZEN, L. B. LAPSON, N. T. ALLEN, T. F. HANISCO, J. F. OLIVER, N. W. LANHAM, J. N. DEMUSZ, and J. G. ANDERSON Review of Scientific Instruments (ISSN 0034-6748) vol. 65, no. 6 June 1994 p. 1858-1876 refs (BTN-95-EIX95072499029) Copyright

A singular measurement and detection of hydroxyl radical has been extremely difficult to accomplish. This paper described the design and initial findings from a device developed specifically to address the issue of the ozone photochemistry of the lower stratosphere. Preliminary results indicated that the technique should be feasible throughout most of the lower atmosphere. This instrument represented the first aircraft-borne instrument that rendered results of sufficient high caliber to provide a real test of understanding of odd-hydrogen photochemistry of the lower atmosphere. OH and HO₂ measurements with signal-to-noise ratio of over 30 were generated with short integration times. The new HO(x) instrument capability increased a suite of in situ instruments aboard the NASA ER-2 aircraft that has the ability to detect, simultaneously, the majority of the species thought crucial in controlling the ozone concentration in the lower stratosphere. EI

**A95-72393
AIRCRAFT MEASUREMENTS OF WATER VAPOUR
CONTINUUM ABSORPTION AT MILLIMETRE
WAVELENGTHS**

S. J. ENGLISH Meteorological Office, UK, C. GUILLOU CNRS, France, C. PRIGENT CNRS, France, and D. C. JONES Meteorological Office, UK Royal Meteorological Society, Quarterly Journal (ISSN 0035-9009) vol. 120, no. 517 April 1994 p. 603-625 (HTN-95-90884) Copyright

In preparation for the future Advanced Microwave Sounding Unit-B (AMSU-B) mission, measurements of clear-air radiative transfer at 89 and 157 GHz were made using a radiometer operating on the C-130 aircraft on the UK Meteorological Research Flight. Observations of water vapor and oxygen absorption in arctic, middle latitude and tropical atmospheres were obtained. Four different empirical models of continuum absorption are compared and tested; three are found to be more representative of the observations in middle-latitude conditions. In the tropical Atlantic, large model deficits are found for these models. The fourth is more representative of observations in the tropics but over-estimates absorption at middle and arctic latitudes. The results confirm observations taken during other atmospheric field experiments, and laboratory measurements, that a model absorption deficit at high humidity exists in the microwave and millimeter wavelength regions. Author (Hemer)

A95-72411* National Aeronautics and Space Administration. Wallops Flight Facility, Wallops Island, VA.

ORBITAL VELOCITIES INDUCED BY SURFACE WAVES

LYNN K. SHAY University of Miami, Miami, FL, US, EDWARD J. WALSH NASA, Wallops Flight Facility, Wallops Island, VA, US, and PEN CHEN ZHANG University of Miami, Miami, FL, US Journal of Atmospheric and Oceanic Technology (ISSN 0739-0572) vol. 11, no. 4, pt. 2 August 1994 p. 1117-1125 Research sponsored by NASA

(Contract(s)/Grant(s): N00014-91-J-1042)
(HTN-95-90902) Copyright

During the third intensive observational period of the Surface Wave Dynamics Experiment (SWADE), an aircraft-based experiment was conducted on 5 March 1991 by deploying slow-fall airborne expendable current profilers (AXCPs) and airborne expendable bathythermographs (AXBTs) during a scanning radar altimeter (SRA) flight on the NASA NP-3A research aircraft. As the Gulf Stream (GS) moved into the SWADE domain in late February, maximum upper-layer currents of 1.98 m/s were observed in the core of the baroclinic jet where the vertical current shears were $O(10(\exp -2)/s)$. The SRA concurrently measured the sea surface topography, which was transformed into two-dimensional directional wave spectra at 5-6-km intervals along the flight tracks. The wave spectra indicated a local wave field with wavelengths of 40-60 m propagating southward between 120 deg and 180 deg, and a northward-moving swell field from 300 deg to 70 deg associated with significant wave heights of 2-4 m. As the AXCP descended through the upper ocean, the profiler sensed orbital velocity amplitudes of 0.2-0.5 m/s due to low-frequency surface waves. These orbital velocities were isolated by fitting the observed current profiles to the three-layer model based on a monochromatic surface wave, including the steady and current shear terms within each layer. The depth-integrated differences between the observed and modeled velocity profiles were typically less than 3 cm/s. For 17 of the 21 AXCP drop sites, the rms orbital velocity amplitudes, estimated by integrating the wave spectra over direction and frequency, were correlated at a level of 0.61 with those derived from the current profiles. The direction of wave propagation inferred from the AXCP-derived orbital velocities was in the same direction observed by the SRA. These mean wave directions were highly correlated (0.87) and differed only by about 5 deg. Author (Hemer)

A95-72423* National Aeronautics and Space Administration. Ames Research Center, Moffett Field, CA.

**PERFORMANCE OF A FOCUSED CAVITY AEROSOL
SPECTROMETER FOR MEASUREMENTS IN THE
STRATOSPHERE OF PARTICLE SIZE IN THE 0.06-2.0-
MICROMETER-DIAMETER RANGE**

H. H. JONSSON University of Denver, Denver, CO, US, J. C. WILSON University of Denver, Denver, CO, US, C. A. BROCK University of Denver, Denver, CO, US, R. G. KNOLLENBERG Particle Measuring Systems, Inc., Boulder, CO, US, R. NEWTON Particle Measuring Systems, Inc., Boulder, CO, US, J. E. DYE National Center for Atmospheric Research, Boulder, CO, US, D. BAUMGARDNER National Center for Atmospheric Research, Boulder, CO, US, S. BORRMANN University of Mainz, Mainz, Germany, G. V. FERRY NASA, Ames Research Center, Moffett Field, CA, US, and R. PUESCHEL NASA, Ames Research Center, Moffett Field, CA, US Journal of Atmospheric and Oceanic Technology (ISSN 0739-0572) vol. 12, no. 1 February 1995 p. 115-129

(Contract(s)/Grant(s): NAG2-458)
(HTN-95-90914) Copyright

A focused cavity aerosol spectrometer aboard a NASA ER-2 high-altitude aircraft provided high-resolution measurements of the size of the stratospheric particles in the 0.06-2.0-micrometer-diameter range in flights following the eruption of Mount Pinatubo in 1991. Effects of anisokinetic sampling and evaporation in the sampling system were accounted for by means adapted and specifically developed for this instrument. Calibrations with monodisperse aerosol particles provided the instrument's response matrix, which upon

13 GEOSCIENCES

inversion during data reduction yielded the particle size distributions. The resultant dataset is internally consistent and generally shows agreement to within a factor of 2 with comparable measurements simultaneously obtained by a condensation nuclei counter, a forward-scattering spectrometer probe, and aerosol particle impactors, as well as with nearby extinction profiles obtained by satellite measurements and with lidar measurements of backscatter.

Author (Herner)

A95-72495

POTENTIAL APPLICATIONS OF THE SSM/I CLOUD LIQUID WATER PARAMETER TO THE ESTIMATION OF MARINE AIRCRAFT ICING

THOMAS F. LEE Naval Research Laboratory, Monterey, CA, US, JAMES R. CLARK Naval Research Laboratory, Monterey, CA, US, and STEVEN D. SWADLEY Computer Sciences Corporation, Monterey, CA, US Weather and Forecasting (ISSN 0882-8156) vol. 9, no. 2 June 1994 p. 173-182 Research sponsored by the Space and Naval Warfare Systems Command (HTN-95-80651) Copyright

Images of integrated cloud liquid water derived from the Special Sensor Microwave Imager (SSM/I) aboard the Defense Meteorological Satellite Program (DMSP) polar-orbiting satellite are presented. Examples with infrared and visible images and synoptic charts are shown for the Gulf of Alaska and Bering Sea for March 1992. The SSM/I images often show detailed, low-level cloud circulations not suggested by infrared satellite images. A prototype system for forecasting the potential for aircraft icing, which combines the SSM/I cloud liquid water parameter with numerical model output, is also presented. Where integrated cloud liquid water exceeds a specific threshold, an icing watch region is specified. The top of the icing watch layer is set to the model -20 C level or infrared cloud top, whichever is lower. The base of the icing watch layer is set to the 0 C level from model output. No watch areas are specified where the infrared cloud top temperature is above freezing, regardless of integrated cloud liquid water amount. Author (Herner)

A95-72500

AN ALGORITHM FOR FORECASTING MOUNTAIN WAVE-RELATED TURBULENCE IN THE STRATOSPHERE

JULIO T. BACMEISTER Naval Research Laboratory, Washington, DC, US, PAUL A. NEWMAN NASA, Goddard Space Flight Center, Greenbelt, MD, US, BRUCE L. GARY NASA, Jet Propulsion Laboratory, Pasadena, CA, US, and K. ROLAND CHAN NASA, Ames Research Center, Moffet Field, CA, US Weather and Forecasting (ISSN 0882-8156) vol. 9, no. 2 June 1994 p. 241-253 (HTN-95-80656) Copyright

A global mountain wave parameterization for prediction of wave-related displacements and turbulence is described. The parameterization is used with input from National Meteorological Center (NMC) analyses of wind and temperature to examine small-scale disturbances encountered by the National Aeronautics and Space Administration high-altitude ER-2 during the Second Airborne Arctic Stratosphere Experiment (AASE-II). The magnitude and location of observed large wave events are well reproduced. A strong correlation is suggested between patches of moderate turbulence encountered by the ER-2 and locations where breaking mountain waves are predicted by the parameterization. These facts suggest that useful forecasts of global mountain wave activity, including wave-related clear-air turbulence, can be made quickly and inexpensively using our mountain wave parameterization with input from current numerical forecast models. Author (Herner)

A95-72543

SNOW-BAND FORMATION AND EVOLUTION DURING THE 15 NOVEMBER 1987 AIRCRAFT ACCIDENT AT DENVER AIRPORT

ROY M. RASMUSSEN National Center for Atmospheric Research, Boulder, CO, US, ANDREW CROOK National Center for Atmospheric Research, Boulder, CO, US, and CATHY KESSINGER National Center for Atmospheric Research, Boulder, CO, US

Weather and Forecasting (ISSN 0882-8156) vol. 8, no. 4 December 1993 p. 453-480

(Contract(s)/Grant(s): DTFA01-90-25001)

(HTN-95-80699) Copyright

The formation and evolution of convective rain and snow bands prior to and during the crash of Continental Airlines flight 1713 on 15 November 1987 at Denver Stapleton Airport are discussed. Convective rain occurred during early stages of the storm in association with the approach of an upper-level trough from the west. Snow bands were observed following the passage of a shallow Canadian cold front from the north. These bands formed above the cold front and moved from southeast to northwest at 7 m/s with a horizontal spacing of 10-30 km. The winds within the cloud layer were southeasterly from 5 to 10 m/s, suggesting that the bands were advected by the mean, cloud-layer flow. The most likely mechanism producing these bands was a convective instability in the shear layer above the cold front. As the upper-level trough moved to the east, the winds in the cloud layer shifted to northerly, causing the bands to move southward with the major axis of the band oriented north-south. The high snowfall rate just prior to the takeoff of flight 1713 occurred as a result of one of these north-south-oriented bands moving over Denver Stapleton Airport from the north during the latter stages of the storm. Author (Herner)

A95-72545

TROPICAL CYCLONE OBSERVATION AND FORECASTING WITH AND WITHOUT AIRCRAFT RECONNAISSANCE

JOEL D. MARTIN Colorado State Univ., Fort Collins, CO, US and WILLIAM M. GRAY Colorado State Univ., Fort Collins, CO, US Weather and Forecasting (ISSN 0882-8156) vol. 8, no. 4 December 1993 p. 519-532 Research sponsored by the USAF, ONR and Phillips Laboratory (HTN-95-80701) Copyright

The contributions of aircraft reconnaissance to the accuracy of tropical cyclone center positioning, motion, and intensity determinations are examined, along with their impact on the accuracy of track and intensity forecasting. The analyses concentrate on differences in cyclone position and intensity diagnosis, as well as track forecasting during periods when aircraft measurements were made versus times when aircraft data were not available. Northwest Pacific data for the period 1979-86, which contain over 200 tropical cyclone cases with approximately 5000 center fix positions, were used for the analyses. Aircraft versus no-aircraft situations are examined with respect to the class of satellite data that were available and for day versus night measurements. Differences in positioning and intensity estimates made from simultaneous independent satellite observations are also examined. Results show that satellite analysts operating independently frequently obtain large differences in their estimates of tropical cyclone positions, as well as their intensity estimates. Aircraft reconnaissance of cyclone position and intensity, as were flown in the western Pacific, does not appear to improve track forecasts beyond 24-h, nor does it affect the current 12-h motion vector estimate. Other areas of tropical cyclone warning services, including estimates of current position and intensity as well as short-term estimates of motion, especially for recurvature forecasts, appear to be improved by aircraft data. Author (Herner)

A95-72546

VOLCANIC ASH FORECAST TRANSPORT AND DISPERSION (VAFTAD) MODEL

JEROME L. HEFFTER NOAA Air Resources Laboratory, Silver Spring, MD, US and BARBARA J. B. STUNDER NOAA Air Resources Laboratory, Silver Spring, MD, US Weather and Forecasting (ISSN 0882-8156) vol. 8, no. 4 December 1993 p. 533-541 (HTN-95-80702) Copyright

The National Oceanic and Atmospheric Administration (NOAA) Air Resources Laboratory (ARL) has developed a Volcanic Ash Forecast Transport And Dispersion (VAFTAD) model for emergency response use focusing on hazards to aircraft flight operations. The model is run on a workstation at ARL. Meteorological input for the model is automatically downloaded from the NOAA National Me-

teorological Center (NMC) twice-daily forecast model runs to ARL. Additional input for VAFTAD regarding the volcanic eruption is supplied by the user guided by monitor prompts. The model calculates transport and dispersion of volcanic ash from an initial ash cloud that has reached its maximum height within 3 h of eruption time. The model assumes that spherical ash particles of diameters ranging from 0.3 to 30 micrometers are distributed throughout the initial cloud with a particle number distribution based on Mount St. Helens and Redoubt Volcano eruptions. Particles are advected horizontally and vertically by the winds and fall according to Stoke's law with a slip correction. A bivariate-normal distribution is used for horizontally diffusing the cloud and determining ash concentrations. Model output gives maps with symbols representing relative concentrations in three flight layers, and throughout the entire ash cloud, for sequential 6- and 12-h time intervals. A verification program for VAFTAD has been started. Results subjectively comparing model ash cloud forecasts with satellite imagery for three separate 1992 eruptions of Mount Spurr in Alaska have been most encouraging.

Author (Herner)

A95-73180

MICROPHYSICAL AND RADIATIVE PROPERTIES OF SMALL CUMULUS CLOUDS OVER THE SEA

G. B. RAGA Manchester Univ. Inst. of Science and Technology, Manchester, UK and P. R. JONAS Manchester Univ. Inst. of Science and Technology, Manchester, UK Royal Meteorological Society, Quarterly Journal (ISSN 0035-9009) vol. 119, no. 514 October 1993 p. 1399-1417 Research sponsored by International Petroleum Industry Environmental Conservation Association (HTN-95-A0526) Copyright

Microphysical and radiative data obtained in fields of cumulus clouds over the sea around the United Kingdom are presented. The Meteorological Research Flight C-130 aircraft was used to make radiation and cloud microphysical measurements in situ on four different occasions. The sub-cloud aerosol concentrations ranged from 100 to 5000 per cu cm, from fairly maritime to heavily polluted. Vertical profiles of microphysical variable indicate that small cumuli over the sea have some properties that are more similar to marine stratocumuli than to continental cumuli. Nonetheless, variables, such as liquid-water content and droplet-number concentration, exhibit a larger variability than in stratocumuli, owing to more vigorous entrainment in cumuli. Mie theory was used to compute extinction cross-sections, single scattering albedo, back-scattering cross-sections, and asymmetry parameters for all in-cloud samples. The average vertical profiles are in agreement upon the background aerosol concentrations. A simple two-stream radiative-transfer model, using the back-scattering cross-section, is presented and shows good agreement with run-averaged radiometric observations.

Author (Herner)

A95-73181

ON THE LINK BETWEEN CLOUD-TOP RADIATIVE PROPERTIES AND SUB-CLOUD AEROSOL CONCENTRATIONS

G. B. RAGA Manchester Univ. Inst. of Science and Technology, Manchester, UK and P. R. JONAS Manchester Univ. Inst. of Science and Technology, Manchester, UK Royal Meteorological Society, Quarterly Journal (ISSN 0035-9009) vol. 119, no. 514 October 1993 p. 1419-1425 Research sponsored by International Petroleum Industry Environmental Conservation Association (HTN-95-A0527) Copyright

Microphysical observations obtained in cumulus clouds over the sea are presented and related to background pollution levels. The sub-cloud aerosol concentrations vary from 50 to 5000 per cu cm, which can hardly be considered 'maritime'. Observed droplet size distributions are used to determine radiative properties using Mie theory. Functional expressions are derived for the extinction cross-section and the single scattering albedo as functions of the sub-cloud aerosol concentrations.

Author (Herner)

N95-19921 Sorbent Technologies Corp., Twinsburg, OH. LABORATORY EVALUATION OF A REACTIVE BAFFLE APPROACH TO NOX CONTROL Final Technical Report,

Feb. - Apr. 1993

S. G. NELSON, D. A. VANSTONE, R. C. LITTLE, and R. A. PETERSON Sep. 1993 41 p Limited Reproducibility: More than 20% of this document may be affected by microfiche quality (Contract(s)/Grant(s): F08635-90-C-0053) (AD-A283802; AL/EQ-TR-1993-0017) Avail: CASI HC A03

Vermiculite, vermiculite coated with magnesia, and activated carbon sorbents have successfully removed NOx (and carbon monoxide and particles) from combustion exhausts in a subscale drone jet engine test cell (JETC), but back pressure so generated elevated the temperature of the JETC and of the engine. The objective of this effort was to explore the feasibility of locating the sorbents in the face of the duct or of baffles parallel to the direction of flow within the ducts. Jet engine test cells (JETC's) are stationary sources of oxides of nitrogen (NOx), soot, and unburned or partially oxidized carbon compounds that form as byproducts of imperfect combustion. Regulation of NOx emissions is being considered for implementation under the Clean Air Act Amendments of 1990. Several principles have been examined as candidate methods to control NOx emissions from JETC's. DTIC

N95-19989# Army Research Lab., Aberdeen Proving Ground, MD. COMPARISON OF METEOROLOGICAL DATA WITH FITTED VALUES EXTRACTED FROM PROJECTILE TRAJECTORY Final Report, Jul. 1993 - Jul. 1994

GENE R. COOPER and KEVIN S. FANSLER Oct. 1994 35 p (AD-A285921; ARL-TR-603) Avail: CASI HC A03/MF A01

In this report, the atmospheric conditions are found by knowing only the projectile's flight trajectory and its flight coefficients together with the initial atmospheric conditions on the ground. The test trajectories were generated as solutions of the modified point mass (MPM) equations of motion. The correct atmospheric conditions for the generated flight trajectory are obtained from data collected during a weather balloon flight. A nonlinear least squares method was then used to fit the MPM equations to the test trajectory by varying the meteorological parameters. Density, sound speed, and wind profiles agreed well. Further tests of the method involved the flight coefficients, which we perturbed to observe the corresponding variation for the fitted values. Also, Gaussian noise was introduced onto the trajectory values to simulate the uncertainty in trajectory measurements. The results of the analysis shows that the whole trajectory should be fitted, and not small trajectory segments, to obtain accurate atmospheric parameters with the location precision provided by current radar and Global Positioning Satellite System (GPS) techniques. DTIC

N95-20441 Army Construction Engineering Research Lab., Champaign, IL.

ENVIRONMENTAL COMPLIANCE ASSESSMENT AND MANAGEMENT PROGRAM Final Report

CAROLYN OROURKE and LISA A. GIFFORD Apr. 1994 243 p Limited Reproducibility: More than 20% of this document may be affected by microfiche quality (AD-A279605; CERL-SR-EC-94/15) Avail: CASI HC A11

The number of environmental laws and regulations has continued to grow in the United States and worldwide, making compliance with these regulations increasingly difficult. Environmental assessments became a way to determine compliance with current environmental regulations. The U.S. Air Force has adopted an environmental compliance program that identifies compliance problems before they are cited as violations by the U.S. Environmental Protection Agency (USEPA). Beginning in 1984, the U.S. Army Construction Engineering Research Laboratories (USACERL), in cooperation with the Air Force Engineering and Services Center, began research on the U.S. Environmental Compliance Assessment and Management Program (ECAMP). The concept was to combine Federal, Department of Defense (DOD), and Air Force environmental regulations, along with existing checklists from the USEPA and private industry, and documentation of good management practices and risk-management issues, into a series of checklists that list legal requirements and specify items or operations to review. Each assessment protocol lists a point of contact to help assessors review

13 GEOSCIENCES

the checklists as effectively as possible. The Hawaii Supplement was developed to be used in conjunction with the U.S. ECAMP manual, using existing Hawaii state environmental legislation and regulations as well as suggested management practices. DTIC

N95-20985# National Renewable Energy Lab., Golden, CO. ADVANCED WIND TURBINE DESIGN STUDIES: ADVANCED CONCEPTUAL STUDY

P. HUGHES and R. SHERWIN Aug. 1994 246 p Prepared in cooperation with Atlantic Orient Corp., Norwich, VT (Contract(s)/Grant(s): DE-AC36-83CH-10093) (DE93-000031; NREL/TP-442-4740) Avail: CASI HC A11/MF A03

In conjunction with the US Department of Energy and the National Renewable Energy Laboratory's Advanced Wind Turbine Program, the Atlantic Orient Corporation developed preliminary designs for the next generation of wind turbines. These 50 kW and 350 kW turbines are based upon the concept of simplicity. By adhering to a design philosophy that emphasizes simplicity, we project that these turbines will produce energy at extremely competitive rates which will unlock the potential of wind energy domestically and internationally. The program consisted of three distinct phases. First, we evaluated the operational history of the Enertech 44 series wind turbines. As a result of this evaluation, we developed, in the second phase, a preliminary design for a new 50 kW turbine for the near-term market. In the third phase, we took a clean-sheet-of-paper approach to designing a 350 kW turbine focused on the mid-1990s utility market that incorporated past experience and advanced technology. DOE

N95-21552# Lawrence Livermore National Lab., Livermore, CA. OVERVIEW OF REMOTE SENSING LASER DEVELOPMENT AND SEMICONDUCTOR LASER TECHNOLOGY

N. W. CARLSON, R. BEACH, B. COMASKEY, M. EMANUEL, T. SCHARLEMANN, J. SKIDMORE, S. VELSKO, B. KRUPKE, and R. SOLARZ Jul. 1994 19 p Presented at the 1994 Chemical Analysis By Laser Interrogation of Proliferation Effluents (CALIOPETR) Interim Technical Review, Livermore, CA, 26-28 Apr. 1994 (Contract(s)/Grant(s): W-7405-ENG-48) (DE94-019103; UCRL-JC-118149; CONF-9404162-12) Avail: CASI HC A03/MF A01

There are many new requirements for remote detection in the atmosphere that have been generated by government agencies. The associated field scenarios anticipated for carrying out the measurements, in many cases, are extremely demanding on the existing technology. Moreover, additional innovations in remote-sensing technology will be needed to satisfy requirements for longer measurement ranges, detection of low concentration levels of target species, new laser wavelengths for a growing list of species, and compact/efficient systems for deployment in airborne platforms. Remote-sensing laser transmitter architectures based on diode-pumped, solid-state lasers offer the most promise in terms of meeting these demanding requirements, although in order to realize this promise, the present level of power performance must be extended by one to two orders of magnitude. The LLNL remote sensing laser development program is aimed at developing those necessary solid-state laser systems with performance characteristics that go well beyond the state-of-the-art. This paper will cover: (1) an overview of the remote sensing laser development program, which includes high-average power solid-state lasers, tunable laser/OPO systems, temperature-insensitive nonlinear materials, and new solid-state/semiconductor laser materials; and (2) a review of the technical progress on semiconductor laser technology development. DOE

15

MATHEMATICAL AND COMPUTER SCIENCES

Includes mathematical and computer sciences (general); computer operations and hardware; computer programming and software; computer systems; cybernetics; numerical analysis; statistics and probability; systems analysis; and theoretical mathematics.

N95-20719# Stanford Univ., CA. COMPUTING METHODS FOR THE APPROXIMATE SOLUTION OF TIME DEPENDENT PROBLEMS Final Report, Jul. 1989 - Sep. 1993

JOSEPH OLIGER Nov. 1994 6 p (Contract(s)/Grant(s): N00014-89-J-1815) (AD-A286007) Avail: CASI HC A02/MF A01

The research dealt with computing methods for applications in aerodynamics, geophysics, hydrodynamics, meteorology, and oceanography. Analysis was done of adaptive numerical methods for time-dependent problems in complicated physical domains which can efficiently and reliably approximate singular and near singular features of the solution such as fronts and shocks. Work focused on development of algorithms which could be executed on parallel architectures and upon data structures and language constructs which allow this to be done efficiently and effectively.

Author (DTIC)

N95-20828# Michigan Univ., Ann Arbor, Mi. Dept. of Electrical Engineering and Computer Science.

DESIGN OF A CONTROLLER FOR A FLEXIBLE POINTING SYSTEM USING H(INFINITY) SYNTHESIS Final Report, Jun. - Sep. 1993

MICHAEL S. MATTICE, S. S. AMBERKAR, N. SIVASHANKAR, and P. P. KHARGONEKAR Oct. 1994 22 p (Contract(s)/Grant(s): AF-AFOSR-0053-90; DAAL03-90-G-0008) (AD-A286572; ARFSD-TR-94010) Avail: CASI HC A03/MF A01

This report presents the results of a digital controller design implementation using the H-infinity synthesis method on the ATB 1000 test fixture at the Army Research Development Engineering Center (ARDEC), Picatinny Arsenal, NJ. The objective was to design a robust tracking controller to make the beam tip track a reference command applied to the base in the face of nominal disturbances. In this report, the salient features of the design approach will be reviewed and the implementation issues that arose will be discussed at length. DTIC

N95-21913 Drexel Univ., Philadelphia, PA. DESIGN OF ROBUST OPTIMAL CONTROL SYSTEMS AND STABILITY ANALYSIS OF REAL STRUCTURED UNCERTAINTIES Final Report, Aug. 1990 - Mar. 1994

BOR-CHIN CHANG and AJMAL YOUSUFF Mar. 1994 149 p Limited Reproducibility: More than 20% of this document may be affected by microfiche quality (Contract(s)/Grant(s): F33615-90-C-3613) (AD-A279089; WL-TR-94-3030) Avail: Issuing Activity (Defense Technical Information Center (DTIC))

This report addresses the computational problems arising in the design of robust controllers via H-inf optimization and mu-synthesis and proposes several new controller reduction approaches. Through our discovery of the convexity and monotonicity properties of the general parameter dependent H-inf Riccati equation, a quadratically convergent algorithm which is faster than the other existing search schemes is developed to compute the optimal H-inf norm. It is desired to preserve the closed-loop stability and performance while reducing the order of the controller. A structured truncation technique based on the closed-loop controllability and observability diagrams, an H-inf controller parameterization and reduction method, and an observer-based controller parameterization and reduction procedure are employed to achieve this objective. DTIC

N95-22216# Michigan Univ., Ann Arbor, MI. Dept. of Aerospace Engineering.

ROBUST FIXED-STRUCTURE CONTROL Final Report, 1
Feb. 1992 - 30 Sep. 1994

DENNIS S. BERNSTEIN 30 Oct. 1994 27 p
(Contract(s)/Grant(s): F49620-92-J-0127)
(AD-A286515; AFOSR-94-0741TR) Avail: CASI HC A03/MF A01

This final report for AFOSR Grant F49620-92-J-0127 summarizes results obtained in five areas, namely, robust control, linear control, sampled-data control, tracking and disturbance rejection, and nonlinear control. Principal results include new bounds for the structured singular value, implementation of structured singular value synthesis using fixed-structure optimization techniques, a more rigorous foundation for the Maximum Entropy control technique, extensions of linear-quadratic control to stable stabilizing controllers, determination of the achievable performance of sampled-data controllers in the presence of sample-rate constraints, control of noise in an acoustic duct, stability theory for second-order systems, a rigorous treatment of Guyan reduction, a deterministic foundation for energy flow theory, a unified treatment of quadratic optimality and servo-compensation, nonlinear control of the spinning top and rotating bodies with known and unknown mass imbalance, global stabilization of the oscillating eccentric rotor using integrator backstepping, and Lyapunov theory for finite-time convergence. DTIC

16

PHYSICS

Includes physics (general); acoustics; atomic and molecular physics; nuclear and high-energy physics; optics; plasma physics; solid-state physics; and thermodynamics and statistical physics.

A95-69970

VORTEX SHEDDING NOISE CONTROL IN IDLING CIRCULAR SAWS USING AIR EJECTION AT THE TEETH

K. YANAGIMOTO Tsuruoka Natl Coll of Technology, Yamagata, Japan, C. D. MOTE, and R. ICHIMIYA Journal of Sound and Vibration (ISSN 0022-460X) vol. 172, no. 2 April 28, 1994 p. 277-282 refs
(BTN-94-EIX94371347214) Copyright

Aerodynamically induced noise from an idling circular saw can be very intense. The purpose of the present investigation is noise reduction through vortex shedding control in idling circular saws. Reduction of aerodynamic noise in idling circular saws may be possible by controlling the shed vortices and flow structures in the space between teeth, based on the earlier observations. EI

A95-70797

SOUND PROPAGATION FROM AN ARBITRARILY ORIENTED MULTIPOLE PLACED NEAR A PLANE, FINITE IMPEDANCE SURFACE

Z. HU Purdue Univ, West Lafayette, IN, United States and J. S. BOLTON Journal of Sound and Vibration (ISSN 0022-460X) vol. 170, no. 5 March 10, 1994 p. 637-669 refs
(BTN-94-EIX94371338964) Copyright

Theories that have been developed for the purpose of predicting sound propagation over plane, finite impedance surfaces have usually been expressed in terms of sound radiation from point monopoles, or at least in terms of sources that generate cylindrically symmetric sound fields. However, not all practical noise sources are monopolar in character, nor do they necessarily generate cylindrically symmetric sound fields. In this paper, a two-dimensional finite Hankel transform technique is described that makes it possible to predict sound propagation from sources that generate non-cylindrically symmetric sound fields: e.g., arbitrarily oriented dipoles and quadrupoles. As a result, the proposed technique may prove useful for predicting sound propagation from aerodynamic noise sources placed near plane outdoor surfaces. EI

A95-71738

SECONDARY SOURCE LOCATIONS IN ACTIVE NOISE CONTROL: SELECTION OR OPTIMIZATION?

E. BENZARIA IMT, Marseille, France and V. MARTIN Journal of Sound and Vibration (ISSN 0022-460X) vol. 173, no. 1 May 26, 1994 p. 137-144 refs
(BTN-94-EIX94381352222) Copyright

In this paper, two strategies are combined to obtain good results in determining locations in the field of active noise control. The first strategy originates from both an interpolation method and a gradient algorithm. The second strategy is to select the best-controlled sources from among many at prescribed locations. EI

A95-72675

ELECTRO-OPTIC CHARACTERIZATION OF ULTRAFAST PHOTODETECTORS USING ADIABATICALLY COMPRESSED SOLITON PULSES

T. NAGATSUMA, M. YAITA, M. SHINAGAWA, K. KATO, A. KOZEN, K. IWATSUKI, and K. SUZUKI Electronics Letters (ISSN 0013-5194) vol. 30, no. 10 May 12, 1994 p. 814-816 refs
(BTN-94-EIX94381359637) Copyright

The response of ultrafast photodetectors at 1.55 micron wavelength has been measured by electro-optic sampling using adiabatically compressed soliton pulses. 750 fs-duration pulses with no wings were used to both pump and probe the waveguide pin photodiode. The measured bandwidth of the photodiode is more than 110 GHz, which is the highest value for a detector operating at 1.55 micron. Author (EI)

N95-20652# Deutsche Aerospace A.G., Munich (Germany). Military Aircraft Div.

OPTICAL BACKPLANE FOR MODULAR AVIONICS

R. BOGENBERGER and O. KRUMPHOLZ In AGARD, Advanced Packaging Concepts for Digital Avionics 6 p Oct. 1994 Copyright Avail: CASI HC A02/MF A03

An experimental study was carried out by DASA and Daimler Benz Research to demonstrate the feasibility of fiber optic technology for use in Modular Avionics. In the first step of the study an inter module communication up to 16 subscribers, with interconnection length of about 1 m was demonstrated. Backplanes being composed of multimode and monomode fibers were tested in a configuration of 4 parallel data channels, each running with 1 GBit/s. This paper will resume results of investigations as: power budget, influence of modal noise with multimode fibers, effects of feedback, as well as optical interference caused by reflections. The paper then goes on to describe the transparency for given protocols (e.g., Pt-bus). A prospect of problems arising of optical interconnections of a relatively large number of subscribers and possible solutions by using in-line amplifiers (optically) are reviewed. The backplane implementation is prepared to be arranged as a serial/parallel bus or a part of a switched network. Finally, this paper will give a synopsis of optical backplane solutions. Author

N95-20963 Naval Surface Warfare Center, Dahlgren, VA.

WAVELET TRANSFORMATIONS FOR HELICOPTER IDENTIFICATION VIA ACOUSTIC SIGNATURES

JEFFREY L. SOLKA, CAREY E. PRIEBE, HALFORD I. HAYES, and GEORGE W. ROGERS May 1994 25 p Limited Reproducibility: More than 20% of this document may be affected by microfiche quality

(AD-A279980; NSWCDD/TR-93/169) Avail: CASI HC A03

The ability to classify helicopters based on their acoustic signature has applications to both detection and tracking. The current approach to this problem uses standard signal-processing techniques to extract features based on the fundamental harmonics of the helicopters' blades. This document examines the role that the wavelet transformation might play in this feature extraction process. It addresses ways to use the wavelet transform both to improve the performance of the existing approach and to expand the capabilities of the classification system. DTIC

16 PHYSICS

N95-21100 Department of the Navy, Washington, DC.
PASSIVE RANGE MEASUREMENT SYSTEM Patent Application

WALTER L. HARRIMAN, inventor (to Navy) 27 Jul. 1992 14 p
Limited Reproducibility: More than 20% of this document may be affected by microfiche quality
(AD-D016222; US-PATENT-APPL-SN-921863) Avail: Issuing Activity (Defense Technical Information Center (DTIC))

A method and apparatus provides instantaneous passive range measurement onboard an aircraft for determining the range between the aircraft and a target. The target may either be stationary and on the earth's surface, or a slower moving vehicle. Calculation of the desired range is achieved using the formula: $\text{Range} = (\sin a / \sin b) V$; where 'a' = angle from aircraft heading to target, 'b' = turning rate; and 'V' ground velocity. The apparatus consists of an automatic video tracker, a video camera, and a servo controlled aiming platform. A resolver on the aiming platform is utilized to determine the angle from the aircraft axis to the target. This angle is added to the aircraft drift angle to determine the total angle from the aircraft heading to the target. The video tracker is utilized to determine the turning rate of the aiming platform. Using the difference in contrast between the target and the background of the video scene, the tracker provides error signals (azimuth and elevation) to keep the aiming platform pointed at the target. DTIC

N95-21170* Georgia Tech Research Inst., Atlanta, GA.
TEMPERATURE EFFECTS ON ACOUSTIC INTERACTIONS BETWEEN ALTITUDE TEST FACILITIES AND JET ENGINE PLUMES Final Report, Feb. 1992 - May 1994
K. K. AHUJA, K. C. MASSEY, C. K. TAN, and R. R. JONES Oct. 1994 300 p
(Contract(s)/Grant(s): NAS1-19061)
(NASA-CR-197638; NAS 1.26:197638; AD-A286058; AEDC-TR-94-10) Avail: CASI HC A13/MF A03

The overall objective of the present investigation was to determine the mechanisms responsible for engine/test cell resonance observed at the AEDC facility. The specific objective was to determine the effect of heating the jet on its coupling with the diffuser used in a typical engine/test cell facility. This objective was to be accomplished through systematic measurements of cold and heated free and ducted jets using a subscale facility. An additional objective was to analytically examine the behavior of jet instability waves as a function of temperature, and to identify any potential of strong coupling between the jet instabilities and diffuser duct resonance modes directly attributable to heating of the jet. Model cold and heated jet experiments are performed with an axisymmetric convergent nozzle in a test setup that simulates a supersonic jet exhausting into a cylindrical diffuser. The measured data consist of a free and ducted plume for a range of jet exit Mach numbers and four reservoir temperatures: ambient, 400 F, 750 F, and 1,000 F. Analytical results on the growth of instability waves and the duct resonance have been introduced. It is shown that the screech frequency increases with increasing operating temperature ratio. The measured in-duct microphone signatures contain a number of discrete tones, and almost all of them can be associated with duct resonances. The amplitudes increase with increasing Mach number and operating temperature ratios. At certain operating conditions, the acoustic fluctuations associated with these ejector duct modes excite the most amplified wave of the jet. DTIC

N95-21388# Argonne National Lab., IL.
MHD-FLOW IN SLOTTED CHANNELS WITH CONDUCTING WALLS
I. A. EVTUSHENKO (Efremov, D. V. Scientific Research Inst., Saint Petersburg, Russia.), I. R. KIRILLOV (Efremov, D. V. Scientific Research Inst., Saint Petersburg, Russia.), and C. B. REED Jul. 1994 22 p Presented at the ISFNT-3: 3rd International Symposium on Fusion Nuclear Technology, Los Angeles, CA, 27 Jun. - 1 Jul. 1994
(Contract(s)/Grant(s): W-31-109-ENG-38)

(DE94-018370; ANL/TD/CP-83927; CONF-940664-29) Avail: CASI HC A03/MF A01

A review of experimental results is presented for magnetohydrodynamic (MHD) flow in rectangular channels with conducting walls and high aspect ratios (longer side parallel to the applied magnetic field), which are called slotted channels. The slotted channel concept was conceived at Efremov Institute as a method for reducing MHD pressure drop in liquid metal cooled blanket design. The experiments conducted by the authors were aimed at studying both fully developed MHD-flow, and the effect of a magnetic field on the hydrodynamics of 3-D flows in slotted channels. Tests were carried out on five models of the slotted geometry. A good agreement between test and theoretical results for the pressure drop in slotted channels was demonstrated. Application of a 'one-electrode movable probe' for velocity measurement permitted measurement of the M-shape velocity profiles in the slotted channels. Suppression of 3-D inertial effects in slotted channels of complex geometry was demonstrated based on potential distribution data. DOE

N95-21673 Office of Naval Research, Arlington, VA.
FIBER-OPTIC ROTARY JOINT WITH BUNDLE COLLIMATOR ASSEMBLIES Patent Application
GREGORY H. AMES, inventor 8 Aug. 1994 15 p Limited Reproducibility: More than 20% of this document may be affected by microfiche quality
(AD-D016504; US-PATENT-APPL-SN-287027) Avail: Issuing Activity (Defense Technical Information Center (DTIC))

There is presented a fiber-optic rotary joint with first and second bundle collimator assemblies, the joint comprising a generally cup-shaped main rotor, a first bundle collimator assembly fixed in a central opening in a bottom wall of the main rotor, a generally cup-shaped stator disposed within the main rotor, the stator having a bottom wall opposed to the main rotor bottom wall, and a second bundle collimator assembly disposed in a central opening in the bottom wall of the stator. The joint further includes a prism mounted in a prism rotor in the joint between the first and second collimator assemblies, and gear means for causing rotation of the main rotor at twice the speed of rotation of the prism rotor. Azimuthal adjustment structure is disposed on one of the first and second collimator assemblies for azimuthal alignment of the one collimator assembly with the other of the collimator assemblies. DTIC

N95-21882# Naval Postgraduate School, Monterey, CA. Dept. of Electrical and Computer Engineering.
A COMPUTER-BASED MULTIMEDIA PROTOTYPE FOR NIGHT VISION GOGGLES M.S. Thesis
BOBBY BRYANT and GLENROY E. DAY, JR. Sep. 1994 44 p
(AD-A286208) Avail: CASI HC A03/MF A01

Naval aviators who employ night vision goggles (NVG) face additional risks during nighttime operations. In an effort to reduce these risks, increased training with NVG's is suggested. Our goal was to design a computer-based, interactive multimedia system that would assist in the training of pilots who use NVG's. This thesis details the methods and techniques used in the development of the NVG multimedia prototype. It describes which hardware components and software applications were utilized as well as how the prototype was developed. Several facets of multimedia technology (sound, animation, video, and three dimensional graphics) have been incorporated into the interactive prototype. For a more robust successive prototype, recommendations are submitted for future enhancements that include alternative methodologies as well as expanded interactions. DTIC

N95-21888* General Electric Co., Cincinnati, OH. Aircraft Engines.
ACTIVE CONTROL OF FAN NOISE-FEASIBILITY STUDY. VOLUME 1: FLYOVER SYSTEM NOISE STUDIES Final Report
ROBERT E. KRAFT, B. A. JANARDAN, G. C. KONTOS, and P. R. GLIEBE Oct. 1994 42 p

(Contract(s)/Grant(s): NAS3-26617; RTOP 538-03-11)
 (NASA-CR-195392-VOL-1; E-9170-VOL-1; NAS 1.26:195392-VOL-1)
 Avail: CASI HC A03/MF A01

A study has been completed to examine the potential reduction of aircraft flyover noise by the method of active noise control (ANC). It is assumed that the ANC system will be designed such that it cancels discrete tones radiating from the engine fan inlet or fan exhaust duct. Thus, without considering the engineering details of the ANC system design, tone levels are arbitrarily removed from the engine component noise spectrum and the flyover noise EPNL levels are compared with and without the presence of tones. The study was conducted for a range of engine cycles, corresponding to fan pressure ratios from 1.3 to 1.75. The major conclusions that can be drawn are that, for a fan pressure ratio of 1.75, ANC of tones gives about the same suppression as acoustic treatment without ANC, and for a fan pressure ratio of 1.45, ANC appears to offer less effectiveness than passive treatment. Additionally, ANC appears to be more effective at sideline and cutback conditions than at approach. Overall EPNL suppressions due to tone removal range from about 1 to 3 dB at takeoff engine speeds and from 1 to 5 db at approach speeds. Studies of economic impact of the installation of an ANC system for the four engine cases indicate increases of DOC ranging from 1 to 2 percent, favoring the lower fan pressure ratio engines. Further study is needed to confirm the results by examining additional engine data, particularly at low fan pressure ratios, and studying the details of the current results to obtain a more complete understanding. Further studies should also include determining the effects of combining passive and active treatment. Author

of luning. The results indicated that the divergent display mode systematically induced more luning than the convergent display mode under the null contour condition. Adding black contours reduced luning in both the convergent and divergent display modes, where the convergent mode retained its relatively lower magnitude of luning. The display luminance level had no effect on luning for the null or black contour conditions. DTIC

N95-21975 Wright Lab., Wright-Patterson AFB, OH.
OPTICAL PROCESSING AND CONTROL Final Report, Oct. 1986 - Sep. 1992

ANDREW SUZUKI, DALE STEVENS, MIKE PRAIRIE, JAMES GROTE, and ANTONIO CRESPO Jan. 1994 69 p Limited Reproducibility: More than 20% of this document may be affected by microfiche quality
 (AD-A279157; WL-TR-94-5005) Avail: Issuing Activity (Defense Technical Information Center (DTIC))

The effort is divided into specific topics applicable to data processing. Those topics include the Dember effect, alignment of a ring laser gyro, measurement of the Fresnel drag coefficient, integrated optical switches, aluminum gallium arsenide waveguides, Fredkin gates, optically reconfigurable superconductive circuits, and an initial investigation into the application of an acoustooptical tunable filter to the interrogation of fiber optic Bragg sensors.

DTIC

N95-22044# Army Aeromedical Research Lab., Fort Rucker, AL.
FACTORS AFFECTING THE PERCEPTION OF LUNING IN MONOCULAR REGIONS OF PARTIAL BINOCULAR OVERLAP DISPLAYS

VICTOR KLYMENKO, ROBERT W. VERONA, JOHN S. MARTIN, HOWARD H. BEASLEY, and WILLIAM E. MCLEAN Aug. 1994 54 p

(Contract(s)/Grant(s): DA PROJ. 3E1-62787-A-879)
 (AD-A286287; USAARL-94-47) Avail: CASI HC A04/MF A01

Luning is a detrimental visual effect characterized by a subjective darkening of the visual field in the monocular regions of partial binocular overlap displays. The effect of a number of factors on the magnitude of luning was investigated. These factors include: (1) the convergent versus the divergent display modes for presenting a partial binocular overlapping field-of-view; (2) the display luminance level; (3) the placement of either black or white contours versus no (null) contours on the binocular overlap border; and (4) the increasing or decreasing of the luminance of the monocular side regions relative to the binocular overlap region. Eighteen Army student aviators served as subjects in a repeated measures design. The percentage of time luning was seen was the measure of the degree

AERONAUTICAL ENGINEERING

Aeronautical engineering: A continuing bibliography with indexes (supplement 315)
[NASA-SP-7037(315)] p 219 N95-21640

AEROSOLS

Performance of a focused cavity aerosol spectrometer for measurements in the stratosphere of particle size in the 0.06-2.0-micrometer-diameter range
[HTN-95-90914] p 253 A95-72423

Microphysical and radiative properties of small cumulus clouds over the sea
[HTN-95-A0526] p 255 A95-73180

On the link between cloud-top radiative properties and sub-cloud aerosol concentrations
[HTN-95-A0527] p 255 A95-73181

AEROSPACE SAFETY

Independent review of Aviation Technology and Research Information Analysis System (ATRIAS) database
[AD-A284049] p 226 N95-21518

AEROTHERMOCHEMISTRY

Thermochemical nonequilibrium viscous shock-layer analysis for a Mars aerocapture vehicle
[BTN-95-EIX95082502732] p 239 A95-70139

AEROTHERMODYNAMICS

Thermochemical nonequilibrium viscous shock-layer analysis for a Mars aerocapture vehicle
[BTN-95-EIX95082502732] p 239 A95-70139

Adaptive remeshing for convective heat transfer with variable fluid properties
[BTN-95-EIX95082502720] p 243 A95-71033

Experimental study of vane heat transfer and aerodynamics at elevated levels of turbulence
[NASA-CR-4633] p 244 N95-19912

A computer code (SKINTEMP) for predicting transient missile and aircraft heat transfer characteristics
[AD-A286044] p 248 N95-21001

AH-64 HELICOPTER

Design optimization of rotor blades for improved performance and vibration
[HTN-95-A0498] p 229 A95-72569

Using the backward transfer paradigm to validate the AH-64 Simulator Training Research Advanced Testbed for Aviation
[AD-A285758] p 238 N95-19931

AIR DATA SYSTEMS

Response of the B-1B air data sensor to simulated dust cloud environments
[AD-A286134] p 235 N95-22036

AIR FLOW

Vortex shedding noise control in idling circular saws using air ejection at the teeth
[BTN-94-EIX94371347214] p 257 A95-69970

Vapor generator wand
[NASA-CASE-LAR-15058-1] p 238 N95-20080

AIR NAVIGATION

Modular CNI avionics system p 234 N95-20659
The personal aircraft: Status and issues
[NASA-TM-109174] p 223 N95-20688

Assessment of a non-dedicated GPS receiver system for precise airborne attitude determination
[DE94-019309] p 229 N95-21520

A real-time algorithm for integrating differential satellite and inertial navigation information during helicopter approach
[NASA-CR-197409] p 229 N95-21891

Recommendation on transition from primary/secondary radar to secondary-only radar capability
[AD-A286279] p 249 N95-22005

AIR POLLUTION

Subsidence of aircraft engine exhaust in the stratosphere: Implications for calculated ozone depletions
[PAPER-93GL03426] p 251 A95-70297

Volcanic ash forecast transport and dispersion (VAFTAD) model
[HTN-95-80702] p 254 A95-72546

On the link between cloud-top radiative properties and sub-cloud aerosol concentrations
[HTN-95-A0527] p 255 A95-73181

AIR PURIFICATION

Laboratory evaluation of a reactive baffle approach to NOx control
[AD-A283802] p 255 N95-19921

AIR TRAFFIC CONTROL

Crew aiding and automation: A system concept for terminal area operations, and guidelines for automation design
[NASA-CR-4631] p 228 N95-19950

Data link terminal DLT document
[PB95-110805] p 229 N95-21369

Recommendation on transition from primary/secondary radar to secondary-only radar capability
[AD-A286279] p 249 N95-22005

AIR TRANSPORTATION

Census US civil aircraft calendar year 1993
[AD-A286309] p 219 N95-20091

Commuter/air taxi ditchings and water-related impacts that occurred from 1979 to 1989
[AD-A285691] p 226 N95-20275

The personal aircraft: Status and issues
[NASA-TM-109174] p 223 N95-20688

AIRBORNE EQUIPMENT

Aircraft-borne, laser-induced fluorescence instrument for the in situ detection of hydroxyl and hydroperoxyl radicals
[BTN-95-EIX95072499029] p 253 A95-71908

Passive range measurement system
[AD-D016222] p 258 N95-21100

Assessment of a non-dedicated GPS receiver system for precise airborne attitude determination
[DE94-019309] p 229 N95-21520

AIRCRAFT ACCIDENTS

Snow-band formation and evolution during the 15 November 1987 aircraft accident at Denver airport
[HTN-95-80699] p 254 A95-72543

Commuter airplane accident data analysis
[AD-A286315] p 226 N95-20174

Commuter/air taxi ditchings and water-related impacts that occurred from 1979 to 1989
[AD-A285691] p 226 N95-20275

Analysis of test criteria for specifying foam firefighting agents for aircraft rescue and firefighting
[AD-A286381] p 227 N95-22352

Forecasting aircraft mishaps using monthly maintenance reports
[AD-A286049] p 227 N95-22417

AIRCRAFT COMMUNICATION

Crew aiding and automation: A system concept for terminal area operations, and guidelines for automation design
[NASA-CR-4631] p 228 N95-19950

AIRCRAFT CONSTRUCTION MATERIALS

Prediction of energy absorption capability of composite stiffeners
[HTN-95-A0500] p 230 A95-72571

AIRCRAFT CONTROL

Crew aiding and automation: A system concept for terminal area operations, and guidelines for automation design
[NASA-CR-4631] p 228 N95-19950

AIRCRAFT DESIGN

Prediction of energy absorption capability of composite stiffeners
[HTN-95-A0500] p 230 A95-72571

New airfoil-design concept with improved aerodynamic characteristics
[PAPER-4384] p 230 A95-72585

F-16XL interview with Marta Bohn-Meyer
[NASA-TM-110505] p 223 N95-19996

Parallel calculation of sensitivity derivatives for aircraft design using automatic differentiation
[NASA-TM-110103] p 231 N95-20370

Why do airlines want and use thrust reversers? A compilation of airline industry responses to a survey regarding the use of thrust reversers on commercial transport airplanes
[NASA-TM-109158] p 226 N95-20706

AIRCRAFT ENGINES

Engine life measurement and diagnostics
[BTN-95-EIX95041505024] p 235 A95-70133

Subsidence of aircraft engine exhaust in the stratosphere: Implications for calculated ozone depletions
[PAPER-93GL03426] p 251 A95-70297

Turbine design and application
[NASA-SP-290] p 236 N95-22341

AIRCRAFT EQUIPMENT

FASTPACK: Optimized solutions for modular avionics derived from a parametric study. Part 1: Platform features
p 233 N95-20634

Immersion/two phase cooling p 246 N95-20648
Composite cases for airborne electronic equipment: A technology study and EMC p 241 N95-20655

Lightweight electronic enclosures using composite materials p 241 N95-20656
Modular supplies for a distributed architecture — avionics packaging p 234 N95-20657

Modular CNI avionics system p 234 N95-20659
TIM-SCT cable testing protocol
[AD-A286633] p 231 N95-20772

Design of a controller for a flexible pointing system using H(infinity) synthesis
[AD-A286572] p 256 N95-20828

AIRCRAFT FUELS

Analysis of test criteria for specifying foam firefighting agents for aircraft rescue and firefighting
[AD-A286381] p 227 N95-22352

AIRCRAFT ICING

Ice accretion on aircraft wings
[BTN-95-EIX95082502224] p 225 A95-71021

Potential applications of the SSM/I cloud liquid water parameter to the estimation of marine aircraft icing
[HTN-95-80651] p 254 A95-72495

Snow-band formation and evolution during the 15 November 1987 aircraft accident at Denver airport
[HTN-95-80699] p 254 A95-72543

AIRCRAFT INDUSTRY

Public-sector aviation issues: Graduate research award papers, 1992-1993
[PB94-217478] p 219 N95-19967

AIRCRAFT LANDING

Comments on effect of wet snow on the null-reference ILS system
[BTN-95-EIX95142555488] p 227 A95-72885

Super-heavy aircraft study
[AD-A279602] p 238 N95-19955

F-15 resource tape
[NASA-TM-110502] p 230 N95-19994

Minima reduction simulation test results
[AD-A285626] p 228 N95-21148

AIRCRAFT MAINTENANCE

Bonded composite repair of cracked load-bearing holes
[BTN-94-EIX94401360553] p 243 A95-71867

Why do airlines want and use thrust reversers? A compilation of airline industry responses to a survey regarding the use of thrust reversers on commercial transport airplanes
[NASA-TM-109158] p 226 N95-20706

Damage tolerant repair techniques for pressurized aircraft fuselages
[AD-A286298] p 219 N95-22046

Forecasting aircraft mishaps using monthly maintenance reports
[AD-A286049] p 227 N95-22417

AIRCRAFT MANEUVERS

F-15 resource tape
[NASA-TM-110502] p 230 N95-19994

AIRCRAFT MODELS

RCS measurements, transformations, and comparisons under cylindrical and plane wave illumination
[BTN-94-EIX94371347126] p 242 A95-69976

Effects of yaw and pitch motion on model attitude measurements
[NASA-TM-4641] p 250 N95-22109

AIRCRAFT NOISE

Acoustic climb to cruise test
[NASA-TM-110504] p 230 N95-20155

Effect of atmospheric pressure on measured aircraft noise levels
[PB95-130423] p 232 N95-21425

AIRCRAFT PARTS

Electrochemical impedance pattern recognition for detection of hidden chemical corrosion on aircraft components
[AD-A285998] p 241 N95-20716

AIRCRAFT PERFORMANCE

F-15 resource tape
[NASA-TM-110502] p 230 N95-19994

Naval aviation: F-14 upgrades are not adequately justified. Report to Congressional Committees
[AD-A286338] p 231 N95-20212

Why do airlines want and use thrust reversers? A compilation of airline industry responses to a survey regarding the use of thrust reversers on commercial transport airplanes
[NASA-TM-109158] p 226 N95-20706

AIRCRAFT POWER SUPPLIES

Photovoltaic electric power applied to Unmanned Aerial Vehicles (UAV) p 245 N95-20530

AIRCRAFT SAFETY

Ice accretion on aircraft wings
[BTN-95-EIX95082502224] p 225 A95-71021

Potential applications of the SSM/I cloud liquid water parameter to the estimation of marine aircraft icing
[HTN-95-80651] p 254 A95-72495

Volcanic ash forecast transport and dispersion (VAFTAD) model
[HTN-95-80702] p 254 A95-72546

Commuter airplane accident data analysis
[AD-A286315] p 226 N95-20174

Commuter/air taxi ditchings and water-related impacts that occurred from 1979 to 1989
[AD-A285691] p 226 N95-20275

Fuselage burnthrough from large exterior fuel fires
[AD-A286295] p 226 N95-22318

Forecasting aircraft mishaps using monthly maintenance reports
[AD-A286049] p 227 N95-22417

AIRCRAFT SPECIFICATIONS

Analysis of test criteria for specifying foam firefighting agents for aircraft rescue and firefighting
[AD-A286381] p 227 N95-22352

AIRCRAFT STRUCTURES

Corrosion of aircraft materials: Correlation between nanometer scale and macroscopic structural damage parameters
[AD-A285930] p 241 N95-20299

Eddy current for detecting second-layer cracks under installed fasteners
[AD-A279871] p 244 N95-20414

Electrochemical impedance pattern recognition for detection of hidden chemical corrosion on aircraft components
[AD-A284998] p 241 N95-20481

AIRCRAFT SURVIVABILITY

Commuter airplane accident data analysis
[AD-A286315] p 226 N95-20174

Commuter/air taxi ditchings and water-related impacts that occurred from 1979 to 1989
[AD-A285691] p 226 N95-20275

AIRFOILS

Ground effect calculation of two-dimensional airfoil
[BTN-94-EIX94371347710] p 219 A95-69969

Ice accretion on aircraft wings
[BTN-95-EIX95082502224] p 225 A95-71021

Effects of leading and trailing edge flaps on the aerodynamics of airfoil/vortex interactions
[HTN-95-31011] p 221 A95-71181

New airfoil-design concept with improved aerodynamic characteristics
[PAPER-4384] p 230 A95-72585

Public-sector aviation issues: Graduate research award papers, 1992-1993
[PB94-217478] p 219 N95-19967

F-16XL interview with Marta Bohn-Meyer
[NASA-TM-110505] p 223 N95-19996

Computation of transonic flow on composite overlapping grids in 2 D
[PB95-131348] p 248 N95-21132

Unstructured-grid large-eddy simulation of flow over an airfoil
p 225 N95-22448

AIRFRAMES

Smart structures in the control of airframe vibrations
[HTN-95-31014] p 236 A95-71184

Lift enhancement device
[AD-D016522] p 224 N95-21864

AIRLINE OPERATIONS

Public-sector aviation issues: Graduate research award papers, 1992-1993
[PB94-217478] p 219 N95-19967

Test and evaluation report for the Manual Domestic Passive Profiling System (MDPPS)
[AD-A286312] p 225 N95-20093

AIRPORT SECURITY

Test and evaluation report for the Manual Domestic Passive Profiling System (MDPPS)
[AD-A286312] p 225 N95-20093

AIRPORTS

Test and Evaluation Plan (TEP) for Improved Explosive Device Screening Systems (IEDSS)
[AD-A286382] p 227 N95-22319

Analysis of test criteria for specifying foam firefighting agents for aircraft rescue and firefighting
[AD-A286381] p 227 N95-22352

AIRSHIPS

CALOPE and TAISIR airborne experiment platform
[DE94-018328] p 250 N95-22299

AIRSPEED

A real-time algorithm for integrating differential satellite and inertial navigation information during helicopter approach
[NASA-CR-197409] p 229 N95-21891

ALBEDO

Microphysical and radiative properties of small cumulus clouds over the sea
[HTN-95-A0526] p 255 A95-73180

On the link between cloud-top radiative properties and sub-cloud aerosol concentrations
[HTN-95-A0527] p 255 A95-73181

ALGORITHMS

Comparison of parameter identification algorithms for flight vehicles
[BTN-94-EIX94371347708] p 219 A95-69967

Behavior of an inversion-based precipitation retrieval algorithm with high-resolution AMPR measurements including a low-frequency 10.7-GHz channel
[HTN-95-70134] p 252 A95-70656

Comments on 'correction of inertial navigation with Loran C on NOAA's P-3 aircraft'
[HTN-95-70149] p 227 A95-70671

Large-scale computational fluid dynamics by the finite element method
[BTN-94-EIX94381359154] p 243 A95-71744

An algorithm for forecasting mountain wave-related turbulence in the stratosphere
[HTN-95-80656] p 254 A95-72500

A generalized algorithm for inverse simulation applied to helicopter maneuvering flight
[HTN-95-A0493] p 236 A95-72564

Buckling and vibration analysis of laminated panels using VICONOPT
[PAPER-1746] p 230 A95-72580

Computing methods for the approximate solution of time dependent problems
[AD-A286007] p 256 N95-20719

A real-time algorithm for integrating differential satellite and inertial navigation information during helicopter approach
[NASA-CR-197409] p 229 N95-21891

Direct numerical simulations of on-demand vortex generators: Mathematical formulation
p 251 N95-22452

ALL-WEATHER AIR NAVIGATION

Comments on effect of wet snow on the null-reference ILS system
[BTN-95-EIX95142555488] p 227 A95-72885

ALTITUDE

Ascent wind model for launch vehicle design
[BTN-95-EIX95041503799] p 239 A95-70124

ALTITUDE TESTS

Temperature effects on acoustic interactions between altitude test facilities and jet engine plumes
[NASA-CR-197638] p 258 N95-21170

ALUMINUM

Corrosion of aircraft materials: Correlation between nanometer scale and macroscopic structural damage parameters
[AD-A285930] p 241 N95-20299

ALUMINUM ALLOYS

Electrochemical impedance pattern recognition for detection of hidden chemical corrosion on aircraft components
[AD-A284998] p 241 N95-20481

Electrochemical impedance pattern recognition for detection of hidden chemical corrosion on aircraft components
[AD-A285998] p 241 N95-20716

Aircraft corrosion study
[AD-A279527] p 241 N95-21687

AMOUNT

Analysis of test criteria for specifying foam firefighting agents for aircraft rescue and firefighting
[AD-A286381] p 227 N95-22352

ANGLE OF ATTACK

T-45A High Angle of Attack Testing: US Naval Test Pilot School 46th Annual Reunion and Symposium
[AD-A284000] p 231 N95-20466

Pressure measurements on an F/A-18 twin vertical tail in buffeting flow. Volume 1: Wind tunnel test summary
[AD-A279126] p 225 N95-21877

Effect of juncture fillets on double-delta wings undergoing sideslip at high angles of attack
[AD-A286165] p 232 N95-22039

ANGULAR VELOCITY

Effects of yaw and pitch motion on model attitude measurements
[NASA-TM-4641] p 250 N95-22109

ANODIZING

Aircraft corrosion study
[AD-A279527] p 241 N95-21687

ANTENNA RADIATION PATTERNS

Comments on effect of wet snow on the null-reference ILS system
[BTN-95-EIX95142555488] p 227 A95-72885

ANTENNAS

Attitude determination using dedicated and nondedicated multiantenna GPS sensors
[BTN-95-EIX95142555482] p 228 A95-72891

APPLICATIONS OF MATHEMATICS

Computing methods for the approximate solution of time dependent problems
[AD-A286007] p 256 N95-20719

APPLICATIONS PROGRAMS (COMPUTERS)

Statistical analysis of Turbine Engine Diagnostic (TED) field test data
[AD-A286032] p 248 N95-20988

A computer code (SKINTEMP) for predicting transient missile and aircraft heat transfer characteristics
[AD-A286044] p 248 N95-21001

Investigation of shear layer transition using various turbulence models
p 248 N95-21096

A user's guide to LUGSAN 1.1: A computer program to calculate and archive lug and sway brace loads for aircraft-carried stores
[DE95-001919] p 232 N95-21730

APPROACH

A real-time algorithm for integrating differential satellite and inertial navigation information during helicopter approach
[NASA-CR-197409] p 229 N95-21891

APPROACH CONTROL

Crew aiding and automation: A system concept for terminal area operations, and guidelines for automation design
[NASA-CR-4631] p 228 N95-19950

APPROACH INDICATORS

Minima reduction simulation test results
[AD-A285626] p 228 N95-21148

APPROXIMATION

Computing methods for the approximate solution of time dependent problems
[AD-A286007] p 256 N95-20719

ARCHITECTURE (COMPUTERS)

The impact of advanced packaging technology on modular avionics architectures
p 233 N95-20632

Standard Hardware Acquisition and Reliability Program (SHARP) advanced SEM-E packaging
p 233 N95-20633

The IEEE scalable coherent interface: An approach for a unified avionics network
p 234 N95-20650

Optical backplane for modular avionics
p 257 N95-20652

High performance backplane components for modular avionics
p 247 N95-20653

The opportunities for and challenges of common integrated electronics
[AD-A279991] p 248 N95-20966

ARCTIC REGIONS

An algorithm for forecasting mountain wave-related turbulence in the stratosphere
[HTN-95-80656] p 254 A95-72500

AREA NAVIGATION

Crew aiding and automation: A system concept for terminal area operations, and guidelines for automation design
[NASA-CR-4631] p 228 N95-19950

Bomber force 2000: Operational concepts for long-range combat aircraft
[AD-A279378] p 230 N95-20181

ARTIFICIAL INTELLIGENCE

Engine life measurement and diagnostics
[BTN-95-EIX95041505024] p 235 A95-70133

Collected papers of the Soar/IFOR project, Spring 1994
[AD-A280063] p 238 N95-20624

ASHES

Volcanic ash forecast transport and dispersion (VAFTAD) model
[HTN-95-80702] p 254 A95-72546

ASYMMETRY

Large-eddy simulation of flow through a plane, asymmetric diffuser
p 250 N95-22449

ATMOSPHERIC CHEMISTRY

An Echelle Grating Spectrometer (EGS) for mid-IR remote chemical detection
[DE94-019310] p 249 N95-21478

ATMOSPHERIC CIRCULATION

Potential applications of the SSM/I cloud liquid water parameter to the estimation of marine aircraft icing
[HTN-95-80651] p 254 A95-72495

Volcanic ash forecast transport and dispersion (VAFTAD) model
[HTN-95-80702] p 254 A95-72546

ATMOSPHERIC COMPOSITION

Subsidence of aircraft engine exhaust in the stratosphere: Implications for calculated ozone depletions
[PAPER-93GL03426] p 251 A95-70297

Aircraft-borne, laser-induced fluorescence instrument for the in situ detection of hydroxyl and hydroperoxyl radicals
[BTN-95-EIX95072499029] p 253 A95-71908

ATMOSPHERIC MODELS

Ascent wind model for launch vehicle design
[BTN-95-EIX95041503799] p 239 A95-70124

Water vapor continuum absorption in mid-latitudes: Aircraft measurements and model comparisons
[HTN-95-40756] p 252 A95-71186

Aircraft measurements of water vapour continuum absorption at millimetre wavelengths
[HTN-95-90884] p 253 A95-72393

Potential applications of the SSM/I cloud liquid water parameter to the estimation of marine aircraft icing
[HTN-95-80651] p 254 A95-72495

An algorithm for forecasting mountain wave-related turbulence in the stratosphere
[HTN-95-80656] p 254 A95-72500

Snow-band formation and evolution during the 15 November 1987 aircraft accident at Denver airport
[HTN-95-80699] p 254 A95-72543

Volcanic ash forecast transport and dispersion (VAFTAD) model
[HTN-95-80702] p 254 A95-72546

ATMOSPHERIC MOISTURE

Response of the B-1B air data sensor to simulated dust cloud environments
[AD-A286134] p 235 N95-22036

ATMOSPHERIC PRESSURE

Effect of atmospheric pressure on measured aircraft noise levels
[PB95-130423] p 232 N95-21425

ATMOSPHERIC RADIATION

Aircraft measurements of water vapour continuum absorption at millimetre wavelengths
[HTN-95-90884] p 253 A95-72393

ATMOSPHERIC TEMPERATURE

Potential applications of the SSM/I cloud liquid water parameter to the estimation of marine aircraft icing
[HTN-95-80651] p 254 A95-72495

ATTACK AIRCRAFT

Naval aviation: F-14 upgrades are not adequately justified. Report to Congressional Committees
[AD-A286338] p 231 N95-20212

Design of a controller for a flexible pointing system using H(infinity) synthesis
[AD-A286572] p 256 N95-20828

ATTITUDE (INCLINATION)

Attitude determination using dedicated and nondedicated multiantenna GPS sensors
[BTN-95-EIX9514255482] p 228 A95-72891

ATTITUDE INDICATORS

Assessment of a non-dedicated GPS receiver system for precise airborne attitude determination
[DE94-019309] p 229 N95-21520

AUTOMATA THEORY

GPS-Scuttler capacity analysis
[AD-A280037] p 245 N95-20599

AUTOMATIC PILOTS

Collected papers of the Soar/IFOR project, Spring 1994
[AD-A280063] p 238 N95-20624

AVIONICS

Integrated IR sensors
[BTN-95-EIX95041505023] p 242 A95-70132

Foliage transmission measurements using a ground-based ultrawide band (300-1300 MHz) SAR system
[BTN-94-EIX94381351617] p 252 A95-70950

Advanced Packaging Concepts for Digital Avionics
[AGARD-CP-562] p 233 N95-20631

The impact of advanced packaging technology on modular avionics architectures
[AD-A286239] p 233 N95-20632

Standard Hardware Acquisition and Reliability Program (SHARP) advanced SEM-E packaging
[AD-A286239] p 233 N95-20633

FASTPACK: Optimized solutions for modular avionics derived from a parametric study. Part 1: Platform features
[AD-A286239] p 233 N95-20634

FASTPACK: Optimized solutions for modular avionics derived from a parametric study. Part 2: Avionics
[AD-A286239] p 233 N95-20635

The Advanced Avionics Subsystem Technology Demonstration Program
[AD-A286239] p 234 N95-20636

Ultra-Reliable Digital Avionics (URDA) processor
[AD-A286239] p 245 N95-20638

MCMs for avionics: Technology selection and intermodule interconnection
[AD-A286239] p 234 N95-20641

High density monolithic packaging technology for digital/microwave avionics
[AD-A286239] p 240 N95-20646

High performance backplane components for modular avionics
[AD-A286239] p 247 N95-20653

Composite cases for airborne electronic equipment: A technology study and EMC
[AD-A286239] p 241 N95-20655

Modular supplies for a distributed architecture — avionics packaging
[AD-A286239] p 234 N95-20657

Modular CNI avionics system
[AD-A286239] p 234 N95-20659

The opportunities for and challenges of common integrated electronics
[AD-A279991] p 248 N95-20966

Systems engineering design and technical analyses for Strategic Avionics Crew-station Design Evaluation Facility (SACDEF)
[AD-A286239] p 235 N95-22024

Evaluation of the Haworth-Newman avionics Display Readability Scale
[AD-A286127] p 235 N95-22232

B

BACKSCATTERING

Electromagnetic backscattering from a helicopter rotor in the decametric wave band regime
[BTN-94-EIX94381353130] p 243 A95-72648

BAGGAGE

Test and Evaluation Plan (TEP) for Improvised Explosive Device Screening Systems (IEDSS)
[AD-A286382] p 227 N95-22319

BALLOON FLIGHT

Comparison of meteorological data with fitted values extracted from projectile trajectory
[AD-A285921] p 255 N95-19899

BALLOON-BORNE INSTRUMENTS

CALIOPE and TAISIR airborne experiment platform
[DE94-018328] p 250 N95-22299

BANDWIDTH

Foliage transmission measurements using a ground-based ultrawide band (300-1300 MHz) SAR system
[BTN-94-EIX94381351617] p 252 A95-70950

BAROCLINITY

Radar studies of aviation hazards
[AD-A285845] p 226 N95-21831

BIBLIOGRAPHIES

Aeronautical engineering: A continuing bibliography with indexes (supplement 315)
[NASA-SP-7037(315)] p 219 N95-21640

BINOCULAR VISION

Factors affecting the perception of luning in monocular regions of partial binocular overlap displays
[AD-A286287] p 259 N95-22044

BLADE-VORTEX INTERACTION

Aerodynamic and wake methodology evaluation using Model UH-60A experimental data
[HTN-95-31009] p 220 A95-71179

Effects of leading and trailing edge flaps on the aerodynamics of airfoil/vortex interactions
[HTN-95-31011] p 221 A95-71181

BLANKETS (FUSION REACTORS)

MHD-flow in slotted channels with conducting walls
[DE94-018370] p 258 N95-21388

BLOWDOWN WIND TUNNELS

The dynamic approach to rotor blade research: ARA's oscillatory test facility
[ARA-MEMO-405] p 223 N95-20758

BLUFF BODIES

Research on bluff body vortex wakes
[AD-A286319] p 223 N95-20177

BLUNT BODIES

Flow resolution and domain influence in rarefied hypersonic blunt-body flows
[BTN-95-EIX95082502729] p 220 A95-70136

Shock wave interactions in hypervelocity flow
[AD-A286507] p 250 N95-22212

BO-105 HELICOPTER

A generalized algorithm for inverse simulation applied to helicopter maneuvering flight
[HTN-95-A0483] p 236 A95-72564

BODY-WING CONFIGURATIONS

Time-resolved surface heat flux measurements in the wing/body junction vortex
[BTN-95-EIX95082502716] p 220 A95-71029

Open Skies project computational fluid dynamic analysis
[AD-A285928] p 223 N95-19991

BOMBER AIRCRAFT

Bomber force 2000: Operational concepts for long-range combat aircraft
[AD-A279378] p 230 N95-20181

Systems engineering design and technical analyses for Strategic Avionics Crew-station Design Evaluation Facility (SACDEF)
[AD-A286239] p 235 N95-22024

BONDED JOINTS

Bonded composite repair of cracked load-bearing holes
[BTN-94-EIX94401360553] p 243 A95-71867

BONDING

Reliability assessment of Multichip Module technologies via the Triservice/NASA RELTECH program
[AD-A286239] p 245 N95-20643

Assuring Known Good Die (KGD) for reliable, cost effective MCMs
[AD-A286239] p 246 N95-20644

BOUNDARY LAYER CONTROL

Flow coefficient behavior for boundary layer bleed holes and slots
[NASA-TM-106846] p 244 N95-19953

Supersonic laminar flow control research
[NASA-CR-196049] p 249 N95-21340

Experimental investigations of on-demand vortex generators
[AD-A286239] p 250 N95-22451

BOUNDARY LAYER FLOW

Aerodynamic mechanism of galloping
[BTN-94-EIX94371347709] p 219 A95-69968

Experiments on the flow field physics of confluent boundary layers for high-lift systems
[NASA-CR-197318] p 224 N95-21343

Acoustics of laminar boundary layers breakdown
[AD-A285622] p 251 N95-22455

BOUNDARY LAYER STABILITY

Computational studies of laminar to turbulence transition
[AD-A285622] p 248 N95-21146

Supersonic laminar flow control research
[NASA-CR-196049] p 249 N95-21340

BOUNDARY LAYER TRANSITION

Application of Direct and Large Eddy Simulation to Transition and Turbulence
[AGARD-CP-551] p 248 N95-21061

Investigation of shear layer transition using various turbulence models
[AD-A285622] p 248 N95-21096

Computational studies of laminar to turbulence transition
[AD-A285622] p 248 N95-21146

Acoustic receptivity due to weak surface inhomogeneities in adverse pressure gradient boundary layers
[NASA-TM-4577] p 249 N95-21258

Supersonic laminar flow control research
[NASA-CR-196049] p 249 N95-21340

Acoustics of laminar boundary layers breakdown
[AD-A285622] p 251 N95-22455

BOUNDARY LAYERS

Open Skies project computational fluid dynamic analysis
[AD-A285928] p 223 N95-19991

BOUNDARY LUBRICATION

Lubricant evaluation and performance, 2
[AD-A279144] p 242 N95-21969

BRAGG CELLS

A three-dimensional orthogonal laser velocimeter for the NASA Ames 7- by 10-foot wind tunnel
[NASA-TM-108864] p 249 N95-21323

BREADBOARD MODELS

Eddy current for detecting second-layer cracks under installed fasteners
[AD-A279871] p 244 N95-20414

BRIGHTNESS TEMPERATURE

Behavior of an inversion-based precipitation retrieval algorithm with high-resolution AMPR measurements including a low-frequency 10.7-GHz channel
[HTN-95-70134] p 252 A95-70656

Water vapor continuum absorption in mid-latitudes: Aircraft measurements and model comparisons
[HTN-95-40756] p 252 A95-71186

Aircraft measurements of water vapour continuum absorption at millimetre wavelengths
[HTN-95-90884] p 253 A95-72393

BUCKLING

Buckling and vibration analysis of laminated panels using VICONOPT
[PAPER-1746] p 230 A95-72580

BUFFETING

Pressure measurements on an F/A-18 twin vertical tail in buffeting flow. Volume 4, part 1: Buffet cross spectral densities
[AD-A285593] p 237 N95-21214

Pressure measurements on an F/A-18 twin vertical tail in buffeting flow. Volume 1: Wind tunnel test summary
[AD-A279126] p 225 N95-21877

BUNDLES

Fiber-optic rotary joint with bundle collimator assemblies
[AD-D016504] p 258 N95-21673

BUOYANCY

Investigation of a thermal buoyancy effect on the drag of half models tested in the ARA Transonic Wind Tunnel
[ARA-MEMO-407] p 222 N95-19946

BURN-IN

Assuring Known Good Die (KGD) for reliable, cost effective MCMs
[AD-A286239] p 246 N95-20644

BY-PRODUCTS

Laboratory evaluation of a reactive baffle approach to NOx control
[AD-A283802] p 255 N95-19921

C

C++ (PROGRAMMING LANGUAGE)

The navigation toolkit
[NASA-CR-197290] p 229 N95-22161

CALIBRATING

Precise orbit determination with a short-arc technique — Abstract only
[AD-A286239] p 240 A95-70543

16-foot transonic tunnel test section flowfield survey
[NASA-TM-109157] p 238 N95-20669

CAMERAS

Passive range measurement system
[AD-D016222] p 258 N95-21100

CANTILEVER BEAMS

Corrosion behavior of landing gear steels
[AD-A285862] p 242 N95-22132

CARBON MONOXIDE

Laboratory evaluation of a reactive baffle approach to NOx control
[AD-A283802] p 255 N95-19921

- CARRIAGES**
A user's guide to LUGSAN 1.1: A computer program to calculate and archive lug and sway brace loads for aircraft-carried stores
[DE95-001919] p 232 N95-21730
- CASCADE FLOW**
Experimental study of vane heat transfer and aerodynamics at elevated levels of turbulence
[NASA-CR-4633] p 244 N95-19912
- CASES (CONTAINERS)**
Composite cases for airborne electronic equipment: A technology study and EMC
p 241 N95-20655
- CAVITIES**
Measurements of shielding effectiveness and cavity characteristics of airplanes
[PB94-210051] p 244 N95-20191
- CENSUS**
Census US civil aircraft calendar year 1993
[AD-A286309] p 219 N95-20091
- CERAMIC MATRIX COMPOSITES**
Toughened Silcomp composites for gas turbine engine applications
[DE95-002851] p 235 N95-21243
- CERAMICS**
Reliability assessment of Multichip Module technologies via the Triservice/NASA RELTECH program
p 245 N95-20643
- CERTIFICATION**
An evaluation of Automatic Terminal Information Service (ATIS) flight deck display presentation options
[AD-A280100] p 228 N95-21020
- CHANNEL FLOW**
Large-eddy simulation of flow through a plane, asymmetric diffuser
p 250 N95-22449
- CHANNELS (DATA TRANSMISSION)**
Optical backplane for modular avionics
p 257 N95-20652
- CHEMICAL ANALYSIS**
An Echelle Grating Spectrometer (EGS) for mid-IR remote chemical detection
[DE94-019310] p 249 N95-21478
- CHEMICAL EQUILIBRIUM**
Thermochemical nonequilibrium viscous shock-layer analysis for a Mars aerocapture vehicle
[BTN-95-EIX95082502732] p 239 A95-70139
- CHEMICAL VAPOR INFILTRATION**
Scale-up and modeling of forced chemical vapor infiltration
[DE94-017769] p 247 N95-20781
- CHIPS**
MCMs for avionics: Technology selection and intermodule interconnection
p 234 N95-20641
Reliability assessment of Multichip Module technologies via the Triservice/NASA RELTECH program
p 245 N95-20643
Assuring Known Good Die (KGD) for reliable, cost effective MCMs
p 246 N95-20644
- CIRCULAR CYLINDERS**
Research on bluff body vortex wakes
[AD-A286319] p 223 N95-20177
- CIVIL AVIATION**
Census US civil aircraft calendar year 1993
[AD-A286309] p 219 N95-20091
Test and evaluation report for the Manual Domestic Passive Profiling System (MDPPS)
[AD-A286312] p 225 N95-20093
- CLIMBING FLIGHT**
Acoustic climb to cruise test
[NASA-TM-110504] p 230 N95-20155
- CLOUD PHYSICS**
High-resolution imaging of rain systems with the advanced microwave precipitation radiometer
[HTN-95-70133] p 252 A95-70655
Behavior of an inversion-based precipitation retrieval algorithm with high-resolution AMPR measurements including a low-frequency 10.7-GHz channel
[HTN-95-70134] p 252 A95-70656
Potential applications of the SSM/I cloud liquid water parameter to the estimation of marine aircraft icing
[HTN-95-80651] p 254 A95-72495
Microphysical and radiative properties of small cumulus clouds over the sea
[HTN-95-A0526] p 255 A95-73180
On the link between cloud-top radiative properties and sub-cloud aerosol concentrations
[HTN-95-A0527] p 255 A95-73181
- CLOUDS (METEOROLOGY)**
High-resolution imaging of rain systems with the advanced microwave precipitation radiometer
[HTN-95-70133] p 252 A95-70655
Behavior of an inversion-based precipitation retrieval algorithm with high-resolution AMPR measurements including a low-frequency 10.7-GHz channel
[HTN-95-70134] p 252 A95-70656
- COANDA EFFECT**
Static investigation of two fluidic thrust-vectoring concepts on a two-dimensional convergent-divergent nozzle
[NASA-TM-4574] p 222 N95-19913
- COATING**
Aircraft corrosion study
[AD-A279527] p 241 N95-21687
- COATINGS**
Aircraft corrosion study
[AD-A279527] p 241 N95-21687
- COLLIMATION**
RCS measurements, transformations, and comparisons under cylindrical and plane wave illumination
[BTN-94-EIX94371347126] p 242 A95-69976
- COLLIMATORS**
Fiber-optic rotary joint with bundle collimator assemblies
[AD-D016504] p 258 N95-21673
- COLOR**
Color control in a multichannel simulator display: The display for advanced research and training
[AD-A279717] p 239 N95-20992
Test and Evaluation Plan (TEP) for Improved Explosive Device Screening Systems (IEDSS)
[AD-A286382] p 227 N95-22319
- COLORADO**
Snow-band formation and evolution during the 15 November 1987 aircraft accident at Denver airport
[HTN-95-80699] p 254 A95-72543
- COMBAT**
Bomber force 2000: Operational concepts for long-range combat aircraft
[AD-A279378] p 230 N95-20181
- COMBUSTIBLE FLOW**
Two-dimensional imaging of OH in a lean burning high pressure combustor
[NASA-TM-106854] p 236 N95-21383
- COMBUSTION**
Two-dimensional imaging of OH in a lean burning high pressure combustor
[NASA-TM-106854] p 236 N95-21383
- COMBUSTION PRODUCTS**
Laboratory evaluation of a reactive baffle approach to NOx control
[AD-A283802] p 255 N95-19921
- COMMERCIAL AIRCRAFT**
Census US civil aircraft calendar year 1993
[AD-A286309] p 219 N95-20091
Commuter/air taxi ditchings and water-related impacts that occurred from 1979 to 1989
[AD-A285691] p 226 N95-20275
Why do airlines want and use thrust reversers? A compilation of airline industry responses to a survey regarding the use of thrust reversers on commercial transport airplanes
[NASA-TM-109158] p 226 N95-20706
- COMMONALITY**
The opportunities for and challenges of common integrated electronics
[AD-A278991] p 248 N95-20966
- COMMUNICATION**
Independent review of Aviation Technology and Research Information Analysis System (ATRIAS) database
[AD-A284049] p 226 N95-21518
- COMMUNICATION NETWORKS**
Optical backplane for modular avionics
p 257 N95-20652
- COMMUTER AIRCRAFT**
Commuter airplane accident data analysis
[AD-A286315] p 226 N95-20174
- COMPOSITE MATERIALS**
Numerical modelling of transverse impact on composite coupons
[BTN-95-EIX95082502225] p 240 A95-71022
Composite cases for airborne electronic equipment: A technology study and EMC
p 241 N95-20655
Lightweight electronic enclosures using composite materials
p 241 N95-20656
- COMPOSITE STRUCTURES**
Bonded composite repair of cracked load-bearing holes
[BTN-94-EIX94401360553] p 243 A95-71867
Air and ground resonance of helicopters with elastically tailored composite rotor blades
[HTN-95-A0497] p 222 A95-72568
- COMPRESSIBLE FLOW**
Investigation of shear layer transition using various turbulence models
p 248 N95-21096
- COMPRESSORS**
Malone-brayton cycle engine/heat pump
[AD-D016573] p 244 N95-20295
- COMPUTATIONAL FLUID DYNAMICS**
Measurement around a rotor blade excited in pitch. Part 1: Dynamic inflow
[HTN-95-31007] p 220 A95-71177
Measurement around a rotor blade excited in pitch. Part 2: Unsteady surface pressure
[HTN-95-31008] p 220 A95-71178
Aerodynamic and wake methodology evaluation using Model UH-60A experimental data
[HTN-95-31009] p 220 A95-71179
Vorticity concentration at the edge of the inboard vortex sheet
[HTN-95-31010] p 221 A95-71180
Effects of leading and trailing edge flaps on the aerodynamics of airfoil/vortex interactions
[HTN-95-31011] p 221 A95-71181
Large-scale computational fluid dynamics by the finite element method
[BTN-94-EIX94381359154] p 243 A95-71744
A generalized algorithm for inverse simulation applied to helicopter maneuvering flight
[HTN-95-A0493] p 236 A95-72564
High-order state space simulation models of helicopter flight mechanics
[HTN-95-A0494] p 237 A95-72565
On the choice of appropriate bases for nonlinear dynamic modal analysis
[HTN-95-A0495] p 221 A95-72566
Flap-lag damping in hover and forward flight with a three-dimensional wake
[HTN-95-A0496] p 221 A95-72567
Air and ground resonance of helicopters with elastically tailored composite rotor blades
[HTN-95-A0497] p 222 A95-72568
Design optimization of rotor blades for improved performance and vibration
[HTN-95-A0498] p 229 A95-72569
Parametric studies for tiltrotor aeroelastic stability in highspeed flight
[HTN-95-A0499] p 222 A95-72570
Open Skies project computational fluid dynamic analysis
[AD-A285928] p 223 N95-19991
Application of Direct and Large Eddy Simulation to Transition and Turbulence
[AGARD-CP-551] p 248 N95-21061
Investigation of shear layer transition using various turbulence models
p 248 N95-21096
Computational studies of laminar to turbulence transition
[AD-A285622] p 248 N95-21146
Application of Navier-Stokes code PAB3D with kappa-epsilon turbulence model to attached and separated flows
[NASA-TP-3480] p 224 N95-21338
Effects of yaw and pitch motion on model attitude measurements
[NASA-TM-4641] p 250 N95-22109
Unstructured-grid large-eddy simulation of flow over an airfoil
p 225 N95-22448
Large-eddy simulation of flow through a plane, asymmetric diffuser
p 250 N95-22449
Direct numerical simulations of on-demand vortex generators: Mathematical formulation
p 251 N95-22452
- COMPUTATIONAL GRIDS**
Flow resolution and domain influence in rarefied hypersonic blunt-body flows
[BTN-95-EIX95082502729] p 220 A95-70136
Adaptive remeshing for convective heat transfer with variable fluid properties
[BTN-95-EIX95082502720] p 243 A95-71033
Large-scale computational fluid dynamics by the finite element method
[BTN-94-EIX94381359154] p 243 A95-71744
Unstructured-grid large-eddy simulation of flow over an airfoil
p 225 N95-22448
- COMPUTER AIDED DESIGN**
Design optimization of rotor blades for improved performance and vibration
[HTN-95-A0498] p 229 A95-72569
Buckling and vibration analysis of laminated panels using VICONOPT
[PAPER-1748] p 230 A95-72580
Parallel calculation of sensitivity derivatives for aircraft design using automatic differentiation
[NASA-TM-110103] p 231 N95-20370
Development of quiet-flow supersonic wind tunnels for laminar-turbulent transition research
[NASA-CR-197286] p 239 N95-21436
- COMPUTER ASSISTED INSTRUCTION**
A computer-based multimedia prototype for night vision goggles
[AD-A286208] p 258 N95-21882

COMPUTER NETWORKS

- The IEEE scalable coherent interface: An approach for a unified avionics network p 234 N95-20650
High performance backbone components for modular avionics p 247 N95-20653
- COMPUTER PROGRAMS**
Buckling and vibration analysis of laminated panels using VICONOPT [PAPER-1746] p 230 A95-72580
Prediction of rotor-blade deformations due to unsteady airloads [AD-A286593] p 231 N95-20860
The opportunities for and challenges of common integrated electronics [AD-A279991] p 248 N95-20966
Data link terminal DLT document [PB95-110805] p 229 N95-21369
- COMPUTER SYSTEMS DESIGN**
The Advanced Avionics Subsystem Technology Demonstration Program p 234 N95-20636
The IEEE scalable coherent interface: An approach for a unified avionics network p 234 N95-20650
Independent review of Aviation Technology and Research Information Analysis System (ATRIAS) database [AD-A284049] p 226 N95-21518
The navigation toolkit [NASA-CR-197290] p 229 N95-22161
- COMPUTER TECHNIQUES**
The IEEE scalable coherent interface: An approach for a unified avionics network p 234 N95-20650
- COMPUTERIZED SIMULATION**
Numerical modelling of transverse impact on composite coupons [BTN-95-EIX95082502225] p 240 A95-71022
High-order state space simulation models of helicopter flight mechanics [HTN-95-A0494] p 237 A95-72565
Collected papers of the Soar/IFOR project, Spring 1994 [AD-A280063] p 238 N95-20624
Application of Direct and Large Eddy Simulation to Transition and Turbulence [AGARD-CP-551] p 248 N95-21061
Simulation of rotor blade element turbulence [NASA-TM-108862] p 232 N95-21186
A preliminary study of the airwake model used in an existing SH-60B/FFG-7 helicopter/ship simulation program [DSTO-TR-0015] p 224 N95-21659
Unstructured-grid large-eddy simulation of flow over an airfoil p 225 N95-22448
Large-eddy simulation of flow through a plane, asymmetric diffuser p 250 N95-22449
Direct numerical simulations of on-demand vortex generators: Mathematical formulation p 251 N95-22452
- COMPUTERS**
The opportunities for and challenges of common integrated electronics [AD-A279991] p 248 N95-20966
- CONDENSATION NUCLEI**
On the link between cloud-top radiative properties and sub-cloud aerosol concentrations [HTN-95-A0527] p 255 A95-73181
- CONFERENCES**
T-45A High Angle of Attack Testing: US Naval Test Pilot School 46th Annual Reunion and Symposium [AD-A284000] p 231 N95-20466
Advanced Packaging Concepts for Digital Avionics [AGARD-CP-562] p 233 N95-20631
Application of Direct and Large Eddy Simulation to Transition and Turbulence [AGARD-CP-551] p 248 N95-21061
- CONGRESSIONAL REPORTS**
Naval aviation: F-14 upgrades are not adequately justified. Report to Congressional Committees [AD-A286338] p 231 N95-20212
- CONSTRUCTION**
Aeronautical engineering: A continuing bibliography with indexes (supplement 315) [NASA-SP-7037(315)] p 219 N95-21640
- CONTINUOUS SPECTRA**
Aircraft measurements of water vapour continuum absorption at millimetre wavelengths [HTN-95-90884] p 253 A95-72393
- CONTROL SYSTEMS DESIGN**
Rotorcraft control system design for uncertain vehicle dynamics using quantitative feedback theory [HTN-95-31012] p 236 A95-71182
Smart structures in the control of airframe vibrations [HTN-95-31014] p 236 A95-71184
A generalized algorithm for inverse simulation applied to helicopter maneuvering flight [HTN-95-A0493] p 236 A95-72564
Design of a controller for a flexible pointing system using H(infinity) synthesis [AD-A286572] p 256 N95-20828
Design of robust optimal control systems and stability analysis of real structured uncertainties [AD-A279089] p 256 N95-21913
- CONTROL THEORY**
Summary of a joint program of research into aircraft flight control concepts [AD-A280012] p 237 N95-20004
- CONTROLLERS**
Design of a controller for a flexible pointing system using H(infinity) synthesis [AD-A286572] p 256 N95-20828
Robust fixed-structure control [AD-A286515] p 257 N95-22216
- CONVECTIVE HEAT TRANSFER**
Adaptive remeshing for convective heat transfer with variable fluid properties [BTN-95-EIX95082502720] p 243 A95-71033
A computer code (SKINTEMP) for predicting transient missile and aircraft heat transfer characteristics [AD-A286044] p 248 N95-21001
- CONVERGENT-DIVERGENT NOZZLES**
Static investigation of two fluidic thrust-vectoring concepts on a two-dimensional convergent-divergent nozzle [NASA-TM-4574] p 222 N95-19913
- CONVEXITY**
Design of robust optimal control systems and stability analysis of real structured uncertainties [AD-A279089] p 256 N95-21913
- COOLANTS**
Immersion/two phase cooling p 246 N95-20648
- COOLING**
FASTPACK: Optimized solutions for modular avionics derived from a parametric study. Part 2: Avionics p 233 N95-20635
Immersion/two phase cooling p 246 N95-20648
Toughened Silcomp composites for gas turbine engine applications [DE95-002851] p 235 N95-21243
- COORDINATES**
SAR image registration in absolute coordinates using GPS carrier phase position and velocity information [DE94-018738] p 228 N95-20195
- CORRELATION**
Precise navigation using adaptive FIR filtering and time domain spectral estimation [BTN-95-EIX95142555485] p 227 A95-72888
- CORROSION**
Modelling of pilling due to corrosion in fuselage lap joints [BTN-95-EIX95082502227] p 240 A95-71024
Corrosion of aircraft materials: Correlation between nanometer scale and macroscopic structural damage parameters [AD-A285930] p 241 N95-20289
Electrochemical impedance pattern recognition for detection of hidden chemical corrosion on aircraft components [AD-A284998] p 241 N95-20481
Electrochemical impedance pattern recognition for detection of hidden chemical corrosion on aircraft components [AD-A285998] p 241 N95-20716
Aircraft corrosion study [AD-A279527] p 241 N95-21687
- CORROSION TESTS**
Corrosion behavior of landing gear steels [AD-A285862] p 242 N95-22132
- COST ANALYSIS**
The personal aircraft: Status and issues [NASA-TM-109174] p 223 N95-20688
- COST EFFECTIVENESS**
Naval aviation: F-14 upgrades are not adequately justified. Report to Congressional Committees [AD-A286338] p 231 N95-20212
Assuring Known Good Die (KGD) for reliable, cost effective MCMs p 246 N95-20644
- COST REDUCTION**
Reliability assessment of Multichip Module technologies via the Triservice/NASA RELTECH program p 245 N95-20643
The opportunities for and challenges of common integrated electronics [AD-A279991] p 248 N95-20966
- COSTS**
MCMs for avionics: Technology selection and intermodule interconnection p 234 N95-20641
- CRACK PROPAGATION**
Bonded composite repair of cracked load-bearing holes [BTN-94-EIX94401360553] p 243 A95-71867

CRACKS

- Eddy current for detecting second-layer cracks under installed fasteners [AD-A279871] p 244 N95-20414
Damage tolerant repair techniques for pressurized aircraft fuselages [AD-A286298] p 219 N95-22046
- CRASH LANDING**
Commuter/air taxi ditchings and water-related impacts that occurred from 1979 to 1989 [AD-A285691] p 226 N95-20275
- CRASHES**
Commuter airplane accident data analysis [AD-A286315] p 226 N95-20174
- CRASHWORTHINESS**
Prediction of energy absorption capability of composite stiffeners [HTN-95-A0500] p 230 A95-72571
Commuter airplane accident data analysis [AD-A286315] p 226 N95-20174
Commuter/air taxi ditchings and water-related impacts that occurred from 1979 to 1989 [AD-A285691] p 226 N95-20275
- CREW WORKSTATIONS**
Systems engineering design and technical analyses for Strategic Avionics Crew-station Design Evaluation Facility (SACDEF) [AD-A286239] p 235 N95-22024
- CROSS FLOW**
Computational studies of laminar to turbulence transition [AD-A285622] p 248 N95-21146
- CUMULUS CLOUDS**
Microphysical and radiative properties of small cumulus clouds over the sea [HTN-95-A0526] p 255 A95-73180
On the link between cloud-top radiative properties and sub-cloud aerosol concentrations [HTN-95-A0527] p 255 A95-73181
- CV-880 AIRCRAFT**
Fuselage burnthrough from large exterior fuel fires [AD-A286295] p 226 N95-22318
- CYCLOGENESIS**
Tropical cyclone observation and forecasting with and without aircraft reconnaissance [HTN-95-80701] p 254 A95-72545
- CYLINDRICAL BODIES**
Aerodynamic mechanism of galloping [BTN-94-EIX94371347709] p 219 A95-69968
Time-resolved surface heat flux measurements in the wing/body junction vortex [BTN-95-EIX95082502716] p 220 A95-71029
- CYLINDRICAL WAVES**
RCS measurements, transformations, and comparisons under cylindrical and plane wave illumination [BTN-94-EIX94371347126] p 242 A95-69976
- D**
- DAMPING**
Flap-lag damping in hover and forward flight with a three-dimensional wake [HTN-95-A0496] p 221 A95-72567
Prediction of energy absorption capability of composite stiffeners [HTN-95-A0500] p 230 A95-72571
- DARKENING**
Factors affecting the perception of tuning in monocular regions of partial binocular overlap displays [AD-A286287] p 259 N95-22044
- DATA BASES**
Description and flow characterization of hypersonic facilities [AD-A284291] p 223 N95-20248
Data link terminal DLT document [PB95-110805] p 229 N95-21369
Independent review of Aviation Technology and Research Information Analysis System (ATRIAS) database [AD-A284049] p 226 N95-21518
A user's guide to LUGSAN 1.1: A computer program to calculate and archive lug and sway brace loads for aircraft-carried stores [DE95-001919] p 232 N95-21730
- DATA LINKS**
GPS-Squitter capacity analysis [AD-A280037] p 245 N95-20599
Data link terminal DLT document [PB95-110805] p 229 N95-21369
- DATA PROCESSING**
SAR image registration in absolute coordinates using GPS carrier phase position and velocity information [DE94-018738] p 228 N95-20195
Optical processing and control [AD-A279157] p 259 N95-21975

DATA PROCESSING EQUIPMENT

The impact of advanced packaging technology on modular avionics architectures p 233 N95-20632

DATA PROCESSING TERMINALS

Evaluation of the Haworth-Newman avionics Display Readability Scale [AD-A286127] p 235 N95-22232

DATA RECORDERS

Investigation of flight data recorder fire test requirements [AD-A285832] p 232 N95-20032

DATA REDUCTION

SAR image registration in absolute coordinates using GPS carrier phase position and velocity information [DE94-018738] p 228 N95-20195

DATA STRUCTURES

Computing methods for the approximate solution of time dependent problems [AD-A286007] p 256 N95-20719

DATA TRANSMISSION

Electromagnetic compatibility effects of advanced packaging configurations p 247 N95-20658

DC 8 AIRCRAFT

Fuselage burnthrough from large exterior fuel fires [AD-A286295] p 226 N95-22318

DEACTIVATION

Recommendation on transition from primary/secondary radar to secondary-only radar capability [AD-A286279] p 249 N95-22005

DECAMETRIC WAVES

Electromagnetic backscattering from a helicopter rotor in the decametric wave band regime [BTN-94-EIX94381353130] p 243 A95-72648

DEFENSE PROGRAM

Environmental Compliance Assessment and Management Program [AD-A279605] p 255 N95-20441

DEFORMATION

Modelling of pillowing due to corrosion in fuselage lap joints [BTN-95-EIX95082502227] p 240 A95-71024
Prediction of rotor-blade deformations due to unsteady airloads [AD-A286593] p 231 N95-20860

DEGREES OF FREEDOM

Aerodynamic mechanism of galloping [BTN-94-EIX94371347709] p 219 A95-69968
High-order state space simulation models of helicopter flight mechanics [HTN-95-A0494] p 237 A95-72565

DELTA WINGS

Effect of juncture fillets on double-delta wings undergoing sideslip at high angles of attack [AD-A286165] p 232 N95-22039

DEPTH MEASUREMENT

Evaluation of the Sparton tight-tolerance AXBT [HTN-95-40728] p 251 A95-70473

DESIGN ANALYSIS

Super-heavy aircraft study [AD-A279602] p 238 N95-19955
Parallel calculation of sensitivity derivatives for aircraft design using automatic differentiation [NASA-TM-110103] p 231 N95-20370
An evaluation of Automatic Terminal Information Service (ATIS) flight deck display presentation options [AD-A280100] p 228 N95-21020
CALIOPE and TAISIR airborne experiment platform [DE94-018328] p 250 N95-22299

DETECTION

Electrochemical impedance pattern recognition for detection of hidden chemical corrosion on aircraft components [AD-A285998] p 241 N95-20716

DIELECTRICS

Reliability assessment of Multichip Module technologies via the Triservice/NASA RELTECH program p 245 N95-20643

DIFFERENCE EQUATIONS

Computation of transonic flow on composite overlapping grids in 2 D [PB95-131348] p 248 N95-21132

DIFFERENTIAL EQUATIONS

Computation of transonic flow on composite overlapping grids in 2 D [PB95-131348] p 248 N95-21132

DIFFUSERS

Large-eddy simulation of flow through a plane, asymmetric diffuser p 250 N95-22449

DIGITAL ELECTRONICS

Advanced Packaging Concepts for Digital Avionics [AGARD-CP-562] p 233 N95-20631
High density monolithic packaging technology for digital/microwave avionics p 240 N95-20646
Modular supplies for a distributed architecture --- avionics packaging p 234 N95-20657

DIGITAL FILTERS

Precise navigation using adaptive FIR filtering and time domain spectral estimation [BTN-95-EIX95142555485] p 227 A95-72888

DIGITAL NAVIGATION

Precise navigation using adaptive FIR filtering and time domain spectral estimation [BTN-95-EIX95142555485] p 227 A95-72888

DIGITAL SYSTEMS

Ultra-Reliable Digital Avionics (URDA) processor p 245 N95-20638

DIMENSIONAL MEASUREMENT

Effects of yaw and pitch motion on model attitude measurements [NASA-TM-4641] p 250 N95-22109

DISPLAY DEVICES

The impact of advanced packaging technology on modular avionics architectures p 233 N95-20632
Color control in a multichannel simulator display: The display for advanced research and training [AD-A279717] p 239 N95-20992
Data link terminal DLT document [PB95-110805] p 229 N95-21369
Evaluation of the Haworth-Newman avionics Display Readability Scale [AD-A286127] p 235 N95-22232

DOPPLER RADAR

Radar studies of aviation hazards [AD-A285845] p 226 N95-21831

DRAG MEASUREMENT

Investigation of a thermal buoyancy effect on the drag of half models tested in the ARA Transonic Wind Tunnel [ARA-MEMO-407] p 222 N95-19946

Optical processing and control [AD-A279157] p 259 N95-21975

DROP SIZE

A review of water mist technology for fire suppression [AD-A285738] p 225 N95-20071

DUST

Response of the B-1B air data sensor to simulated dust cloud environments [AD-A286134] p 235 N95-22036

DYNAMIC MODELS

Large-eddy simulation of flow through a plane, asymmetric diffuser p 250 N95-22449

DYNAMIC PRESSURE

Pressure measurements on an F/A-18 twin vertical tail in buffeting flow. Volume 1: Wind tunnel test summary [AD-A279126] p 225 N95-21877

DYNAMIC RESPONSE

Effects of yaw and pitch motion on model attitude measurements [NASA-TM-4641] p 250 N95-22109

DYNAMIC TESTS

Effect of atmospheric pressure on measured aircraft noise levels [PB95-130423] p 232 N95-21425

E**EARTH ATMOSPHERE**

Overview of remote sensing laser development and semiconductor laser technology [DE94-018103] p 256 N95-21552

ECHELLE GRATINGS

An Echelle Grating Spectrometer (EGS) for mid-IR remote chemical detection [DE94-019310] p 249 N95-21478

EDDY CURRENTS

Eddy current for detecting second-layer cracks under installed fasteners [AD-A279871] p 244 N95-20414

EFFECTIVE PERCEIVED NOISE LEVELS

Effect of atmospheric pressure on measured aircraft noise levels [PB95-130423] p 232 N95-21425

Active control of fan noise-feasibility study. Volume 1: Flyover system noise studies [NASA-CR-195392-VOL-1] p 258 N95-21888

ELECTRIC EQUIPMENT TESTS

Fault detection techniques for complex cable shield topologies [AD-A286632] p 247 N95-20771

ELECTRIC NETWORKS

Modeling resonance in waveguide-to-microstrip junctions by unilateral fin line resonators [BTN-94-EIX94381323445] p 242 A95-70844

ELECTRICAL FAULTS

Fault detection techniques for complex cable shield topologies [AD-A286632] p 247 N95-20771

ELECTRO-OPTICS

Electro-optic characterization of ultrafast photodetectors using adiabatically compressed soliton pulses [BTN-94-EIX94381359637] p 257 A95-72675

ELECTROCHEMISTRY

Electrochemical impedance pattern recognition for detection of hidden chemical corrosion on aircraft components [AD-A285998] p 241 N95-20716

ELECTROMAGNETIC COMPATIBILITY

FASTPACK: Optimized solutions for modular avionics derived from a parametric study. Part 2: Avionics p 233 N95-20635

Composite cases for airborne electronic equipment: A technology study and EMC p 241 N95-20655
Electromagnetic compatibility effects of advanced packaging configurations p 247 N95-20658

ELECTROMAGNETIC FIELDS

Measurements of shielding effectiveness and cavity characteristics of airplanes [PB94-210051] p 244 N95-20191

ELECTROMAGNETIC INTERFERENCE

Measurements of shielding effectiveness and cavity characteristics of airplanes [PB94-210051] p 244 N95-20191

ELECTROMAGNETIC MEASUREMENT

Measurements of shielding effectiveness and cavity characteristics of airplanes [PB94-210051] p 244 N95-20191

ELECTROMAGNETIC RADIATION

RCS measurements, transformations, and comparisons under cylindrical and plane wave illumination [BTN-94-EIX94371347126] p 242 A95-69976

Comments on effect of wet snow on the null-reference ILS system [BTN-95-EIX95142555488] p 227 A95-72885

ELECTROMAGNETIC SHIELDING

Measurements of shielding effectiveness and cavity characteristics of airplanes [PB94-210051] p 244 N95-20191

Composite cases for airborne electronic equipment: A technology study and EMC p 241 N95-20655

Lightweight electronic enclosures using composite materials p 241 N95-20656
Fault detection techniques for complex cable shield topologies [AD-A286632] p 247 N95-20771

TIM-SCT cable testing protocol [AD-A286633] p 231 N95-20772

ELECTROMAGNETIC WAVE TRANSMISSION

Measurements of shielding effectiveness and cavity characteristics of airplanes [PB94-210051] p 244 N95-20191

ELECTROMECHANICS

High density monolithic packaging technology for digital/microwave avionics p 240 N95-20646

ELECTRON ENERGY

Measurement and analysis of nitric oxide radiation in an arcjet flow [BTN-95-EIX95082502727] p 243 A95-71040

A survey of bidirectional greater than or equal to MeV ion flows during the Helios 1 and Helios 2 mission: Observations from the Goddard Space Flight Center instruments [HTN-95-70542] p 237 A95-71656

ELECTRONIC EQUIPMENT

Composite cases for airborne electronic equipment: A technology study and EMC p 241 N95-20655

Lightweight electronic enclosures using composite materials p 241 N95-20656

ELECTRONIC EQUIPMENT TESTS

Assessment of a non-dedicated GPS receiver system for precise airborne attitude determination [DE94-019309] p 229 N95-21520

ELECTRONIC MODULES

MCMs for avionics: Technology selection and intermodule interconnection p 234 N95-20641

Liquid flow-through cooling of electronic modules p 246 N95-20647
Immersion/two phase cooling p 246 N95-20648

ELECTRONIC PACKAGING

High density monolithic packaging technology for digital/microwave avionics p 240 N95-20646

Liquid flow-through cooling of electronic modules p 246 N95-20647

Electromagnetic compatibility effects of advanced packaging configurations p 247 N95-20658

ELECTRONIC WARFARE

Systems engineering design and technical analyses for Strategic Avionics Crew-station Design Evaluation Facility (SACDEF) [AD-A286239] p 235 N95-22024

EMISSION SPECTRA

Two-dimensional imaging of OH in a lean burning high pressure combustor [NASA-TM-106854] p 236 N95-21383

EMITTANCE

Measurement and analysis of nitric oxide radiation in an arcjet flow [BTN-95-EIX95082502727] p 243 A95-71040

- ENERGY ABSORPTION**
Prediction of energy absorption capability of composite stiffeners
[HTN-95-A0500] p 230 A95-72571
- ENERGY TRANSFER**
State-to-state collisional dynamics of atmospheric species
[AD-A285053] p 245 N95-20484
- ENGINE DESIGN**
Turbine design and application
[NASA-SP-290] p 236 N95-22341
- ENGINE INLETS**
Active control of fan noise-feasibility study. Volume 1: Flyover system noise studies
[NASA-CR-195392-VOL-1] p 258 N95-21888
- ENGINE MONITORING INSTRUMENTS**
Engine life measurement and diagnostics
[BTN-95-EIX95041505024] p 235 A95-70133
- ENGINE NOISE**
Active control of fan noise-feasibility study. Volume 1: Flyover system noise studies
[NASA-CR-195392-VOL-1] p 258 N95-21888
- ENGINE PARTS**
Toughened Silcomp composites for gas turbine engine applications
[DE95-002851] p 235 N95-21243
- ENGINE TESTS**
Statistical analysis of Turbine Engine Diagnostic (TED) field test data
[AD-A286032] p 248 N95-20998
Portable static test facility for small, expendable, turbojet engines, phase 1
[AD-A286337] p 239 N95-21719
- ENVIRONMENT EFFECTS**
Corrosion of aircraft materials: Correlation between nanometer scale and macroscopic structural damage parameters
[AD-A285930] p 241 N95-20299
- ENVIRONMENT MANAGEMENT**
Environmental Compliance Assessment and Management Program
[AD-A279605] p 255 N95-20441
- ENVIRONMENT POLLUTION**
Environmental Compliance Assessment and Management Program.
[AD-A279605] p 255 N95-20441
- ENVIRONMENT PROTECTION**
Environmental Compliance Assessment and Management Program
[AD-A279605] p 255 N95-20441
- ENVIRONMENTAL MONITORING**
Environmental Compliance Assessment and Management Program
[AD-A279605] p 255 N95-20441
- EQUATIONS OF MOTION**
Comparison of meteorological data with fitted values extracted from projectile trajectory
[AD-A285921] p 255 N95-19989
Direct numerical simulations of on-demand vortex generators: Mathematical formulation
p 251 N95-22452
- EROSION**
Aircraft corrosion study
[AD-A279527] p 241 N95-21687
- EULER EQUATIONS OF MOTION**
Ground effect calculation of two-dimensional airfoil
[BTN-94-EIX94371347710] p 219 A95-69969
- EXCITATION**
Aerodynamic mechanism of galloping
[BTN-94-EIX94371347709] p 219 A95-69968
Measurement around a rotor blade excited in pitch. Part 1: Dynamic inflow
[HTN-95-31007] p 220 A95-71177
Measurement around a rotor blade excited in pitch. Part 2: Unsteady surface pressure
[HTN-95-31008] p 220 A95-71178
- EXHAUST EMISSION**
Subsidence of aircraft engine exhaust in the stratosphere: Implications for calculated ozone depletions
[PAPER-93GL03426] p 251 A95-70297
Two-dimensional imaging of OH in a lean burning high pressure combustor
[NASA-TM-106854] p 236 N95-21383
- EXHAUST SYSTEMS**
Active control of fan noise-feasibility study. Volume 1: Flyover system noise studies
[NASA-CR-195392-VOL-1] p 258 N95-21888
- EXPERIMENT DESIGN**
Statistical analysis of Turbine Engine Diagnostic (TED) field test data
[AD-A286032] p 248 N95-20998
- EXPLOSIVE DEVICES**
Test and Evaluation Plan (TEP) for Improvised Explosive Device Screening Systems (IEDSS)
[AD-A286382] p 227 N95-22319
- EXTINGUISHING**
A review of water mist technology for fire suppression
[AD-A285738] p 225 N95-20071
- F**
- F-14 AIRCRAFT**
Naval aviation: F-14 upgrades are not adequately justified. Report to Congressional Committees
[AD-A286338] p 231 N95-20212
- F-15 AIRCRAFT**
F-15 resource tape
[NASA-TM-110502] p 230 N95-19994
- F-16 AIRCRAFT**
F-16XL interview with Marta Bohn-Meyer
[NASA-TM-110505] p 223 N95-19996
- F-18 AIRCRAFT**
Pressure measurements on an F/A-18 twin vertical tail in buffeting flow. Volume 1: Wind tunnel test summary
[AD-A279126] p 225 N95-21877
- FABRICATION**
Scale-up and modeling of forced chemical vapor infiltration
[DE94-017769] p 247 N95-20781
- FAILURE ANALYSIS**
Modeling of pilowing due to corrosion in fuselage lap joints
[BTN-95-EIX95082502227] p 240 A95-71024
- FAILURE MODES**
Advanced Packaging Concepts for Digital Avionics
[AGARD-CP-562] p 233 N95-20631
- FALKNER-SKAN EQUATION**
Acoustic receptivity due to weak surface inhomogeneities in adverse pressure gradient boundary layers
[NASA-TM-4577] p 249 N95-21258
- FAST FOURIER TRANSFORMATIONS**
Electrochemical impedance pattern recognition for detection of hidden chemical corrosion on aircraft components
[AD-A284998] p 241 N95-20481
- FASTENERS**
Eddy current for detecting second-layer cracks under installed fasteners
[AD-A278871] p 244 N95-20414
- FATIGUE (MATERIALS)**
Derived gust spectra for the Macchi MB326H
[ARL-TN-3] p 225 N95-21892
- FATIGUE TESTS**
Bonded composite repair of cracked load-bearing holes
[BTN-94-EIX94401360553] p 243 A95-71867
Lubricant evaluation and performance, 2
[AD-A279144] p 242 N95-21969
- FAULT DETECTION**
Engine life measurement and diagnostics
[BTN-95-EIX95041505024] p 235 A95-70133
Fault detection techniques for complex cable shield topologies
[AD-A286632] p 247 N95-20771
- FAULT TOLERANCE**
The Advanced Avionics Subsystem Technology Demonstration Program
p 234 N95-20636
- FEASIBILITY ANALYSIS**
The personal aircraft: Status and issues
[NASA-TM-109174] p 223 N95-20688
- FEEDBACK CONTROL**
Rotorcraft control system design for uncertain vehicle dynamics using quantitative feedback theory
[HTN-95-31012] p 236 A95-71182
Design of robust optimal control systems and stability analysis of real structured uncertainties
[AD-A279089] p 256 N95-21913
- FEEDFORWARD CONTROL**
A neural expert approach to self designing flight control systems
[AD-A279965] p 237 N95-21122
- FIBER COMPOSITES**
Toughened Silcomp composites for gas turbine engine applications
[DE95-002851] p 235 N95-21243
- FIBER OPTICS**
Optical backplane for modular avionics
p 257 N95-20652
High performance backplane components for modular avionics
p 247 N95-20653
A three-dimensional orthogonal laser velocimeter for the NASA Ames 7- by 10-foot wind tunnel
[NASA-TM-108864] p 249 N95-21323
Fiber-optic rotary joint with bundle collimator assemblies
[AD-D016504] p 258 N95-21673
Optical processing and control
[AD-A279157] p 259 N95-21975
- FIELD OF VIEW**
Factors affecting the perception of tuning in monocular regions of partial binocular overlap displays
[AD-A286287] p 259 N95-22044
- FIGHTER AIRCRAFT**
Integrated IR sensors
[BTN-95-EIX95041505023] p 242 A95-70132
- FILLETs**
Effect of juncture fillets on double-delta wings undergoing sideslip at high angles of attack
[AD-A286165] p 232 N95-22039
- FILTRATION**
Precise navigation using adaptive FIR filtering and time domain spectral estimation
[BTN-95-EIX95142555485] p 227 A95-72888
- FINITE DIFFERENCE THEORY**
Effects of leading and trailing edge flaps on the aerodynamics of airfoil/vortex interactions
[HTN-95-31011] p 221 A95-71181
A computer code (SKINTEMP) for predicting transient missile and aircraft heat transfer characteristics
[AD-A286044] p 248 N95-21001
Computation of transonic flow on composite overlapping grids in 2 D
[PB95-131348] p 248 N95-21132
- FINITE ELEMENT METHOD**
Numerical modelling of transverse impact on composite coupons
[BTN-95-EIX95082502225] p 240 A95-71022
Modelling of pilowing due to corrosion in fuselage lap joints
[BTN-95-EIX95082502227] p 240 A95-71024
Adaptive remeshing for convective heat transfer with variable fluid properties
[BTN-95-EIX95082502720] p 243 A95-71033
Advance finite element modeling of rotor blade aeroelasticity
[HTN-95-31013] p 221 A95-71183
Large-scale computational fluid dynamics by the finite element method
[BTN-94-EIX94381359154] p 243 A95-71744
On the choice of appropriate bases for nonlinear dynamic modal analysis
[HTN-95-A0495] p 221 A95-72566
Parametric studies for titrotor aeroelastic stability in highspeed flight
[HTN-95-A0489] p 222 A95-72570
Unstructured-grid large-eddy simulation of flow over an airfoil
p 225 N95-22448
- FINS**
Modeling resonance in waveguide-to-microstrip junctions by unilateral fin line resonators
[BTN-94-EIX94381323445] p 242 A95-70844
- FIR FILTERS**
Precise navigation using adaptive FIR filtering and time domain spectral estimation
[BTN-95-EIX95142555485] p 227 A95-72888
- FIRE EXTINGUISHERS**
A review of water mist technology for fire suppression
[AD-A285738] p 225 N95-20071
- FIRE FIGHTING**
A review of water mist technology for fire suppression
[AD-A285738] p 225 N95-20071
Analysis of test criteria for specifying foam firefighting agents for aircraft rescue and firefighting
[AD-A286381] p 227 N95-22352
- FIRES**
Investigation of flight data recorder fire test requirements
[AD-A285832] p 232 N95-20032
Fuselage burnthrough from large exterior fuel fires
[AD-A286295] p 226 N95-22318
- FLAME PROPAGATION**
Fuselage burnthrough from large exterior fuel fires
[AD-A286295] p 226 N95-22318
- FLAMMABILITY**
Investigation of flight data recorder fire test requirements
[AD-A285832] p 232 N95-20032
Fuselage burnthrough from large exterior fuel fires
[AD-A286295] p 226 N95-22318
- FLAT PLATES**
Time-resolved surface heat flux measurements in the wing/body junction vortex
[BTN-95-EIX95082502716] p 220 A95-71029
- FLIGHT CHARACTERISTICS**
T-45A High Angle of Attack Testing: US Naval Test Pilot School 46th Annual Reunion and Symposium
[AD-A284000] p 231 N95-20466
- FLIGHT CONDITIONS**
Derived gust spectra for the Macchi MB326H
[ARL-TN-3] p 225 N95-21892
- FLIGHT CONTROL**
Rotorcraft control system design for uncertain vehicle dynamics using quantitative feedback theory
[HTN-95-31012] p 236 A95-71182

A generalized algorithm for inverse simulation applied to helicopter maneuvering flight
[HTN-95-A0493] p 236 A95-72564

Summary of a joint program of research into aircraft flight control concepts
[AD-A280012] p 237 N95-20004

A neural expert approach to self designing flight control systems
[AD-A279965] p 237 N95-21122

FLIGHT MANAGEMENT SYSTEMS
Crew aiding and automation: A system concept for terminal area operations, and guidelines for automation design
[NASA-CR-4631] p 228 N95-19950

FLIGHT MECHANICS
High-order state space simulation models of helicopter flight mechanics
[HTN-95-A0494] p 237 A95-72565

FLIGHT PATHS
Comparison of meteorological data with fitted values extracted from projectile trajectory
[AD-A285921] p 255 N95-19989

FLIGHT RECORDERS
Investigation of flight data recorder fire test requirements
[AD-A285832] p 232 N95-20032

FLIGHT SAFETY
Commuter/air taxi ditchings and water-related impacts that occurred from 1979 to 1989
[AD-A285691] p 226 N95-20275

Forecasting aircraft mishaps using monthly maintenance reports
[AD-A286049] p 227 N95-22417

FLIGHT SIMULATION
Comparison of parameter identification algorithms for flight vehicles
[BTN-94-EIX94371347708] p 219 A95-69967

A generalized algorithm for inverse simulation applied to helicopter maneuvering flight
[HTN-95-A0493] p 236 A95-72564

High-order state space simulation models of helicopter flight mechanics
[HTN-95-A0494] p 237 A95-72565

Summary of a joint program of research into aircraft flight control concepts
[AD-A280012] p 237 N95-20004

Collected papers of the Soar/IFOR project, Spring 1994
[AD-A280063] p 238 N95-20624

Minima reduction simulation test results
[AD-A285626] p 228 N95-21148

A preliminary study of the airwake model used in an existing SH-60B/FFG-7 helicopter/ship simulation program
[DSTO-TR-0015] p 224 N95-21659

FLIGHT SIMULATORS
Using the backward transfer paradigm to validate the AH-64 Simulator Training Research Advanced Testbed for Aviation
[AD-A285758] p 238 N95-19931

Summary of a joint program of research into aircraft flight control concepts
[AD-A280012] p 237 N95-20004

FLIGHT TESTS
Open Skies project computational fluid dynamic analysis
[AD-A285928] p 223 N95-19991

F-15 resource tape
[NASA-TM-110502] p 230 N95-19994

Acoustic climb to cruise test
[NASA-TM-110504] p 230 N95-20155

SAR image registration in absolute coordinates using GPS carrier phase position and velocity information
[DE94-018738] p 228 N95-20195

Assessment of a non-dedicated GPS receiver system for precise airborne attitude determination
[DE94-019309] p 229 N95-21520

FLIGHT TRAINING
Public-sector aviation issues: Graduate research award papers, 1992-1993
[PB94-217478] p 219 N95-19967

T-45A High Angle of Attack Testing: US Naval Test Pilot School 46th Annual Reunion and Symposium
[AD-A284000] p 231 N95-20466

A computer-based multimedia prototype for night vision goggles
[AD-A286208] p 258 N95-21882

FLOW COEFFICIENTS
Flow coefficient behavior for boundary layer bleed holes and slots
[NASA-TM-106846] p 244 N95-19953

FLOW DEFLECTION
Static investigation of two fluidic thrust-vectoring concepts on a two-dimensional convergent-divergent nozzle
[NASA-TM-4574] p 222 N95-19913

FLOW DISTRIBUTION
16-foot transonic tunnel test section flowfield survey
[NASA-TM-109157] p 238 N95-20669

Wake measurements in a strong adverse pressure gradient
[NASA-CR-197272] p 224 N95-21031

Application of Navier-Stokes code PAB3D with kappa-epsilon turbulence model to attached and separated flows
[NASA-TP-3480] p 224 N95-21338

Experiments on the flow field physics of confluent boundary layers for high-lift systems
[NASA-CR-197318] p 224 N95-21343

FLOW EQUATIONS
Application of Navier-Stokes code PAB3D with kappa-epsilon turbulence model to attached and separated flows
[NASA-TP-3480] p 224 N95-21338

FLOW GEOMETRY
A survey of bidirectional greater than or equal to MeV ion flows during the Helios 1 and Helios 2 mission: Observations from the Goddard Space Flight Center instruments
[HTN-95-70542] p 237 A95-71656

FLOW MEASUREMENT
Vorticity concentration at the edge of the inboard vortex sheet
[HTN-95-31010] p 221 A95-71180

Transverse vorticity measurements in the NASA Ames 80 x 120 wind tunnel boundary layer
p 251 N95-22457

FLOW THEORY
Robust fixed-structure control
[AD-A286515] p 257 N95-22216

FLOW VISUALIZATION
Vorticity concentration at the edge of the inboard vortex sheet
[HTN-95-31010] p 221 A95-71180

Effect of juncture fillets on double-delta wings undergoing sideslip at high angles of attack
[AD-A286165] p 232 N95-22039

Experimental investigations of on-demand vortex generators
p 250 N95-22451

FLUID DYNAMICS
Description and flow characterization of hypersonic facilities
[AD-A284291] p 223 N95-20248

Turbine design and application
[NASA-SP-290] p 236 N95-22341

FLUID FLOW
Application of Direct and Large Eddy Simulation to Transition and Turbulence
[AGARD-CP-551] p 248 N95-21061

FLUIDICS
Static investigation of two fluidic thrust-vectoring concepts on a two-dimensional convergent-divergent nozzle
[NASA-TM-4574] p 222 N95-19913

FLYING PLATFORMS
CALIOPE and TAISIR airborne experiment platform
[DE94-018328] p 250 N95-22299

FOAMS
Analysis of test criteria for specifying foam firefighting agents for aircraft rescue and firefighting
[AD-A286381] p 227 N95-22352

FOLIAGE
Foliage transmission measurements using a ground-based ultrawide band (300-1300 MHz) SAR system
[BTN-94-EIX94381351617] p 252 A95-70950

FORCED CONVECTION
A computer code (SKINTEMP) for predicting transient missile and aircraft heat transfer characteristics
[AD-A286044] p 248 N95-21001

FORECASTING
Radar studies of aviation hazards
[AD-A285845] p 226 N95-21831

FORESTS
Foliage transmission measurements using a ground-based ultrawide band (300-1300 MHz) SAR system
[BTN-94-EIX94381351617] p 252 A95-70950

FORM FACTORS
Ultra-Reliable Digital Avionics (URDA) processor
p 245 N95-20638

FORMAT
FASTPACK: Optimized solutions for modular avionics derived from a parametric study. Part 2: Avionics
p 233 N95-20635

An evaluation of Automatic Terminal Information Service (ATIS) flight deck display presentation options
[AD-A280100] p 228 N95-21020

FORTTRAN
Buckling and vibration analysis of laminated panels using VICONOPT
[PAPER-1746] p 230 A95-72580

FREE JETS
Temperature effects on acoustic interactions between altitude test facilities and jet engine plumes
[NASA-CR-197638] p 258 N95-21170

FREE MOLECULAR FLOW
Cercignani-Lampis-Lord gas-surface interaction model: Comparisons between theory and simulation
[BTN-95-EIX95041503806] p 242 A95-70131

FREQUENCIES
Foliage transmission measurements using a ground-based ultrawide band (300-1300 MHz) SAR system
[BTN-94-EIX94381351617] p 252 A95-70950

Rotorcraft control system design for uncertain vehicle dynamics using quantitative feedback theory
[HTN-95-31012] p 236 A95-71182

Experimental study of the helicopter-mobile radioelectrical channel and possible extension to the satellite-mobile channel
p 247 N95-20945

FREQUENCY MODULATION
Electromagnetic backscattering from a helicopter rotor in the decimeter wave band regime
[BTN-94-EIX94381353130] p 243 A95-72648

FREQUENCY RESPONSE
Precise navigation using adaptive FIR filtering and time domain spectral estimation
[BTN-95-EIX95142555485] p 227 A95-72888

FUEL COMBUSTION
Fuselage burnthrough from large exterior fuel fires
[AD-A286295] p 226 N95-22318

FUSELAGES
Modelling of pillowing due to corrosion in fuselage lap joints
[BTN-95-EIX95082502227] p 240 A95-71024

Design optimization of rotor blades for improved performance and vibration
[HTN-95-A0498] p 229 A95-72569

Damage tolerant repair techniques for pressurized aircraft fuselages
[AD-A286298] p 219 N95-22046

Fuselage burnthrough from large exterior fuel fires
[AD-A286295] p 226 N95-22318

G

GALLIUM ARSENIDES
Photovoltaic electric power applied to Unmanned Aerial Vehicles (UAV)
p 245 N95-20530

GAS DETECTORS
Aircraft-borne, laser-induced fluorescence instrument for the in situ detection of hydroxyl and hydroperoxyl radicals
[BTN-95-EIX95072499029] p 253 A95-71908

GAS DYNAMICS
State-to-state collisional dynamics of atmospheric species
[AD-A285053] p 245 N95-20484

GAS GENERATORS
Integral rocket ramjets
[AD-A285135] p 240 N95-20906

GAS TURBINE ENGINES
Engine life measurement and diagnostics
[BTN-95-EIX95041505024] p 235 A95-70133

Experimental study of vane heat transfer and aerodynamics at elevated levels of turbulence
[NASA-CR-4633] p 244 N95-19912

Toughened Silcomp composites for gas turbine engine applications
[DE95-002851] p 235 N95-21243

GAS TURBINES
Toughened Silcomp composites for gas turbine engine applications
[DE95-002851] p 235 N95-21243

GAS-SOLID INTERACTIONS
Cercignani-Lampis-Lord gas-surface interaction model: Comparisons between theory and simulation
[BTN-95-EIX95041503806] p 242 A95-70131

GATES (CIRCUITS)
Optical processing and control
[AD-A279157] p 259 N95-21975

GAUSSIAN ELIMINATION
Large-scale computational fluid dynamics by the finite element method
[BTN-94-EIX94381359154] p 243 A95-71744

GENERAL AVIATION AIRCRAFT
Census US civil aircraft calendar year 1993
[AD-A286309] p 219 N95-20091

The personal aircraft: Status and issues
[NASA-TM-109174] p 223 N95-20688

GLOBAL POSITIONING SYSTEM
Attitude determination using dedicated and nondedicated multiantenna GPS sensors
[BTN-95-EIX95142555482] p 228 A95-72891

GPS-Squitter capacity analysis
[AD-A280037] p 245 N95-20599

- Assessment of a non-dedicated GPS receiver system for precise airborne attitude determination
[DE94-019309] p 229 N95-21520
- GOERTLER INSTABILITY**
Computational studies of laminar to turbulence transition
[AD-A285622] p 248 N95-21146
- GOOGLES**
A computer-based multimedia prototype for night vision goggles
[AD-A286208] p 258 N95-21882
- GOVERNMENT/INDUSTRY RELATIONS**
Environmental Compliance Assessment and Management Program
[AD-A279605] p 255 N95-20441
- GRAPHITE-EPOXY COMPOSITES**
Prediction of energy absorption capability of composite stiffeners
[HTN-95-A0500] p 230 A95-72571
- GRAUPEL**
High-resolution imaging of rain systems with the advanced microwave precipitation radiometer
[HTN-95-70133] p 252 A95-70655
- GRAVITY WAVES**
An algorithm for forecasting mountain wave-related turbulence in the stratosphere
[HTN-95-80656] p 254 A95-72500
- GRID GENERATION (MATHEMATICS)**
Open Skies project computational fluid dynamic analysis
[AD-A285928] p 223 N95-19991
Unstructured-grid large-eddy simulation of flow over an airfoil
[HTN-95-22448] p 225 N95-22448
- GROUND EFFECT (AERODYNAMICS)**
Ground effect calculation of two-dimensional airfoil
[BTN-94-EIX94371347710] p 219 A95-69969
Air and ground resonance of helicopters with elastically tailored composite rotor blades
[HTN-95-A0497] p 222 A95-72568
- GROUND RESONANCE**
Air and ground resonance of helicopters with elastically tailored composite rotor blades
[HTN-95-A0497] p 222 A95-72568
- GROUND STATIONS**
GPS-Scuttler capacity analysis
[AD-A280037] p 245 N95-20599
- GROUND TESTS**
Description and flow characterization of hypersonic facilities
[AD-A284291] p 223 N95-20248
- GUIDANCE SENSORS**
Assessment of a non-dedicated GPS receiver system for precise airborne attitude determination
[DE94-019309] p 229 N95-21520
- GULF STREAM**
Orbital velocities induced by surface waves
[HTN-95-90902] p 253 A95-72411
- GUST LOADS**
Derived gust spectra for the Macchi MB326H
[ARL-TN-3] p 225 N95-21892

H

- H-INFINITY CONTROL**
Design of robust optimal control systems and stability analysis of real structured uncertainties
[AD-A279089] p 256 N95-21913
- HARRIER AIRCRAFT**
Forecasting aircraft mishaps using monthly maintenance reports
[AD-A286049] p 227 N95-22417
- HAZARDS**
Assuring Known Good Die (KGD) for reliable, cost effective MCMs
[AD-A285845] p 226 N95-21831
- HEAT EXCHANGERS**
Malone-brayton cycle engine/heat pump
[AD-D016573] p 244 N95-20295
Microchannel heat pipe cooling of modules
[AD-A286507] p 246 N95-20649
- HEAT FLUX**
Time-resolved surface heat flux measurements in the wing/body junction vortex
[BTN-95-EIX95082502716] p 220 A95-71029
- HEAT PIPES**
Microchannel heat pipe cooling of modules
[AD-A286507] p 246 N95-20649
- HEAT PUMPS**
Malone-brayton cycle engine/heat pump
[AD-D016573] p 244 N95-20295
- HEAT TRANSFER**
Time-resolved surface heat flux measurements in the wing/body junction vortex
[BTN-95-EIX95082502716] p 220 A95-71029

- Measurement and analysis of nitric oxide radiation in an arcjet flow
[BTN-95-EIX95082502727] p 243 A95-71040
- Experimental study of vane heat transfer and aerodynamics at elevated levels of turbulence
[NASA-CR-4633] p 244 N95-19912
- Investigation of a thermal buoyancy effect on the drag of half models tested in the ARA Transonic Wind Tunnel
[ARA-MEMO-407] p 222 N95-19946
- Microchannel heat pipe cooling of modules
[AD-A286507] p 246 N95-20649
- Shock wave interactions in hypervelocity flow
[AD-A286507] p 250 N95-22212
- HEATING**
Vapor generator wand
[NASA-CASE-LAR-15058-1] p 238 N95-20080
- HELICOPTER CONTROL**
Rotorcraft control system design for uncertain vehicle dynamics using quantitative feedback theory
[HTN-95-31012] p 236 A95-71182
- Smart structures in the control of airframe vibrations
[HTN-95-31014] p 236 A95-71184
- A generalized algorithm for inverse simulation applied to helicopter maneuvering flight
[HTN-95-A0493] p 236 A95-72564
- High-order state space simulation models of helicopter flight mechanics
[HTN-95-A0494] p 237 A95-72565
- HELICOPTER DESIGN**
Design optimization of rotor blades for improved performance and vibration
[HTN-95-A0498] p 229 A95-72569
- HELICOPTER PERFORMANCE**
A generalized algorithm for inverse simulation applied to helicopter maneuvering flight
[HTN-95-A0493] p 236 A95-72564
- High-order state space simulation models of helicopter flight mechanics
[HTN-95-A0494] p 237 A95-72565
- Air and ground resonance of helicopters with elastically tailored composite rotor blades
[HTN-95-A0497] p 222 A95-72568
- Design optimization of rotor blades for improved performance and vibration
[HTN-95-A0498] p 229 A95-72569
- HELICOPTER WAKES**
Aerodynamic and wake methodology evaluation using Model UH-60A experimental data
[HTN-95-31009] p 220 A95-71179
- Vorticity concentration at the edge of the inboard vortex sheet
[HTN-95-31010] p 221 A95-71180
- Flap-lag damping in hover and forward flight with a three-dimensional wake
[HTN-95-A0496] p 221 A95-72567
- HELICOPTERS**
Measurement around a rotor blade excited in pitch. Part 2: Unsteady surface pressure
[HTN-95-31008] p 220 A95-71178
- Rotorcraft control system design for uncertain vehicle dynamics using quantitative feedback theory
[HTN-95-31012] p 236 A95-71182
- Advance finite element modeling of rotor blade aeroelasticity
[HTN-95-31013] p 221 A95-71183
- Smart structures in the control of airframe vibrations
[HTN-95-31014] p 236 A95-71184
- Air and ground resonance of helicopters with elastically tailored composite rotor blades
[HTN-95-A0497] p 222 A95-72568
- The personal aircraft: Status and issues
[NASA-TM-109174] p 223 N95-20688
- Experimental study of the helicopter-mobile radioelectrical channel and possible extension to the satellite-mobile channel
[AD-A286287] p 247 N95-20945
- Wavelet transformations for helicopter identification via acoustic signatures
[AD-A279980] p 257 N95-20963
- HELMET MOUNTED DISPLAYS**
Factors affecting the perception of tuning in monocular regions of partial binocular overlap displays
[AD-A286287] p 259 N95-22044
- HIGH ALTITUDE**
Photovoltaic electric power applied to Unmanned Aerial Vehicles (UAV)
[AD-A286507] p 245 N95-20530
- HIGH TEMPERATURE**
Toughened Silcomp composites for gas turbine engine applications
[DE95-002851] p 235 N95-21243
- HIGH TEMPERATURE GASES**
Temperature effects on acoustic interactions between altitude test facilities and jet engine plumes
[NASA-CR-197638] p 258 N95-21170
- Toughened Silcomp composites for gas turbine engine applications
[DE95-002851] p 235 N95-21243

HIGH TEMPERATURE TESTS

- Investigation of flight data recorder fire test requirements
[AD-A285832] p 232 N95-20032
- HISTORIES**
The personal aircraft: Status and issues
[NASA-TM-109174] p 223 N95-20688
- HOLES (MECHANICS)**
Bonded composite repair of cracked load-bearing holes
[BTN-94-EIX94401360553] p 243 A95-71867
- HOT-WIRE FLOWMETERS**
Transverse vorticity measurements in the NASA Ames 80 x 120 wind tunnel boundary layer
[AD-A286507] p 251 N95-22457
- HOVERING**
Measurement around a rotor blade excited in pitch. Part 1: Dynamic inflow
[HTN-95-31007] p 220 A95-71177
- Measurement around a rotor blade excited in pitch. Part 2: Unsteady surface pressure
[HTN-95-31008] p 220 A95-71178
- Rotorcraft control system design for uncertain vehicle dynamics using quantitative feedback theory
[HTN-95-31012] p 236 A95-71182
- Flap-lag damping in hover and forward flight with a three-dimensional wake
[HTN-95-A0496] p 221 A95-72567
- Air and ground resonance of helicopters with elastically tailored composite rotor blades
[HTN-95-A0497] p 222 A95-72568
- HUMAN FACTORS ENGINEERING**
Crew aiding and automation: A system concept for terminal area operations, and guidelines for automation design
[NASA-CR-4631] p 228 N95-19950
- An evaluation of Automatic Terminal Information Service (ATIS) flight deck display presentation options
[AD-A280100] p 228 N95-21020
- Independent review of Aviation Technology and Research Information Analysis System (ATRIAS) database
[AD-A284049] p 226 N95-21518
- Systems engineering design and technical analyses for Strategic Avionics Crew-station Design Evaluation Facility (SACDEF)
[AD-A286239] p 235 N95-22024
- HYDROCARBON FUELS**
Analysis of test criteria for specifying foam firefighting agents for aircraft rescue and firefighting
[AD-A286381] p 227 N95-22352
- HYDROXYL EMISSION**
Two-dimensional imaging of OH in a lean burning high pressure combustor
[NASA-TM-106854] p 236 N95-21383
- HYDROXYL RADICALS**
Aircraft-borne, laser-induced fluorescence instrument for the in situ detection of hydroxyl and hydroperoxyl radicals
[BTN-95-EIX95072499029] p 253 A95-71908
- Two-dimensional imaging of OH in a lean burning high pressure combustor
[NASA-TM-106854] p 236 N95-21383
- HYPERSONIC FLOW**
Flow resolution and domain influence in rarefied hypersonic blunt-body flows
[BTN-95-EIX95082502729] p 220 A95-70136
- Application of pressure sensitive paint in hypersonic flows
[NASA-TM-106824] p 223 N95-20794
- Shock wave interactions in hypervelocity flow
[AD-A286507] p 250 N95-22212
- HYPERSONIC VEHICLES**
Description and flow characterization of hypersonic facilities
[AD-A284291] p 223 N95-20248
- HYPERSONICS**
Description and flow characterization of hypersonic facilities
[AD-A284291] p 223 N95-20248
- HYPERVELOCITY FLOW**
Shock wave interactions in hypervelocity flow
[AD-A286507] p 250 N95-22212
- ICE**
High-resolution imaging of rain systems with the advanced microwave precipitation radiometer
[HTN-95-70133] p 252 A95-70655
- Ice accretion on aircraft wings
[BTN-95-EIX95082502224] p 225 A95-71021
- IDEAL GAS**
Shock wave interactions in hypervelocity flow
[AD-A286507] p 250 N95-22212

IMAGE PROCESSING

SAR image registration in absolute coordinates using GPS carrier phase position and velocity information [DE94-018738] p 228 N95-20195

IMAGERY

Color control in a multichannel simulator display: The display for advanced research and training [AD-A279717] p 239 N95-20992

IMAGING RADAR

Foliage transmission measurements using a ground-based ultrawide band (300-1300 MHz) SAR system [BTN-94-EIX94381351617] p 252 A95-70950

IMAGING TECHNIQUES

Corrosion of aircraft materials: Correlation between nanometer scale and macroscopic structural damage parameters [AD-A285930] p 241 N95-20289

Two-dimensional imaging of OH in a lean burning high pressure combustor [NASA-TM-106854] p 236 N95-21383

IMPACT DAMAGE

Numerical modelling of transverse impact on composite coupons [BTN-95-EIX95082502225] p 240 A95-71022

IMPACT LOADS

Super-heavy aircraft study [AD-A279602] p 238 N95-19955

IMPEDANCE

Electrochemical impedance pattern recognition for detection of hidden chemical corrosion on aircraft components [AD-A284998] p 241 N95-20481

IMPEDANCE MEASUREMENT

Fault detection techniques for complex cable shield topologies [AD-A286632] p 247 N95-20771

TIM-SCT cable testing protocol [AD-A286633] p 231 N95-20772

IMPINGEMENT

Shock wave interactions in hypervelocity flow [AD-A286507] p 250 N95-22212

INCOMPRESSIBLE FLOW

Time-resolved surface heat flux measurements in the wing/body junction vortex [BTN-95-EIX95082502716] p 220 A95-71029

Adaptive remeshing for convective heat transfer with variable fluid properties [BTN-95-EIX95082502720] p 243 A95-71033

Direct numerical simulations of on-demand vortex generators: Mathematical formulation p 251 N95-22452

INDEXES (DOCUMENTATION)

Aeronautical engineering: A continuing bibliography with indexes (supplement 315) [NASA-SP-7037(315)] p 219 N95-21640

INDIUM ARSENIDES

An Echelle Grating Spectrometer (EGS) for mid-IR remote chemical detection [DE94-019310] p 249 N95-21478

INDUSTRIES

Standard Hardware Acquisition and Reliability Program (SHARP) advanced SEM-E packaging p 233 N95-20633

INERTIAL NAVIGATION

Comments on 'correction of inertial navigation with Loran C on NOAA's P-3 aircraft' [HTN-95-70149] p 227 A95-70671

Assessment of a non-dedicated GPS receiver system for precise airborne attitude determination [DE94-019309] p 229 N95-21520

A real-time algorithm for integrating differential satellite and inertial navigation information during helicopter approach [NASA-CR-197409] p 229 N95-21891

INFORMATION FLOW

The IEEE scalable coherent interface: An approach for a unified avionics network p 234 N95-20650

INFORMATION MANAGEMENT

Collected papers of the Soar/IFOR project, Spring 1994 [AD-A280063] p 238 N95-20624

INFORMATION SYSTEMS

Independent review of Aviation Technology and Research Information Analysis System (ATRIAS) database [AD-A284049] p 226 N95-21518

Aeronautical engineering: A continuing bibliography with indexes (supplement 315) [NASA-SP-7037(315)] p 219 N95-21640

INFRARED ABSORPTION

Water vapor continuum absorption in mid-latitudes: Aircraft measurements and model comparisons [HTN-95-40756] p 252 A95-71186

INFRARED DETECTORS

Integrated IR sensors [BTN-95-EIX95041505023] p 242 A95-70132

State-to-state collisional dynamics of atmospheric species [AD-A285053] p 245 N95-20484

INFRARED LASERS

State-to-state collisional dynamics of atmospheric species [AD-A285053] p 245 N95-20484

INFRARED RADIATION

An Echelle Grating Spectrometer (EGS) for mid-IR remote chemical detection [DE94-019310] p 249 N95-21478

INFRARED SPECTROMETERS

An Echelle Grating Spectrometer (EGS) for mid-IR remote chemical detection [DE94-019310] p 249 N95-21478

INSTRUMENT LANDING SYSTEMS

Comments on effect of wet snow on the null-reference ILS system [BTN-95-EIX95142555488] p 227 A95-72885

INTEGRAL ROCKET RAMJETS

Integral rocket ramjets [AD-A285135] p 240 N95-20906

INTEGRATED CIRCUITS

Ultra-Reliable Digital Avionics (URDA) processor p 245 N95-20638
Assuring Known Good Die (KGD) for reliable, cost effective MCMs p 246 N95-20644
Liquid flow-through cooling of electronic modules p 246 N95-20647

INTEGRATED OPTICS

Integrated IR sensors [BTN-95-EIX95041505023] p 242 A95-70132

INTERMOLECULAR FORCES

Flow resolution and domain influence in rarefied hypersonic blunt-body flows [BTN-95-EIX95082502729] p 220 A95-70136

INTERNAL FLOW

Experimental study of vane heat transfer and aerodynamics at elevated levels of turbulence [NASA-CR-4633] p 244 N95-19912

INTERPOLATION

Secondary source locations in active noise control: Selection or optimization? [BTN-94-EIX94381352222] p 257 A95-71738

INTERPROCESSOR COMMUNICATION

The IEEE scalable coherent interface: An approach for a unified avionics network p 234 N95-20650

ION CONCENTRATION

A survey of bidirectional greater than or equal to MeV ion flows during the Helios 1 and Helios 2 mission: Observations from the Goddard Space Flight Center instruments [HTN-95-70542] p 237 A95-71656

ISOTROPIC TURBULENCE

Application of Direct and Large Eddy Simulation to Transition and Turbulence [AGARD-CP-551] p 248 N95-21061

J

JET AIRCRAFT NOISE

Active control of fan noise-feasibility study. Volume 1: Flyover system noise studies [NASA-CR-195392-VOL-1] p 258 N95-21888

JET ENGINE FUELS

Investigation of flight data recorder fire test requirements [AD-A285832] p 232 N95-20032

Two-dimensional imaging of OH in a lean burning high pressure combustor [NASA-TM-106854] p 236 N95-21383

JET ENGINES

Temperature effects on acoustic interactions between altitude test facilities and jet engine plumes [NASA-CR-197638] p 258 N95-21170

JET MIXING FLOW

Experimental investigations of on-demand vortex generators p 250 N95-22451

JET THRUST

Static investigation of two fluidic thrust-vectoring concepts on a two-dimensional convergent-divergent nozzle [NASA-TM-4574] p 222 N95-18913

JOINTS (JUNCTIONS)

Reliability assessment of Multichip Module technologies via the Triservice/NASA RELTECH program p 245 N95-20643

Fiber-optic rotary joint with bundle collimator assemblies [AD-D016504] p 258 N95-21673

K

K-EPSILON TURBULENCE MODEL

Application of Navier-Stokes code PAB3D with kappa-epsilon turbulence model to attached and separated flows [NASA-TP-3480] p 224 N95-21338

KALMAN FILTERS

Comparison of parameter identification algorithms for flight vehicles [BTN-94-EIX94371347708] p 219 A95-69967

Comments on 'correction of inertial navigation with Loran C on NOAA's P-3 aircraft' [HTN-95-70149] p 227 A95-70671

A real-time algorithm for integrating differential satellite and inertial navigation information during helicopter approach [NASA-CR-197409] p 229 N95-21891

L

LAGRANGE MULTIPLIERS

Large-scale computational fluid dynamics by the finite element method [BTN-94-EIX94381359154] p 243 A95-71744

A neural expert approach to self designing flight control systems [AD-A279965] p 237 N95-21122

LAMINAR BOUNDARY LAYER

Acoustic receptivity due to weak surface inhomogeneities in adverse pressure gradient boundary layers [NASA-TM-4577] p 249 N95-21258

Supersonic laminar flow control research [NASA-CR-196049] p 249 N95-21340

Development of quiet-flow supersonic wind tunnels for laminar-turbulent transition research [NASA-CR-197286] p 239 N95-21436

Acoustics of laminar boundary layers breakdown p 251 N95-22455

LAMINATES

Prediction of energy absorption capability of composite stiffeners [HTN-95-A0500] p 230 A95-72571

Reliability assessment of Multichip Module technologies via the Triservice/NASA RELTECH program p 245 N95-20643

Damage tolerant repair techniques for pressurized aircraft fuselages [AD-A286298] p 219 N95-22046

LANDING GEAR

Corrosion behavior of landing gear steels [AD-A285862] p 242 N95-22132

LANDING LOADS

Super-heavy aircraft study [AD-A279602] p 238 N95-19955

LAP JOINTS

Modelling of pillowwing due to corrosion in fuselage lap joints [BTN-95-EIX95082502227] p 240 A95-71024

LASER APPLICATIONS

Overview of remote sensing laser development and semiconductor laser technology [DE94-019103] p 256 N95-21552

LASER DOPPLER VELOCIMETERS

Measurement around a rotor blade excited in pitch. Part 1: Dynamic inflow [HTN-95-31007] p 220 A95-71177

A three-dimensional orthogonal laser velocimeter for the NASA Ames 7-by-10-foot wind tunnel [NASA-TM-108864] p 249 N95-21323

LASER GYROSCOPES

Optical processing and control [AD-A279157] p 259 N95-21975

LASER INDUCED FLUORESCENCE

Aircraft-borne, laser-induced fluorescence instrument for the in situ detection of hydroxyl and hydroperoxyl radicals [BTN-95-EIX95072499029] p 253 A95-71908

Two-dimensional imaging of OH in a lean burning high pressure combustor [NASA-TM-106854] p 236 N95-21383

LAW (JURISPRUDENCE)

Environmental Compliance Assessment and Management Program [AD-A279605] p 255 N95-20441

LEADING EDGE FLAPS

Effects of leading and trailing edge flaps on the aerodynamics of airfoil/vortex interactions [HTN-95-31011] p 221 A95-71181

LEAST SQUARES METHOD

Attitude determination using dedicated and nondedicated multi-antenna GPS sensors [BTN-95-EIX95142555482] p 228 A95-72891

- Comparison of meteorological data with fitted values extracted from projectile trajectory
[AD-A285921] p 255 N95-19989
- LEGIBILITY**
Evaluation of the Haworth-Newman avionics Display Readability Scale
[AD-A286127] p 235 N95-22232
- LIFT**
Cercignani-Lampis-Lord gas-surface interaction model: Comparisons between theory and simulation
[BTN-95-EIX95041503806] p 242 A95-70131
New airfoil-design concept with improved aerodynamic characteristics
[PAPER-4384] p 230 A95-72585
Lift enhancement device
[AD-DO16522] p 224 N95-21864
- LIFT AUGMENTATION**
Experiments on the flow field physics of confluent boundary layers for high-lift systems
[NASA-CR-197318] p 224 N95-21343
- LIFT DEVICES**
Wake measurements in a strong adverse pressure gradient
[NASA-CR-197272] p 224 N95-21031
Experiments on the flow field physics of confluent boundary layers for high-lift systems
[NASA-CR-197318] p 224 N95-21343
Lift enhancement device
[AD-DO16522] p 224 N95-21864
Experimental investigations of on-demand vortex generators
p 250 N95-22451
- LIGHTHILL GAS MODEL**
Acoustics of laminar boundary layers breakdown
p 251 N95-22455
- LIQUID COOLING**
Liquid flow-through cooling of electronic modules
p 246 N95-20647
Microchannel heat pipe cooling of modules
p 246 N95-20649
- LIQUID METALS**
MHD-flow in slotted channels with conducting walls
[DE94-018370] p 258 N95-21388
- LOADS (FORCES)**
A user's guide to LUGSAN 1.1: A computer program to calculate and archive lug and sway brace loads for aircraft-carried stores
[DE95-001919] p 232 N95-21730
- LONGITUDINAL CONTROL**
Rotorcraft control system design for uncertain vehicle dynamics using quantitative feedback theory
[HTN-95-31012] p 236 A95-71182
- LORAN C**
Comments on 'correction of inertial navigation with Loran C on NOAA's P-3 aircraft'
[HTN-95-70149] p 227 A95-70671
- LOW FREQUENCIES**
Behavior of an inversion-based precipitation retrieval algorithm with high-resolution AMPR measurements including a low-frequency 10.7-GHz channel
[HTN-95-70134] p 252 A95-70656
- LOW SPEED WIND TUNNELS**
Vapor generator wand
[NASA-CASE-LAR-15058-1] p 238 N95-20080
- LOW TEMPERATURE**
High density monolithic packaging technology for digital/microwave avionics
p 240 N95-20646
- LOWER ATMOSPHERE**
Aircraft-borne, laser-induced fluorescence instrument for the *in situ* detection of hydroxyl and hydroperoxy radicals
[BTN-95-EIX95072499029] p 253 A95-71908
- LUBRICANTS**
Lubricant evaluation and performance, 2
[AD-A279144] p 242 N95-21969
- LUGS**
A user's guide to LUGSAN 1.1: A computer program to calculate and archive lug and sway brace loads for aircraft-carried stores
[DE95-001919] p 232 N95-21730
- LUMINANCE**
Factors affecting the perception of furling in monocular regions of partial binocular overlap displays
[AD-A286287] p 259 N95-22044
- LUMINOUS INTENSITY**
Application of pressure sensitive paint in hypersonic flows
[NASA-TM-106824] p 223 N95-20794
- M**
- MACH NUMBER**
Flow resolution and domain influence in rarefied hypersonic blunt-body flows
[BTN-95-EIX95082502729] p 220 A95-70136
- Flow coefficient behavior for boundary layer bleed holes and slots
[NASA-TM-106846] p 244 N95-19953
- MACHINE LEARNING**
A neural expert approach to self designing flight control systems
[AD-A279965] p 237 N95-21122
- MAGNETOHYDRODYNAMIC FLOW**
MHD-flow in slotted channels with conducting walls
[DE94-018370] p 258 N95-21388
- MAGNETOHYDRODYNAMICS**
MHD-flow in slotted channels with conducting walls
[DE94-018370] p 258 N95-21388
- MAINTENANCE**
Public-sector aviation issues: Graduate research award papers, 1992-1993
[PB94-217478] p 219 N95-19967
- MAN MACHINE SYSTEMS**
Crew aiding and automation: A system concept for terminal area operations, and guidelines for automation design
[NASA-CR-4631] p 228 N95-19950
Collected papers of the Scar/IFOR project, Spring 1994
[AD-A280063] p 238 N95-20624
Systems engineering design and technical analyses for Strategic Avionics Crew-station Design Evaluation Facility (SACDEF)
[AD-A286239] p 235 N95-22024
- MANEUVERS**
A generalized algorithm for inverse simulation applied to helicopter maneuvering flight
[HTN-95-A0493] p 236 A95-72564
- MANUFACTURING**
High density monolithic packaging technology for digital/microwave avionics
p 240 N95-20646
- MARINE ENVIRONMENTS**
Potential applications of the SSM/I cloud liquid water parameter to the estimation of marine aircraft icing
[HTN-95-80651] p 254 A95-72495
- MARINE METEOROLOGY**
Microphysical and radiative properties of small cumulus clouds over the sea
[HTN-95-A0526] p 255 A95-73180
On the link between cloud-top radiative properties and sub-cloud aerosol concentrations
[HTN-95-A0527] p 255 A95-73181
- MARS PROBES**
Thermochemical nonequilibrium viscous shock-layer analysis for a Mars aerocapture vehicle
[BTN-95-EIX95082502732] p 239 A95-70139
- MATHEMATICAL MODELS**
Ascent wind model for launch vehicle design
[BTN-95-EIX95041503799] p 239 A95-70124
Modeling resonance in waveguide-to-microstrip junctions by unilateral fin line resonators
[BTN-94-EIX94381323445] p 242 A95-70844
Numerical modelling of transverse impact on composite coupons
[BTN-95-EIX95082502225] p 240 A95-71022
Modelling of pillowing due to corrosion in fuselage lap joints
[BTN-95-EIX95082502227] p 240 A95-71024
Measurement and analysis of nitric oxide radiation in an arcjet flow
[BTN-95-EIX95082502727] p 243 A95-71040
Secondary source locations in active noise control: Selection or optimization?
[BTN-94-EIX94381352222] p 257 A95-71738
Large-scale computational fluid dynamics by the finite element method
[BTN-94-EIX94381359154] p 243 A95-71744
High-order state space simulation models of helicopter flight mechanics
[HTN-95-A0494] p 237 A95-72565
Microphysical and radiative properties of small cumulus clouds over the sea
[HTN-95-A0526] p 255 A95-73180
Computing methods for the approximate solution of time dependent problems
[AD-A286007] p 256 N95-20719
Scale-up and modeling of forced chemical vapor infiltration
[DE94-017769] p 247 N95-20781
Effects of yaw and pitch motion on model attitude measurements
[NASA-TM-4841] p 250 N95-22109
Direct numerical simulations of on-demand vortex generators: Mathematical formulation
p 251 N95-22452
- MAXIMUM ENTROPY METHOD**
Robust fixed-structure control
[AD-A286515] p 257 N95-22216
- MAXIMUM LIKELIHOOD ESTIMATES**
Comparison of parameter identification algorithms for flight vehicles
[BTN-94-EIX94371347708] p 219 A95-69967
- MEAN FREE PATH**
A preliminary study of the airwake model used in an existing SH-60B/FFG-7 helicopter/ship simulation program
[DSTO-TR-0015] p 224 N95-21659
- MECHANICAL IMPEDANCE**
Sound propagation from an arbitrarily oriented multipole placed near a plane, finite impedance surface
[BTN-94-EIX94371338964] p 257 A95-70797
- MECHANICAL PROPERTIES**
Corrosion behavior of landing gear steels
[AD-A285862] p 242 N95-22132
- MECHANIZATION**
An evaluation of Automatic Terminal Information Service (ATIS) flight deck display presentation options
[AD-A280100] p 228 N95-21020
- MESOMETEOROLOGY**
Snow-band formation and evolution during the 15 November 1987 aircraft accident at Denver airport
[HTN-95-80699] p 254 A95-72543
- METEOROLOGICAL BALLOONS**
Comparison of meteorological data with fitted values extracted from projectile trajectory
[AD-A285921] p 255 N95-19989
- METEOROLOGICAL PARAMETERS**
Comparison of meteorological data with fitted values extracted from projectile trajectory
[AD-A285921] p 255 N95-19989
- METEOROLOGICAL RADAR**
Radar studies of aviation hazards
[AD-A285845] p 226 N95-21831
- METEOROLOGY**
Comparison of meteorological data with fitted values extracted from projectile trajectory
[AD-A285921] p 255 N95-19989
- METHODOLOGY**
The navigation toolkit
[NASA-CR-197290] p 229 N95-22161
- MICROCHANNELS**
Microchannel heat pipe cooling of modules
p 246 N95-20649
- MICROELECTRONICS**
Lightweight electronic enclosures using composite materials
p 241 N95-20656
- MICROSTRIP DEVICES**
Modeling resonance in waveguide-to-microstrip junctions by unilateral fin line resonators
[BTN-94-EIX94381323445] p 242 A95-70844
- MICROWAVE ABSORPTION**
Aircraft measurements of water vapour continuum absorption at millimetre wavelengths
[HTN-95-90884] p 253 A95-72393
- MICROWAVE LANDING SYSTEMS**
Minima reduction simulation test results
[AD-A285826] p 228 N95-21148
- MICROWAVE RADIOMETERS**
High-resolution imaging of rain systems with the advanced microwave precipitation radiometer
[HTN-95-70133] p 252 A95-70655
Behavior of an inversion-based precipitation retrieval algorithm with high-resolution AMPR measurements including a low-frequency 10.7-GHz channel
[HTN-95-70134] p 252 A95-70656
- MICROWAVE SOUNDING**
Aircraft measurements of water vapour continuum absorption at millimetre wavelengths
[HTN-95-90884] p 253 A95-72393
- MIE SCATTERING**
Microphysical and radiative properties of small cumulus clouds over the sea
[HTN-95-A0526] p 255 A95-73180
On the link between cloud-top radiative properties and sub-cloud aerosol concentrations
[HTN-95-A0527] p 255 A95-73181
- MILITARY AVIATION**
Forecasting aircraft mishaps using monthly maintenance reports
[AD-A286049] p 227 N95-22417
- MILITARY OPERATIONS**
Bomber force 2000: Operational concepts for long-range combat aircraft
[AD-A279378] p 230 N95-20181
- MILITARY TECHNOLOGY**
Unmanned aerial vehicles
[AD-A286190] p 231 N95-20329
Standard Hardware Acquisition and Reliability Program (SHARP) advanced SEM-E packaging
p 233 N95-20633
- MISSILES**
A computer code (SKINTEMP) for predicting transient missile and aircraft heat transfer characteristics
[AD-A286044] p 248 N95-21001

MIST

A review of water mist technology for fire suppression
[AD-A285738] p 225 N95-20071

MOBILE COMMUNICATION SYSTEMS

Experimental study of the helicopter-mobile radioelectrical channel and possible extension to the satellite-mobile channel
p 247 N95-20945

MODAL RESPONSE

On the choice of appropriate bases for nonlinear dynamic modal analysis
[HTN-95-A0495] p 221 A95-72566

MODULES

FASTPACK: Optimized solutions for modular avionics derived from a parametric study. Part 2: Avionics
p 233 N95-20635

Ultra-Reliable Digital Avionics (URDA) processor
p 245 N95-20638

Assuring Known Good Die (KGD) for reliable, cost effective MCMs
p 246 N95-20644

Modular supplies for a distributed architecture — avionics packaging
p 234 N95-20657

MOLECULAR BEAMS

State-to-state collisional dynamics of atmospheric species
[AD-A285053] p 245 N95-20484

MOLECULAR EXCITATION

Two-dimensional imaging of OH in a lean burning high pressure combustor
[NASA-TM-106854] p 236 N95-21383

MONOTONE FUNCTIONS

Design of robust optimal control systems and stability analysis of real structured uncertainties
[AD-A278089] p 256 N95-21913

MOTION SIMULATION

Simulation of rotor blade element turbulence
[NASA-TM-108862] p 232 N95-21186

A preliminary study of the airwake model used in an existing SH-60B/FFG-7 helicopter/ship simulation program
[DSTO-TR-0015] p 224 N95-21659

MOUNTAINS

An algorithm for forecasting mountain wave-related turbulence in the stratosphere
[HTN-95-80656] p 254 A95-72500

MULTIMEDIA

A computer-based multimedia prototype for night vision goggles
[AD-A286208] p 258 N95-21882

MULTIPOLES

Sound propagation from an arbitrarily oriented multipole placed near a plane, finite impedance surface
[BTN-94-EIX94371338964] p 257 A95-70797

N**NATURAL LANGUAGE PROCESSING**

Collected papers of the Soar/IFOR project, Spring 1994
[AD-A280063] p 238 N95-20624

NAVIER-STOKES EQUATION

Large-scale computational fluid dynamics by the finite element method
[BTN-94-EIX94381359154] p 243 A95-71744

Open Skies project computational fluid dynamic analysis
[AD-A285928] p 223 N95-19991

Application of Navier-Stokes code PAB3D with kappa-epsilon turbulence model to attached and separated flows
[NASA-TP-3480] p 224 N95-21338

Unstructured-grid large-eddy simulation of flow over an airfoil
p 225 N95-22448

Large-eddy simulation of flow through a plane, asymmetric diffuser
p 250 N95-22449

NAVIGATION

The navigation toolkit
[NASA-CR-197290] p 229 N95-22161

NAVIGATION AIDS

Precise navigation using adaptive FIR filtering and time domain spectral estimation
[BTN-95-EIX95142555485] p 227 A95-72888

GPS-Squitter capacity analysis
[AD-A280037] p 245 N95-20599

Minima reduction simulation test results
[AD-A285626] p 228 N95-21148

NAVIGATION INSTRUMENTS

Comments on effect of wet snow on the null-reference ILS system
[BTN-95-EIX95142555488] p 227 A95-72885

Assessment of a non-dedicated GPS receiver system for precise airborne attitude determination
[DE94-019309] p 229 N95-21520

NEAR WAKES

Research on bluff body vortex wakes
[AD-A286319] p 223 N95-20177

NEURAL NETS

A neural expert approach to self designing flight control systems
[AD-A279965] p 237 N95-21122

NIGHT FLIGHTS (AIRCRAFT)

A computer-based multimedia prototype for night vision goggles
[AD-A286208] p 258 N95-21882

NIGHT VISION

Ultra-Reliable Digital Avionics (URDA) processor
p 245 N95-20638

A computer-based multimedia prototype for night vision goggles
[AD-A286208] p 258 N95-21882

NITRIC OXIDE

Measurement and analysis of nitric oxide radiation in an arcjet flow
[BTN-95-EIX95082502727] p 243 A95-71040

NITROGEN OXIDES

Laboratory evaluation of a reactive baffle approach to NOx control
[AD-A283802] p 255 N95-19921

NOISE (SOUND)

Secondary source locations in active noise control: Selection or optimization?
[BTN-94-EIX94381352222] p 257 A95-71738

NOISE INTENSITY

Acoustic climb to cruise test
[NASA-TM-110504] p 230 N95-20155

NOISE PROPAGATION

Effect of atmospheric pressure on measured aircraft noise levels
[PB95-130423] p 232 N95-21425

NOISE REDUCTION

Vortex shedding noise control in idling circular saws using air ejection at the teeth
[BTN-94-EIX94371347214] p 257 A95-69970

Secondary source locations in active noise control: Selection or optimization?
[BTN-94-EIX94381352222] p 257 A95-71738

Active control of fan noise-feasibility study. Volume 1: Flyover system noise studies
[NASA-CR-195392-VOL-1] p 258 N95-21888

NONDESTRUCTIVE TESTS

Eddy current for detecting second-layer cracks under installed fasteners
[AD-A279871] p 244 N95-20414

NONEQUILIBRIUM FLOW

Thermochemical nonequilibrium viscous shock-layer analysis for a Mars aerocapture vehicle
[BTN-95-EIX95082502732] p 239 A95-70139

NONEQUILIBRIUM RADIATION

Measurement and analysis of nitric oxide radiation in an arcjet flow
[BTN-95-EIX95082502727] p 243 A95-71040

NONLINEAR SYSTEMS

On the choice of appropriate bases for nonlinear dynamic modal analysis
[HTN-95-A0495] p 221 A95-72566

A neural expert approach to self designing flight control systems
[AD-A279965] p 237 N95-21122

NONLINEARITY

Robust fixed-structure control
[AD-A286515] p 257 N95-22216

NOZZLE DESIGN

Development of quiet-flow supersonic wind tunnels for laminar-turbulent transition research
[NASA-CR-197286] p 239 N95-21436

NOZZLE FLOW

Measurement and analysis of nitric oxide radiation in an arcjet flow
[BTN-95-EIX95082502727] p 243 A95-71040

Static investigation of two fluidic thrust-vectoring concepts on a two-dimensional convergent-divergent nozzle
[NASA-TM-4574] p 222 N95-19913

NUMERICAL WEATHER FORECASTING

An algorithm for forecasting mountain wave-related turbulence in the stratosphere
[HTN-95-80656] p 254 A95-72500

O**OBJECT-ORIENTED PROGRAMMING**

The navigation toolkit
[NASA-CR-197290] p 229 N95-22161

OBLIQUE SHOCK WAVES

Shock wave interactions in hypervelocity flow
[AD-A286507] p 250 N95-22212

OCEAN MODELS

Orbital velocities induced by surface waves
[HTN-95-90902] p 253 A95-72411

OCEAN TEMPERATURE

Evaluation of the Spartan tight-tolerance AXBT
[HTN-95-40728] p 251 A95-70473

OPERATING TEMPERATURE

Temperature effects on acoustic interactions between altitude test facilities and jet engine plumes
[NASA-CR-197638] p 258 N95-21170

OPTICAL COMMUNICATION

Optical backplane for modular avionics
p 257 N95-20652

OPTICAL COMPUTERS

High performance backplane components for modular avionics
p 247 N95-20653

OPTICAL FIBERS

A three-dimensional orthogonal laser velocimeter for the NASA Ames 7- by 10-foot wind tunnel
[NASA-TM-108864] p 249 N95-21323

OPTICAL MEASURING INSTRUMENTS

State-to-state collisional dynamics of atmospheric species
[AD-A285053] p 245 N95-20484

Optical processing and control
[AD-A279157] p 259 N95-21975

OPTICAL SWITCHING

Optical processing and control
[AD-A279157] p 259 N95-21975

OPTICAL THICKNESS

Microphysical and radiative properties of small cumulus clouds over the sea
[HTN-95-A0526] p 255 A95-73180

OPTICAL TRACKING

Passive range measurement system
[AD-D016222] p 258 N95-21100

OPTIMIZATION

Secondary source locations in active noise control: Selection or optimization?
[BTN-94-EIX94381352222] p 257 A95-71738

Parallel calculation of sensitivity derivatives for aircraft design using automatic differentiation
[NASA-TM-110103] p 231 N95-20370

Robust fixed-structure control
[AD-A286515] p 257 N95-22216

OPTOELECTRONIC DEVICES

Integrated IR sensors
[BTN-95-EIX95041505023] p 242 A95-70132

High performance backplane components for modular avionics
p 247 N95-20653

ORBITAL VELOCITY

Orbital velocities induced by surface waves
[HTN-95-90902] p 253 A95-72411

ORIFICES

Flow coefficient behavior for boundary layer bleed holes and slots
[NASA-TM-106846] p 244 N95-19953

OSCILLATIONS

Measurement around a rotor blade excited in pitch. Part 1: Dynamic inflow
[HTN-95-31007] p 220 A95-71177

Measurement around a rotor blade excited in pitch. Part 2: Unsteady surface pressure
[HTN-95-31008] p 220 A95-71178

Smart structures in the control of airframe vibrations
[HTN-95-31014] p 236 A95-71184

Design optimization of rotor blades for improved performance and vibration
[HTN-95-A0498] p 229 A95-72569

Robust fixed-structure control
[AD-A286515] p 257 N95-22216

OXIDATION RESISTANCE

Toughened Silcomp composites for gas turbine engine applications
[DE95-002851] p 235 N95-21243

Lubricant evaluation and performance, 2
[AD-A279144] p 242 N95-21969

OXYGEN

Aircraft measurements of water vapour continuum absorption at millimetre wavelengths
[HTN-95-90884] p 253 A95-72393

OZONE

Subsidence of aircraft engine exhaust in the stratosphere: Implications for calculated ozone depletions
[PAPER-93GL03426] p 251 A95-70297

Aircraft-borne, laser-induced fluorescence instrument for the in situ detection of hydroxyl and hydroperoxyl radicals
[BTN-95-EIX95072499029] p 253 A95-71908

OZONE DEPLETION

Subsidence of aircraft engine exhaust in the stratosphere: Implications for calculated ozone depletions
[PAPER-93GL03426] p 251 A95-70297

P

P-I-N JUNCTIONS

Electro-optic characterization of ultrafast photodetectors using adiabatically compressed soliton pulses
[BTN-94-EIX94381359637] p 257 A95-72675

P-3 AIRCRAFT

Comments on 'correction of inertial navigation with Lorán C on NOAA's P-3 aircraft'
[HTN-95-70149] p 227 A95-70671

PACKAGING

Advanced Packaging Concepts for Digital Avionics [AGARD-CP-562] p 233 N95-20631
The impact of advanced packaging technology on modular avionics architectures p 233 N95-20632
Standard Hardware Acquisition and Reliability Program (SHARP) advanced SEM-E packaging p 233 N95-20633
FASTPACK: Optimized solutions for modular avionics derived from a parametric study. Part 2: Avionics p 233 N95-20635
Ultra-Reliable Digital Avionics (URDA) processor p 245 N95-20638

PAINTS

Application of pressure sensitive paint in hypersonic flows
[NASA-TM-106824] p 223 N95-20794

PANEL METHOD (FLUID DYNAMICS)

Ice accretion on aircraft wings
[BTN-95-EIX95082502224] p 225 A95-71021
Open Skies project computational fluid dynamic analysis
[AD-A285928] p 223 N95-19991

PANELS

Buckling and vibration analysis of laminated panels using VICONOPT
[PAPER-1746] p 230 A95-72580

PARABOLIC BODIES

Experimental study of the helicopter-mobile radioelectrical channel and possible extension to the satellite-mobile channel p 247 N95-20945

PARALLEL PROCESSING (COMPUTERS)

Large-scale computational fluid dynamics by the finite element method
[BTN-94-EIX94381359154] p 243 A95-71744
Computing methods for the approximate solution of time dependent problems
[AD-A286007] p 256 N95-20719

PARAMETER IDENTIFICATION

Comparison of parameter identification algorithms for flight vehicles
[BTN-94-EIX94371347708] p 219 A95-69967
Attitude determination using dedicated and nondedicated multiantenna GPS sensors
[BTN-95-EIX95142555482] p 228 A95-72891

PARAMETERIZATION

An algorithm for forecasting mountain wave-related turbulence in the stratosphere
[HTN-95-80656] p 254 A95-72500

PARTICLE COLLISIONS

State-to-state collisional dynamics of atmospheric species
[AD-A285053] p 245 N95-20484

PARTICLE SIZE DISTRIBUTION

Performance of a focused cavity aerosol spectrometer for measurements in the stratosphere of particle size in the 0.06-2.0-micrometer-diameter range
[HTN-95-90914] p 253 A95-72423
Microphysical and radiative properties of small cumulus clouds over the sea
[HTN-95-A0526] p 255 A95-73180
On the link between cloud-top radiative properties and sub-cloud aerosol concentrations
[HTN-95-A0527] p 255 A95-73181

PASSENGER AIRCRAFT

Commuter/air taxi ditchings and water-related impacts that occurred from 1979 to 1989
[AD-A285691] p 226 N95-20275

PASSENGERS

Test and evaluation report for the Manual Domestic Passive Profiling System (MDPPS)
[AD-A286312] p 225 N95-20093

PATTERN RECOGNITION

Electrochemical impedance pattern recognition for detection of hidden chemical corrosion on aircraft components
[AD-A284998] p 241 N95-20481

PATTERN REGISTRATION

SAR image registration in absolute coordinates using GPS carrier phase position and velocity information
[DE94-018738] p 228 N95-20195

PAVEMENTS

Super-heavy aircraft study
[AD-A279602] p 238 N95-19955

PERFORMANCE PREDICTION

Lubricant evaluation and performance, 2
[AD-A279144] p 242 N95-21969

PERFORMANCE TESTS

A review of water mist technology for fire suppression
[AD-A285738] p 225 N95-20071

GPS-Squitter capacity analysis
[AD-A280037] p 245 N95-20599

An Echelle Grating Spectrometer (EGS) for mid-IR remote chemical detection
[DE94-019310] p 249 N95-21478

Response of the B-1B air data sensor to simulated dust cloud environments
[AD-A286134] p 235 N95-22036

PHASE VELOCITY

SAR image registration in absolute coordinates using GPS carrier phase position and velocity information
[DE94-018738] p 228 N95-20195

PHOSPHORESCENCE

Application of pressure sensitive paint in hypersonic flows
[NASA-TM-106824] p 223 N95-20794

PHOTODIODES

Electro-optic characterization of ultrafast photodetectors using adiabatically compressed soliton pulses
[BTN-94-EIX94381359637] p 257 A95-72675

PHOTOMETERS

Electro-optic characterization of ultrafast photodetectors using adiabatically compressed soliton pulses
[BTN-94-EIX94381359637] p 257 A95-72675

PHOTOVOLTAIC CONVERSION

Photovoltaic electric power applied to Unmanned Aerial Vehicles (UAV)
p 245 N95-20530

PHOTOVOLTAIC EFFECT

Optical processing and control
[AD-A279157] p 259 N95-21975

PIEZOELECTRIC TRANSDUCERS

Smart structures in the control of airframe vibrations
[HTN-95-31014] p 236 A95-71184

PILOT PERFORMANCE

Using the backward transfer paradigm to validate the AH-64 Simulator Training Research Advanced Testbed for Aviation
[AD-A285758] p 238 N95-19931

PILOT TRAINING

A computer-based multimedia prototype for night vision goggles
[AD-A286208] p 258 N95-21882

PILOTLESS AIRCRAFT

Unmanned aerial vehicles
[AD-A286190] p 231 N95-20329
Photovoltaic electric power applied to Unmanned Aerial Vehicles (UAV)
p 245 N95-20530

PITCH (INCLINATION)

Measurement around a rotor blade excited in pitch. Part 1: Dynamic inflow
[HTN-95-31007] p 220 A95-71177
Measurement around a rotor blade excited in pitch. Part 2: Unsteady surface pressure
[HTN-95-31008] p 220 A95-71178

PITCHING MOMENTS

Effects of yaw and pitch motion on model attitude measurements
[NASA-TM-4641] p 250 N95-22109

PITOT TUBES

Response of the B-1B air data sensor to simulated dust cloud environments
[AD-A286134] p 235 N95-22036

PITTING

Corrosion of aircraft materials: Correlation between nanometer scale and macroscopic structural damage parameters
[AD-A285930] p 241 N95-20299

PLANE WAVES

RCS measurements, transformations, and comparisons under cylindrical and plane wave illumination
[BTN-94-EIX94371347126] p 242 A95-69976

PLUMES

Temperature effects on acoustic interactions between attitude test facilities and jet engine plumes
[NASA-CR-187638] p 258 N95-21170

POLARIMETRY

Foliage transmission measurements using a ground-based ultrawide band (300-1300 MHz) SAR system
[BTN-94-EIX94381351617] p 252 A95-70950

POLLUTION CONTROL

Environmental Compliance Assessment and Management Program
[AD-A279605] p 255 N95-20441

POLLUTION MONITORING

Environmental Compliance Assessment and Management Program
[AD-A279605] p 255 N95-20441

POLYCHLORINATED BIPHENYLS

The impact of advanced packaging technology on modular avionics architectures p 233 N95-20632

POLYPHENYL ETHER

Lubricant evaluation and performance, 2
[AD-A279144] p 242 N95-21969

POSITION (LOCATION)

Secondary source locations in active noise control: Selection or optimization?
[BTN-94-EIX94381352222] p 257 A95-71738
SAR image registration in absolute coordinates using GPS carrier phase position and velocity information
[DE94-018738] p 228 N95-20195

POTENTIAL FLOW

Effects of leading and trailing edge flaps on the aerodynamics of airfoil/vortex interactions
[HTN-95-31011] p 221 A95-71181

POWER LINES

Fault detection techniques for complex cable shield topologies
[AD-A286632] p 247 N95-20771
TIM-SCT cable testing protocol
[AD-A286633] p 231 N95-20772

POWER SPECTRA

A preliminary study of the airwake model used in an existing SH-60B/FFG-7 helicopter/ship simulation program
[DSTO-TR-0015] p 224 N95-21659
Derived gust spectra for the Macchi MB326H
[ARL-TN-3] p 225 N95-21892

PRECONDITIONING

Large-scale computational fluid dynamics by the finite element method
[BTN-94-EIX94381359154] p 243 A95-71744

PREDICTION ANALYSIS TECHNIQUES

Forecasting aircraft mishaps using monthly maintenance reports
[AD-A286049] p 227 N95-22417

PRESSURE DISTRIBUTION

Measurement around a rotor blade excited in pitch. Part 2: Unsteady surface pressure
[HTN-95-31008] p 220 A95-71178
Application of pressure sensitive paint in hypersonic flows
[NASA-TM-106824] p 223 N95-20794

PRESSURE EFFECTS

Wake measurements in a strong adverse pressure gradient
[NASA-CR-197272] p 224 N95-21031
Effect of atmospheric pressure on measured aircraft noise levels
[PB95-130423] p 232 N95-21425

PRESSURE GRADIENTS

Wake measurements in a strong adverse pressure gradient
[NASA-CR-197272] p 224 N95-21031
Acoustic receptivity due to weak surface inhomogeneities in adverse pressure gradient boundary layers
[NASA-TM-4577] p 249 N95-21258
Large-eddy simulation of flow through a plane, asymmetric diffuser p 250 N95-22449

PRESSURE MEASUREMENT

Application of pressure sensitive paint in hypersonic flows
[NASA-TM-106824] p 223 N95-20794
Pressure measurements on an F/A-18 twin vertical tail in buffeting flow. Volume 4, part 1: Buffet cross spectral densities
[AD-A285593] p 237 N95-21214

PRESSURE REDUCTION

MHD-flow in slotted channels with conducting walls
[DE94-018730] p 258 N95-21388

PRESSURE SENSORS

Response of the B-1B air data sensor to simulated dust cloud environments
[AD-A286134] p 235 N95-22036

PRINTED CIRCUITS

Ultra-Reliable Digital Avionics (URDA) processor p 245 N95-20638

PROBLEM SOLVING

Computing methods for the approximate solution of time dependent problems
[AD-A286007] p 256 N95-20719

PROCUREMENT

The Advanced Avionics Subsystem Technology Demonstration Program p 234 N95-20636

PROFILES

Test and evaluation report for the Manual Domestic Passive Profiling System (MDPPS)
[AD-A286312] p 225 N95-20093

PROJECTILES

Comparison of meteorological data with fitted values extracted from projectile trajectory
[AD-A285921] p 255 N95-19989

PROPULSION

T-45A High Angle of Attack Testing: US Naval Test Pilot School 46th Annual Reunion and Symposium
[AD-A284000] p 231 N95-20466

PROTOCOL (COMPUTERS)

High performance backplane components for modular avionics p 247 N95-20653

Q

Q VALUES

Measurements of shielding effectiveness and cavity characteristics of airplanes
[PB94-210051] p 244 N95-20191

R

RADAR BEACONS

GPS-Scuttler capacity analysis
[AD-A280037] p 245 N95-20599

Recommendation on transition from primary/secondary radar to secondary-only radar capability
[AD-A286279] p 249 N95-22005

RADAR CROSS SECTIONS

Electromagnetic backscattering from a helicopter rotor in the decametric wave band regime
[BTN-94-EIX94381353130] p 243 A95-72648

RADAR IMAGERY

SAR image registration in absolute coordinates using GPS carrier phase position and velocity information
[DE94-018738] p 228 N95-20195

RADAR NAVIGATION

Recommendation on transition from primary/secondary radar to secondary-only radar capability
[AD-A286279] p 249 N95-22005

RADIANCE

Water vapor continuum absorption in mid-latitudes: Aircraft measurements and model comparisons
[HTN-95-40756] p 252 A95-71186

RADIATIVE TRANSFER

Microphysical and radiative properties of small cumulus clouds over the sea
[HTN-95-A0526] p 255 A95-73180

On the link between cloud-top radiative properties and sub-cloud aerosol concentrations
[HTN-95-A0527] p 255 A95-73181

RADIO COMMUNICATION

Modular CNI avionics system p 234 N95-20659

RADIO FREQUENCIES

The impact of advanced packaging technology on modular avionics architectures p 233 N95-20632
High density monolithic packaging technology for digital/microwave avionics p 240 N95-20646

RAIN

High-resolution imaging of rain systems with the advanced microwave precipitation radiometer
[HTN-95-70133] p 252 A95-70655

Behavior of an inversion-based precipitation retrieval algorithm with high-resolution AMPR measurements including a low-frequency 10.7-GHz channel
[HTN-95-70134] p 252 A95-70656

Snow-band formation and evolution during the 15 November 1987 aircraft accident at Denver airport
[HTN-95-80699] p 254 A95-72543

RAINDROPS

Aircraft corrosion study
[AD-A279527] p 241 N95-21687

RAMJET ENGINES

Integral rocket ramjets
[AD-A285135] p 240 N95-20906

RANGEFINDING

Passive range measurement system
[AD-D016222] p 258 N95-21100

RAREFIED GAS DYNAMICS

Cercignani-Lampis-Lord gas-surface interaction model: Comparisons between theory and simulation
[BTN-95-EIX95041503806] p 242 A95-70131

Flow resolution and domain influence in rarefied hypersonic blunt-body flows
[BTN-95-EIX95082502729] p 220 A95-70136

REACTIVITY

Laboratory evaluation of a reactive baffle approach to NOx control
[AD-A283802] p 255 N95-19921

READING

Evaluation of the Haworth-Newman avionics Display Readability Scale
[AD-A286127] p 235 N95-22232

REAL TIME OPERATION

High-order state space simulation models of helicopter flight mechanics
[HTN-95-A0494] p 237 A95-72565

The impact of advanced packaging technology on modular avionics architectures p 233 N95-20632

A real-time algorithm for integrating differential satellite and inertial navigation information during helicopter approach
[NASA-CR-197409] p 229 N95-21891

RECEIVERS

Attitude determination using dedicated and nondedicated multi-antenna GPS sensors
[BTN-95-EIX95142555482] p 228 A95-72891
Assessment of a non-dedicated GPS receiver system for precise airborne attitude determination
[DE94-019309] p 229 N95-21520

RECIRCULATIVE FLUID FLOW

Application of Direct and Large Eddy Simulation to Transition and Turbulence
[AGARD-CP-551] p 248 N95-21061

RECONNAISSANCE AIRCRAFT

Unmanned aerial vehicles
[AD-A286190] p 231 N95-20329
Passive range measurement system
[AD-D016222] p 258 N95-21100

REGULATIONS

Environmental Compliance Assessment and Management Program
[AD-A279605] p 255 N95-20441

REINFORCEMENT (STRUCTURES)

Prediction of energy absorption capability of composite stiffeners
[HTN-95-A0500] p 230 A95-72571

RELIABILITY

Standard Hardware Acquisition and Reliability Program (SHARP) advanced SEM-E packaging p 233 N95-20633

Reliability assessment of Multichip Module technologies via the Triservice/NASA RELTECH program p 245 N95-20643

Assuring Known Good Die (KGD) for reliable, cost effective MCMs p 246 N95-20644

REMOTE SENSING

High-resolution imaging of rain systems with the advanced microwave precipitation radiometer
[HTN-95-70133] p 252 A95-70655

An Echelle Grating Spectrometer (EGS) for mid-IR remote chemical detection
[DE94-019310] p 249 N95-21478

Overview of remote sensing laser development and semiconductor laser technology
[DE94-019103] p 256 N95-21552

REMOTE SENSORS

Attitude determination using dedicated and nondedicated multi-antenna GPS sensors
[BTN-95-EIX95142555482] p 228 A95-72891

REMOTELY PILOTED VEHICLES

Unmanned aerial vehicles
[AD-A286190] p 231 N95-20329

RESCUE OPERATIONS

Analysis of test criteria for specifying foam firefighting agents for aircraft rescue and firefighting
[AD-A286381] p 227 N95-22352

RESONANCE

Modeling resonance in waveguide-to-microstrip junctions by unilateral fin line resonators
[BTN-94-EIX94381323445] p 242 A95-70844

Temperature effects on acoustic interactions between altitude test facilities and jet engine plumes
[NASA-CR-197638] p 258 N95-21170

RESONANT FREQUENCIES

On the choice of appropriate bases for nonlinear dynamic modal analysis
[HTN-95-A0495] p 221 A95-72566

RESONATORS

Modeling resonance in waveguide-to-microstrip junctions by unilateral fin line resonators
[BTN-94-EIX94381323445] p 242 A95-70844

RESOURCES MANAGEMENT

Public-sector aviation issues: Graduate research award papers, 1992-1993
[PB94-217478] p 219 N95-19967

REYNOLDS NUMBER

Research on bluff body vortex wakes
[AD-A286319] p 223 N95-20177

Acoustic receptivity due to weak surface inhomogeneities in adverse pressure gradient boundary layers
[NASA-TM-4577] p 249 N95-21258

Experiments on the flow field physics of confluent boundary layers for high-lift systems
[NASA-CR-197318] p 224 N95-21343

RICCATI EQUATION

Design of robust optimal control systems and stability analysis of real structured uncertainties
[AD-A279089] p 256 N95-21913

RING LASERS

Optical processing and control
[AD-A279157] p 259 N95-21975

RIVETING

Damage tolerant repair techniques for pressurized aircraft fuselages
[AD-A286298] p 219 N95-22046

ROTORARY WING AIRCRAFT

Measurement around a rotor blade excited in pitch. Part 1: Dynamic inflow
[HTN-95-31007] p 220 A95-71177

ROTORARY WINGS

Measurement around a rotor blade excited in pitch. Part 1: Dynamic inflow
[HTN-95-31007] p 220 A95-71177

Measurement around a rotor blade excited in pitch. Part 2: Unsteady surface pressure
[HTN-95-31008] p 220 A95-71178

Aerodynamic and wake methodology evaluation using Model UH-60A experimental data
[HTN-95-31009] p 220 A95-71179

Effects of leading and trailing edge flaps on the aerodynamics of airfoil/vortex interactions
[HTN-95-31011] p 221 A95-71181

Advance finite element modeling of rotor blade aeroelasticity
[HTN-95-31013] p 221 A95-71183

On the choice of appropriate bases for nonlinear dynamic modal analysis
[HTN-95-A0495] p 221 A95-72566

Flap-lag damping in hover and forward flight with a three-dimensional wake
[HTN-95-A0496] p 221 A95-72567

Air and ground resonance of helicopters with elastically tailored composite rotor blades
[HTN-95-A0497] p 222 A95-72568

Design optimization of rotor blades for improved performance and vibration
[HTN-95-A0498] p 229 A95-72569

Electromagnetic backscattering from a helicopter rotor in the decametric wave band regime
[BTN-94-EIX94381353130] p 243 A95-72648

Prediction of rotor-blade deformations due to unsteady airloads
[AD-A286593] p 231 N95-20860

Simulation of rotor blade element turbulence
[NASA-TM-108862] p 232 N95-21186

ROTATING BODIES

Robust fixed-structure control
[AD-A286515] p 257 N95-22216

ROTOR AERODYNAMICS

Measurement around a rotor blade excited in pitch. Part 1: Dynamic inflow
[HTN-95-31007] p 220 A95-71177

Measurement around a rotor blade excited in pitch. Part 2: Unsteady surface pressure
[HTN-95-31008] p 220 A95-71178

Vorticity concentration at the edge of the inboard vortex sheet
[HTN-95-31010] p 221 A95-71180

Effects of leading and trailing edge flaps on the aerodynamics of airfoil/vortex interactions
[HTN-95-31011] p 221 A95-71181

Advance finite element modeling of rotor blade aeroelasticity
[HTN-95-31013] p 221 A95-71183

High-order state space simulation models of helicopter flight mechanics
[HTN-95-A0494] p 237 A95-72565

On the choice of appropriate bases for nonlinear dynamic modal analysis
[HTN-95-A0495] p 221 A95-72566

Flap-lag damping in hover and forward flight with a three-dimensional wake
[HTN-95-A0496] p 221 A95-72567

Design optimization of rotor blades for improved performance and vibration
[HTN-95-A0498] p 229 A95-72569

Parametric studies for tiltrotor aeroelastic stability in highspeed flight
[HTN-95-A0499] p 222 A95-72570

The dynamic approach to rotor blade research: ARA's oscillatory test facility
[ARA-MEMO-405] p 223 N95-20758

ROTOR BLADES (TURBOMACHINERY)

Prediction of rotor-blade deformations due to unsteady airloads
[AD-A286593] p 231 N95-20860

ROTOR BODY INTERACTIONS

High-order state space simulation models of helicopter flight mechanics
[HTN-95-A0494] p 237 A95-72565

Design optimization of rotor blades for improved performance and vibration
[HTN-95-A0498] p 229 A95-72569

ROTOR DYNAMICS

Measurement around a rotor blade excited in pitch. Part 1: Dynamic inflow
[HTN-95-31007] p 220 A95-71177

ROTORS

- Measurement around a rotor blade excited in pitch. Part 2: Unsteady surface pressure
[HTN-95-31008] p 220 A95-71178
- Air and ground resonance of helicopters with elastically tailored composite rotor blades
[HTN-95-A0497] p 222 A95-72568
- The dynamic approach to rotor blade research: ARA's oscillatory test facility
[ARA-MEMO-405] p 223 N95-20758
- ROTORS**
- Variations observed in the AC generator signal period of a Sea King helicopter
[AD-A284280] p 230 N95-19963
- Scale-up and modeling of forced chemical vapor infiltration
[DE94-017769] p 247 N95-20781
- Advanced wind turbine design studies: Advanced conceptual study
[DE93-000031] p 256 N95-20985
- RUNWAYS**
- Super-heavy aircraft study
[AD-A279602] p 238 N95-19955

S

SAFETY FACTORS

- The personal aircraft: Status and issues
[NASA-TM-109174] p 223 N95-20688
- Analysis of test criteria for specifying foam firefighting agents for aircraft rescue and firefighting
[AD-A286381] p 227 N95-22352

SAMPLING

- Electro-optic characterization of ultrafast photodetectors using adiabatically compressed soliton pulses
[BTN-94-EIX94381359637] p 257 A95-72675

SATELLITE ALTIMETRY

- Precise orbit determination with a short-arc technique
— Abstract only p 240 A95-70543

SATELLITE ORBITS

- Precise orbit determination with a short-arc technique
— Abstract only p 240 A95-70543

SATELLITE TRACKING

- Precise orbit determination with a short-arc technique
— Abstract only p 240 A95-70543
- Tropical cyclone observation and forecasting with and without aircraft reconnaissance
[HTN-95-80701] p 254 A95-72545

SAWS

- Vortex shedding noise control in idling circular saws using air ejection at the teeth
[BTN-94-EIX94371347214] p 257 A95-69970

SCANNERS

- Foliage transmission measurements using a ground-based ultrawide band (300-1300 MHz) SAR system
[BTN-94-EIX94381351617] p 252 A95-70950
- Test and Evaluation Plan (TEP) for Improvised Explosive Device Screening Systems (IEDSS)
[AD-A286382] p 227 N95-22319

SELECTION

- MCMs for avionics: Technology selection and intermodule interconnection p 234 N95-20641

SELECTIVE FADING

- Experimental study of the helicopter-mobile radioelectrical channel and possible extension to the satellite-mobile channel p 247 N95-20945

SELF ADAPTIVE CONTROL SYSTEMS

- A neural expert approach to self designing flight control systems
[AD-A279965] p 237 N95-21122

SEMICONDUCTOR JUNCTIONS

- Modeling resonance in waveguide-to-microstrip junctions by unilateral fin line resonators
[BTN-94-EIX94381323445] p 242 A95-70844

SEMICONDUCTOR LASERS

- Overview of remote sensing laser development and semiconductor laser technology
[DE94-019103] p 256 N95-21552

SEPARATED FLOW

- Application of Navier-Stokes code PAB3D with kappa-epsilon turbulence model to attached and separated flows
[NASA-TP-3480] p 224 N95-21338

SERVICE LIFE

- Engine life measurement and diagnostics
[BTN-95-EIX95041505024] p 235 A95-70133

SH-3 HELICOPTER

- Variations observed in the AC generator signal period of a Sea King helicopter
[AD-A284280] p 230 N95-19963

SHEAR FLOW

- Aerodynamic mechanism of galloping
[BTN-94-EIX94371347709] p 219 A95-69968
- Investigation of shear layer transition using various turbulence models p 248 N95-21096

SHEAR LAYERS

- Investigation of shear layer transition using various turbulence models p 248 N95-21096

SHOCK LAYERS

- Thermochemical nonequilibrium viscous shock-layer analysis for a Mars aerocapture vehicle
[BTN-95-EIX95082502732] p 239 A95-70139

SHOCK WAVE INTERACTION

- Shock wave interactions in hypervelocity flow
[AD-A286507] p 250 N95-22212

SHOCK WAVES

- Shock wave interactions in hypervelocity flow
[AD-A286507] p 250 N95-22212

SIDESLIP

- Pressure measurements on an F/A-18 twin vertical tail in buffeting flow. Volume 1: Wind tunnel test summary
[AD-A279126] p 225 N95-21877
- Effect of juncture fillets on double-delta wings undergoing sideslip at high angles of attack
[AD-A286165] p 232 N95-22039

SIGNAL ANALYZERS

- The impact of advanced packaging technology on modular avionics architectures p 233 N95-20632

SIGNAL PROCESSING

- Precise navigation using adaptive FIR filtering and time domain spectral estimation
[BTN-95-EIX95142555485] p 227 A95-72888
- Variations observed in the AC generator signal period of a Sea King helicopter
[AD-A284280] p 230 N95-19963
- The impact of advanced packaging technology on modular avionics architectures p 233 N95-20632
- Wavelet transformations for helicopter identification via acoustic signatures
[AD-A279980] p 257 N95-20963

SIGNAL TRANSMISSION

- Attitude determination using dedicated and nondedicated multiantenna GPS sensors
[BTN-95-EIX95142555482] p 228 A95-72891

SIGNATURES

- Application of wavelet-filtering techniques to intermittent turbulent and wall pressure events. Part 1: Exploratory results
[AD-A286077] p 247 N95-20849

SIMULATORS

- Color control in a multichannel simulator display: The display for advanced research and training
[AD-A279717] p 239 N95-20992
- An evaluation of Automatic Terminal Information Service (ATIS) flight deck display presentation options
[AD-A280100] p 228 N95-21020

SITE SELECTION

- Secondary source locations in active noise control: Selection or optimization?
[BTN-94-EIX94381352222] p 257 A95-71738

SIZE (DIMENSIONS)

- Scale-up and modeling of forced chemical vapor infiltration
[DE94-017769] p 247 N95-20781

SKIN FRICTION

- Application of Navier-Stokes code PAB3D with kappa-epsilon turbulence model to attached and separated flows
[NASA-TP-3480] p 224 N95-21338

SMART STRUCTURES

- Smart structures in the control of airframe vibrations
[HTN-95-31014] p 236 A95-71184
- Collected papers of the Soar/IFOR project, Spring 1994
[AD-A280063] p 238 N95-20624

SNOW

- Snow-band formation and evolution during the 15 November 1987 aircraft accident at Denver airport
[HTN-95-80699] p 254 A95-72543
- Comments on effect of wet snow on the null-reference ILS system
[BTN-95-EIX95142555488] p 227 A95-72885

SNOWSTORMS

- Snow-band formation and evolution during the 15 November 1987 aircraft accident at Denver airport
[HTN-95-80699] p 254 A95-72543

SOFTWARE TOOLS

- The navigation toolkit
[NASA-CR-197290] p 229 N95-22161

SOLAR CELLS

- Photovoltaic electric power applied to Unmanned Aerial Vehicles (UAV) p 245 N95-20530

SOLAR ELECTRIC PROPULSION

- CALJOE and TAISIR airborne experiment platform
[DE94-018328] p 250 N95-22299

SOLAR WIND

- A survey of bidirectional greater than or equal to MeV ion flows during the Helios 1 and Helios 2 mission: Observations from the Goddard Space Flight Center instruments
[HTN-95-70542] p 237 A95-71656

SOLID PROPELLANTS

- Integral rocket ramjets
[AD-A285135] p 240 N95-20906

SORBENTS

- Laboratory evaluation of a reactive baffle approach to NOx control
[AD-A283802] p 255 N95-19921

SOUND PROPAGATION

- Sound propagation from an arbitrarily oriented multipole placed near a plane, finite impedance surface
[BTN-94-EIX94371338964] p 257 A95-70797

SOUND WAVES

- Sound propagation from an arbitrarily oriented multipole placed near a plane, finite impedance surface
[BTN-94-EIX94371338964] p 257 A95-70797
- Temperature effects on acoustic interactions between altitude test facilities and jet engine plumes
[NASA-CR-197638] p 258 N95-21170
- Acoustic receptivity due to weak surface inhomogeneities in adverse pressure gradient boundary layers
[NASA-TM-4577] p 249 N95-21258
- Effect of atmospheric pressure on measured aircraft noise levels
[PB95-130423] p 232 N95-21425

SPALLING

- Aircraft corrosion study
[AD-A279527] p 241 N95-21687

SPECTRAL METHODS

- Derived gust spectra for the Macchi MB326H
[ARL-TN-3] p 225 N95-21892

SPECTROMETERS

- Performance of a focused cavity aerosol spectrometer for measurements in the stratosphere of particle size in the 0.06-2.0-micrometer-diameter range
[HTN-95-90914] p 253 A95-72423

SPECTROSCOPIC ANALYSIS

- Electrochemical impedance pattern recognition for detection of hidden chemical corrosion on aircraft components
[AD-A284998] p 241 N95-20481

SPECTRUM ANALYSIS

- Measurement around a rotor blade excited in pitch. Part 1: Dynamic inflow
[HTN-95-31007] p 220 A95-71177
- Precise navigation using adaptive FIR filtering and time domain spectral estimation
[BTN-95-EIX95142555485] p 227 A95-72888

SPRAYING

- A review of water mist technology for fire suppression
[AD-A285738] p 225 N95-20071

STABILITY

- Robust fixed-structure control
[AD-A286515] p 257 N95-22216

STABILITY TESTS

- Design of robust optimal control systems and stability analysis of real structured uncertainties
[AD-A279089] p 256 N95-21913

STABILIZATION

- Robust fixed-structure control
[AD-A286515] p 257 N95-22216

STABILIZERS (FLUID DYNAMICS)

- Pressure measurements on an F/A-18 twin vertical tail in buffeting flow. Volume 4, part 1: Buffet cross spectral densities
[AD-A285593] p 237 N95-21214
- Pressure measurements on an F/A-18 twin vertical tail in buffeting flow. Volume 1: Wind tunnel test summary
[AD-A279126] p 225 N95-21877

STANDARDIZATION

- TIM-SCT cable testing protocol
[AD-A286633] p 231 N95-20772

STATIC TESTS

- Static investigation of two fluidic thrust-vectoring concepts on a two-dimensional convergent-divergent nozzle
[NASA-TM-4574] p 222 N95-19913
- Portable static test facility for small, expendable, turbojet engines, phase 1
[AD-A286337] p 239 N95-21719

STATISTICAL ANALYSIS

- Statistical analysis of Turbine Engine Diagnostic (TED) field test data
[AD-A286032] p 248 N95-20998

STEADY FLOW

- Shock wave interactions in hypervelocity flow
[AD-A286507] p 250 N95-22212

STEELS

- Corrosion behavior of landing gear steels
[AD-A285862] p 242 N95-22132

STIFFENING

- Prediction of energy absorption capability of composite stiffeners
[HTN-95-A0500] p 230 A95-72571

STORMS (METEOROLOGY)

Radar studies of aviation hazards
[AD-A285845] p 226 N95-21831

STRAIN GAGES

Vapor generator wand
[NASA-CASE-LAR-15058-1] p 238 N95-20080

STRATEGY

Bomber force 2000: Operational concepts for long-range combat aircraft
[AD-A279378] p 230 N95-20181

STRATOSPHERE

Subsidence of aircraft engine exhaust in the stratosphere: Implications for calculated ozone depletions
[PAPER-93GL03426] p 251 A95-70297

Aircraft-borne, laser-induced fluorescence instrument for the in situ detection of hydroxyl and hydroperoxy radicals
[BTN-95-EIX95072499029] p 253 A95-71908

Performance of a focused cavity aerosol spectrometer for measurements in the stratosphere of particle size in the 0.06-2.0-micrometer-diameter range
[HTN-95-90914] p 253 A95-72423

An algorithm for forecasting mountain wave-related turbulence in the stratosphere
[HTN-95-80656] p 254 A95-72500

STRESS CORROSION CRACKING

Corrosion behavior of landing gear steels
[AD-A285862] p 242 N95-22132

STRESS INTENSITY FACTORS

Bonded composite repair of cracked load-bearing holes
[BTN-94-EIX94401360553] p 243 A95-71867

STRUCTURAL ANALYSIS

Numerical modelling of transverse impact on composite coupons
[BTN-95-EIX95082502225] p 240 A95-71022

Super-heavy aircraft study
[AD-A279602] p 238 N95-19955

STRUCTURAL DESIGN

Design optimization of rotor blades for improved performance and vibration
[HTN-95-A0498] p 229 A95-72569

STRUCTURAL DESIGN CRITERIA

An Echelle Grating Spectrometer (EGS) for mid-IR remote chemical detection
[DE94-019310] p 249 N95-21478

STRUCTURAL FAILURE

Prediction of energy absorption capability of composite stiffeners
[HTN-95-A0500] p 230 A95-72571

Corrosion of aircraft materials: Correlation between nanometer scale and macroscopic structural damage parameters
[AD-A285930] p 241 N95-20299

SUBMERGING

Immersion/two phase cooling
p 246 N95-20648

SUBROUTINES

A preliminary study of the airwake model used in an existing SH-60B/FFG-7 helicopter/ship simulation program
[DSTO-TR-0015] p 224 N95-21659

SUPERSONIC BOUNDARY LAYERS

Supersonic laminar flow control research
[NASA-CR-196049] p 249 N95-21340

SUPERSONIC FLOW

Application of Navier-Stokes code PAB3D with kappa-epsilon turbulence model to attached and separated flows
[NASA-TP-3480] p 224 N95-21338

Shock wave interactions in hypervelocity flow
[AD-A286507] p 250 N95-22212

SUPERSONIC JET FLOW

Temperature effects on acoustic interactions between altitude test facilities and jet engine plumes
[NASA-CR-197638] p 258 N95-21170

SUPERSONIC NOZZLES

Development of quiet-flow supersonic wind tunnels for laminar-turbulent transition research
[NASA-CR-197286] p 239 N95-21436

SUPERSONIC SPEED

Flow coefficient behavior for boundary layer bleed holes and slots
[NASA-TM-106846] p 244 N95-19953

SUPERSONIC WIND TUNNELS

Supersonic laminar flow control research
[NASA-CR-196049] p 249 N95-21340

Development of quiet-flow supersonic wind tunnels for laminar-turbulent transition research
[NASA-CR-197286] p 239 N95-21436

SURFACE ROUGHNESS

Aircraft corrosion study
[AD-A279527] p 241 N95-21687

SURFACE TEMPERATURE

Flow resolution and domain influence in rarefied hypersonic blunt-body flows
[BTN-95-EIX95082502729] p 220 A95-70136

SURFACE TREATMENT

Aircraft corrosion study
[AD-A279527] p 241 N95-21687

SURFACE WATER

Orbital velocities induced by surface waves
[HTN-95-90902] p 253 A95-72411

SURFACE WAVES

Orbital velocities induced by surface waves
[HTN-95-90902] p 253 A95-72411

SURVEILLANCE

GPS-Squitter capacity analysis
[AD-A280037] p 245 N95-20599

SURVEILLANCE RADAR

Recommendation on transition from primary/secondary radar to secondary-only radar capability
[AD-A286279] p 249 N95-22005

SWEPT WINGS

Computational studies of laminar to turbulence transition
[AD-A285622] p 248 N95-21146

Lift enhancement device
[AD-DO16522] p 224 N95-21864

SYSTEM IDENTIFICATION

Modular CNI avionics system
p 234 N95-20659

SYSTEMS ENGINEERING

FASTPACK: Optimized solutions for modular avionics derived from a parametric study. Part 1: Platform features
p 233 N95-20634

Advanced wind turbine design studies: Advanced conceptual study
[DE93-000031] p 256 N95-20985

SYSTEMS INTEGRATION

FASTPACK: Optimized solutions for modular avionics derived from a parametric study. Part 1: Platform features
p 233 N95-20634

T

TACHOMETERS

Variations observed in the AC generator signal period of a Sea King helicopter
[AD-A284280] p 230 N95-19963

TAIL ASSEMBLIES

Pressure measurements on an F/A-18 twin vertical tail in buffet flow. Volume 4, part 1: Buffet cross spectral densities
[AD-A285593] p 237 N95-21214

Pressure measurements on an F/A-18 twin vertical tail in buffet flow. Volume 1: Wind tunnel test summary
[AD-A279126] p 225 N95-21877

TAIL SURFACES

Pressure measurements on an F/A-18 twin vertical tail in buffet flow. Volume 4, part 1: Buffet cross spectral densities
[AD-A285593] p 237 N95-21214

Pressure measurements on an F/A-18 twin vertical tail in buffet flow. Volume 1: Wind tunnel test summary
[AD-A279126] p 225 N95-21877

TAKEOFF

F-15 resource tape
[NASA-TM-110502] p 230 N95-19994

TECHNOLOGY ASSESSMENT

Reliability assessment of Multichip Module technologies via the Triservice/NASA RELTECH program
p 245 N95-20643

High density monolithic packaging technology for digital/microwave avionics
p 240 N95-20646

TECHNOLOGY UTILIZATION

Independent review of Aviation Technology and Research Information Analysis System (ATRIAS) database
[AD-A284049] p 226 N95-21518

TELECOMMUNICATION

Experimental study of the helicopter-mobile radioelectrical channel and possible extension to the satellite-mobile channel
p 247 N95-20945

TEMPERATURE CONTROL

Liquid flow-through cooling of electronic modules
p 246 N95-20647

TEMPERATURE EFFECTS

Investigation of a thermal buoyancy effect on the drag of half models tested in the ARA Transonic Wind Tunnel
[ARA-MEMO-407] p 222 N95-19946

Temperature effects on acoustic interactions between altitude test facilities and jet engine plumes
[NASA-CR-197638] p 258 N95-21170

Effect of atmospheric pressure on measured aircraft noise levels
[PB95-130423] p 232 N95-21425

TEMPERATURE MEASUREMENT

Time-resolved surface heat flux measurements in the wing/body junction vortex
[BTN-95-EIX95082502716] p 220 A95-71029

TEMPERATURE PROFILES

Evaluation of the Sparton tight-tolerance AXBT
[HTN-95-40728] p 251 A95-70473

TEST CHAMBERS

16-foot transonic tunnel test section flowfield survey
[NASA-TM-109157] p 238 N95-20669

TEST FACILITIES

Description and flow characterization of hypersonic facilities
[AD-A284291] p 223 N95-20248

Portable static test facility for small, expendable, turbojet engines, phase 1
[AD-A286377] p 239 N95-21719

TEST PILOTS

T-45A High Angle of Attack Testing: US Naval Test Pilot School 46th Annual Reunion and Symposium
[AD-A284000] p 231 N95-20466

TETHERED BALLOONS

CALIOPE and TAISIR airborne experiment platform
[DE94-018328] p 250 N95-22299

THERMAL ANALYSIS

Lubricant evaluation and performance, 2
[AD-A279144] p 242 N95-21969

THERMAL CONDUCTIVITY

Evaluation of the Sparton tight-tolerance AXBT
[HTN-95-40728] p 251 A95-70473

THERMAL ENVIRONMENTS

MCMs for avionics: Technology selection and intermodule interconnection
p 234 N95-20641

THERMAL STABILITY

Toughened Silcomp composites for gas turbine engine applications
[DE95-002851] p 235 N95-21243

Lubricant evaluation and performance, 2
[AD-A279144] p 242 N95-21969

THERMODYNAMIC CYCLES

Malone-brayton cycle engine/heat pump
[AD-DO16573] p 244 N95-20295

THERMODYNAMIC EQUILIBRIUM

Thermochemical nonequilibrium viscous shock-layer analysis for a Mars aerocapture vehicle
[BTN-95-EIX95082502732] p 239 A95-70139

THERMODYNAMICS

Turbine design and application
[NASA-SF-290] p 236 N95-22341

THIN FILMS

Reliability assessment of Multichip Module technologies via the Triservice/NASA RELTECH program
p 245 N95-20643

THREAT EVALUATION

Test and evaluation report for the Manual Domestic Passive Profiling System (MDPPS)
[AD-A286312] p 225 N95-20093

THREE DIMENSIONAL FLOW

Flap-lag damping in hover and forward flight with a three-dimensional wake
[HTN-95-A0496] p 221 A95-72567

Application of Direct and Large Eddy Simulation to Transition and Turbulence
[AGARD-CP-551] p 248 N95-21061

THREE DIMENSIONAL MODELS

Open Skies project computational fluid dynamic analysis
[AD-A285928] p 223 N95-19991

THRUST REVERSAL

Why do airlines want and use thrust reversers? A compilation of airline industry responses to a survey regarding the use of thrust reversers on commercial transport airplanes
[NASA-TM-109158] p 226 N95-20706

THRUST VECTOR CONTROL

Static investigation of two fluidic thrust-vectoring concepts on a two-dimensional convergent-divergent nozzle
[NASA-TM-4574] p 222 N95-19913

TILT ROTOR AIRCRAFT

Parametric studies for tiltrotor aeroelastic stability in highspeed flight
[HTN-95-A0499] p 222 A95-72570

TILTING ROTORS

Parametric studies for tiltrotor aeroelastic stability in highspeed flight
[HTN-95-A0499] p 222 A95-72570

TIME DEPENDENCE

Computing methods for the approximate solution of time dependent problems
[AD-A286007] p 256 N95-20719

TIME MARCHING

Computation of transonic flow on composite overlapping grids in 2 D
[PB95-131348] p 248 N95-21132

TITANIUM ALLOYS

- Electrochemical impedance pattern recognition for detection of hidden chemical corrosion on aircraft components
[AD-A284998] p 241 N95-20481
- Electrochemical impedance pattern recognition for detection of hidden chemical corrosion on aircraft components
[AD-A285998] p 241 N95-20716
- TOLERANCES (MECHANICS)**
Toughened Sicomposites for gas turbine engine applications
[DE95-002851] p 235 N95-21243
- TOUCHDOWN**
F-15 resource tape
[NASA-TM-110502] p 230 N95-19994
- TOWERS**
An evaluation of Automatic Terminal Information Service (ATIS) flight deck display presentation options
[AD-A280100] p 228 N95-21020
- TRACKING (POSITION)**
Tropical cyclone observation and forecasting with and without aircraft reconnaissance
[HTN-95-80701] p 254 A95-72545
- TRAILING EDGE FLAPS**
Effects of leading and trailing edge flaps on the aerodynamics of airfoil/vortex interactions
[HTN-95-31011] p 221 A95-71181
- Lift enhancement device
[AD-D016522] p 224 N95-21864
- TRAINING ANALYSIS**
Using the backward transfer paradigm to validate the AH-64 Simulator Training Research Advanced Testbed for Aviation
[AD-A285758] p 238 N95-19931
- TRAJECTORIES**
Comparison of meteorological data with fitted values extracted from projectile trajectory
[AD-A285921] p 255 N95-19989
- TRAJECTORY CONTROL**
A generalized algorithm for inverse simulation applied to helicopter maneuvering flight
[HTN-95-A0493] p 236 A95-72564
- TRANSFER FUNCTIONS**
Precise navigation using adaptive FIR filtering and time domain spectral estimation
[BTN-95-EIX95142555485] p 227 A95-72888
- TRANSFER OF TRAINING**
Using the backward transfer paradigm to validate the AH-64 Simulator Training Research Advanced Testbed for Aviation
[AD-A285758] p 238 N95-19931
- TRANSITION FLOW**
Application of Direct and Large Eddy Simulation to Transition and Turbulence
[AGARD-CP-551] p 248 N95-21061
- Acoustic receptivity due to weak surface inhomogeneities in adverse pressure gradient boundary layers
[NASA-TM-4577] p 249 N95-21258
- TRANSMISSION RATE (COMMUNICATIONS)**
Electromagnetic compatibility effects of advanced packaging configurations
p 247 N95-20658
- TRANSMITTER RECEIVERS**
High performance backplane components for modular avionics
p 247 N95-20653
- TRANSONIC FLOW**
Aerodynamic and wake methodology evaluation using Model UH-60A experimental data
[HTN-95-31009] p 220 A95-71179
- Computation of transonic flow on composite overlapping grids in 2 D
[PB95-131348] p 248 N95-21132
- TRANSONIC WIND TUNNELS**
Investigation of a thermal buoyancy effect on the drag of half models tested in the ARA Transonic Wind Tunnel
[ARA-MEMO-407] p 222 N95-19946
- 16-foot transonic tunnel test section flowfield survey
[NASA-TM-109157] p 238 N95-20669
- Testing in the ARA Transonic Wind Tunnel
[ARA-MEMO-395] p 239 N95-20799
- TRANSPORT AIRCRAFT**
Why do airlines want and use thrust reversers? A compilation of airline industry responses to a survey regarding the use of thrust reversers on commercial transport airplanes
[NASA-TM-109158] p 226 N95-20706
- TROPICAL METEOROLOGY**
Tropical cyclone observation and forecasting with and without aircraft reconnaissance
[HTN-95-80701] p 254 A95-72545
- TURBINE BLADES**
Advanced wind turbine design studies: Advanced conceptual study
[DE93-000031] p 256 N95-20985

TURBINE ENGINES

- Statistical analysis of Turbine Engine Diagnostic (TED) field test data
[AD-A286032] p 248 N95-20998
- Turbine design and application
[NASA-SP-290] p 236 N95-22341
- TURBINES**
Scale-up and modeling of forced chemical vapor infiltration
[DE94-017769] p 247 N95-20781
- Turbine design and application
[NASA-SP-290] p 236 N95-22341
- TURBOJET ENGINES**
Portable static test facility for small, expendable, turbojet engines, phase 1
[AD-A286337] p 239 N95-21719
- TURBOMACHINE BLADES**
Investigation of shear layer transition using various turbulence models
p 248 N95-21096
- TURBULENCE**
An algorithm for forecasting mountain wave-related turbulence in the stratosphere
[HTN-95-80656] p 254 A95-72500
- Experimental study of vane heat transfer and aerodynamics at elevated levels of turbulence
[NASA-CR-4633] p 244 N95-19912
- Application of wavelet-filtering techniques to intermittent turbulent and wall pressure events. Part 1: Exploratory results
[AD-A286077] p 247 N95-20849
- Experimental investigations of on-demand vortex generators
p 250 N95-22451
- TURBULENCE EFFECTS**
Simulation of rotor blade element turbulence
[NASA-TM-108862] p 232 N95-21186
- A preliminary study of the airwake model used in an existing SH-60B/FFG-7 helicopter/ship simulation program
[DSTO-TR-0015] p 224 N95-21659
- TURBULENCE MODELS**
Open Skies project computational fluid dynamic analysis
[AD-A285928] p 223 N95-19991
- Investigation of shear layer transition using various turbulence models
p 248 N95-21096
- Simulation of rotor blade element turbulence
[NASA-TM-108862] p 232 N95-21186
- Large-eddy simulation of flow through a plane, asymmetric diffuser
p 250 N95-22449
- TURBULENT BOUNDARY LAYER**
Application of wavelet-filtering techniques to intermittent turbulent and wall pressure events. Part 1: Exploratory results
[AD-A286077] p 247 N95-20849
- Experimental investigations of on-demand vortex generators
p 250 N95-22451
- Transverse vorticity measurements in the NASA Ames 80 x 120 wind tunnel boundary layer
p 251 N95-22457
- TURBULENT FLOW**
Time-resolved surface heat flux measurements in the wing/body junction vortex
[BTN-95-EIX95082502716] p 220 A95-71029
- Application of wavelet-filtering techniques to intermittent turbulent and wall pressure events. Part 1: Exploratory results
[AD-A286077] p 247 N95-20849
- A computer code (SKINTEMP) for predicting transient missile and aircraft heat transfer characteristics
[AD-A286044] p 248 N95-21001
- Application of Direct and Large Eddy Simulation to Transition and Turbulence
[AGARD-CP-551] p 248 N95-21061
- Large-eddy simulation of flow through a plane, asymmetric diffuser
p 250 N95-22449
- TURBULENT JETS**
Application of Direct and Large Eddy Simulation to Transition and Turbulence
[AGARD-CP-551] p 248 N95-21061
- TURBULENT WAKES**
Application of Direct and Large Eddy Simulation to Transition and Turbulence
[AGARD-CP-551] p 248 N95-21061
- TWO DIMENSIONAL BODIES**
Ground effect calculation of two-dimensional airfoil
[BTN-84-EIX94371347710] p 219 A95-69969
- TWO DIMENSIONAL FLOW**
Effects of leading and trailing edge flaps on the aerodynamics of airfoil/vortex interactions
[HTN-95-31011] p 221 A95-71181
- Static investigation of two fluidic thrust-vectoring concepts on a two-dimensional convergent-divergent nozzle
[NASA-TM-4574] p 222 N95-19913
- Investigation of shear layer transition using various turbulence models
p 248 N95-21096

- Two-dimensional imaging of OH in a lean burning high pressure combustor
[NASA-TM-106854] p 236 N95-21383
- Shock wave interactions in hypervelocity flow
[AD-A286507] p 250 N95-22212
- Direct numerical simulations of on-demand vortex generators: Mathematical formulation
p 251 N95-22452

TWO DIMENSIONAL MODELS

- Open Skies project computational fluid dynamic analysis
[AD-A285928] p 223 N95-19991
- An Echelle Grating Spectrometer (EGS) for mid-IR remote chemical detection
[DE94-019310] p 249 N95-21478

U

UH-60A HELICOPTER

- Aerodynamic and wake methodology evaluation using Model UH-60A experimental data
[HTN-95-31009] p 220 A95-71179
- UNITED STATES**
Census US civil aircraft calendar year 1993
[AD-A286309] p 219 N95-20091
- UNSTEADY AERODYNAMICS**
Measurement around a rotor blade excited in pitch. Part 2: Unsteady surface pressure
[HTN-95-31008] p 220 A95-71178
- Aerodynamic and wake methodology evaluation using Model UH-60A experimental data
[HTN-95-31009] p 220 A95-71179
- Effects of leading and trailing edge flaps on the aerodynamics of airfoil/vortex interactions
[HTN-95-31011] p 221 A95-71181
- The dynamic approach to rotor blade research: ARA's oscillatory test facility
[ARA-MEMO-405] p 223 N95-20758
- Prediction of rotor-blade deformations due to unsteady airloads
[AD-A286593] p 231 N95-20860
- Pressure measurements on an F/A-18 twin vertical tail in buffeting flow. Volume 4, part 1: Buffet cross spectral densities
[AD-A285593] p 237 N95-21214
- Pressure measurements on an F/A-18 twin vertical tail in buffeting flow. Volume 1: Wind tunnel test summary
[AD-A279126] p 225 N95-21877
- Direct numerical simulations of on-demand vortex generators: Mathematical formulation
p 251 N95-22452

UNSTEADY FLOW

- Simulation of rotor blade element turbulence
[NASA-TM-108862] p 232 N95-21186
- Direct numerical simulations of on-demand vortex generators: Mathematical formulation
p 251 N95-22452
- Acoustics of laminar boundary layers breakdown
p 251 N95-22455
- USER MANUALS (COMPUTER PROGRAMS)**
A user's guide to LUGSAN 1.1: A computer program to calculate and archive lug and sway brace loads for aircraft-carried stores
[DE95-001919] p 232 N95-21730

V

VANES

- Experimental study of vane heat transfer and aerodynamics at elevated levels of turbulence
[NASA-CR-4633] p 244 N95-19912
- VAPORIZERS**
Vapor generator wand
[NASA-CASE-LAR-15058-1] p 238 N95-20080
- VELOCITY DISTRIBUTION**
A preliminary study of the airwake model used in an existing SH-60B/FFG-7 helicopter/ship simulation program
[DSTO-TR-0015] p 224 N95-21659
- VELOCITY MEASUREMENT**
A three-dimensional orthogonal laser velocimeter for the NASA Ames 7- by 10-foot wind tunnel
[NASA-TM-108864] p 249 N95-21323
- MHD-flow in slotted channels with conducting walls
[DE94-018370] p 258 N95-21388
- A preliminary study of the airwake model used in an existing SH-60B/FFG-7 helicopter/ship simulation program
[DSTO-TR-0015] p 224 N95-21659
- VERMICULITE**
Laboratory evaluation of a reactive baffle approach to NOx control
[AD-A283802] p 255 N95-19921

- VERTICAL AIR CURRENTS**
Simulation of rotor blade element turbulence
[NASA-TM-108862] p 232 N95-21186
- VERTICAL DISTRIBUTION**
Ascent wind model for launch vehicle design
[BTN-95-EIX95041503799] p 239 A95-70124
- VERTICAL FLIGHT**
Comments on effect of wet snow on the null-reference ILS system
[BTN-95-EIX9514255488] p 227 A95-72885
- VERTICAL TAKEOFF AIRCRAFT**
The personal aircraft: Status and issues
[NASA-TM-109174] p 223 N95-20688
- VIBRATION**
Measurement and analysis of nitric oxide radiation in an arcjet flow
[BTN-95-EIX95082502727] p 243 A95-71040
Buckling and vibration analysis of laminated panels using VICONOPT
[PAPER-1746] p 230 A95-72580
Variations observed in the AC generator signal period of a Sea King helicopter
[AD-A264280] p 230 N95-19963
- VIBRATION TESTS**
An Echelle Grating Spectrometer (EGS) for mid-IR remote chemical detection
[DE94-018310] p 249 N95-21478
- VIDEO EQUIPMENT**
Color control in a multichannel simulator display: The display for advanced research and training
[AD-A279717] p 239 N95-20992
Evaluation of the Haworth-Newman avionics Display Readability Scale
[AD-A286127] p 235 N95-22232
- VIDEO SIGNALS**
Passive range measurement system
[AD-D016222] p 258 N95-21100
- VISCOSITY**
Large-scale computational fluid dynamics by the finite element method
[BTN-94-EIX94381359154] p 243 A95-71744
- VISCOUS FLOW**
Thermochemical nonequilibrium viscous shock-layer analysis for a Mars aerocapture vehicle
[BTN-95-EIX95082502732] p 239 A95-70139
Adaptive remeshing for convective heat transfer with variable fluid properties
[BTN-95-EIX95082502720] p 243 A95-71033
Experiments on the flow field physics of confluent boundary layers for high-lift systems
[NASA-CR-197318] p 224 N95-21343
- VISCOUS FLUIDS**
Direct numerical simulations of on-demand vortex generators: Mathematical formulation
p 251 N95-22452
- VISUAL FIELDS**
Factors affecting the perception of luning in monocular regions of partial binocular overlap displays
[AD-A286287] p 259 N95-22044
- VISUAL PERCEPTION**
Factors affecting the perception of luning in monocular regions of partial binocular overlap displays
[AD-A286287] p 259 N95-22044
- VOLCANOES**
Volcanic ash forecast transport and dispersion (VAFTAD) model
[HTN-95-80702] p 254 A95-72546
- VORTEX BREAKDOWN**
Effect of juncture fillets on double-delta wings undergoing sideslip at high angles of attack
[AD-A286165] p 232 N95-22039
- VORTEX GENERATORS**
Experimental investigations of on-demand vortex generators
p 250 N95-22451
Direct numerical simulations of on-demand vortex generators: Mathematical formulation
p 251 N95-22452
- VORTEX SHEDDING**
Vortex shedding noise control in idling circular saws using air ejection at the teeth
[BTN-94-EIX94371347214] p 257 A95-69970
Research on bluff body vortex wakes
[AD-A286319] p 223 N95-20177
- VORTEX SHEETS**
Vorticity concentration at the edge of the inboard vortex sheet
[HTN-95-31010] p 221 A95-71180
- VORTICES**
Time-resolved surface heat flux measurements in the wing/body junction vortex
[BTN-95-EIX95082502716] p 220 A95-71029
Research on bluff body vortex wakes
[AD-A286319] p 223 N95-20177
Application of Direct and Large Eddy Simulation to Transition and Turbulence
[AGARD-CP-551] p 248 N95-21061
- Computational studies of laminar to turbulence transition
[AD-A285622] p 248 N95-21146
Effect of juncture fillets on double-delta wings undergoing sideslip at high angles of attack
[AD-A286165] p 232 N95-22039
Unstructured-grid large-eddy simulation of flow over an airfoil
p 225 N95-22448
Large-eddy simulation of flow through a plane, asymmetric diffuser
p 250 N95-22449
- VORTICITY**
Measurement around a rotor blade excited in pitch. Part 1: Dynamic inflow
[HTN-95-31007] p 220 A95-71177
Measurement around a rotor blade excited in pitch. Part 2: Unsteady surface pressure
[HTN-95-31008] p 220 A95-71178
Aerodynamic and wake methodology evaluation using Model UH-60A experimental data
[HTN-95-31009] p 220 A95-71179
Transverse vorticity measurements in the NASA Ames 80 x 120 wind tunnel boundary layer
p 251 N95-22457
- W**
- WAFERS**
Assuring Known Good Die (KGD) for reliable, cost effective MCMs
p 246 N95-20644
- WAKES**
Experimental study of vane heat transfer and aerodynamics at elevated levels of turbulence
[NASA-CR-4633] p 244 N95-19912
Wake measurements in a strong adverse pressure gradient
[NASA-CR-197272] p 224 N95-21031
Direct numerical simulations of on-demand vortex generators: Mathematical formulation
p 251 N95-22452
- WALL PRESSURE**
Application of wavelet-filtering techniques to intermittent turbulent and wall pressure events. Part 1: Exploratory results
[AD-A286077] p 247 N95-20849
- WARFARE**
Bomber force 2000: Operational concepts for long-range combat aircraft
[AD-A279378] p 230 N95-20181
- WATER**
A review of water mist technology for fire suppression
[AD-A285738] p 225 N95-20071
- WATER CURRENTS**
Orbital velocities induced by surface waves
[HTN-95-90902] p 253 A95-72411
- WATER TUNNEL TESTS**
Effect of juncture fillets on double-delta wings undergoing sideslip at high angles of attack
[AD-A286165] p 232 N95-22039
- WATER VAPOR**
Water vapor continuum absorption in mid-latitudes: Aircraft measurements and model comparisons
[HTN-95-40756] p 252 A95-71186
Aircraft measurements of water vapour continuum absorption at millimetre wavelengths
[HTN-95-90884] p 253 A95-72393
- WATER WAVES**
Orbital velocities induced by surface waves
[HTN-95-90902] p 253 A95-72411
- WAVE INTERACTION**
Computational studies of laminar to turbulence transition
[AD-A285622] p 248 N95-21146
- WAVE REFLECTION**
Comments on effect of wet snow on the null-reference ILS system
[BTN-95-EIX9514255488] p 227 A95-72885
- WAVEGUIDES**
Modeling resonance in waveguide-to-microstrip junctions by unilateral fin line resonators
[BTN-94-EIX94381323445] p 242 A95-70844
Electro-optic characterization of ultrafast photodetectors using adiabatically compressed soliton pulses
[BTN-94-EIX94381359637] p 257 A95-72675
- WAVELET ANALYSIS**
Wavelet transformations for helicopter identification via acoustic signatures
[AD-A279980] p 257 N95-20963
- WEAPON SYSTEMS**
Design of a controller for a flexible pointing system using H(infinity) synthesis
[AD-A286572] p 256 N95-20828
- WEAR TESTS**
Lubricant evaluation and performance, 2
[AD-A279144] p 242 N95-21969
- WEATHER**
Radar studies of aviation hazards
[AD-A285845] p 226 N95-21831
- WEATHER FORECASTING**
Snow-band formation and evolution during the 15 November 1987 aircraft accident at Denver airport
[HTN-95-80699] p 254 A95-72543
Tropical cyclone observation and forecasting with and without aircraft reconnaissance
[HTN-95-80701] p 254 A95-72545
Volcanic ash forecast transport and dispersion (VAFTAD) model
[HTN-95-80702] p 254 A95-72546
- WIND DIRECTION**
Ascent wind model for launch vehicle design
[BTN-95-EIX95041503799] p 239 A95-70124
- WIND PROFILES**
Ascent wind model for launch vehicle design
[BTN-95-EIX95041503799] p 239 A95-70124
Comparison of meteorological data with fitted values extracted from projectile trajectory
[AD-A285921] p 255 N95-19989
- WIND TUNNEL APPARATUS**
The dynamic approach to rotor blade research: ARA's oscillatory test facility
[ARA-MEMO-405] p 223 N95-20758
Testing in the ARA Transonic Wind Tunnel
[ARA-MEMO-395] p 239 N95-20799
- WIND TUNNEL CALIBRATION**
The dynamic approach to rotor blade research: ARA's oscillatory test facility
[ARA-MEMO-405] p 223 N95-20758
- WIND TUNNEL MODELS**
The dynamic approach to rotor blade research: ARA's oscillatory test facility
[ARA-MEMO-405] p 223 N95-20758
Testing in the ARA Transonic Wind Tunnel
[ARA-MEMO-395] p 239 N95-20799
- WIND TUNNEL TESTS**
Aerodynamic mechanism of galloping
[BTN-94-EIX94371347709] p 219 A95-69968
Static investigation of two fluidic thrust-vectoring concepts on a two-dimensional convergent-divergent nozzle
[NASA-TM-4574] p 222 N95-19913
Investigation of a thermal buoyancy effect on the drag of half models tested in the ARA Transonic Wind Tunnel
[ARA-MEMO-407] p 222 N95-19946
Flow coefficient behavior for boundary layer bleed holes and slots
[NASA-TM-106846] p 244 N95-19953
16-foot transonic tunnel test section flowfield survey
[NASA-TM-109157] p 238 N95-20669
The dynamic approach to rotor blade research: ARA's oscillatory test facility
[ARA-MEMO-405] p 223 N95-20758
Application of pressure sensitive paint in hypersonic flows
[NASA-TM-106824] p 223 N95-20794
Testing in the ARA Transonic Wind Tunnel
[ARA-MEMO-395] p 239 N95-20799
Wake measurements in a strong adverse pressure gradient
[NASA-CR-197272] p 224 N95-21031
Pressure measurements on an F/A-18 twin vertical tail in buffeting flow. Volume 4, part 1: Buffet cross spectral densities
[AD-A285593] p 237 N95-21214
Experiments on the flow field physics of confluent boundary layers for high-lift systems
[NASA-CR-197318] p 224 N95-21343
Pressure measurements on an F/A-18 twin vertical tail in buffeting flow. Volume 1: Wind tunnel test summary
[AD-A279126] p 225 N95-21877
Effects of yaw and pitch motion on model attitude measurements
[NASA-TM-4641] p 250 N95-22109
Large-eddy simulation of flow through a plane, asymmetric diffuser
p 250 N95-22449
Experimental investigations of on-demand vortex generators
p 250 N95-22451
Transverse vorticity measurements in the NASA Ames 80 x 120 wind tunnel boundary layer
p 251 N95-22457
- WIND TUNNEL WALLS**
Investigation of a thermal buoyancy effect on the drag of half models tested in the ARA Transonic Wind Tunnel
[ARA-MEMO-407] p 222 N95-19946
- WIND TUNNELS**
Measurement and analysis of nitric oxide radiation in an arcjet flow
[BTN-95-EIX95082502727] p 243 A95-71040
Application of wavelet-filtering techniques to intermittent turbulent and wall pressure events. Part 1: Exploratory results
[AD-A286077] p 247 N95-20849

WIND TURBINES

A three-dimensional orthogonal laser velocimeter for the
NASA Ames 7- by 10-foot wind tunnel
[NASA-TM-108864] p 249 N95-21323

WIND TURBINES

Advanced wind turbine design studies: Advanced
conceptual study
[DE93-000031] p 256 N95-20985

WIND VELOCITY

Ascent wind model for launch vehicle design
[BTN-95-EIX95041503789] p 239 A95-70124

WINDPOWER UTILIZATION

Advanced wind turbine design studies: Advanced
conceptual study
[DE93-000031] p 256 N95-20985

WING LOADING

Derived gust spectra for the Macchi MB326H
[ARL-TN-3] p 225 N95-21892

WINGS

Ice accretion on aircraft wings
[BTN-95-EIX95082502224] p 225 A95-71021

Time-resolved surface heat flux measurements in the
wing/body junction vortex
[BTN-95-EIX95082502716] p 220 A95-71029

Electro-optic characterization of ultrafast photodetectors
using adiabatically compressed soliton pulses
[BTN-94-EIX94381359637] p 257 A95-72675

WIRE

Reliability assessment of Multichip Module technologies
via the Triservice/NASA RELTECH program
p 245 N95-20643

WORKING FLUIDS

Malone-brayton cycle engine/heat pump
[AD-D016573] p 244 N95-20295

WORKSTATIONS

An evaluation of Automatic Terminal Information Service
(ATIS) flight deck display presentation options
[AD-A280100] p 228 N95-21020

X**X RAYS**

Test and Evaluation Plan (TEP) for Improvised Explosive
Device Screening Systems (IEDSS)
[AD-A286382] p 227 N95-22319

Y**YAW**

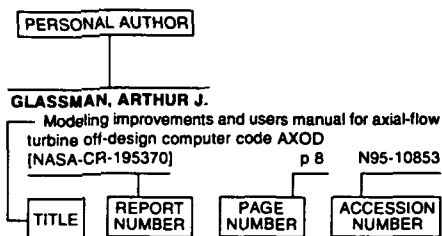
Effects of yaw and pitch motion on model attitude
measurements
[NASA-TM-4641] p 250 N95-22109

PERSONAL AUTHOR INDEX

AERONAUTICAL ENGINEERING / A Continuing Bibliography (Supplement 318)

June 1995

Typical Personal Author Index Listing



Listings in this index are arranged alphabetically by personal author. The title of the document is used to provide a brief description of the subject matter. The report number helps to indicate the type of document (e.g., NASA report, translation, NASA contractor report). The page and accession numbers are located beneath and to the right of the title. Under any one author's name the accession numbers are arranged in sequence.

A

- ABDOL-HAMID, KHALED S.**
Application of Navier-Stokes code PAB3D with kappa-epsilon turbulence model to attached and separated flows
[NASA-TP-3480] p 224 N95-21338
- ABE, TAKASHI**
Thermochemical nonequilibrium viscous shock-layer analysis for a Mars aerocapture vehicle
[BTN-95-EIX95082502732] p 239 A95-70139
- ABEYOUNIS, W. K.**
16-foot transonic tunnel test section flowfield survey
[NASA-TM-109157] p 238 N95-20669
- ABRAHAM, JACOB**
The Advanced Avionics Subsystem Technology Demonstration Program p 234 N95-20636
- ADELFGANG, S. I.**
Ascent wind model for launch vehicle design
[BTN-95-EIX95041503799] p 239 A95-70124
- AHUJA, K. K.**
Temperature effects on acoustic interactions between altitude test facilities and jet engine plumes
[NASA-CR-197638] p 258 N95-21170
- ALGER, T.**
An Echelle Grating Spectrometer (EGS) for mid-IR remote chemical detection
[DE94-019310] p 249 N95-21478
- ALLEN, N. T.**
Aircraft-borne, laser-induced fluorescence instrument for the in situ detection of hydroxyl and hydroperoxyl radicals
[BTN-95-EIX95072499029] p 253 A95-71908
- AMBERKAR, S. S.**
Design of a controller for a flexible pointing system using H(infinity) synthesis
[AD-A286572] p 256 N95-20828
- AMES, FORREST E.**
Experimental study of vane heat transfer and aerodynamics at elevated levels of turbulence
[NASA-CR-4633] p 244 N95-19912
- AMES, GREGORY H.**
Fiber-optic rotary joint with bundle collimator assemblies
[AD-D016504] p 258 N95-21673

- ANDERS, SCOTT G.**
The personal aircraft: Status and issues
[NASA-TM-109174] p 223 N95-20688
- ANDERSON, A.**
Description and flow characterization of hypersonic facilities
[AD-A284291] p 223 N95-20248
- ANDERSON, J. G.**
Aircraft-borne, laser-induced fluorescence instrument for the in situ detection of hydroxyl and hydroperoxyl radicals
[BTN-95-EIX95072499029] p 253 A95-71908
- ANDERSON, MELVIN S.**
Buckling and vibration analysis of laminated panels using VICONOPT
[PAPER-1746] p 230 A95-72580
- ANDERSON, R. C.**
Two-dimensional imaging of OH in a lean burning high pressure combustor
[NASA-TM-106854] p 236 N95-21383
- ANDERSSON, BRODD LEIF**
Computation of transonic flow on composite overlapping grids in 2 D
[PB95-131348] p 248 N95-21132
- ANDREWS, C.**
Corrosion of aircraft materials: Correlation between nanometer scale and macroscopic structural damage parameters
[AD-A285930] p 241 N95-20299
- ARNOLD, JACK H.**
Photovoltaic electric power applied to Unmanned Aerial Vehicles (UAV) p 245 N95-20530
- ASBURY, SCOTT C.**
The personal aircraft: Status and issues
[NASA-TM-109174] p 223 N95-20688
- AUDONE, B.**
Electromagnetic compatibility effects of advanced packaging configurations p 247 N95-20658

B

- BABIKIAN, DIKRAN S.**
Measurement and analysis of nitric oxide radiation in an arcjet flow
[BTN-95-EIX95082502727] p 243 A95-71040
- BACK, G. G.**
A review of water mist technology for fire suppression
[AD-A285738] p 225 N95-20071
- BACMEISTER, JULIO T.**
An algorithm for forecasting mountain wave-related turbulence in the stratosphere
[HTN-95-80656] p 254 A95-72500
- BALANIS, CONSTANTINE A.**
RCS measurements, transformations, and comparisons under cylindrical and plane wave illumination
[BTN-94-EIX94371347126] p 242 A95-69976
- BALLMANN, JOSEF**
Prediction of rotor-blade deformations due to unsteady airloads
[AD-A286593] p 231 N95-20860
- BANFORD, MICHAEL**
Pressure measurements on an F/A-18 twin vertical tail in buffeting flow. Volume 4, part 1: Buffet cross spectral densities
[AD-A285593] p 237 N95-21214
- BANFORD, MICHAEL**
Pressure measurements on an F/A-18 twin vertical tail in buffeting flow. Volume 1: Wind tunnel test summary
[AD-A279126] p 225 N95-21877
- BARBAGOLETA, S.**
FASTPACK: Optimized solutions for modular avionics derived from a parametric study. Part 1: Platform features p 233 N95-20634
- BARKER, WALTER R.**
Super-heavy aircraft study
[AD-A278602] p 238 N95-19955
- BARTHOLOMEUSZ, R. A.**
Bonded composite repair of cracked load-bearing holes
[BTN-94-EIX94401360553] p 243 A95-71867
- BATTS, G. W.**
Ascent wind model for launch vehicle design
[BTN-95-EIX95041503799] p 239 A95-70124
- BAUCHAU, O. A.**
On the choice of appropriate bases for nonlinear dynamic modal analysis
[HTN-95-A0495] p 221 A95-72566
- BAUMGARDNER, D.**
Performance of a focused cavity aerosol spectrometer for measurements in the stratosphere of particle size in the 0.06-2.0-micrometer-diameter range
[HTN-95-90914] p 253 A95-72423
- BEACH, R.**
Overview of remote sensing laser development and semiconductor laser technology
[DE94-019103] p 256 N95-21552
- BEASLEY, HOWARD H.**
Factors affecting the perception of luning in monocular regions of partial binocular overlap displays
[AD-A286287] p 259 N95-22044
- BEENE, JEFFREY K.**
Bomber force 2000: Operational concepts for long-range combat aircraft
[AD-A279378] p 230 N95-20181
- BEISSNER, ROBERT E.**
Eddy current for detecting second-layer cracks under installed fasteners
[AD-A279871] p 244 N95-20414
- BELLINGER, N. C.**
Modelling of pilowing due to corrosion in fuselage lap joints
[BTN-95-EIX95082502227] p 240 A95-71024
- BENZARIA, E.**
Secondary source locations in active noise control: Selection or optimization?
[BTN-94-EIX94381352222] p 257 A95-71738
- BEREZIN, CHARLES R.**
Aerodynamic and wake methodology evaluation using Model UH-60A experimental data
[HTN-95-31009] p 220 A95-71179
- BERKOWITZ, J. P.**
Test and evaluation report for the Manual Domestic Passive Profiling System (MDPPS)
[AD-A286312] p 225 N95-20093
- BERKOWITZ, JACK**
Test and Evaluation Plan (TEP) for Improved Explosive Device Screening Systems (IEDSS)
[AD-A286382] p 227 N95-22319
- BERNSTEIN, DENNIS S.**
Robust fixed-structure control
[AD-A286515] p 257 N95-22216
- BESMANN, T. M.**
Scale-up and modeling of forced chemical vapor infiltration
[DE94-017769] p 247 N95-20781
- BEYLER, C. L.**
A review of water mist technology for fire suppression
[AD-A285738] p 225 N95-20071
- BHOL, D. G.**
Transverse vorticity measurements in the NASA Ames 80 x 120 wind tunnel boundary layer p 251 N95-22457
- BILLMANN, BARRY**
Minima reduction simulation test results
[AD-A285626] p 228 N95-21148
- BIRTCHEK, CRAIG R.**
RCS measurements, transformations, and comparisons under cylindrical and plane wave illumination
[BTN-94-EIX94371347126] p 242 A95-69976
- BISCHOF, C. H.**
Parallel calculation of sensitivity derivatives for aircraft design using automatic differentiation
[NASA-TM-110103] p 231 N95-20370
- BLANCHETIERE-CIARLETTI, V.**
Experimental study of the helicopter-mobile radioelectrical channel and possible extension to the satellite-mobile channel p 247 N95-20945
- BLEICHER, P.**
FASTPACK: Optimized solutions for modular avionics derived from a parametric study. Part 2: Avionics p 233 N95-20635

AUTHOR

BLUNT, D. M.

- BLUNT, D. M.**
Variations observed in the AC generator signal period of a Sea King helicopter
[AD-A284280] p 230 N95-18963
- BOGENBERGER, R.**
Optical backplane for modular avionics
p 257 N95-20652
- BOGGS, S. L.**
Independent review of Aviation Technology and Research Information Analysis System (ATRIAS) database
[AD-A284049] p 226 N95-21518
- BOLLA, L.**
Electromagnetic compatibility effects of advanced packaging configurations
p 247 N95-20658
- BOLTON, J. S.**
Sound propagation from an arbitrarily oriented multipole placed near a plane, finite impedance surface
[BTN-94-EIX94371338964] p 257 A95-70797
- BOLUKBASI, AKIF O.**
Prediction of energy absorption capability of composite stiffeners
[HTN-95-A0500] p 230 A95-72571
- BONNEFOND, P.**
Precise orbit determination with a short-arc technique
p 240 A95-70543
- BORCHERS, MARY F.**
Lubricant evaluation and performance, 2
[AD-A279144] p 242 N95-21969
- BORRMANN, S.**
Performance of a focused cavity aerosol spectrometer for measurements in the stratosphere of particle size in the 0.06-2.0-micrometer-diameter range
[HTN-95-90914] p 253 A95-72423
- BOTROS, SHERIF M.**
A neural expert approach to self designing flight control systems
[AD-A279965] p 237 N95-21122
- BOWERS, JAMES S.**
Electrochemical impedance pattern recognition for detection of hidden chemical corrosion on aircraft components
[AD-A284998] p 241 N95-20481
Electrochemical impedance pattern recognition for detection of hidden chemical corrosion on aircraft components
[AD-A285998] p 241 N95-20716
- BOYD, JANICE D.**
Evaluation of the Spartan tight-tolerance AXBT
[HTN-95-40728] p 251 A95-70473
- BRAHIMI, M. T.**
Ice accretion on aircraft wings
[BTN-95-EIX95082502224] p 225 A95-71021
- BRAMKAMP, F. D.**
Transverse vorticity measurements in the NASA Ames 80 x 120 wind tunnel boundary layer
p 251 N95-22457
- BRANSTETTER, REAGAN**
Ultra-Reliable Digital Avionics (URDA) processor
p 245 N95-20638
- BRENTNER, KENNETH S.**
The personal aircraft: Status and issues
[NASA-TM-109174] p 223 N95-20688
- BROCK, C. A.**
Performance of a focused cavity aerosol spectrometer for measurements in the stratosphere of particle size in the 0.06-2.0-micrometer-diameter range
[HTN-95-90914] p 253 A95-72423
- BROWN, DANSEN**
Pressure measurements on an F/A-18 twin vertical tail in buffeting flow. Volume 4, part 1: Buffet cross spectral densities
[AD-A285593] p 237 N95-21214
Pressure measurements on an F/A-18 twin vertical tail in buffeting flow. Volume 1: Wind tunnel test summary
[AD-A279126] p 225 N95-21877
- BRUN, M. K.**
Toughened Silcomp composites for gas turbine engine applications
[DE95-002851] p 235 N95-21243
- BRYANT, BOBBY**
A computer-based multimedia prototype for night vision goggles
[AD-A286208] p 258 N95-21882
- BUCKHARDT, GARY L.**
Eddy current for detecting second-layer cracks under installed fasteners
[AD-A279871] p 244 N95-20414
- BUDNICK, E. K.**
A review of water mist technology for fire suppression
[AD-A285738] p 225 N95-20071
- BURGETT, S.**
SAR image registration in absolute coordinates using GPS carrier phase position and velocity information
[DE94-018738] p 228 N95-20195

BURNS, IAN F.

- Investigation of a thermal buoyancy effect on the drag of half models tested in the ARA Transonic Wind Tunnel
[ARA-MEMO-407] p 222 N95-19946
- BUSHNELL, DENNIS M.**
The personal aircraft: Status and issues
[NASA-TM-109174] p 223 N95-20688

C

- CAGLAYAN, ALPER K.**
A neural expert approach to self designing flight control systems
[AD-A279965] p 237 N95-21122
- CALLAHAN, CYNTHIA B.**
Design optimization of rotor blades for improved performance and vibration
[HTN-95-A0498] p 229 A95-72569
- CALZONE, R. F.**
Integral rocket ramjets
[AD-A285135] p 240 N95-20906
- CAMELL, D. G.**
Measurements of shielding effectiveness and cavity characteristics of airplanes
[PB94-210051] p 244 N95-20191
- CANNON, M. E.**
Attitude determination using dedicated and nondedicated multiantenna GPS sensors
[BTN-95-EIX95142555482] p 228 A95-72891
Assessment of a non-dedicated GPS receiver system for precise airborne attitude determination
[DE94-019309] p 229 N95-21520
- CAPLOT, M.**
FASTPACK: Optimized solutions for modular avionics derived from a parametric study. Part 2: Avionics
p 233 N95-20635
Composite cases for airborne electronic equipment: A technology study and EMC
p 241 N95-20655
Modular supplies for a distributed architecture
p 234 N95-20657
- CAPOGNA, C.**
FASTPACK: Optimized solutions for modular avionics derived from a parametric study. Part 2: Avionics
p 233 N95-20635
- CARBONARO, MARIO**
Application of pressure sensitive paint in hypersonic flows
[NASA-TM-106824] p 223 N95-20794
- CARBONELL, J. M.**
Liquid flow-through cooling of electronic modules
p 246 N95-20647
- CARLSON, JOHN R.**
Application of Navier-Stokes code PAB3D with kappa-epsilon turbulence model to attached and separated flows
[NASA-TP-3480] p 224 N95-21338
- CARLSON, N. W.**
Overview of remote sensing laser development and semiconductor laser technology
[DE94-019103] p 256 N95-21552
- CASARELLA, MARIO J.**
Application of wavelet-filtering techniques to intermittent turbulent and wall pressure events. Part 1: Exploratory results
[AD-A286077] p 247 N95-20849
- CELLI, ROBERTO**
High-order state space simulation models of helicopter flight mechanics
[HTN-95-A0494] p 237 A95-72565
- CHAN, K. ROLAND**
An algorithm for forecasting mountain wave-related turbulence in the stratosphere
[HTN-95-80656] p 254 A95-72500
- CHANDLER, N.**
MCMs for avionics: Technology selection and intermodule interconnection
p 234 N95-20641
- CHANG, BOR-CHIN**
Design of robust optimal control systems and stability analysis of real structured uncertainties
[AD-A279089] p 256 N95-21913
- CHANG, WEN-HUAN**
Effect of juncture fillets on double-delta wings undergoing sideslip at high angles of attack
[AD-A286185] p 232 N95-22039
- CHAO, KENNETH K.**
Lubricant evaluation and performance, 2
[AD-A279144] p 242 N95-21969
- CHEN, CHARLES C.**
Commuter/air taxi ditchings and water-related impacts that occurred from 1979 to 1989
[AD-A285691] p 226 N95-20275
- CHIAPPETTI, CHARLES F.**
Evaluation of the Haworth-Newman avionics Display Readability Scale
[AD-A286127] p 235 N95-22232

CHOCOL, C. J.

- CALOPE and TAISIR airborne experiment platform
[DE94-018328] p 250 N95-22299
- CHOPRA, INDERJIT**
Air and ground resonance of helicopters with elastically tailored composite rotor blades
[HTN-95-A0497] p 222 A95-72568
- CHOUDHARI, MEELAN**
Acoustic receptivity due to weak surface inhomogeneities in adverse pressure gradient boundary layers
[NASA-TM-4577] p 249 N95-21258
- CHU, H. C.**
Experiments on the flow field physics of confluent boundary layers for high-lift systems
[NASA-CR-197318] p 224 N95-21343
- CLARK, JAMES R.**
Potential applications of the SSM/I cloud liquid water parameter to the estimation of marine aircraft icing
[HTN-95-80651] p 254 A95-72495
- CLOUD, HARLEY A.**
The opportunities for and challenges of common integrated electronics
[AD-A279991] p 248 N95-20966
- COHEN, R. C.**
Aircraft-borne, laser-induced fluorescence instrument for the in situ detection of hydroxyl and hydroperoxyl radicals
[BTN-95-EIX95072499029] p 253 A95-71908
- COMASKEY, B.**
Overview of remote sensing laser development and semiconductor laser technology
[DE94-019103] p 256 N95-21552
- COONROD, KURT H.**
Fault detection techniques for complex cable shield topologies
[AD-A286632] p 247 N95-20771
TIM-SCT cable testing protocol
[AD-A286633] p 231 N95-20772
- COOPER, DONALD L.**
A three-dimensional orthogonal laser velocimeter for the NASA Ames 7- by 10-foot wind tunnel
[NASA-TM-108864] p 249 N95-21323
- COOPER, GENE R.**
Comparison of meteorological data with fitted values extracted from projectile trajectory
[AD-A285921] p 255 N95-19989
- CORMAN, G. S.**
Toughened Silcomp composites for gas turbine engine applications
[DE95-002851] p 235 N95-21243
- CRAWFORD, M. L.**
Measurements of shielding effectiveness and cavity characteristics of airplanes
[PB94-210051] p 244 N95-20191
- CRAWFORD, R. A.**
Description and flow characterization of hypersonic facilities
[AD-A284291] p 223 N95-20248
- CREEK, EDITH A.**
Eddy current for detecting second-layer cracks under installed fasteners
[AD-A279871] p 244 N95-20414
- CRESPO, ANTONIO**
Optical processing and control
[AD-A279157] p 259 N95-21975
- CROOK, ANDREW**
Snow-band formation and evolution during the 15 November 1987 aircraft accident at Denver airport
[HTN-95-80699] p 254 A95-72543
- CROSTON, I. R.**
MCMs for avionics: Technology selection and intermodule interconnection
p 234 N95-20641
- CUMMINGS, MARY L.**
A computer code (SKINTEMP) for predicting transient missile and aircraft heat transfer characteristics
[AD-A286044] p 248 N95-21001
- CURRAN, LAWRENCE J., JR.**
Investigation of flight data recorder fire test requirements
[AD-A285832] p 232 N95-20032

D

- DASKIEWICH, DANIEL E.**
Assuring Known Good Die (KGD) for reliable, cost effective MCMs
p 246 N95-20644
- DAVIS, D. O.**
Flow coefficient behavior for boundary layer bleed holes and slots
[NASA-TM-106846] p 244 N95-19953
- DAVIS, STUART L.**
Fault detection techniques for complex cable shield topologies
[AD-A286632] p 247 N95-20771

- DAY, GLENROY E., JR.**
A computer-based multimedia prototype for night vision goggles
[AD-A286208] p 258 N95-21882
- DELVINQUIER, J. P.**
Modular supplies for a distributed architecture
p 234 N95-20657
- DEMUSZ, J. N.**
Aircraft-borne, laser-induced fluorescence instrument for the in situ detection of hydroxyl and hydroperoxyl radicals
[BTN-95-EIX95072499029] p 253 A95-71908
- DHAUSSY, J. C.**
FASTPACK: Optimized solutions for modular avionics derived from a parametric study. Part 2: Avionics
p 233 N95-20635
- DILLER, T. E.**
Time-resolved surface heat flux measurements in the wing/body junction vortex
[BTN-95-EIX95082502716] p 220 A95-71029
- DINENNO, P. J.**
A review of water mist technology for fire suppression
[AD-A285738] p 225 N95-20071
- DOLAN, N. J.**
Test and evaluation report for the Manual Domestic Passive Profiling System (MDPPS)
[AD-A286312] p 225 N95-20093
- DONALDSON, RALPH S., JR.**
Radar studies of aviation hazards
[AD-A285845] p 226 N95-21831
- DUISENBERG, KEN**
Simulation of rotor blade element turbulence
[NASA-TM-108862] p 232 N95-21186
- DUMONT, B.**
Composite cases for airborne electronic equipment: A technology study and EMC
p 241 N95-20655
- DUNAGAN, STEPHEN E.**
A three-dimensional orthogonal laser velocimeter for the NASA Ames 7- by 10-foot wind tunnel
[NASA-TM-108864] p 249 N95-21323
- DUNN, W. N.**
A user's guide to LUGSAN 1.1: A computer program to calculate and archive lug and sway brace loads for aircraft-carried stores
[DE95-001919] p 232 N95-21730
- DWYER, JOHN P.**
Crew aiding and automation: A system concept for terminal area operations, and guidelines for automation design
[NASA-CR-4631] p 228 N95-19950
- DYE, J. E.**
Performance of a focused cavity aerosol spectrometer for measurements in the stratosphere of particle size in the 0.06-2.0-micrometer-diameter range
[HTN-95-90914] p 253 A95-72423
- E**
- EKSTROM, M.**
Bonded composite repair of cracked load-bearing holes
[BTN-94-EIX94401360553] p 243 A95-71867
- EMANUEL, M.**
Overview of remote sensing laser development and semiconductor laser technology
[DE94-019103] p 256 N95-21552
- ENGLISH, S. J.**
Aircraft measurements of water vapour continuum absorption at millimetre wavelengths
[HTN-95-90884] p 253 A95-72393
- ERM, LINCOLN P.**
A preliminary study of the airwake model used in an existing SH-60B/FFG-7 helicopter/ship simulation program
[DSTO-TR-0015] p 224 N95-21659
- EVERBERG, CARL**
Minima reduction simulation test results
[AD-A285626] p 228 N95-21148
- EVTUSHENKO, I. A.**
MHD-flow in slotted channels with conducting walls
[DE94-018370] p 258 N95-21388
- EXERTIER, P.**
Precise orbit determination with a short-arc technique
p 240 A95-70543
- F**
- FALLAVOLLITA, MICHAEL A.**
Flow resolution and domain influence in rarefied hypersonic blunt-body flows
[BTN-95-EIX95082502729] p 220 A95-70136
- FANSLER, KEVIN S.**
Comparison of meteorological data with fitted values extracted from projectile trajectory
[AD-A285921] p 255 N95-19989
- FAYETTE, DANIEL F.**
Reliability assessment of Multichip Module technologies via the Triservice/NASA RELTECH program
p 245 N95-20643
- FERRY, G. V.**
Performance of a focused cavity aerosol spectrometer for measurements in the stratosphere of particle size in the 0.06-2.0-micrometer-diameter range
[HTN-95-90914] p 253 A95-72423
- FERTIG, TIMOTHY**
High density monolithic packaging technology for digital/microwave avionics
p 240 N95-20646
- FERTIS, DEMETER G.**
New airfoil-design concept with improved aerodynamic characteristics
[PAPER-4384] p 230 A95-72585
- FINCH, STEVE**
Systems engineering design and technical analyses for Strategic Avionics Crew-station Design Evaluation Facility (SACDEF)
[AD-A286239] p 235 N95-22024
- FINLEY, TOM D.**
Effects of yaw and pitch motion on model attitude measurements
[NASA-TM-4641] p 250 N95-22109
- FISCHER, D. S.**
Test and evaluation report for the Manual Domestic Passive Profiling System (MDPPS)
[AD-A286312] p 225 N95-20093
- FISCHER, DOUGLAS S.**
Test and Evaluation Plan (TEP) for Improvised Explosive Device Screening Systems (IEDSS)
[AD-A286382] p 227 N95-22319
- FISHER, JAY L.**
Eddy current for detecting second-layer cracks under installed fasteners
[AD-A279871] p 244 N95-20414
- FOBES, J. L.**
Test and evaluation report for the Manual Domestic Passive Profiling System (MDPPS)
[AD-A286312] p 225 N95-20093
- FOBES, JAMES L.**
Test and Evaluation Plan (TEP) for Improvised Explosive Device Screening Systems (IEDSS)
[AD-A286382] p 227 N95-22319
- FORTIN, M.**
Large-scale computational fluid dynamics by the finite element method
[BTN-94-EIX94381359154] p 243 A95-71744
- FOSS, JOHN F.**
Transverse vorticity measurements in the NASA Ames 80 x 120 wind tunnel boundary layer
p 251 N95-22457
- FREDELL, ROBERT S.**
Damage tolerant repair techniques for pressurized aircraft fuselages
[AD-A286298] p 219 N95-22046
- G**
- GALLIANO, JOE**
High-resolution imaging of rain systems with the advanced microwave precipitation radiometer
[HTN-95-70133] p 252 A95-70655
- GAO, C.**
A generalized algorithm for inverse simulation applied to helicopter maneuvering flight
[HTN-95-A0493] p 236 A95-72564
- GAONKAR, GOPAL H.**
Flap-lag damping in hover and forward flight with a three-dimensional wake
[HTN-95-A0496] p 221 A95-72567
- GARY, BRUCE L.**
An algorithm for forecasting mountain wave-related turbulence in the stratosphere
[HTN-95-80656] p 254 A95-72500
- GAVER, ERIC**
High density monolithic packaging technology for digital/microwave avionics
p 240 N95-20646
- GEIS, JACK**
Photovoltaic electric power applied to Unmanned Aerial Vehicles (UAV)
p 245 N95-20530
- GEORGANTOPOULOS, G. A.**
Investigation of shear layer transition using various turbulence models
p 248 N95-21096
- GHALY, K. S.**
Large-scale computational fluid dynamics by the finite element method
[BTN-94-EIX94381359154] p 243 A95-71744
- GHARIB, MORTEZA**
Research on bluff body vortex wakes
[AD-A286319] p 223 N95-20177
- GIFFORD, LISA A.**
Environmental Compliance Assessment and Management Program
[AD-A279605] p 255 N95-20441
- GILMOUR, THOMAS A.**
Malone-brayton cycle engine/heat pump
[AD-D016573] p 244 N95-20295
- GLASS, CHRISTOPHER E.**
The personal aircraft: Status and issues
[NASA-TM-109174] p 223 N95-20688
- GLASSMAN, ARTHUR J.**
Turbine design and application
[NASA-SP-290] p 236 N95-22341
- GLIEBE, P. R.**
Active control of fan noise-feasibility study. Volume 1: Flyover system noise studies
[NASA-CR-195392-VOL-1] p 258 N95-21888
- GLYNN, G.**
High performance backplane components for modular avionics
p 247 N95-20653
- GONZALES-MARTIN, A.**
Corrosion of aircraft materials: Correlation between nanometer scale and macroscopic structural damage parameters
[AD-A285930] p 241 N95-20299
- GONZALEZ, CARLOS R.**
Super-heavy aircraft study
[AD-A279602] p 238 N95-19955
- GOODFELLOW, R. C.**
High performance backplane components for modular avionics
p 247 N95-20653
- GOODWIN, M. J.**
High performance backplane components for modular avionics
p 247 N95-20653
- GOPAUL, NIGEL K. J. M.**
Measurement and analysis of nitric oxide radiation in an arcjet flow
[BTN-95-EIX95082502727] p 243 A95-71040
- GRAY, WILLIAM M.**
Tropical cyclone observation and forecasting with and without aircraft reconnaissance
[HTN-95-80701] p 254 A95-72545
- GREEN, HARRY E.**
Electromagnetic backscattering from a helicopter rotor in the decametric wave band regime
[BTN-94-EIX94381353130] p 243 A95-72648
- GREEN, JOHN E.**
Investigation of a thermal buoyancy effect on the drag of half models tested in the ARA Transonic Wind Tunnel
[ARA-MEMO-407] p 222 N95-19946
- GREEN, L. L.**
Parallel calculation of sensitivity derivatives for aircraft design using automatic differentiation
[NASA-TM-110103] p 231 N95-20370
- GREENHALGH, SAMUEL**
Lift enhancement device
[AD-D016522] p 224 N95-21864
- GRIFFIN, VANESSA L.**
High-resolution imaging of rain systems with the advanced microwave precipitation radiometer
[HTN-95-70133] p 252 A95-70655
- GROTE, JAMES**
Optical processing and control
[AD-A279157] p 259 N95-21975
- GROVES-KIRKBY, C. J.**
High performance backplane components for modular avionics
p 247 N95-20653
- GUERNSEY, D.**
On the choice of appropriate bases for nonlinear dynamic modal analysis
[HTN-95-A0495] p 221 A95-72566
- GUILLOU, C.**
Aircraft measurements of water vapour continuum absorption at millimetre wavelengths
[HTN-95-90884] p 253 A95-72393
- H**
- HAAS, BRIAN L.**
Flow resolution and domain influence in rarefied hypersonic blunt-body flows
[BTN-95-EIX95082502729] p 220 A95-70136
- HABASHI, W. G.**
Large-scale computational fluid dynamics by the finite element method
[BTN-94-EIX94381359154] p 243 A95-71744
- HAIGLER, K. J.**
Parallel calculation of sensitivity derivatives for aircraft design using automatic differentiation
[NASA-TM-110103] p 231 N95-20370

- HALL, J. P.**
High performance backplane components for modular avionics p 247 N95-20653
- MAMILL, T. G.**
MCMs for avionics: Technology selection and intermodule interconnection p 234 N95-20641
- HANAGUD, S.**
Smart structures in the control of airframe vibrations [HTN-95-31014] p 236 A95-71184
- HANISCO, T. F.**
Aircraft-borne, laser-induced fluorescence instrument for the in situ detection of hydroxyl and hydroperoxyl radicals [BTN-95-EIX95072499029] p 253 A95-71908
- HANKEY, J.**
High performance backplane components for modular avionics p 247 N95-20653
- HARMAN, WILLIAM H.**
GPS-Squitter capacity analysis [AD-A260037] p 245 N95-20599
- HARRIMAN, WALTER L.**
Passive range measurement system [AD-D016222] p 258 N95-21100
- HARRIS, F. I.**
Radar studies of aviation hazards [AD-A285845] p 226 N95-21831
- HASSAN, AHMED A.**
Effects of leading and trailing edge flaps on the aerodynamics of airfoil/vortex interactions [HTN-95-31011] p 221 A95-71181
- HAWKINS, ANTHONY**
Standard Hardware Acquisition and Reliability Program (SHARP) advanced SEM-E packaging p 233 N95-20633
- HAYES, HALFORD I.**
Wavelet transformations for helicopter identification via acoustic signatures [AD-A279980] p 257 N95-20963
- HAZEN, N. L.**
Aircraft-borne, laser-induced fluorescence instrument for the in situ detection of hydroxyl and hydroperoxyl radicals [BTN-95-EIX95072499029] p 253 A95-71908
- HEATON, HARRY**
Systems engineering design and technical analyses for Strategic Avionics Crew-station Design Evaluation Facility (SACDEF) [AD-A286239] p 235 N95-22024
- HEFFTER, JEROME L.**
Volcanic ash forecast transport and dispersion (VAFTAD) model [HTN-95-80702] p 254 A95-72546
- HEISEY, C. W.**
Subsidence of aircraft engine exhaust in the stratosphere: Implications for calculated ozone depletions [PAPER-93GL03426] p 251 A95-70297
- HELLIE, P.**
FASTPACK: Optimized solutions for modular avionics derived from a parametric study. Part 1: Platform features p 233 N95-20634
- HENDRICKSON, J. T.**
TIM-SCT cable testing protocol [AD-A286633] p 231 N95-20772
- HEROLD, K. E.**
Liquid flow-through cooling of electronic modules p 246 N95-20647
- HERREWYN, J.**
FASTPACK: Optimized solutions for modular avionics derived from a parametric study. Part 2: Avionics p 233 N95-20635
- HESS, R. A.**
Rotorcraft control system design for uncertain vehicle dynamics using quantitative feedback theory [HTN-95-31012] p 236 A95-71182
A generalized algorithm for inverse simulation applied to helicopter maneuvering flight [HTN-95-A0493] p 236 A95-72564
- HETU, JEAN-FRANCOIS**
Adaptive remeshing for convective heat transfer with variable fluid properties [BTN-95-EIX95082502720] p 243 A95-71033
- HICKS, Y. R.**
Two-dimensional imaging of OH in a lean burning high pressure combustor [NASA-TM-106854] p 236 N95-21383
- HILL, D. A.**
Measurements of shielding effectiveness and cavity characteristics of airplanes [PB94-210051] p 244 N95-20191
- HINGST, W. R.**
Flow coefficient behavior for boundary layer bleed holes and slots [NASA-TM-106846] p 244 N95-19953
- HIRATA, KATSUYA**
Aerodynamic mechanism of galloping [BTN-94-EIX94371347709] p 219 A95-69968
- HITCHCOCK, L.**
Independent review of Aviation Technology and Research Information Analysis System (ATRIAS) database [AD-A284049] p 226 N95-21518
- HOANG, TY**
A real-time algorithm for integrating differential satellite and inertial navigation information during helicopter approach [NASA-CR-197409] p 229 N95-21891
- HODGES, WILLIAM T.**
The personal aircraft: Status and issues [NASA-TM-109174] p 223 N95-20688
- HODKO, D.**
Corrosion of aircraft materials: Correlation between nanometer scale and macroscopic structural damage parameters [AD-A285930] p 241 N95-20299
- HOFFENBERG, R.**
Wake measurements in a strong adverse pressure gradient [NASA-CR-197272] p 224 N95-21031
- HOLBOURN, P. E.**
MCMs for avionics: Technology selection and intermodule interconnection p 234 N95-20641
- HOOD, R. E.**
Behavior of an inversion-based precipitation retrieval algorithm with high-resolution AMPR measurements including a low-frequency 10.7-GHz channel [HTN-95-70134] p 252 A95-70656
- HOOD, ROBBIE E.**
High-resolution imaging of rain systems with the advanced microwave precipitation radiometer [HTN-95-70133] p 252 A95-70655
- HOPPER, JAMES**
Systems engineering design and technical analyses for Strategic Avionics Crew-station Design Evaluation Facility (SACDEF) [AD-A286239] p 235 N95-22024
- HOWARD, CELESTE M.**
Color control in a multichannel simulator display: The display for advanced research and training [AD-A279717] p 239 N95-20992
- HU, Z.**
Sound propagation from an arbitrarily oriented multipole placed near a plane, finite impedance surface [BTN-94-EIX94371338964] p 257 A95-70797
- HUGHES, P.**
Advanced wind turbine design studies: Advanced conceptual study [DE93-000031] p 256 N95-20985
- HUMPHREYS, CAROLINE M.**
The dynamic approach to rotor blade research: ARA's oscillatory test facility [ARA-MEMO-405] p 223 N95-20758
- ICHIMIYA, R.**
Vortex shedding noise control in idling circular saws using air ejection at the teeth [BTN-94-EIX94371347214] p 257 A95-69970
- ILINCA, FLORIN**
Adaptive remeshing for convective heat transfer with variable fluid properties [BTN-95-EIX95082502720] p 243 A95-71033
- IWATSUKI, K.**
Electro-optic characterization of ultrafast photodetectors using adiabatically compressed soliton pulses [BTN-94-EIX94381359637] p 257 A95-72675
- IVY, RAVI**
The Advanced Avionics Subsystem Technology Demonstration Program p 234 N95-20636
- JANARDAN, B. A.**
Active control of fan noise-feasibility study. Volume 1: Flyover system noise studies [NASA-CR-195392-VOL-1] p 258 N95-21888
- JANSEN, KENNETH**
Unstructured-grid large-eddy simulation of flow over an airfoil p 225 N95-22448
- JIBB, D. J.**
High performance backplane components for modular avionics p 247 N95-20653
- JOHNK, R. T.**
Measurements of shielding effectiveness and cavity characteristics of airplanes [PB94-210051] p 244 N95-20191
- JOHNSON, W. L.**
Collected papers of the Soar/IFOR project, Spring 1994 [AD-A280063] p 238 N95-20624
- JONAS, P. R.**
Microphysical and radiative properties of small cumulus clouds over the sea [HTN-95-A0526] p 255 A95-73180
On the link between cloud-top radiative properties and sub-cloud aerosol concentrations [HTN-95-A0527] p 255 A95-73181
- JONES, D. C.**
Aircraft measurements of water vapour continuum absorption at millimetre wavelengths [HTN-95-90884] p 253 A95-72393
- JONES, JACK**
Immersion/two phase cooling p 246 N95-20648
- JONES, R.**
Bonded composite repair of cracked load-bearing holes [BTN-94-EIX94401360553] p 243 A95-71867
- JONES, R. R.**
Temperature effects on acoustic interactions between altitude test facilities and jet engine plumes [NASA-CR-197638] p 258 N95-21170
- JONES, RANDOLPH M.**
Collected papers of the Soar/IFOR project, Spring 1994 [AD-A280063] p 238 N95-20624
- JONSSON, H. H.**
Performance of a focused cavity aerosol spectrometer for measurements in the stratosphere of particle size in the 0.06-2.0-micrometer-diameter range [HTN-95-90914] p 253 A95-72423
- JORDAN, DICK**
Testing in the ARA Transonic Wind Tunnel [ARA-MEMO-395] p 239 N95-20799
- JULES, KENOL**
Application of pressure sensitive paint in hypersonic flows [NASA-TM-106824] p 223 N95-20794
- JURISSON, KARL R.**
TIM-SCT cable testing protocol [AD-A286633] p 231 N95-20772
- JURKOVICH, MARK S.**
Open Skies project computational fluid dynamic analysis [AD-A285928] p 223 N95-19991
- K**
- KALDELLIS, J. K.**
Investigation of shear layer transition using various turbulence models p 248 N95-21096
- KALTENBACH, HANS-JAKOB**
Large-eddy simulation of flow through a plane, asymmetric diffuser p 250 N95-22449
- KAMMEYER, MARK**
Application of wavelet-filtering techniques to intermittent turbulent and wall pressure events. Part 1: Exploratory results [AD-A286077] p 247 N95-20849
- KANAWATI, GHANI**
The Advanced Avionics Subsystem Technology Demonstration Program p 234 N95-20636
- KATO, K.**
Electro-optic characterization of ultrafast photodetectors using adiabatically compressed soliton pulses [BTN-94-EIX94381359637] p 257 A95-72675
- KEIRSEY, DAVID**
Collected papers of the Soar/IFOR project, Spring 1994 [AD-A280063] p 238 N95-20624
- KELLER, MICHAEL A.**
Lubricant evaluation and performance, 2 [AD-A279144] p 242 N95-21969
- KENNEDY, DAVID**
Buckling and vibration analysis of laminated panels using VICONOPT [PAPER-1746] p 230 A95-72580
- KESSINGER, CATHY**
Snow-band formation and evolution during the 15 November 1987 aircraft accident at Denver airport [HTN-95-80699] p 254 A95-72543
- KEZAI, TAHAR**
Modeling resonance in waveguide-to-microstrip junctions by unilateral fin line resonators [BTN-94-EIX94381323445] p 242 A95-70844
- KHARGONEKAR, P. P.**
Design of a controller for a flexible pointing system using H(infinity) synthesis [AD-A286572] p 256 N95-20828

- KIELLAND, P.**
Attitude determination using dedicated and nondedicated multi-antenna GPS sensors
[BTN-95-EIX95142555482] p 228 A95-72891
- KILSBY, C. G.**
Water vapor continuum absorption in mid-latitudes: Aircraft measurements and model comparisons
[HTN-95-40756] p 252 A95-71186
- KIM, FREDERICK D.**
High-order state space simulation models of helicopter flight mechanics
[HTN-95-A0494] p 237 A95-72565
- KIM, J. M.**
Vorticity concentration at the edge of the inboard vortex sheet
[HTN-95-31010] p 221 A95-71180
- KIRILLOV, I. R.**
MHD-flow in slotted channels with conducting walls
[DE94-018370] p 258 N95-21388
- KLETZLI, D. W., JR.**
Foliage transmission measurements using a ground-based ultrawide band (300-1300 MHz) SAR system
[BTN-94-EIX94381351617] p 252 A95-70950
- KLEWICKI, J. G.**
Transverse vorticity measurements in the NASA Ames 80 x 120 wind tunnel boundary layer
p 251 N95-22457
- KLYMENKO, VICTOR**
Factors affecting the perception of luning in monocular regions of partial binocular overlap displays
[AD-A286287] p 259 N95-22044
- KNAUFF, T. L., JR.**
Parallel calculation of sensitivity derivatives for aircraft design using automatic differentiation
[NASA-TM-110103] p 231 N95-20370
- KNOLLENBERG, R. G.**
Performance of a focused cavity aerosol spectrometer for measurements in the stratosphere of particle size in the 0.06-2.0-micrometer-diameter range
[HTN-95-90914] p 253 A95-72423
- KO, M. K. W.**
Subsidence of aircraft engine exhaust in the stratosphere: Implications for calculated ozone depletions
[PAPER-93GL03426] p 251 A95-70297
- KOLB, C. E.**
Subsidence of aircraft engine exhaust in the stratosphere: Implications for calculated ozone depletions
[PAPER-93GL03426] p 251 A95-70297
- KOMERATH, N. M.**
Measurement around a rotor blade excited in pitch. Part 1: Dynamic inflow
[HTN-95-31007] p 220 A95-71177
Measurement around a rotor blade excited in pitch. Part 2: Unsteady surface pressure
[HTN-95-31008] p 220 A95-71178
Vorticity concentration at the edge of the inboard vortex sheet
[HTN-95-31010] p 221 A95-71180
- KOMOROWSKI, J. P.**
Modelling of pillowing due to corrosion in fuselage lap joints
[BTN-95-EIX95082502227] p 240 A95-71024
- KONTOS, G. C.**
Active control of fan noise-feasibility study. Volume 1: Flyover system noise studies
[NASA-CR-195392-VOL-1] p 258 N95-21888
- KOSS, FRANK V.**
Collected papers of the Soar/IFOR project, Spring 1994
[AD-A280063] p 238 N95-20624
- KOUMOUTSAKOS, PETROS**
Direct numerical simulations of on-demand vortex generators: Mathematical formulation
p 251 N95-22452
- KOZEN, A.**
Electro-optic characterization of ultrafast photodetectors using adiabatically compressed soliton pulses
[BTN-94-EIX94381359637] p 257 A95-72675
- KRAFT, ROBERT E.**
Active control of fan noise-feasibility study. Volume 1: Flyover system noise studies
[NASA-CR-195392-VOL-1] p 258 N95-21888
- KRISHNAKUMAR, S.**
Modelling of pillowing due to corrosion in fuselage lap joints
[BTN-95-EIX95082502227] p 240 A95-71024
- KRUMPHOLZ, O.**
Optical backplane for modular avionics
p 257 N95-20652
- KRUPKE, B.**
Overview of remote sensing laser development and semiconductor laser technology
[DE94-019103] p 256 N95-21552
- KUZMENKO, P.**
An Echelle Grating Spectrometer (EGS) for mid-IR remote chemical detection
[DE94-019310] p 249 N95-21478
- LAANANEN, DAVID H.**
Prediction of energy absorption capability of composite stiffeners
[HTN-95-A0500] p 230 A95-72571
- LABAUNE, G.**
FASTPACK: Optimized solutions for modular avionics derived from a parametric study. Part 2: Avionics
p 233 N95-20635
- Composite cases for airborne electronic equipment: A technology study and EMC
p 241 N95-20655
- LACHAPPELLE, G.**
Attitude determination using dedicated and nondedicated multi-antenna GPS sensors
[BTN-95-EIX95142555482] p 228 A95-72891
- LACHENMAIER, RALPH**
The IEEE scalable coherent interface: An approach for a unified avionics network
p 234 N95-20650
- LAFONTAINE, FRANK J.**
High-resolution imaging of rain systems with the advanced microwave precipitation radiometer
[HTN-95-70133] p 252 A95-70655
- LAFORET, S.**
Composite cases for airborne electronic equipment: A technology study and EMC
p 241 N95-20655
- LAIRD, JOHN E.**
Collected papers of the Soar/IFOR project, Spring 1994
[AD-A280063] p 238 N95-20624
- LAKSHMANAN, B.**
Application of Navier-Stokes code PAB3D with kappa-epsilon turbulence model to attached and separated flows
[NASA-TP-3480] p 224 N95-21338
- LAL, MIHIR KUMAR**
Measurement around a rotor blade excited in pitch. Part 1: Dynamic inflow
[HTN-95-31007] p 220 A95-71177
Measurement around a rotor blade excited in pitch. Part 2: Unsteady surface pressure
[HTN-95-31008] p 220 A95-71178
- LANHAM, N. W.**
Aircraft-borne, laser-induced fluorescence instrument for the in situ detection of hydroxyl and hydroperoxyl radicals
[BTN-95-EIX95072499029] p 253 A95-71908
- LAPSON, L. B.**
Aircraft-borne, laser-induced fluorescence instrument for the in situ detection of hydroxyl and hydroperoxyl radicals
[BTN-95-EIX95072499029] p 253 A95-71908
- LAY, RICHARD J.**
Recommendation on transition from primary/secondary radar to secondary-only radar capability
[AD-A286279] p 249 N95-22005
- LEACH, BARRIE W.**
Comments on 'correction of inertial navigation with Loran C on NOAA's P-3 aircraft'
[HTN-95-70149] p 227 A95-70671
- LEAHY, KEVIN**
High density monolithic packaging technology for digital/microwave avionics
p 240 N95-20646
- LECUELLET, J.**
Composite cases for airborne electronic equipment: A technology study and EMC
p 241 N95-20655
- LEE, DAL HO**
Comparison of parameter identification algorithms for flight vehicles
[BTN-94-EIX94371347708] p 219 A95-69967
- LEE, EUN U.**
Corrosion behavior of landing gear steels
[AD-A285862] p 242 N95-22132
- LEE, JANG GYU**
Comparison of parameter identification algorithms for flight vehicles
[BTN-94-EIX94371347708] p 219 A95-69967
- LEE, THOMAS F.**
Potential applications of the SSM/I cloud liquid water parameter to the estimation of marine aircraft icing
[HTN-95-80651] p 254 A95-72495
- LEGGETT, DAVID B.**
Summary of a joint program of research into aircraft flight control concepts
[AD-A280012] p 237 N95-20004
- LEMENN, P.**
Experimental study of the helicopter-mobile radioelectrical channel and possible extension to the satellite-mobile channel
p 247 N95-20945
- LEONARD, ANTHONY**
Research on bluff body vortex wakes
[AD-A286319] p 223 N95-20177
- LEWIS, D. J.**
Time-resolved surface heat flux measurements in the wing/body junction vortex
[BTN-95-EIX95082502716] p 220 A95-71029
- LEWIS, T. B.**
Foliage transmission measurements using a ground-based ultrawide band (300-1300 MHz) SAR system
[BTN-94-EIX94381351617] p 252 A95-70950
- LI, FEI**
Computational studies of laminar to turbulence transition
[AD-A285622] p 248 N95-21146
- LINZELL, ROBERT S.**
Evaluation of the Spartan tight-tolerance AXBT
[HTN-95-40728] p 251 A95-70473
- LIQU, S. G.**
Vorticity concentration at the edge of the inboard vortex sheet
[HTN-95-31010] p 221 A95-71180
- LIQU, SHIUH-GUANG**
Measurement around a rotor blade excited in pitch. Part 1: Dynamic inflow
[HTN-95-31007] p 220 A95-71177
Measurement around a rotor blade excited in pitch. Part 2: Unsteady surface pressure
[HTN-95-31008] p 220 A95-71178
- LITTLE, R. C.**
Laboratory evaluation of a reactive baffle approach to NOx control
[AD-A2863802] p 255 N95-19921
- LIU, J. W. H.**
Large-scale computational fluid dynamics by the finite element method
[BTN-94-EIX94381359154] p 243 A95-71744
- LO, CHING F.**
Supersonic laminar flow control research
[NASA-CR-196049] p 249 N95-21340
- LOBL, ELENA**
High-resolution imaging of rain systems with the advanced microwave precipitation radiometer
[HTN-95-70133] p 252 A95-70655
- LOCKE, R. J.**
Two-dimensional imaging of OH in a lean burning high pressure combustor
[NASA-TM-106854] p 236 N95-21383
- LOFARO, RONALD J.**
Test and evaluation report for the Manual Domestic Passive Profiling System (MDPPS)
[AD-A286312] p 225 N95-20093
Independent review of Aviation Technology and Research Information Analysis System (ATRIAS) database
[AD-A284049] p 226 N95-21518
Test and Evaluation Plan (TEP) for Improvised Explosive Device Screening Systems (IEDSS)
[AD-A286382] p 227 N95-22319
- LOPEZ, ALFRED R.**
Comments on effect of wet snow on the null-reference ILS system
[BTN-95-EIX95142555488] p 227 A95-72885
- LU, G.**
Attitude determination using dedicated and nondedicated multi-antenna GPS sensors
[BTN-95-EIX95142555482] p 228 A95-72891
- LUTHRA, K. L.**
Toughened Silcomp composites for gas turbine engine applications
[DE95-002851] p 235 N95-21243

M

- MACPHERSON, J. IAN**
Comments on 'correction of inertial navigation with Loran C on NOAA's P-3 aircraft'
[HTN-95-70149] p 227 A95-70671
- MAJED, O.**
Numerical modelling of transverse impact on composite coupons
[BTN-95-EIX95082502225] p 240 A95-71022
- MALIK, MUJEEB R.**
Computational studies of laminar to turbulence transition
[AD-A285622] p 248 N95-21146
- MALINAS, N. P.**
Foliage transmission measurements using a ground-based ultrawide band (300-1300 MHz) SAR system
[BTN-94-EIX94381351617] p 252 A95-70950

- MALONE, ROBERT L.**
Test and Evaluation Plan (TEP) for Improvised Explosive Device Screening Systems (IEDSS)
[AD-A286382] p 227 N95-22319
- MANJUNATH, A. R.**
Flap-lag damping in hover and forward flight with a three-dimensional wake
[HTN-95-A0496] p 221 A95-72567
- MARTIN, JOEL D.**
Tropical cyclone observation and forecasting with and without aircraft reconnaissance
[NASA-95-80701] p 254 A95-72545
- MARTIN, JOHN S.**
Factors affecting the perception of luning in monocular regions of partial binocular overlap displays
[AD-A286287] p 259 N95-22044
- MARTIN, V.**
Secondary source locations in active noise control: Selection or optimization?
[BTN-94-EIX94381352222] p 257 A95-71738
- MASON, RALPH**
Precise navigation using adaptive FIR filtering and time domain spectral estimation
[BTN-95-EIX95142555485] p 227 A95-72888
- MASSEY, K. C.**
Temperature effects on acoustic interactions between altitude test facilities and jet engine plumes
[NASA-CR-197638] p 258 N95-21170
- MATESKI, J. E.**
Independent review of Aviation Technology and Research Information Analysis System (ATRIAS) database
[AD-A284049] p 226 N95-21518
- MATTHEWS, R. K.**
Description and flow characterization of hypersonic facilities
[AD-A284291] p 223 N95-20248
- MATTICE, MICHAEL S.**
Design of a controller for a flexible pointing system using H(infinity) synthesis
[AD-A286572] p 256 N95-20828
- MAUS, J. R.**
Description and flow characterization of hypersonic facilities
[AD-A284291] p 223 N95-20248
- MCFARLAND, R. E.**
Simulation of rotor blade element turbulence
[NASA-TM-108862] p 232 N95-21186
- MCKELVEY, TERESA**
Systems engineering design and technical analyses for Strategic Avionics Crew-station Design Evaluation Facility (SACDEF)
[AD-A286239] p 235 N95-22024
- MCLAUGHLIN, J. C.**
Scale-up and modeling of forced chemical vapor infiltration
[DE94-017769] p 247 N95-20781
- MCLEAN, WILLIAM E.**
Factors affecting the perception of luning in monocular regions of partial binocular overlap displays
[AD-A286287] p 259 N95-22044
- MCLEMORE, DONALD P.**
Fault detection techniques for complex cable shield topologies
[AD-A286632] p 247 N95-20771
TIM-SCT cable testing protocol
[AD-A286633] p 231 N95-20772
- MEINDL, M.**
SAR image registration in absolute coordinates using GPS carrier phase position and velocity information
[DE94-018738] p 228 N95-20195
- MEINDL, M. A.**
Assessment of a non-dedicated GPS receiver system for precise airborne attitude determination
[DE94-019309] p 229 N95-21520
- MESCHTER, P. J.**
Toughened Silcomp composites for gas turbine engine applications
[DE95-002851] p 235 N95-21243
- MEY, G.**
Modular CNI avionics system p 234 N95-20659
- MIKAE-LYE, R. C.**
Subsidence of aircraft engine exhaust in the stratosphere: Implications for calculated ozone depletions
[PAPER-93GL03426] p 251 A95-70297
- MILATOVIC, BORISLAV**
Portable static test facility for small, expendable, turbojet engines, phase 1
[AD-A286337] p 239 N95-21719
- MINNETT, P. J.**
Water vapor continuum absorption in mid-latitudes: Aircraft measurements and model comparisons
[HTN-95-40756] p 252 A95-71186
- MIVILLE, FRANK**
Ultra-Reliable Digital Avionics (URDA) processor
p 245 N95-20638
- MONAGHAN, TIM**
The Advanced Avionics Subsystem Technology Demonstration Program p 234 N95-20636
- MONYAK, JOHN T.**
Statistical analysis of Turbine Engine Diagnostic (TED) field test data
[AD-A286032] p 248 N95-20998
- MOREAU, A.**
Modular supplies for a distributed architecture
p 234 N95-20657
- MORGAN, REED**
The impact of advanced packaging technology on modular avionics architectures p 233 N95-20632
- MORISHITA, ETSUO**
Ground effect calculation of two-dimensional airfoil
[BTN-94-EIX94371347710] p 219 A95-69969
- MORRIS, SHELBY J., JR.**
The personal aircraft: Status and issues
[NASA-TM-109174] p 223 N95-20688
- MOSER, G.**
Microchannel heat pipe cooling of modules
p 246 N95-20649
- MOSIER, MARY H.**
Standard Hardware Acquisition and Reliability Program (SHARP) advanced SEM-E packaging
p 233 N95-20633
- MOTE, C. D.**
Vortex shedding noise control in idling circular saws using air ejection at the teeth
[BTN-94-EIX94371347214] p 257 A95-69970
- MUGNAI, A.**
Behavior of an inversion-based precipitation retrieval algorithm with high-resolution AMPR measurements including a low-frequency 10.7-GHz channel
[HTN-95-70134] p 252 A95-70656
- MULLER, MARK**
Commuter/air taxi ditchings and water-related impacts that occurred from 1979 to 1989
[AD-A285691] p 226 N95-20275
- MURPHY, O. J.**
Corrosion of aircraft materials: Correlation between nanometer scale and macroscopic structural damage parameters
[AD-A285930] p 241 N95-20299
- N**
- NAGABHUSHANAM, J.**
Flap-lag damping in hover and forward flight with a three-dimensional wake
[HTN-95-A0496] p 221 A95-72567
- NAGATSUMA, T.**
Electro-optic characterization of ultrafast photodetectors using adiabatically compressed soliton pulses
[BTN-94-EIX94381359637] p 257 A95-72675
- NAGESH BABU, G. L.**
Smart structures in the control of airframe vibrations
[HTN-95-31014] p 236 A95-71184
- NAKAMURA, YASU HARU**
Aerodynamic mechanism of galloping
[BTN-94-EIX94371347709] p 219 A95-69968
- NELSON, J. R.**
The opportunities for and challenges of common integrated electronics
[AD-A279991] p 248 N95-20966
- NELSON, ROBERT C.**
Experiments on the flow field physics of confluent boundary layers for high-lift systems
[NASA-CR-197318] p 224 N95-21343
- NELSON, S. G.**
Laboratory evaluation of a reactive baffle approach to NOx control
[AD-A283802] p 255 N95-19921
- NESBITT, DAVID J.**
State-to-state collisional dynamics of atmospheric species
[AD-A285053] p 245 N95-20484
- NEWMAN, PAUL A.**
An algorithm for forecasting mountain wave-related turbulence in the stratosphere
[HTN-95-80656] p 254 A95-72500
- NEWTON, R.**
Performance of a focused cavity aerosol spectrometer for measurements in the stratosphere of particle size in the 0.06-2.0-micrometer-diameter range
[HTN-95-90914] p 253 A95-72423
- NG, LIAN**
Acoustic receptivity due to weak surface inhomogeneities in adverse pressure gradient boundary layers
[NASA-TM-4577] p 249 N95-21258
- NGUYEN, V.-N.**
Large-scale computational fluid dynamics by the finite element method
[BTN-94-EIX94381359154] p 243 A95-71744
- NIXON, MARK W.**
Parametric studies for titrotor aeroelastic stability in highspeed flight
[HTN-95-A0499] p 222 A95-72570
- NORTH, G. L.**
Two-dimensional imaging of OH in a lean burning high pressure combustor
[NASA-TM-106854] p 236 N95-21383
- O**
- OCKUNZZI, K. A.**
Two-dimensional imaging of OH in a lean burning high pressure combustor
[NASA-TM-106854] p 236 N95-21383
- OEDING, ROBERT G.**
Response of the B-1B air data sensor to simulated dust cloud environments
[AD-A286134] p 235 N95-22036
- OLIGER, JOSEPH**
Computing methods for the approximate solution of time dependent problems
[AD-A286007] p 256 N95-20719
- OLIVER, J. F.**
Aircraft-borne, laser-induced fluorescence instrument for the in situ detection of hydroxyl and hydroperoxyl radicals
[BTN-95-EIX95072499029] p 253 A95-71908
- OLSON, DANIEL**
The Advanced Avionics Subsystem Technology Demonstration Program p 234 N95-20636
- ONDREJKA, A. R.**
Measurements of shielding effectiveness and cavity characteristics of airplanes
[PB94-210051] p 244 N95-20191
- ORLANDO, VINCENT A.**
GPS-Scuttler capacity analysis
[AD-A280037] p 245 N95-20599
- OROURKE, CAROLYN**
Environmental Compliance Assessment and Management Program
[AD-A279605] p 255 N95-20441
- OSTERMAN, M. D.**
Liquid flow-through cooling of electronic modules
p 246 N95-20647
- OSTGAARD, JOHN**
The impact of advanced packaging technology on modular avionics architectures p 233 N95-20632
- OWEN, T. E.**
Assessment of a non-dedicated GPS receiver system for precise airborne attitude determination
[DE94-019309] p 229 N95-21520
- P**
- PANDA, B.**
Advance finite element modeling of rotor blade aeroelasticity
[HTN-95-31013] p 221 A95-71183
- PARASCHIVOIU, I.**
Ice accretion on aircraft wings
[BTN-95-EIX95082502224] p 225 A95-71021
- PARK, CHUL**
Measurement and analysis of nitric oxide radiation in an arcjet flow
[BTN-95-EIX95082502727] p 243 A95-71040
- PAUL, J.**
Bonded composite repair of cracked load-bearing holes
[BTN-94-EIX94401360553] p 243 A95-71867
- PAYNE, R. C.**
Effect of atmospheric pressure on measured aircraft noise levels
[PB95-130423] p 232 N95-21425
- PELLETIER, DOMINIQUE**
Adaptive remeshing for convective heat transfer with variable fluid properties
[BTN-95-EIX95082502720] p 243 A95-71033
- PENAFIEL, PABLO B.**
Application of wavelet-filtering techniques to intermittent turbulent and wall pressure events. Part 1: Exploratory results
[AD-A286077] p 247 N95-20849
- PENDLETON, ED**
Pressure measurements on an F/A-18 twin vertical tail in buffeting flow. Volume 4, part 1: Buffet cross spectral densities
[AD-A285593] p 237 N95-21214

- Pressure measurements on an F/A-18 twin vertical tail in buffeting flow. Volume 1: Wind tunnel test summary [AD-A279126] p 225 N95-21877
- PERKOSKI, EMMETT**
Immersion/two phase cooling p 246 N95-20648
- PERUSSE, PATRICK**
T-45A High Angle of Attack Testing: US Naval Test Pilot School 46th Annual Reunion and Symposium [AD-A284000] p 231 N95-20466
- PETERS, DAVID A.**
Flap-lag damping in hover and forward flight with a three-dimensional wake [HTN-95-A0496] p 221 A95-72567
- PETERSON, R. A.**
Laboratory evaluation of a reactive baffle approach to NOx control [AD-A283802] p 255 N95-19921
- PETTIT, CHRIS**
Pressure measurements on an F/A-18 twin vertical tail in buffeting flow. Volume 4, part 1: Buffet cross spectral densities [AD-A285593] p 237 N95-21214
Pressure measurements on an F/A-18 twin vertical tail in buffeting flow. Volume 1: Wind tunnel test summary [AD-A279126] p 225 N95-21877
- PHILIPPART, A.**
Data link terminal DLT document [PB95-110805] p 229 N95-21369
- PIERCE, G. A.**
Measurement around a rotor blade excited in pitch. Part 2: Unsteady surface pressure [HTN-95-31008] p 220 A95-71178
- PIPERIAS, P.**
Derived gust spectra for the Macchi MB326H [ARL-TN-3] p 225 N95-21892
- PLATT, ROBERT**
High-resolution imaging of rain systems with the advanced microwave precipitation radiometer [HTN-95-70133] p 252 A95-70655
- POMFRET, CHRIS J.**
Engine life measurement and diagnostics [BTN-95-EIX95041505024] p 235 A95-70133
- POON, C.**
Numerical modelling of transverse impact on composite coupons [BTN-95-EIX95082502225] p 240 A95-71022
- PRAIRIE, MIKE**
Optical processing and control [AD-A279157] p 259 N95-21975
- PRIEBE, CAREY E.**
Wavelet transformations for helicopter identification via acoustic signatures [AD-A279980] p 257 N95-20963
- PRIGENT, C.**
Aircraft measurements of water vapour continuum absorption at millimetre wavelengths [HTN-95-90884] p 253 A95-72393
- PUESCHEL, R.**
Performance of a focused cavity aerosol spectrometer for measurements in the stratosphere of particle size in the 0.06-2.0-micrometer-diameter range [HTN-95-90914] p 253 A95-72423
- PUGACZ, EDWARD**
Minima reduction simulation test results [AD-A285626] p 228 N95-21148
- R**
- RAGA, G. B.**
Microphysical and radiative properties of small cumulus clouds over the sea [HTN-95-A0526] p 255 A95-73180
On the link between cloud-top radiative properties and sub-cloud aerosol concentrations [HTN-95-A0527] p 255 A95-73181
- RASMUSSEN, ROY M.**
Snow-band formation and evolution during the 15 November 1987 aircraft accident at Denver airport [HTN-95-80699] p 254 A95-72543
- RAULT, D. F. G.**
Cercignani-Lampis-Lord gas-surface interaction model: Comparisons between theory and simulation [BTN-95-EIX95041503806] p 242 A95-70131
- REED, C. B.**
MHD-flow in slotted channels with conducting walls [DE94-018370] p 258 N95-21388
- REHMANN, ALBERT**
An evaluation of Automatic Terminal Information Service (ATIS) flight deck display presentation options [AD-A280100] p 228 N95-21020
- REITBERGER, P. H.**
Modular CNI avionics system p 234 N95-20659
- REITERER, BERNARD L.**
The opportunities for and challenges of common integrated electronics [AD-A279991] p 248 N95-20966
- REY, J. M.**
Modular supplies for a distributed architecture p 234 N95-20657
- RICH, WILLIAM F.**
The navigation toolkit [NASA-CR-197290] p 229 N95-22161
- RICHARDSON, I. G.**
A survey of bidirectional greater than or equal to MeV ion flows during the Helios 1 and Helios 2 mission: Observations from the Goddard Space Flight Center instruments [HTN-95-70542] p 237 A95-71656
- ROBELEN, DAVID B.**
Vapor generator wand [NASA-CASE-LAR-15058-1] p 238 N95-20080
- ROBICHAUD, M.**
Large-scale computational fluid dynamics by the finite element method [BTN-94-EIX94381359154] p 243 A95-71744
- RODRIGUEZ, J. M.**
Subsidence of aircraft engine exhaust in the stratosphere: Implications for calculated ozone depletions [PAPER-93GL03426] p 251 A95-70297
- ROGERS, GEORGE W.**
Wavelet transformations for helicopter identification via acoustic signatures [AD-A279980] p 257 N95-20963
- ROGERS, MAX**
T-45A High Angle of Attack Testing: US Naval Test Pilot School 46th Annual Reunion and Symposium [AD-A284000] p 231 N95-20466
- ROMAN, JUAN F.**
Foliage transmission measurements using a ground-based ultrawide band (300-1300 MHz) SAR system [BTN-94-EIX94381351617] p 252 A95-70950
- ROSHKO, ANATOL**
Research on bluff body vortex wakes [AD-A286319] p 223 N95-20177
- RUALT, P.**
Data link terminal DLT document [PB95-110805] p 229 N95-21369
- RUDMAN, S. D.**
Water vapor continuum absorption in mid-latitudes: Aircraft measurements and model comparisons [HTN-95-40756] p 252 A95-71186
- RUNTZ, KEN J.**
Precise navigation using adaptive FIR filtering and time domain spectral estimation [BTN-95-EIX95142555485] p 227 A95-72888
- RUSZCZYK, WILLIAM**
Ultra-Reliable Digital Avionics (URDA) processor p 245 N95-20638
- S**
- SABA, COSTANDY S.**
Lubricant evaluation and performance, 2 [AD-A279144] p 242 N95-21969
- SADDOUGHI, SEYED G.**
Experimental investigations of on-demand vortex generators p 250 N95-22451
- SALIK, M. D.**
High performance backplane components for modular avionics p 247 N95-20653
- SAMMELLS, ANTHONY F.**
Electrochemical impedance pattern recognition for detection of hidden chemical corrosion on aircraft components [AD-A284998] p 241 N95-20481
Electrochemical impedance pattern recognition for detection of hidden chemical corrosion on aircraft components [AD-A285998] p 241 N95-20716
- SANDERSON, S. R.**
Shock wave interactions in hypervelocity flow [AD-A286507] p 250 N95-22212
- SANGHA, K. B.**
Advance finite element modeling of rotor blade aeroelasticity [HTN-95-31013] p 221 A95-71183
- SANKAR, L. N.**
Effects of leading and trailing edge flaps on the aerodynamics of airfoil/vortex interactions [HTN-95-31011] p 221 A95-71181
- SARNO, C.**
FASTPACK: Optimized solutions for modular avionics derived from a parametric study. Part 2: Avionics p 233 N95-20635
- Lightweight electronic enclosures using composite materials p 241 N95-20656
- SAUNDERS, R. W.**
Water vapor continuum absorption in mid-latitudes: Aircraft measurements and model comparisons [HTN-95-40756] p 252 A95-71186
- SCHARLEMANN, T.**
Overview of remote sensing laser development and semiconductor laser technology [DE94-019103] p 256 N95-21552
- SCHEFFEY, JOSEPH L.**
Analysis of test criteria for specifying foam firefighting agents for aircraft rescue and firefighting [AD-A286381] p 227 N95-22352
- SCHLECHTRIEM, STEFAN**
Prediction of rotor-blade deformations due to unsteady airloads [AD-A286593] p 231 N95-20860
- SCHNEIDER, S. P.**
Wake measurements in a strong adverse pressure gradient [NASA-CR-197272] p 224 N95-21031
- SCHNEIDER, STEVEN P.**
Development of quiet-flow supersonic wind tunnels for laminar-turbulent transition research [NASA-CR-197286] p 239 N95-21436
- SCOTT, MICHAEL A.**
The personal aircraft: Status and issues [NASA-TM-109174] p 223 N95-20688
- SHAY, LYNN K.**
Orbital velocities induced by surface waves [HTN-95-90902] p 253 A95-72411
- SHEEN, D. R.**
Foliage transmission measurements using a ground-based ultrawide band (300-1300 MHz) SAR system [BTN-94-EIX94381351617] p 252 A95-70950
- SHERWIN, R.**
Advanced wind turbine design studies: Advanced conceptual study [DE93-000031] p 256 N95-20985
- SHIA, R.-L.**
Subsidence of aircraft engine exhaust in the stratosphere: Implications for calculated ozone depletions [PAPER-93GL03426] p 251 A95-70297
- SHINAGAWA, M.**
Electro-optic characterization of ultrafast photodetectors using adiabatically compressed soliton pulses [BTN-94-EIX94381359637] p 257 A95-72675
- SIMPSON, R. L.**
Time-resolved surface heat flux measurements in the wing/body junction vortex [BTN-95-EIX95082502716] p 220 A95-71029
- SIVASHANKAR, N.**
Design of a controller for a flexible pointing system using H(infinity) synthesis [AD-A286572] p 256 N95-20828
- SKIDMORE, J.**
Overview of remote sensing laser development and semiconductor laser technology [DE94-019103] p 256 N95-21552
- SLAVEY, JAMES C.**
Open Skies project computational fluid dynamic analysis [AD-A285928] p 223 N95-19991
- SMALLEY, DAVID J.**
Radar studies of aviation hazards [AD-A285845] p 226 N95-21831
- SMITH, E. A.**
Behavior of an inversion-based precipitation retrieval algorithm with high-resolution AMPR measurements including a low-frequency 10.7-GHz channel [HTN-95-70134] p 252 A95-70656
- SMITH, EDWARD C.**
Air and ground resonance of helicopters with elastically tailored composite rotor blades [HTN-95-A0497] p 222 A95-72568
- SMITH, ERIC A.**
High-resolution imaging of rain systems with the advanced microwave precipitation radiometer [HTN-95-70133] p 252 A95-70655
- SMITH, HOOVER A.**
Lubricant evaluation and performance, 2 [AD-A279144] p 242 N95-21969
- SMITH, O. E.**
Ascent wind model for launch vehicle design [BTN-95-EIX95041503799] p 239 A95-70124
- SMITH, R. D.**
Aircraft corrosion study [AD-A279527] p 241 N95-21687
- SOLARZ, R.**
Overview of remote sensing laser development and semiconductor laser technology [DE94-019103] p 256 N95-21552

SOLKA, JEFFREY L.
Wavelet transformations for helicopter identification via acoustic signatures
[AD-A279980] p 257 N95-20963

SPENCER, R. W.
Behavior of an inversion-based precipitation retrieval algorithm with high-resolution AMPR measurements including a low-frequency 10.7-GHz channel
[HTN-95-70134] p 252 A95-70656

SPENCER, ROY W.
High-resolution imaging of rain systems with the advanced microwave precipitation radiometer
[HTN-95-70133] p 252 A95-70655

SRIDHAR, S.
Liquid flow-through cooling of electronic modules
p 246 N95-20647

STANNILAND, DENNIS R.
Investigation of a thermal buoyancy effect on the drag of half models tested in the ARA Transonic Wind Tunnel [ARA-MEMO-407] p 222 N95-19946

STARR, T. L.
Scale-up and modeling of forced chemical vapor infiltration
[DE94-017769] p 247 N95-20781

STENGEL, JOHN D.
Systems engineering design and technical analyses for Strategic Avionics Crew-station Design Evaluation Facility (SACDEF)
[AD-A286239] p 235 N95-22024

STEVENS, C. G.
An Echelle Grating Spectrometer (EGS) for mid-IR remote chemical detection
[DE94-019310] p 249 N95-21478

STEVENS, DALE
Optical processing and control
[AD-A279157] p 259 N95-21975

STEWART, JOHN E., II
Using the backward transfer paradigm to validate the AH-64 Simulator Training Research Advanced Testbed for Aviation
[AD-A285758] p 238 N95-19931

STRAUB, F. K.
Advance finite element modeling of rotor blade aeroelasticity
[HTN-95-31013] p 221 A95-71183

STRAUB, FREDRICH K.
Design optimization of rotor blades for improved performance and vibration
[HTN-95-A0498] p 229 A95-72569

STRAZNICKY, P. V.
Numerical modelling of transverse impact on composite coupons
[BTN-95-EIX95082502225] p 240 A95-71022

STREETT, CRAIG
Acoustic receptivity due to weak surface inhomogeneities in adverse pressure gradient boundary layers
[NASA-TM-4577] p 249 N95-21258

STRETCH, THOMAS
The IEEE scalable coherent interface: An approach for a unified avionics network
p 234 N95-20650

STROM, STEPHEN W.
The navigation toolkit
[NASA-CR-197290] p 229 N95-22161

STROPKI, J. T.
Aircraft corrosion study
[AD-A279527] p 241 N95-21687

STUNDER, BARBARA J. B.
Volcanic ash forecast transport and dispersion (VAFTAD) model
[HTN-95-80702] p 254 A95-72546

STURTEVANT, B.
Shock wave interactions in hypervelocity flow
[AD-A286507] p 250 N95-22212

SU, AY
Flap-lag damping in hover and forward flight with a three-dimensional wake
[HTN-95-A0496] p 221 A95-72567

SULLIVAN, JOHN P.
Wake measurements in a strong adverse pressure gradient
[NASA-CR-197272] p 224 N95-21031

SUN, H.
Assessment of a non-dedicated GPS receiver system for precise airborne attitude determination
[DE94-018309] p 229 N95-21520

SUZUKI, ANDREW
Optical processing and control
[AD-A279157] p 259 N95-21975

SUZUKI, K.
Electro-optic characterization of ultrafast photodetectors using adiabatically compressed soliton pulses
[BTN-94-EIX94381359637] p 257 A95-72675

SUZUKI, KOJIRO
Thermochemical nonequilibrium viscous shock-layer analysis for a Mars aerocapture vehicle
[BTN-95-EIX95082502732] p 239 A95-70139

SWADLEY, STEVEN D.
Potential applications of the SSM/I cloud liquid water parameter to the estimation of marine aircraft icing
[HTN-95-80651] p 254 A95-72495

SYLVAIN, M.
Experimental study of the helicopter-mobile radioelectrical channel and possible extension to the satellite-mobile channel
p 247 N95-20945

T

TADGHIGHI, H.
Effects of leading and trailing edge flaps on the aerodynamics of airfoil/vortex interactions
[HTN-95-31011] p 221 A95-71181

TAN, C. K.
Temperature effects on acoustic interactions between altitude test facilities and jet engine plumes
[NASA-CR-197638] p 258 N95-21170

TARDUCCI, D.
Electromagnetic compatibility effects of advanced packaging configurations
p 247 N95-20658

TATUM, P. A.
A review of water mist technology for fire suppression
[AD-A285738] p 225 N95-20071

TAYLOR, MALCOLM S.
Statistical analysis of Turbine Engine Diagnostic (TED) field test data
[AD-A286032] p 248 N95-20998

TCHENG, PING
Effects of yaw and pitch motion on model attitude measurements
[NASA-TM-4641] p 250 N95-22109

TEZUKA, KAORU
Ground effect calculation of two-dimensional airfoil
[BTN-94-EIX94371347710] p 219 A95-69969

THOMAS, F. O.
Experiments on the flow field physics of confluent boundary layers for high-lift systems
[NASA-CR-197318] p 224 N95-21343

THOMAS, N.
An Echelle Grating Spectrometer (EGS) for mid-IR remote chemical detection
[DE94-019310] p 249 N95-21478

TISCHLER, MARK B.
High-order state space simulation models of helicopter flight mechanics
[HTN-95-A0494] p 237 A95-72565

TOM, MICHAEL
Integrated IR sensors
[BTN-95-EIX95041505023] p 242 A95-70132

TOROK, MICHAEL S.
Aerodynamic and wake methodology evaluation using Model UH-60A experimental data
[HTN-95-31009] p 220 A95-71179

TOTH, DOUGLAS K.
Lubricant evaluation and performance, 2
[AD-A279144] p 242 N95-21969

TOTH, JOE M.
Precise navigation using adaptive FIR filtering and time domain spectral estimation
[BTN-95-EIX95142555485] p 227 A95-72888

TRAN, P.
Ice accretion on aircraft wings
[BTN-95-EIX95082502224] p 225 A95-71021

TRIPP, JOHN S.
Effects of yaw and pitch motion on model attitude measurements
[NASA-TM-4641] p 250 N95-22109

TRUJILLO, EDWARD
Integrated IR sensors
[BTN-95-EIX95041505023] p 242 A95-70132

TUNG, SHU-LIN
Radar studies of aviation hazards
[AD-A285845] p 226 N95-21831

TYLER, S. G.
MCMs for avionics: Technology selection and intermodule interconnection
p 234 N95-20641

VANDERVOORST, ANDRE
Modeling resonance in waveguide-to-microstrip junctions by unilateral fin line resonators
[BTN-94-EIX94381323445] p 242 A95-70844

VANHOUTEN, JOHN S.
Forecasting aircraft mishaps using monthly maintenance reports
[AD-A286049] p 227 N95-22417

V

VANSTONE, D. A.
Laboratory evaluation of a reactive baffle approach to NOx control
[AD-A283802] p 255 N95-18921

VEBER, G.
FASTPACK: Optimized solutions for modular avionics derived from a parametric study. Part 1: Platform features
p 233 N95-20634

VELSKO, S.
Overview of remote sensing laser development and semiconductor laser technology
[DE94-019103] p 256 N95-21552

VERONA, ROBERT W.
Factors affecting the perception of luring in monocular regions of partial binocular overlap displays
[AD-A286287] p 259 N95-22044

VILCANS, JANIS
Recommendation on transition from primary/secondary radar to secondary-only radar capability
[AD-A286279] p 249 N95-22005

VOKURA, V. J.
RCS measurements, transformations, and comparisons under cylindrical and plane wave illumination
[BTN-94-EIX94371347126] p 242 A95-69976

W

WALSH, EDWARD J.
Orbital velocities induced by surface waves
[HTN-95-90902] p 253 A95-72411

WALTER, THERESA
High density monolithic packaging technology for digital/microwave avionics
p 240 N95-20646

WANG, MENG
Acoustics of laminar boundary layers breakdown
p 251 N95-22455

WEBSTER, HARRY
Fuselage burnthrough from large exterior fuel fires
[AD-A286295] p 226 N95-22318

WEISTENSTEIN, D. K.
Subsidence of aircraft engine exhaust in the stratosphere: Implications for calculated ozone depletions
[PAPER-93GL03426] p 251 A95-70297

WENNBERG, P. O.
Aircraft-borne, laser-induced fluorescence instrument for the in situ detection of hydroxyl and hydroperoxyl radicals
[BTN-95-EIX95072499029] p 253 A95-71908

WEYER, ROBERT M.
Open Skies project computational fluid dynamic analysis
[AD-A285928] p 223 N95-19991

WILHELM, KNUT
Summary of a joint program of research into aircraft flight control concepts
[AD-A280012] p 237 N95-20004

WILLIAMS, FRED W.
Buckling and vibration analysis of laminated panels using VICONOPT
[PAPER-1746] p 230 A95-72580

WILLIS, B. P.
Flow coefficient behavior for boundary layer bleed holes and slots
[NASA-TM-106846] p 244 N95-19953

WILSON, J. C.
Performance of a focused cavity aerosol spectrometer for measurements in the stratosphere of particle size in the 0.06-2.0-micrometer-diameter range
[HTN-95-90914] p 253 A95-72423

WING, DAVID J.
Static investigation of two fluidic thrust-vectoring concepts on a two-dimensional convergent-divergent nozzle
[NASA-TM-4574] p 222 N95-19913

WITTLIN, G.
Commuter airplane accident data analysis
[AD-A286315] p 226 N95-20174

WOODCOCK, ROBERT W.
Summary of a joint program of research into aircraft flight control concepts
[AD-A280012] p 237 N95-20004

WORONOWICZ, M. S.
Cercignani-Lampis-Lord gas-surface interaction model: Comparisons between theory and simulation
[BTN-95-EIX95041503806] p 242 A95-70131

WORSWICK, M. J.
Numerical modelling of transverse impact on composite coupons
[BTN-95-EIX95082502225] p 240 A95-71022

WRIGHT, JOSEPH A.
Analysis of test criteria for specifying foam firefighting agents for aircraft rescue and firefighting
[AD-A286381] p 227 N95-22352

X

XIANG, X.

Behavior of an inversion-based precipitation retrieval algorithm with high-resolution AMPR measurements including a low-frequency 10.7-GHz channel
[HTN-95-70134] p 252 A95-70656

Y

YAITA, M.

Electro-optic characterization of ultrafast photodetectors using adiabatically compressed soliton pulses
[BTN-94-EIX94381359637] p 257 A95-72675

YANAGIMOTO, K.

Vortex shedding noise control in idling circular saws using air ejection at the teeth
[BTN-94-EIX94371347214] p 257 A95-69970

YETTER, J. A.

16-foot transonic tunnel test section flowfield survey
[NASA-TM-109157] p 238 N95-20669

YETTER, JEFFREY A.

Why do airlines want and use thrust reversers? A compilation of airline industry responses to a survey regarding the use of thrust reversers on commercial transport airplanes
[NASA-TM-109158] p 226 N95-20706

YOUSUFF, AJMAL

Design of robust optimal control systems and stability analysis of real structured uncertainties
[AD-A279089] p 256 N95-21913

Z

ZACHARIAS, GREG L.

A neural expert approach to self designing flight control systems
[AD-A279965] p 237 N95-21122

ZEMSCH, STEPHAN

Application of pressure sensitive paint in hypersonic flows
[NASA-TM-106824] p 223 N95-20794

ZHANG, PEN CHEN

Orbital velocities induced by surface waves
[HTN-95-90902] p 253 A95-72411

ZUPPARDO, JOSEPH C.

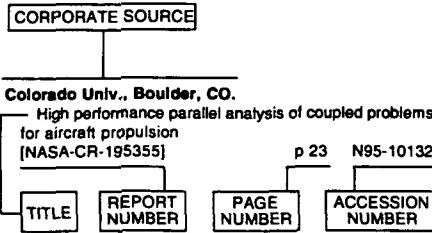
Open Skies project computational fluid dynamic analysis
[AD-A285928] p 223 N95-19991

CORPORATE SOURCE INDEX

AERONAUTICAL ENGINEERING / A Continuing Bibliography (Supplement 318)

June 1995

Typical Corporate Source Index Listing



Listings in this index are arranged alphabetically by corporate source. The title of the document is used to provide a brief description of the subject matter. The page number and the accession number are included in each entry to assist the user in locating the abstract in the abstract section. If applicable, a report number is also included as an aid in identifying the document.

A

- Advisory Group for Aerospace Research and Development, Neuilly-Sur-Seine (France).**
Advanced Packaging Concepts for Digital Avionics [AGARD-CP-562] p 233 N95-20631
Application of Direct and Large Eddy Simulation to Transition and Turbulence [AGARD-CP-551] p 248 N95-21061
- Aeronautical Research Labs., Melbourne (Australia).**
Derived gust spectra for the Macchi MB326H [ARL-TN-3] p 225 N95-21892
- Aeronautical Systems Div., Wright-Patterson AFB, OH.**
Open Skies project computational fluid dynamic analysis [AD-A285928] p 223 N95-19991
- Air Force Systems Command, Wright-Patterson AFB, OH.**
Photovoltaic electric power applied to Unmanned Aerial Vehicles (UAV) p 245 N95-20530
- Aircraft Research Association Ltd., Bedford (England).**
Investigation of a thermal buoyancy effect on the drag of half models tested in the ARA Transonic Wind Tunnel [ARA-MEMO-407] p 222 N95-19946
The dynamic approach to rotor blade research: ARA's oscillatory test facility [ARA-MEMO-405] p 223 N95-20758
Testing in the ARA Transonic Wind Tunnel [ARA-MEMO-395] p 239 N95-20799
- Alenia, Turin (Italy).**
Electromagnetic compatibility effects of advanced packaging configurations p 247 N95-20658
- Argonne National Lab., IL.**
MHD-flow in slotted channels with conducting walls [DE94-018370] p 258 N95-21388
- Army Aeromedical Research Lab., Fort Rucker, AL.**
Factors affecting the perception of luring in monocular regions of partial binocular overlap displays [AD-A286287] p 259 N95-22044

- Army Construction Engineering Research Lab., Champaign, IL.**
Environmental Compliance Assessment and Management Program [AD-A279605] p 255 N95-20441
- Army Engineer Waterways Experiment Station, Vicksburg, MS.**
Super-heavy aircraft study [AD-A279602] p 238 N95-19955
- Army Research Inst. for the Behavioral and Social Sciences, Alexandria, VA.**
Using the backward transfer paradigm to validate the AH-64 Simulator Training Research Advanced Testbed for Aviation [AD-A285758] p 238 N95-19931
- Army Research Lab., Aberdeen Proving Ground, MD.**
Comparison of meteorological data with fitted values extracted from projectile trajectory [AD-A285921] p 255 N95-19989
Statistical analysis of Turbine Engine Diagnostic (TED) field test data [AD-A286032] p 248 N95-20998
- Arnold Engineering Development Center, Arnold AFS, TN.**
Description and flow characterization of hypersonic facilities [AD-A284291] p 223 N95-20248
- Atlantic Orient Corp., Norwich, VT.**
Advanced wind turbine design studies: Advanced conceptual study [DE93-000031] p 256 N95-20985

B

- Battelle Columbus Labs., OH.**
Aircraft corrosion study [AD-A279527] p 241 N95-21687

C

- California Inst. of Tech., Pasadena, CA.**
Research on bluff body vortex wakes [AD-A286319] p 223 N95-20177
Shock wave interactions in hypervelocity flow [AD-A286507] p 250 N95-22212
- California Polytechnic State Univ., San Luis Obispo, CA.**
A real-time algorithm for integrating differential satellite and inertial navigation information during helicopter approach [NASA-CR-197409] p 229 N95-21891
- Carnegie-Mellon Univ., Pittsburgh, PA.**
Collected papers of the Soar/IFOR project, Spring 1994 [AD-A280063] p 238 N95-20624
- Catholic Univ. of America, Washington, DC.**
Application of wavelet-filtering techniques to intermittent turbulent and wall pressure events. Part 1: Exploratory results [AD-A286077] p 247 N95-20849
- Centre de Recherches en Physique de l'Environnement, Velizy (France).**
Experimental study of the helicopter-mobile radioelectrical channel and possible extension to the satellite-mobile channel p 247 N95-20945
- Charles River Analytics, Inc., Cambridge, MA.**
A neural expert approach to self designing flight control systems [AD-A279965] p 237 N95-21122
- Colorado Univ., Boulder, CO.**
State-to-state collisional dynamics of atmospheric species [AD-A285053] p 245 N95-20484

D

- Dassault Aviation, Saint-Cloud (France).**
FASTPACK: Optimized solutions for modular avionics derived from a parametric study. Part 1: Platform features p 233 N95-20634

- Dayton Univ., OH.**
Lubricant evaluation and performance, 2 [AD-A279144] p 242 N95-21969
- Dayton Univ. Research Inst., OH.**
Color control in a multichannel simulator display: The display for advanced research and training [AD-A279717] p 239 N95-20992
- Defence Science and Technology Organization, Melbourne (Australia).**
Variations observed in the AC generator signal period of a Sea King helicopter [AD-A284280] p 230 N95-19963
A preliminary study of the airwake model used in an existing SH-60B/FFG-7 helicopter/ship simulation program [DSTO-TR-0015] p 224 N95-21659
- Department of Defense, Washington, DC.**
Unmanned aerial vehicles [AD-A286190] p 231 N95-20329
- Department of the Navy, Washington, DC.**
Malone-brayton cycle engine/heat pump [AD-D016573] p 244 N95-20295
Passive range measurement system [AD-D016222] p 258 N95-21100
Lift enhancement device [AD-D016522] p 224 N95-21864
- Detroit Diesel Allison, Indianapolis, IN.**
Experimental study of vane heat transfer and aerodynamics at elevated levels of turbulence [NASA-CR-4633] p 244 N95-19912
- Deutsche Aerospace A.G., Munich (Germany).**
Microchannel heat pipe cooling of modules p 246 N95-20649
Optical backplane for modular avionics p 257 N95-20652
- Drexel Univ., Philadelphia, PA.**
Design of robust optimal control systems and stability analysis of real structured uncertainties [AD-A279089] p 256 N95-21913

E

- Eagle Ventures, Rockville, MD.**
Independent review of Aviation Technology and Research Information Analysis System (ATRIAS) database [AD-A284049] p 226 N95-21518
- Eitron Research, Inc., Boulder, CO.**
Electrochemical impedance pattern recognition for detection of hidden chemical corrosion on aircraft components [AD-A284998] p 241 N95-20481
Electrochemical impedance pattern recognition for detection of hidden chemical corrosion on aircraft components [AD-A285998] p 241 N95-20716
- Eurocontrol Experimental Centre, Bretigny (France).**
Data link terminal DLT document [PB95-110805] p 229 N95-21369

F

- Federal Aviation Administration, Atlanta, GA.**
Fuselage burnthrough from large exterior fuel fires [AD-A286295] p 226 N95-22318
- Federal Aviation Administration, Atlantic City, NJ.**
Investigation of flight data recorder fire test requirements [AD-A285832] p 232 N95-20032
An evaluation of Automatic Terminal Information Service (ATIS) flight deck display presentation options [AD-A280100] p 228 N95-21020
Minima reduction simulation test results [AD-A285626] p 228 N95-21148
- Federal Aviation Administration, Cambridge, MA.**
Recommendation on transition from primary/secondary radar to secondary-only radar capability [AD-A286279] p 249 N95-22005
- Federal Aviation Administration, Washington, DC.**
Census US civil aircraft calendar year 1993 [AD-A286309] p 219 N95-20091

SOURCE

G

- Galaxy Scientific Corp., Pleasantville, NJ.**
Test and evaluation report for the Manual Domestic Passive Profiling System (MDPPS)
[AD-A286312] p 225 N95-20093
- Commuter airplane accident data analysis
[AD-A286315] p 226 N95-20174
- Commuter/air taxi ditchings and water-related impacts that occurred from 1979 to 1989
[AD-A285691] p 226 N95-20275
- Test and Evaluation Plan (TEP) for Improvised Explosive Device Screening Systems (IEDSS)
[AD-A286382] p 227 N95-22319
- GEC-Marconi Materials Technology, Towcester (England).**
High performance backplane components for modular avionics
p 247 N95-20653
- GEC-Marconi Research Centre, Great Baddow (England).**
MCMs for avionics: Technology selection and intermodule interconnection
p 234 N95-20641
- General Accounting Office, Washington, DC.**
Naval aviation: F-14 upgrades are not adequately justified. Report to Congressional Committees
[AD-A286338] p 231 N95-20212
- General Electric Co., Cincinnati, OH.**
Active control of fan noise-feasibility study. Volume 1: Flyover system noise studies
[NASA-CR-195392-VOL-1] p 258 N95-21888
- General Electric Co., Schenectady, NY.**
Toughened Silcomp composites for gas turbine engine applications
[DE95-002851] p 235 N95-21243
- Georgia Tech Research Inst., Atlanta, GA.**
Temperature effects on acoustic interactions between altitude test facilities and jet engine plumes
[NASA-CR-197638] p 258 N95-21170

H

- Hellenic Air Force Academy, Athens (Greece).**
Investigation of shear layer transition using various turbulence models
p 248 N95-21096
- High Technology Corp., Hampton, VA.**
Computational studies of laminar to turbulence transition
[AD-A285622] p 248 N95-21146
- Hughes Associates, Inc., Columbia, MD.**
Analysis of test criteria for firefighting foam firefighting agents for aircraft rescue and firefighting
[AD-A286381] p 227 N95-22352
- Hughes STX, Inc., Lexington, MA.**
Radar studies of aviation hazards
[AD-A285845] p 226 N95-21831

I

- Institute for Defense Analyses, Alexandria, VA.**
The opportunities for and challenges of common integrated electronics
[AD-A279991] p 248 N95-20966

K

- Kaman Sciences Corp., Albuquerque, NM.**
Fault detection techniques for complex cable shield topologies
[AD-A286632] p 247 N95-20771
- TIM-SCT cable testing protocol
[AD-A286633] p 231 N95-20772

L

- Lawrence Livermore National Lab., Livermore, CA.**
An Echelle Grating Spectrometer (EGS) for mid-IR remote chemical detection
[DE94-019310] p 249 N95-21478
- Overview of remote sensing laser development and semiconductor laser technology
[DE94-019103] p 256 N95-21552
- CALOPE and TAISIR airborne experiment platform
[DE94-018328] p 250 N95-22299
- Lynntech, Inc., College Station, TX.**
Corrosion of aircraft materials: Correlation between nanometer scale and macroscopic structural damage parameters
[AD-A285930] p 241 N95-20299

M

- Maryland Univ., College Park, MD.**
Liquid flow-through cooling of electronic modules
p 246 N95-20647
- Massachusetts Inst. of Tech., Lexington, MA.**
GPS-Squitter capacity analysis
[AD-A280037] p 245 N95-20599
- McDonnell-Douglas Aerospace, Long Beach, CA.**
Crew aiding and automation: A system concept for terminal area operations, and guidelines for automation design
[NASA-CR-4831] p 228 N95-19950
- McDonnell-Douglas Aerospace, Saint Louis, MO.**
Transverse vorticity measurements in the NASA Ames 80 x 120 wind tunnel boundary layer
p 251 N95-22457
- Michigan Univ., Ann Arbor, MI.**
Design of a controller for a flexible pointing system using H(infinity) synthesis
[AD-A286572] p 256 N95-20828
- Robust fixed-structure control
[AD-A286515] p 257 N95-22216

N

- National Aeronautics and Space Administration, Washington, DC.**
Orbital velocities induced by surface waves
[HTN-95-90902] p 253 A95-72411
- Buckling and vibration analysis of laminated panels using VICONOPT
[PAPER-1746] p 230 A95-72580
- Aeronautical engineering: A continuing bibliography with indexes (supplement 315)
[NASA-SP-7037(315)] p 219 N95-21640
- Turbine design and application
[NASA-SP-290] p 236 N95-22341
- National Aeronautics and Space Administration, Ames Research Center, Moffett Field, CA.**
Flow resolution and domain influence in rarefied hypersonic blunt-body flows
[BTN-95-EI95082502729] p 220 A95-70136
- Measurement and analysis of nitric oxide radiation in an arcjet flow
[BTN-95-EI95082502727] p 243 A95-71040
- Rotorcraft control system design for uncertain vehicle dynamics using quantitative feedback theory
[HTN-95-31012] p 236 A95-71182
- Advance finite element modeling of rotor blade aeroelasticity
[HTN-95-31013] p 221 A95-71183
- Performance of a focused cavity aerosol spectrometer for measurements in the stratosphere of particle size in the 0.06-2.0-micrometer-diameter range
[HTN-95-90914] p 253 A95-72423
- High-order state space simulation models of helicopter flight mechanics
[HTN-95-A0494] p 237 A95-72565
- Flap-lag damping in hover and forward flight with a three-dimensional wake
[HTN-95-A0496] p 221 A95-72567
- Simulation of rotor blade element turbulence
[NASA-TM-108862] p 232 N95-21186
- A three-dimensional orthogonal laser velocimeter for the NASA Ames 7- by 10-foot wind tunnel
[NASA-TM-108864] p 249 N95-21323
- National Aeronautics and Space Administration, Goddard Space Flight Center, Greenbelt, MD.**
Behavior of an inversion-based precipitation retrieval algorithm with high-resolution AMPR measurements including a low-frequency 10.7-GHz channel
[HTN-95-70134] p 252 A95-70656
- A survey of bidirectional greater than or equal to MeV ion flows during the Helios 1 and Helios 2 mission: Observations from the Goddard Space Flight Center instruments
[HTN-95-70542] p 237 A95-71656
- National Aeronautics and Space Administration, Hugh L. Dryden Flight Research Center, Edwards, CA.**
F-15 resource tape
[NASA-TM-110502] p 230 N95-19994
- F-16XL interview with Marta Bohn-Meyer
[NASA-TM-110505] p 223 N95-19996
- Acoustic climb to cruise test
[NASA-TM-110504] p 230 N95-20155
- National Aeronautics and Space Administration, John C. Stennis Space Center, Bay Saint Louis, MS.**
Evaluation of the Sparton tight-tolerance AXBT
[HTN-95-40728] p 251 A95-70473

- National Aeronautics and Space Administration, Langley Research Center, Hampton, VA.**
Subsidence of aircraft engine exhaust in the stratosphere: Implications for calculated ozone depletions
[PAPER-93GL03426] p 251 A95-70297
- Effects of leading and trailing edge flaps on the aerodynamics of airfoil/vortex interactions
[HTN-95-31011] p 221 A95-71181
- Air and ground resonance of helicopters with elastically tailored composite rotor blades
[HTN-95-A0497] p 222 A95-72568
- Buckling and vibration analysis of laminated panels using VICONOPT
[PAPER-1746] p 230 A95-72580
- Static investigation of two fluidic thrust-vectoring concepts on a two-dimensional convergent-divergent nozzle
[NASA-TM-4574] p 222 N95-19913
- Vapor generator wand
[NASA-CASE-LAR-15058-1] p 238 N95-20080
- Parallel calculation of sensitivity derivatives for aircraft design using automatic differentiation
[NASA-TM-110103] p 231 N95-20370
- 16-foot transonic tunnel test section flowfield survey
[NASA-TM-109157] p 238 N95-20669
- The personal aircraft: Status and issues
[NASA-TM-109174] p 223 N95-20688
- Why do airlines want and use thrust reversers? A compilation of airline industry responses to a survey regarding the use of thrust reversers on commercial transport airplanes
[NASA-TM-109158] p 226 N95-20706
- Acoustic receptivity due to weak surface inhomogeneities in adverse pressure gradient boundary layers
[NASA-TM-4577] p 249 N95-21258
- Application of Navier-Stokes code PAB3D with kappa-epsilon turbulence model to attached and separated flows
[NASA-TP-3480] p 224 N95-21338
- Effects of yaw and pitch motion on model attitude measurements
[NASA-TM-4641] p 250 N95-22109
- National Aeronautics and Space Administration, Lewis Research Center, Cleveland, OH.**
Flow coefficient behavior for boundary layer bleed holes and slots
[NASA-TM-106846] p 244 N95-19953
- Application of pressure sensitive paint in hypersonic flows
[NASA-TM-106824] p 223 N95-20794
- Two-dimensional imaging of OH in a lean burning high pressure combustor
[NASA-TM-106854] p 236 N95-21383
- National Aeronautics and Space Administration, Marshall Space Flight Center, Huntsville, AL.**
High-resolution imaging of rain systems with the advanced microwave precipitation radiometer
[HTN-95-70133] p 252 A95-70655
- Behavior of an inversion-based precipitation retrieval algorithm with high-resolution AMPR measurements including a low-frequency 10.7-GHz channel
[HTN-95-70134] p 252 A95-70656
- National Aeronautics and Space Administration, Wallops Flight Facility, Wallops Island, VA.**
Orbital velocities induced by surface waves
[HTN-95-90902] p 253 A95-72411
- National Defence Research Establishment, Stockholm (Sweden).**
Computation of transonic flow on composite overlapping grids in 2 D
[PB95-131348] p 248 N95-21132
- National Inst. of Standards and Technology, Boulder, CO.**
Measurements of shielding effectiveness and cavity characteristics of airplanes
[PB94-210051] p 244 N95-20191
- National Physical Lab., Teddington (England).**
Effect of atmospheric pressure on measured aircraft noise levels
[PB95-130423] p 232 N95-21425
- National Renewable Energy Lab., Golden, CO.**
Advanced wind turbine design studies: Advanced conceptual study
[DE93-000031] p 256 N95-20985
- Naval Air Warfare Center, Indianapolis, IN.**
Standard Hardware Acquisition and Reliability Program (SHARP) advanced SEM-E packaging
p 233 N95-20633
- Immersion/two phase cooling
p 246 N95-20648
- Naval Air Warfare Center, Warminster, PA.**
The Advanced Avionics Subsystem Technology Demonstration Program
p 234 N95-20636
- The IEEE scalable coherent interface: An approach for a unified avionics network
p 234 N95-20650

- Corrosion behavior of landing gear steels
[AD-A285862] p 242 N95-22132
- Naval Postgraduate School, Monterey, CA.**
A computer code (SKINTEMP) for predicting transient missile and aircraft heat transfer characteristics
[AD-A286044] p 248 N95-21001
- A computer-based multimedia prototype for night vision goggles
[AD-A286208] p 258 N95-21882
- Effect of juncture fillets on double-delta wings undergoing sideslip at high angles of attack
[AD-A286165] p 232 N95-22039
- Evaluation of the Haworth-Newman avionics Display Readability Scale
[AD-A286127] p 235 N95-22232
- Forecasting aircraft mishaps using monthly maintenance reports
[AD-A286049] p 227 N95-22417
- Naval Research Lab., Washington, DC.**
A review of water mist technology for fire suppression
[AD-A285738] p 225 N95-20071
- Naval Surface Warfare Center, Dahlgren, VA.**
Wavelet transformations for helicopter identification via acoustic signatures
[AD-A279980] p 257 N95-20963
- Naval Test Pilot School, Patuxent River, MD.**
T-45A High Angle of Attack Testing: US Naval Test Pilot School 46th Annual Reunion and Symposium
[AD-A284000] p 231 N95-20466
- Naval War Coll., Newport, RI.**
Bomber force 2000: Operational concepts for long-range combat aircraft
[AD-A279378] p 230 N95-20181
- Notre Dame Univ., IN.**
Experiments on the flow field physics of confluent boundary layers for high-lift systems
[NASA-CR-197318] p 224 N95-21343

O

- Oak Ridge National Lab., TN.**
Scale-up and modeling of forced chemical vapor infiltration
[DE94-017769] p 247 N95-20781
- Office of Naval Research, Arlington, VA.**
Fiber-optic rotary joint with bundle collimator assemblies
[AD-D016504] p 258 N95-21673

P

- PDA Engineering, Costa Mesa, CA.**
Response of the B-1B air data sensor to simulated dust cloud environments
[AD-A286134] p 235 N95-22036
- Prins Maurits Lab. TNO, Rijswijk (Netherlands).**
Integral rocket ramjets
[AD-A285135] p 240 N95-20906
- Purdue Univ., West Lafayette, IN.**
Wake measurements in a strong adverse pressure gradient
[NASA-CR-197272] p 224 N95-21031
- Development of quiet-flow supersonic wind tunnels for laminar-turbulent transition research
[NASA-CR-197286] p 239 N95-21436

R

- Rockwell Space Operations Co., Houston, TX.**
The navigation toolkit
[NASA-CR-197290] p 229 N95-22161
- Rohde and Schwartz, Munich (Germany).**
Modular CNI avionics system p 234 N95-20659
- Rome Lab., Griffiss AFB, NY.**
Reliability assessment of Multichip Module technologies via the Triservice/NASA RELTECH program
p 245 N95-20643
- Assuring Known Good Die (KGD) for reliable, cost effective MCMs p 246 N95-20644

S

- Sandia National Labs., Albuquerque, NM.**
SAR image registration in absolute coordinates using GPS carrier phase position and velocity information
[DE94-018738] p 228 N95-20185
- Assessment of a non-dedicated GPS receiver system for precise airborne attitude determination
[DE94-019309] p 229 N95-21520
- A user's guide to LUGSAN 1.1: A computer program to calculate and archive lug and sway brace loads for aircraft-carried stores
[DE95-001919] p 232 N95-21730

- Science Applications International Corp., Dayton, OH.**
Systems engineering design and technical analyses for Strategic Avionics Crew-station Design Evaluation Facility (SACDEF)
[AD-A286239] p 235 N95-22024
- Sextant Avionique, Valence (France).**
Lightweight electronic enclosures using composite materials p 241 N95-20656
- Sorbent Technologies Corp., Twinsburg, OH.**
Laboratory evaluation of a reactive baffle approach to NOx control
[AD-A283802] p 255 N95-19921
- Southwest Research Inst., San Antonio, TX.**
Eddy current for detecting second-layer cracks under installed fasteners
[AD-A279871] p 244 N95-20414
- Stanford Univ., CA.**
Computing methods for the approximate solution of time dependent problems
[AD-A286007] p 256 N95-20719
- Unstructured-grid large-eddy simulation of flow over an airfoil p 225 N95-22448
- Large-eddy simulation of flow through a plane, asymmetric diffuser p 250 N95-22449
- Experimental investigations of on-demand vortex generators p 250 N95-22451
- Direct numerical simulations of on-demand vortex generators: Mathematical formulation p 251 N95-22452
- Acoustics of laminar boundary layers breakdown p 251 N95-22455

T

- Technische Hochschule, Aachen (Germany).**
Prediction of rotor-blade deformations due to unsteady airloads
[AD-A286593] p 231 N95-20860
- Tennessee Univ. Space Inst., Tullahoma, TN.**
Supersonic laminar flow control research
[NASA-CR-196049] p 249 N95-21340
- Test Devices, Inc., Hudson, MA.**
Portable static test facility for small, expendable, turbojet engines, phase 1
[AD-A286337] p 239 N95-21719
- Texas Instruments, Inc., Dallas, TX.**
Ultra-Reliable Digital Avionics (URDA) processor p 245 N95-20638
- Thomson-CSF, Paris (France).**
FASTPACK: Optimized solutions for modular avionics derived from a parametric study. Part 2: Avionics p 233 N95-20635
- Composite cases for airborne electronic equipment: A technology study and EMC p 241 N95-20655
- Modular supplies for a distributed architecture p 234 N95-20657
- Transportation Research Board, Washington, DC.**
Public-sector aviation issues: Graduate research award papers, 1992-1993
[PB94-217478] p 219 N95-19967

W

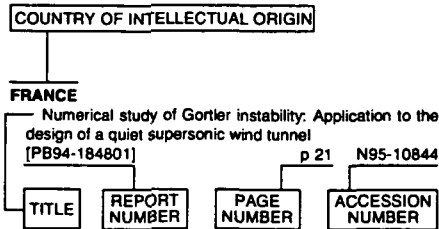
- Westinghouse Electric Corp., Baltimore, MD.**
High density monolithic packaging technology for digital/microwave avionics p 240 N95-20646
- Wright Lab., Wright-Patterson AFB, OH.**
Summary of a joint program of research into aircraft flight control concepts
[AD-A280012] p 237 N95-20004
- The impact of advanced packaging technology on modular avionics architectures p 233 N95-20632
- Pressure measurements on an F/A-18 twin vertical tail in buffeting flow. Volume 4, part 1: Buffet cross spectral densities
[AD-A285593] p 237 N95-21214
- Pressure measurements on an F/A-18 twin vertical tail in buffeting flow. Volume 1: Wind tunnel test summary
[AD-A279126] p 225 N95-21877
- Optical processing and control
[AD-A279157] p 259 N95-21975
- Damage tolerant repair techniques for pressurized aircraft fuselages p 219 N95-22046
- [AD-A286298]

FOREIGN TECHNOLOGY INDEX

AERONAUTICAL ENGINEERING / A Continuing Bibliography (Supplement 318)

June 1995

Typical Foreign Technology Index Listing



Listings in this index are arranged alphabetically by country of intellectual origin. The title of the document is used to provide a brief description of the subject matter. The page number and accession number are included in each entry to assist the user in locating the abstract in the abstract section. If applicable, a report number is also included as an aid in identifying the document.

A

- AUSTRALIA**
Bonded composite repair of cracked load-bearing holes
[BTN-94-EIX94401360553] p 243 A95-71867
Electromagnetic backscattering from a helicopter rotor in the decametric wave band regime
[BTN-94-EIX94381353130] p 243 A95-72648
Variations observed in the AC generator signal period of a Sea King helicopter
[AD-A284280] p 230 N95-19963
A preliminary study of the airwake model used in an existing SH-60B/FFG-7 helicopter/ship simulation program
[DSTO-TR-0015] p 224 N95-21659
Derived gust spectra for the Macchi MB326H
[ARL-TN-3] p 225 N95-21892

B

- BELGIUM**
Modeling resonance in waveguide-to-microstrip junctions by unilateral fin line resonators
[BTN-94-EIX94381323445] p 242 A95-70844

C

- CANADA**
Ice accretion on aircraft wings
[BTN-95-EIX95082502224] p 225 A95-71021
Numerical modelling of transverse impact on composite coupons
[BTN-95-EIX95082502225] p 240 A95-71022
Modelling of pillowing due to corrosion in fuselage lap joints
[BTN-95-EIX95082502227] p 240 A95-71024

- Adaptive remeshing for convective heat transfer with variable fluid properties
[BTN-95-EIX95082502720] p 243 A95-71033
Large-scale computational fluid dynamics by the finite element method
[BTN-94-EIX94381359154] p 243 A95-71744
CHINA
Assessment of a non-dedicated GPS receiver system for precise airborne attitude determination
[DE94-019309] p 229 N95-21520

F

- FRANCE**
Precise orbit determination with a short-arc technique
p 240 A95-70543
Secondary source locations in active noise control: Selection or optimization?
[BTN-94-EIX94381352222] p 257 A95-71738
Advanced Packaging Concepts for Digital Avionics [AGARD-CP-562] p 233 N95-20631
FASTPACK: Optimized solutions for modular avionics derived from a parametric study. Part 1: Platform features
p 233 N95-20634
FASTPACK: Optimized solutions for modular avionics derived from a parametric study. Part 2: Avionics
p 233 N95-20635
Composite cases for airborne electronic equipment: A technology study and EMC
p 241 N95-20655
Lightweight electronic enclosures using composite materials
p 241 N95-20656
Modular supplies for a distributed architecture
p 234 N95-20657
Experimental study of the helicopter-mobile radioelectrical channel and possible extension to the satellite-mobile channel
p 247 N95-20945
Application of Direct and Large Eddy Simulation to Transition and Turbulence
[AGARD-CP-551] p 248 N95-21061
Data link terminal DLT document
[PB95-110805] p 229 N95-21369

G

- GERMANY**
Microchannel heat pipe cooling of modules
p 246 N95-20649
Optical backplane for modular avionics
p 257 N95-20652
Modular CNI avionics system
p 234 N95-20659
Prediction of rotor-blade deformations due to unsteady airloads
[AD-A286593] p 231 N95-20860

- GREECE**
Investigation of shear layer transition using various turbulence models
p 248 N95-21096

I

- ITALY**
Electromagnetic compatibility effects of advanced packaging configurations
p 247 N95-20658

J

- JAPAN**
Aerodynamic mechanism of galloping
[BTN-94-EIX94371347709] p 219 A95-69968
Ground effect calculation of two-dimensional airfoil
[BTN-94-EIX94371347710] p 219 A95-69969
Vortex shedding noise control in idling circular saws using air ejection at the teeth
[BTN-94-EIX94371347214] p 257 A95-69970
Thermochemical nonequilibrium viscous shock-layer analysis for a Mars aerocapture vehicle
[BTN-95-EIX95082502732] p 239 A95-70139

K

- KOREA, REPUBLIC OF**
Comparison of parameter identification algorithms for flight vehicles
[BTN-94-EIX94371347708] p 219 A95-69967

N

- NETHERLANDS**
Integral rocket ramjets
[AD-A285135] p 240 N95-20906

S

- SWEDEN**
Computation of transonic flow on composite overlapping grids in 2 D
[PB95-131348] p 248 N95-21132

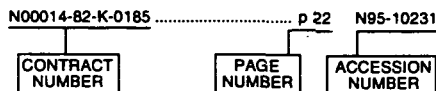
U

- UNITED KINGDOM**
Water vapor continuum absorption in mid-latitudes: Aircraft measurements and model comparisons
[HTN-95-40756] p 252 A95-71186
Aircraft measurements of water vapour continuum absorption at millimetre wavelengths
[HTN-95-90884] p 253 A95-72393
Electro-optic characterization of ultrafast photodetectors using adiabatically compressed soliton pulses
[BTN-94-EIX94381359637] p 257 A95-72675
Microphysical and radiative properties of small cumulus clouds over the sea
[HTN-95-A0526] p 255 A95-73180
On the link between cloud-top radiative properties and sub-cloud aerosol concentrations
[HTN-95-A0527] p 255 A95-73181
Investigation of a thermal buoyancy effect on the drag of half models tested in the ARA Transonic Wind Tunnel
[ARA-MEMO-407] p 222 N95-18946
MCMs for avionics: Technology selection and intermodule interconnection
p 234 N95-20641
High performance backplane components for modular avionics
p 247 N95-20653
The dynamic approach to rotor blade research: ARA's oscillatory test facility
[ARA-MEMO-405] p 223 N95-20758
Testing in the ARA Transonic Wind Tunnel
[ARA-MEMO-395] p 239 N95-20799
Effect of atmospheric pressure on measured aircraft noise levels
[PB95-130423] p 232 N95-21425

FOREIGN

CONTRACT NUMBER INDEX

Typical Contract Number Index Listing



Listings in this index are arranged alphanumerically by contract number. Under each contract number the accession numbers denoting documents that have been produced as a result of research done under the contract are shown. The accession number denotes the number by which the citation is identified in the abstract section. Preceding the accession number is the page number on which the citation may be found.

AF PROJ. 2401	p 237	N95-21214
	p 219	N95-22046
AF PROJ. 2403	p 237	N95-20004
AF-AFOSR-0053-90	p 256	N95-20828
AF-AFOSR-0231-93	p 245	N95-20484
DA PROJ. 3E1-62787-A-879	p 259	N95-22044
DAAH01-94-C-R032	p 239	N95-21719
DAAL03-88-C-0002	p 222	A95-72568
DAAL03-88-C-0003	p 236	A95-71184
DAAL03-88-C-0004	p 221	A95-72566
DAAL03-90-G-0008	p 256	N95-20828
DAAL03-91-G-0007	p 221	A95-72567
DE-AC02-76CH-00016	p 252	A95-71186
DE-AC04-94AL-85000	p 228	N95-20195
	p 229	N95-21520
	p 232	N95-21730
DE-AC05-84OR-21400	p 247	N95-20781
DE-AC36-83CH-10093	p 256	N95-20985
DE-FC02-92CE-41000	p 235	N95-21243
DE-FC05-85ER-250000	p 252	A95-70656
DNA001-91-C-0021	p 235	N95-22036
DTFA01-90-25001	p 254	A95-72543
DTFA01-93-P-02265	p 226	N95-21518
DTFA01-93-Z-02012	p 245	N95-20599
DTFA03-89-C-00043	p 226	N95-20174
	p 226	N95-20275
	p 227	N95-22319
DTFA03-92-C-0035	p 225	N95-20093
ESPRIT 3 PROJ. 6276	p 247	N95-20653
F08635-90-C-0053	p 255	N95-18921
F09603-90-D-2217	p 241	N95-21687
F18628-90-C-0002	p 245	N95-20599
F18628-93-C-0054	p 226	N95-21831
F29601-92-C-0109	p 247	N95-20771
	p 231	N95-20772
F33615-87-C-0531	p 235	N95-22024
F33615-88-C-2817	p 242	N95-21969
F33615-90-C-0005	p 239	N95-20992
F33615-90-C-3613	p 256	N95-21913
F33615-91-C-5661	p 244	N95-20414
F49620-91-C-0014	p 248	N95-21146
F49620-92-J-0127	p 257	N95-22216
F49620-93-C-0050	p 237	N95-21122
F49620-93-1-0338	p 250	N95-22212
F49620-93-1-0444	p 245	N95-20484
F49620-94-C-0040	p 241	N95-20299
F49620-94-C-0043	p 241	N95-20481
	p 241	N95-20716
MDA903-89-C-0003	p 248	N95-20966
NAG-991	p 252	A95-70656
NAG1-1133	p 239	N95-21436

NAG1-1253	p 222	A95-72568
NAG2-458	p 253	A95-72423
NAG2-462	p 221	A95-72567
NAG2-854	p 224	N95-21031
NAG2-881	p 249	N95-21340
NAG2-905	p 224	N95-21343
NAG5-1602	p 252	A95-70656
NAS1-18028	p 228	N95-19950
NAS1-18240	p 249	N95-21258
NAS1-18584	p 230	A95-72580
NAS1-18599	p 249	N95-21258
NAS1-19061	p 258	N95-21170
NAS1-19136	p 221	A95-71181
NAS1-19161	p 251	A95-70297
NAS2-12343	p 221	A95-71183
NAS3-25950	p 244	N95-19912
NAS3-26617	p 258	N95-21888
NAS3-27186	p 236	N95-21383
NAS9-18000	p 229	N95-22161
NATO-CG-890894	p 252	A95-70656
NCA2-S11	p 237	A95-72565
NCCW-2	p 230	A95-72580
NCC2-624	p 236	A95-71182
NCC2-775	p 229	N95-21891
NR PROJ. RH2-1-S-22	p 225	N95-20071
N00014-88-K-0141	p 247	N95-20849
N00014-89-J-1815	p 256	N95-20719
N00014-91-J-1042	p 253	A95-72411
N00014-92-K-2015	p 238	N95-20624
N00014-94-1-0793	p 223	N95-20177
N68171-94-C-9068	p 231	N95-20860
RTOP 232-01-04-01	p 223	N95-20688
RTOP 466-05-02	p 223	N95-20794
RTOP 505-59-10-20	p 224	N95-21338
RTOP 505-59-54-02	p 250	N95-22109
RTOP 505-59-54	p 249	N95-21323
RTOP 505-62-10	p 244	N95-19912
RTOP 505-62-30-01	p 222	N95-19913
RTOP 505-62-52	p 244	N95-19953
RTOP 505-64-13-22	p 228	N95-19950
RTOP 505-64-29	p 232	N95-21186
RTOP 537-02-21	p 236	N95-21383
RTOP 537-03-23-03	p 249	N95-21258
RTOP 538-03-11	p 258	N95-21888
RTOP 538-05-13-01	p 238	N95-20669
	p 226	N95-20706
W-31-109-ENG-38	p 231	N95-20370
	p 258	N95-21388
W-7405-ENG-48	p 249	N95-21478
	p 256	N95-21552
	p 250	N95-22299

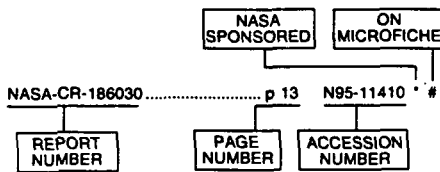
CONTRACT

REPORT NUMBER INDEX

AERONAUTICAL ENGINEERING / A Continuing Bibliography (Supplement 318)

June 1995

Typical Report Number Index Listing



Listings in this index are arranged alphanumerically by report number. The page number indicates the page on which the citation is located. The accession number denotes the number by which the citation is identified. An asterisk (*) indicates that the item is a NASA report. A pound sign (#) indicates that the item is available on microfiche.

A-95028	p 232	N95-21186	* #
A-95032	p 249	N95-21323	* #
AD-A279089	p 256	N95-21913	
AD-A279126	p 225	N95-21877	
AD-A279144	p 242	N95-21969	
AD-A279157	p 259	N95-21975	
AD-A279378	p 230	N95-20181	
AD-A279527	p 241	N95-21687	
AD-A279602	p 238	N95-19955	#
AD-A279605	p 255	N95-20441	
AD-A279717	p 239	N95-20992	
AD-A279871	p 244	N95-20414	
AD-A279965	p 237	N95-21122	
AD-A279980	p 257	N95-20963	
AD-A279991	p 248	N95-20968	
AD-A280012	p 237	N95-20004	#
AD-A280037	p 245	N95-20599	
AD-A280063	p 238	N95-20624	
AD-A280100	p 228	N95-21020	
AD-A283802	p 255	N95-19921	
AD-A284000	p 231	N95-20466	
AD-A284049	p 226	N95-21518	#
AD-A284280	p 230	N95-19963	#
AD-A284291	p 223	N95-20248	#
AD-A284898	p 241	N95-20481	
AD-A285053	p 245	N95-20484	#
AD-A285135	p 240	N95-20906	#
AD-A285593	p 237	N95-21214	#
AD-A285622	p 248	N95-21146	#
AD-A285626	p 228	N95-21148	#
AD-A285691	p 226	N95-20275	#
AD-A285738	p 225	N95-20071	#
AD-A285758	p 238	N95-19931	#
AD-A285832	p 232	N95-20032	#
AD-A285845	p 226	N95-21831	#
AD-A285862	p 242	N95-22132	#
AD-A285921	p 255	N95-19989	#
AD-A285928	p 223	N95-19991	#
AD-A285930	p 241	N95-20299	#
AD-A285998	p 241	N95-20716	#
AD-A286007	p 256	N95-20719	#
AD-A286032	p 248	N95-20998	#
AD-A286044	p 248	N95-21001	#
AD-A286049	p 227	N95-22417	#
AD-A286058	p 258	N95-21170	* #
AD-A286077	p 247	N95-20849	#
AD-A286127	p 235	N95-22232	#
AD-A286134	p 235	N95-22036	#
AD-A286165	p 232	N95-22039	#
AD-A286190	p 231	N95-20329	#
AD-A286208	p 258	N95-21882	#
AD-A286239	p 235	N95-22024	#
AD-A286279	p 249	N95-22005	#
AD-A286287	p 259	N95-22044	#

AD-A286295	p 226	N95-22318	#
AD-A286298	p 219	N95-22046	#
AD-A286309	p 219	N95-20091	
AD-A286312	p 225	N95-20093	
AD-A286315	p 226	N95-20174	#
AD-A286319	p 223	N95-20177	
AD-A286337	p 239	N95-21719	#
AD-A286338	p 231	N95-20212	#
AD-A286381	p 227	N95-22352	#
AD-A286382	p 227	N95-22319	#
AD-A286507	p 250	N95-22212	#
AD-A286515	p 257	N95-22216	#
AD-A286572	p 256	N95-20828	#
AD-A286593	p 231	N95-20860	#
AD-A286632	p 247	N95-20771	#
AD-A286633	p 231	N95-20772	#
AD-D016222	p 258	N95-21100	
AD-D016504	p 258	N95-21673	
AD-D016522	p 224	N95-21864	
AD-D016573	p 244	N95-20295	
AD-E501787	p 248	N95-20986	
AEDC-TR-94-10	p 258	N95-21170	* #
AEDC-TR-94-8	p 223	N95-20248	#
AFOSR-94-0310TR	p 237	N95-21122	
AFOSR-94-0488TR	p 248	N95-21146	#
AFOSR-94-0559TR	p 245	N95-20484	#
AFOSR-94-0608TR	p 241	N95-20481	
AFOSR-94-0673TR	p 241	N95-20716	#
AFOSR-94-0674TR	p 241	N95-20299	#
AFOSR-94-0727TR	p 250	N95-22212	#
AFOSR-94-0741TR	p 257	N95-22216	#
AGARD-CP-551	p 248	N95-21061	#
AGARD-CP-562	p 233	N95-20631	#
AIAA PAPER 94-2613	p 224	N95-21031	* #
AIAA PAPER 95-0031	p 244	N95-19953	* #
AIAA PAPER 95-0173	p 236	N95-21383	* #
AL/CF-TR-1994-0074	p 235	N95-22024	#
AL/EQ-TR-1993-0017	p 255	N95-19921	
AL/HR-TR-1994-0024	p 239	N95-20992	
ANL/MCS/CP-82870	p 231	N95-20370	* #
ANL/TD/CP-83927	p 258	N95-21388	#
AR-007-124	p 225	N95-21892	
AR-008-644	p 224	N95-21659	
ARA-MEMO-395	p 239	N95-20799	#
ARA-MEMO-405	p 223	N95-20758	#
ARA-MEMO-407	p 222	N95-19946	#
ARFSD-TR-94010	p 256	N95-20828	#
ARI-RR-1666	p 238	N95-19931	#
ARL-TN-3	p 225	N95-21892	
ARL-TR-603	p 255	N95-19989	#
ARL-TR-614	p 248	N95-20998	#
ASC-TR-94-5027	p 223	N95-19991	#
ATC-214	p 245	N95-20599	
B-257718	p 231	N95-20212	#
BTN-94-EIX94371338964	p 257	A95-70797	
BTN-94-EIX94371347126	p 242	A95-69976	
BTN-94-EIX94371347214	p 257	A95-69970	
BTN-94-EIX94371347708	p 219	A95-69967	
BTN-94-EIX94371347709	p 219	A95-69968	
BTN-94-EIX94371347710	p 219	A95-69969	
BTN-94-EIX94381323445	p 242	A95-70844	
BTN-94-EIX94381351617	p 252	A95-70950	

BTN-94-EIX94381352222	p 257	A95-71738	
BTN-94-EIX94381353130	p 243	A95-72648	
BTN-94-EIX94381359154	p 243	A95-71744	
BTN-94-EIX94381359637	p 257	A95-72675	
BTN-94-EIX94401360553	p 243	A95-71867	
BTN-95-EIX95041503799	p 239	A95-70124	
BTN-95-EIX95041503806	p 242	A95-70131	
BTN-95-EIX95041505023	p 242	A95-70132	
BTN-95-EIX95041505024	p 235	A95-70133	
BTN-95-EIX95072499029	p 253	A95-71908	
BTN-95-EIX95082502224	p 225	A95-71021	
BTN-95-EIX95082502225	p 240	A95-71022	
BTN-95-EIX95082502227	p 240	A95-71024	
BTN-95-EIX95082502716	p 220	A95-71029	
BTN-95-EIX95082502720	p 243	A95-71033	
BTN-95-EIX95082502727	p 243	A95-71040	
BTN-95-EIX95082502729	p 220	A95-70136	*
BTN-95-EIX95082502732	p 239	A95-70139	*
BTN-95-EIX95142555482	p 228	A95-72891	
BTN-95-EIX95142555485	p 227	A95-72888	
BTN-95-EIX95142555488	p 227	A95-72885	
CERL-SR-EC-94/15	p 255	N95-20441	
CGR/DC-01/94	p 241	N95-21687	
CMU-CS-94-134	p 238	N95-20624	
CONF-940135-9	p 247	N95-20781	#
CONF-9404162-10	p 250	N95-22299	#
CONF-9404162-12	p 256	N95-21552	#
CONF-940664-29	p 258	N95-21388	#
CONF-940723-28	p 249	N95-21478	#
CONF-9408163-1	p 228	N95-20195	#
CONF-9409185-2	p 229	N95-21520	#
CONF-9409187-1	p 231	N95-20370	#
CRAD-9206-TR-8940	p 228	N95-19950	* #
CSE-TR-207-94	p 238	N95-20624	
DE93-000031	p 256	N95-20985	#
DE94-016894	p 231	N95-20370	#
DE94-017769	p 247	N95-20781	#
DE94-018328	p 250	N95-22299	#
DE94-018370	p 258	N95-21388	#
DE94-018738	p 228	N95-20195	#
DE94-019103	p 256	N95-21552	#
DE94-019309	p 229	N95-21520	#
DE94-019310	p 249	N95-21478	#
DE95-001919	p 232	N95-21730	#
DE95-002851	p 235	N95-21243	#
DNA-TR-93-164	p 235	N95-22036	#
DODA-AR-008-545	p 230	N95-19963	#
DOE/CE-41000/2	p 235	N95-21243	#
DOT-VNTSC-FAA-94-10	p 249	N95-22005	#
DOT/FAA/CT-TN92/47	p 228	N95-21148	#
DOT/FAA/CT-TN93/25	p 228	N95-21020	#
DOT/FAA/CT-TN94/23	p 232	N95-20032	#
DOT/FAA/CT-90-10	p 226	N95-22318	#
DOT/FAA/CT-92/4	p 226	N95-20275	#
DOT/FAA/CT-94/04	p 227	N95-22352	#
DOT/FAA/CT-94/12	p 226	N95-21518	#
DOT/FAA/CT-94/75	p 226	N95-20174	#
DOT/FAA/CT-94/86	p 225	N95-20093	#
DOT/FAA/CT-94/87	p 227	N95-22319	#
DOT/FAA/NR-94-1	p 249	N95-22005	#
DSTO-GD-0004	p 230	N95-19963	#
DSTO-TR-0015	p 224	N95-21659	
E-5666	p 236	N95-22341	* #
E-9170-VOL-1	p 258	N95-21888	* #
E-9203	p 244	N95-19912	* #
E-9373	p 223	N95-20794	* #

REPORT

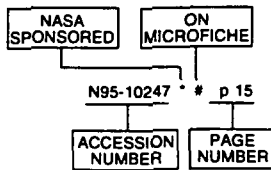
E-9420

REPORT NUMBER INDEX

E-9420	p 244	N95-19953 *	#	NASA-CR-196049	p 249	N95-21340 *	#	US-PATENT-5,327,745	p 244	N95-20295	
E-9444	p 236	N95-21383 *	#	NASA-CR-197272	p 224	N95-21031 *	#	US-PATENT-5,335,886	p 224	N95-21864	
EEC/NOTE-12/94	p 229	N95-21369		NASA-CR-197286	p 239	N95-21436 *	#				
FAA-APO-94-10	p 219	N95-20091		NASA-CR-197290	p 229	N95-22161 *	#	USAARL-94-47	p 259	N95-22044	#
FOA-C-20972-2.5	p 248	N95-21132	#	NASA-CR-197318	p 224	N95-21343 *	#	USCG-D-05-94	p 241	N95-21687	
GAO/NSIAD-95-12	p 231	N95-20212	#	NASA-CR-197409	p 229	N95-21891 *	#	WES/TR/GL-94-12	p 238	N95-19955	#
HTN-95-A0330	p 251	A95-70297 *		NASA-CR-197638	p 258	N95-21170 *	#	WL-TM-94-3039-VOL-1	p 225	N95-21877	
HTN-95-A0493	p 236	A95-72564		NASA-CR-4631	p 228	N95-19950 *	#	WL-TM-94-3112-VOL-4-PT-1	p 237	N95-21214	#
HTN-95-A0494	p 237	A95-72565 *		NASA-CR-4633	p 244	N95-19912 *	#	WL-TR-93-2126-2	p 242	N95-21969	
HTN-95-A0495	p 221	A95-72566		NASA-SP-290	p 236	N95-22341 *	#	WL-TR-93-4125	p 244	N95-20414	
HTN-95-A0496	p 221	A95-72567 *		NASA-SP-7037(315)	p 219	N95-21640 *		WL-TR-94-3030	p 256	N95-21913	
HTN-95-A0497	p 222	A95-72568 *		NASA-TM-106824	p 223	N95-20794 *	#	WL-TR-94-3039	p 237	N95-20004	#
HTN-95-A0498	p 229	A95-72569		NASA-TM-106846	p 244	N95-19953 *	#	WL-TR-94-3134	p 219	N95-22046	#
HTN-95-A0499	p 222	A95-72570		NASA-TM-106854	p 236	N95-21383 *	#	WL-TR-94-5005	p 259	N95-21975	
HTN-95-A0500	p 230	A95-72571 *		NASA-TM-108862	p 232	N95-21186 *	#				
HTN-95-A0509	p 230	A95-72580 *		NASA-TM-108864	p 249	N95-21323 *	#				
HTN-95-A0514	p 230	A95-72585		NASA-TM-109157	p 238	N95-20669 *	#				
HTN-95-A0526	p 255	A95-73180		NASA-TM-109158	p 226	N95-20706 *	#				
HTN-95-A0527	p 255	A95-73181		NASA-TM-109174	p 223	N95-20688 *	#				
HTN-95-31007	p 220	A95-71177		NASA-TM-109174	p 223	N95-20688 *	#				
HTN-95-31008	p 220	A95-71178		NASA-TM-110103	p 231	N95-20370 *	#				
HTN-95-31009	p 220	A95-71179		NASA-TM-110502	p 230	N95-19994 *					
HTN-95-31010	p 221	A95-71180		NASA-TM-110504	p 230	N95-20155 *					
HTN-95-31011	p 221	A95-71181 *		NASA-TM-110505	p 223	N95-19996 *					
HTN-95-31012	p 236	A95-71182 *		NASA-TM-4574	p 222	N95-19913 *	#				
HTN-95-31013	p 221	A95-71183		NASA-TM-4577	p 249	N95-21258 *	#				
HTN-95-31014	p 236	A95-71184		NASA-TM-4641	p 250	N95-22109 *	#				
HTN-95-40728	p 251	A95-70473		NASA-TP-3480	p 224	N95-21338 *	#				
HTN-95-40756	p 252	A95-71186		NAWCADWAR-94001-60	p 242	N95-22132	#				
HTN-95-70133	p 252	A95-70655 *		NISTIR-5023	p 244	N95-20191	#				
HTN-95-70134	p 252	A95-70656 *		NONP-NASA-VT-95-41114	p 230	N95-19994 *					
HTN-95-70149	p 227	A95-70671 *		NONP-NASA-VT-95-41116	p 230	N95-20155 *					
HTN-95-70542	p 237	A95-71656 *		NONP-NASA-VT-95-41117	p 223	N95-19996 *					
HTN-95-80651	p 254	A95-72495		NPL-RSA(EXT)0048	p 232	N95-21425					
HTN-95-80656	p 254	A95-72500		NREL/TP-442-4740	p 256	N95-20985	#				
HTN-95-80699	p 254	A95-72543		NRL/MR/6180-94-7624	p 225	N95-20071	#				
HTN-95-80701	p 254	A95-72545		NSWCDD/TR-93/169	p 257	N95-20963					
HTN-95-80702	p 254	A95-72546		PAPER-1746	p 230	A95-72580 *					
HTN-95-90884	p 253	A95-72393		PAPER-4384	p 230	A95-72585					
HTN-95-90902	p 253	A95-72411 *		PAPER-83GL03426	p 251	A95-70297 *					
HTN-95-90914	p 253	A95-72423 *		PB94-210051	p 244	N95-20191	#				
IDA-D-1490	p 248	N95-20966		PB94-217478	p 219	N95-19967	#				
IDA/HQ-93-44599	p 248	N95-20966		PB95-110805	p 229	N95-21369	#				
ISBN-0-309-05506-7	p 219	N95-19967	#	PB95-130423	p 232	N95-21425					
ISBN-92-836-0004-5	p 233	N95-20631	#	PB95-131348	p 248	N95-21132	#				
ISBN-92-836-0006-1	p 248	N95-21061	#	PDA-TR-1754-02-01	p 235	N95-22036	#				
ISI/SR-94-379	p 238	N95-20624		PL-TR-93-1110	p 231	N95-20772	#				
JILA-153-1236	p 245	N95-20484	#	PL-TR-93-1111	p 247	N95-20771	#				
L-17162	p 249	N95-21258 *	#	PL-TR-94-2146	p 226	N95-21831	#				
L-17350	p 222	N95-19913 *	#	PML-1994-B29	p 240	N95-20906	#				
L-17354	p 224	N95-21338 *	#	R/D-7213-AN-01	p 231	N95-20860	#				
L-17381	p 250	N95-22109 *	#	R93081	p 237	N95-21122					
LC-94-67487	p 236	N95-22341 *	#	SAND-94-1136C	p 229	N95-21520	#				
NAS 1.15:106824	p 223	N95-20794 *	#	SAND-94-1417C	p 228	N95-20195	#				
NAS 1.15:106846	p 244	N95-19953 *	#	SAND-94-1826	p 232	N95-21730	#				
NAS 1.15:106854	p 236	N95-21383 *	#	SR-1	p 226	N95-21831	#				
NAS 1.15:108862	p 232	N95-21186 *	#	SWRI-17-4865	p 244	N95-20414					
NAS 1.15:108864	p 249	N95-21323 *	#	TDCK-93-2570	p 240	N95-20906	#				
NAS 1.15:109157	p 238	N95-20669 *	#	TRB/TRR-1428	p 219	N95-19967	#				
NAS 1.15:109158	p 226	N95-20706 *	#	UCRL-JC-118149	p 256	N95-21552	#				
NAS 1.15:109174	p 223	N95-20688 *	#	UCRL-JC-118226	p 249	N95-21478	#				
NAS 1.15:110103	p 231	N95-20370 *	#	UCRL-JC-118289	p 250	N95-22299	#				
NAS 1.15:4574	p 222	N95-19913 *	#	UDR-TR-93-81-2	p 242	N95-21969					
NAS 1.15:4577	p 249	N95-21258 *	#	US-PATENT-APPL-SN-067763	p 224	N95-21864					
NAS 1.15:4641	p 250	N95-22109 *	#	US-PATENT-APPL-SN-127567	p 244	N95-20295					
NAS 1.21:290	p 236	N95-22341 *	#	US-PATENT-APPL-SN-287027	p 258	N95-21673					
NAS 1.21:7037(315)	p 219	N95-21640 *		US-PATENT-APPL-SN-359320	p 238	N95-20080	#				
NAS 1.26:195392-VOL-1	p 258	N95-21888 *	#	US-PATENT-APPL-SN-921863	p 258	N95-21100					
NAS 1.26:196049	p 249	N95-21340 *	#								
NAS 1.26:197272	p 224	N95-21031 *	#								
NAS 1.26:197286	p 239	N95-21436 *	#								
NAS 1.26:197290	p 229	N95-22161 *	#								
NAS 1.26:197318	p 224	N95-21343 *	#								
NAS 1.26:197409	p 229	N95-21891 *	#								
NAS 1.26:197638	p 258	N95-21170 *	#								
NAS 1.26:4631	p 228	N95-19950 *	#								
NAS 1.26:4633	p 244	N95-19912 *	#								
NAS 1.60:3480	p 224	N95-21338 *	#								
NAS 1.71:LAR-15058-1	p 238	N95-20080 *	#								
NASA-CASE-LAR-15058-1	p 238	N95-20080 *	#								
NASA-CR-195392-VOL-1	p 258	N95-21888 *	#								
				US-PATENT-CLASS-244-21	p 224	N95-21864					
				US-PATENT-CLASS-62-467	p 244	N95-20295					

ACCESSION NUMBER INDEX

Typical Accession Number Index Listing



Listings in this index are arranged alphanumerically by accession number. The page number indicates the page on which the citation is located. The accession number denotes the number by which the citation is identified. An asterisk (*) indicates that the item is a NASA report. A pound sign (#) indicates that the item is available on microfiche.

A95-69967	p 219	A95-72571	p 230	N95-20634	# p 233	N95-21975	p 259
A95-69968	p 219	A95-72580	p 230	N95-20635	# p 233	N95-22005	# p 249
A95-69969	p 219	A95-72585	p 230	N95-20636	# p 234	N95-22024	# p 235
A95-69970	p 257	A95-72648	p 243	N95-20638	# p 245	N95-22036	# p 235
A95-69976	p 242	A95-72675	p 257	N95-20641	# p 234	N95-22039	p 232
A95-70124	p 239	A95-72885	p 227	N95-20643	# p 245	N95-22044	# p 259
A95-70131	p 242	A95-72888	p 227	N95-20644	# p 246	N95-22046	# p 219
A95-70132	p 242	A95-72891	p 228	N95-20646	# p 240	N95-22109	* # p 250
A95-70133	p 235	A95-73180	p 255	N95-20647	# p 246	N95-22132	# p 242
A95-70136	p 220	A95-73181	p 255	N95-20648	# p 246	N95-22161	* # p 229
A95-70139	p 239			N95-20649	# p 246	N95-22212	# p 250
A95-70297	p 251	N95-19912	* # p 244	N95-20650	# p 234	N95-22216	# p 257
A95-70473	p 251	N95-19913	* # p 222	N95-20652	# p 257	N95-22232	# p 235
A95-70543	p 240	N95-19921	p 255	N95-20653	# p 247	N95-22299	# p 250
A95-70655	p 252	N95-19931	# p 238	N95-20655	# p 241	N95-22318	# p 226
A95-70656	p 252	N95-19946	# p 222	N95-20656	# p 241	N95-22319	# p 227
A95-70671	p 227	N95-19950	# p 228	N95-20657	# p 234	N95-22341	* # p 236
A95-70797	p 257	N95-19953	* # p 244	N95-20658	# p 247	N95-22352	# p 227
A95-70844	p 242	N95-19955	# p 238	N95-20659	# p 234	N95-22417	# p 227
A95-70950	p 252	N95-19957	# p 219	N95-20669	# p 238	N95-22448	* # p 225
A95-71021	p 225	N95-19963	# p 230	N95-20688	* # p 223	N95-22449	* # p 250
A95-71022	p 240	N95-19967	# p 219	N95-20706	* # p 226	N95-22451	* # p 250
A95-71024	p 240	N95-19989	# p 255	N95-20716	# p 241	N95-22452	* # p 251
A95-71029	p 220	N95-19991	# p 223	N95-20719	# p 256	N95-22455	* # p 251
A95-71033	p 243	N95-19994	p 230	N95-20758	# p 223	N95-22457	* # p 251
A95-71040	p 243	N95-19996	p 223	N95-20771	# p 247		
A95-71177	p 220	N95-20004	# p 237	N95-20772	# p 231		
A95-71178	p 220	N95-20032	# p 232	N95-20781	# p 247		
A95-71179	p 220	N95-20071	# p 225	N95-20784	* # p 223		
A95-71180	p 221	N95-20080	* # p 238	N95-20799	# p 239		
A95-71181	p 221	N95-20091	p 219	N95-20828	# p 256		
A95-71182	p 236	N95-20093	p 225	N95-20849	# p 247		
A95-71183	p 221	N95-20093	p 225	N95-20860	# p 231		
A95-71184	p 236	N95-20155	* # p 230	N95-20906	# p 240		
A95-71186	p 252	N95-20174	# p 226	N95-20945	# p 247		
A95-71856	p 237	N95-20177	p 223	N95-20963	p 257		
A95-71738	p 257	N95-20181	p 230	N95-20966	p 248		
A95-71744	p 243	N95-20191	# p 244	N95-20985	# p 256		
A95-71867	p 243	N95-20195	# p 228	N95-20992	p 239		
A95-71908	p 253	N95-20212	# p 231	N95-20998	# p 248		
A95-72393	p 253	N95-20248	# p 223	N95-21001	# p 248		
A95-72411	p 253	N95-20275	# p 226	N95-21020	# p 228		
A95-72423	p 253	N95-20295	p 244	N95-21031	* # p 224		
A95-72495	p 254	N95-20299	# p 241	N95-21061	# p 248		
A95-72500	p 254	N95-20329	p 231	N95-21096	# p 248		
A95-72543	p 254	N95-20370	* # p 231	N95-21100	p 258		
A95-72545	p 254	N95-20414	p 244	N95-21122	p 237		
A95-72546	p 254	N95-20441	p 255	N95-21132	# p 248		
A95-72564	p 236	N95-20466	p 231	N95-21146	# p 248		
A95-72565	p 237	N95-20481	p 241	N95-21148	# p 228		
A95-72566	p 221	N95-20484	# p 245	N95-21170	* # p 258		
A95-72567	p 221	N95-20530	* # p 245	N95-21186	* # p 232		
A95-72568	p 222	N95-20599	p 245	N95-21214	# p 237		
A95-72569	p 229	N95-20624	p 238	N95-21243	# p 235		
A95-72570	p 222	N95-20631	# p 233	N95-21258	* # p 249		
		N95-20632	# p 233	N95-21323	* # p 249		
		N95-20633	# p 233	N95-21338	* # p 224		
				N95-21340	* # p 249		
				N95-21343	* # p 224		
				N95-21369	p 229		
				N95-21383	* # p 236		
				N95-21388	# p 258		
				N95-21425	# p 232		
				N95-21436	* # p 239		
				N95-21478	# p 249		
				N95-21518	# p 226		
				N95-21520	# p 229		
				N95-21552	# p 256		
				N95-21640	p 219		
				N95-21659	p 224		
				N95-21673	p 258		
				N95-21687	p 241		
				N95-21719	# p 239		
				N95-21730	# p 232		
				N95-21831	# p 226		
				N95-21864	p 224		
				N95-21877	p 225		
				N95-21882	# p 258		
				N95-21888	* # p 258		
				N95-21891	* # p 229		
				N95-21892	p 225		
				N95-21913	p 256		
				N95-21969	p 242		

AVAILABILITY OF CITED PUBLICATIONS

OPEN LITERATURE ENTRIES (A95-60000 Series)

Inquiries and requests should be addressed to NASA Center for AeroSpace Information, 800 Elkridge Landing Road, Linthicum Heights, MD 21090-2934. Orders are also taken by telephone, (301) 621-0390, e-mail, help@sti.nasa.gov, and fax, (301) 621-0134. Please refer to the accession number when requesting publications.

STAR ENTRIES (N95-10000 Series)

One or more sources from which a document announced in *STAR* is available to the public is ordinarily given on the last line of the citation. The most commonly indicated sources and their acronyms or abbreviations are listed below, and their addresses are listed on page APP-3. If the publication is available from a source other than those listed, the publisher and his address will be displayed on the availability line or in combination with the corporate source line.

Avail: CASI. Sold by the NASA Center for AeroSpace Information. Prices for hard copy (HC) and microfiche (MF) are indicated by a price code following the letters HC or MF in the *STAR* citation. Current values for the price codes are given in the tables on page APP-5.

NOTE ON ORDERING DOCUMENTS: When ordering publications from NASA CASI, use the N accession number or other report number. It is also advisable to cite the title and other bibliographic identification.

Avail: SOD (or GPO). Sold by the Superintendent of Documents, U.S. Government Printing Office, in hard copy.

Avail: BLL (formerly NLL): British Library Lending Division, Boston Spa, Wetherby, Yorkshire, England. Photocopies available from this organization at the price shown. (If none is given, inquiry should be addressed to the BLL.)

Avail: DOE Depository Libraries. Organizations in U.S. cities and abroad that maintain collections of Department of Energy reports, usually in microfiche form, are listed in *Energy Research Abstracts*. Services available from the DOE and its depositories are described in a booklet, *DOE Technical Information Center - Its Functions and Services* (TID-4660), which may be obtained without charge from the DOE Technical Information Center.

Avail: ESDU. Pricing information on specific data, computer programs, and details on Engineering Sciences Data Unit (ESDU) topic categories can be obtained from ESDU International Ltd. Requesters in North America should use the Virginia address while all other requesters should use the London address, both of which are on page APP-3.

Avail: Fachinformationszentrum Karlsruhe. Gesellschaft für wissenschaftlich-technische Information mbH 76344 Eggenstein-Leopoldshafen, Germany.

Avail: HMSO. Publications of Her Majesty's Stationery Office are sold in the U.S. by Pendragon House, Inc. (PHI), Redwood City, CA. The U.S. price (including a service and mailing charge) is given, or a conversion table may be obtained from PHI.

Avail: Issuing Activity, or Corporate Author, or no indication of availability. Inquiries as to the availability of these documents should be addressed to the organization shown in the citation as the corporate author of the document.

Avail: NASA Public Document Rooms. Documents so indicated may be examined at or purchased from the National Aeronautics and Space Administration (JBD-4), Public Documents Room (Room 1H23), Washington, DC 20546-0001, or public document rooms located at NASA installations, and the NASA Pasadena Office at the Jet Propulsion Laboratory.

Avail: NTIS. Sold by the National Technical Information Service. Initially distributed microfiche under the NTIS SRIM (Selected Research in Microfiche) are available. For information concerning this service, consult the NTIS Subscription Section, Springfield, VA 22161.

Avail: Univ. Microfilms. Documents so indicated are dissertations selected from *Dissertation Abstracts* and are sold by University Microfilms as xerographic copy (HC) and microfilm. All requests should cite the author and the Order Number as they appear in the citation.

Avail: US Patent and Trademark Office. Sold by Commissioner of Patents and Trademarks, U.S. Patent and Trademark Office, at the standard price of \$1.50 each, postage free.

Avail: (US Sales Only). These foreign documents are available to users within the United States from the National Technical Information Service (NTIS). They are available to users outside the United States through the International Nuclear Information Service (INIS) representative in their country, or by applying directly to the issuing organization.

Avail: USGS. Originals of many reports from the U.S. Geological Survey, which may contain color illustrations, or otherwise may not have the quality of illustrations preserved in the microfiche or facsimile reproduction, may be examined by the public at the libraries of the USGS field offices whose addresses are listed on page APP-3. The libraries may be queried concerning the availability of specific documents and the possible utilization of local copying services, such as color reproduction.

FEDERAL DEPOSITORY LIBRARY PROGRAM

In order to provide the general public with greater access to U.S. Government publications, Congress established the Federal Depository Library Program under the Government Printing Office (GPO), with 53 regional depositories responsible for permanent retention of material, inter-library loan, and reference services. At least one copy of nearly every NASA and NASA-sponsored publication, either in printed or microfiche format, is received and retained by the 53 regional depositories. A list of the regional GPO libraries, arranged alphabetically by state, appears on the inside back cover of this issue. These libraries are *not* sales outlets. A local library can contact a regional depository to help locate specific reports, or direct contact may be made by an individual.

PUBLIC COLLECTION OF NASA DOCUMENTS

An extensive collection of NASA and NASA-sponsored publications is maintained by the British Library Lending Division, Boston Spa, Wetherby, Yorkshire, England for public access. The British Library Lending Division also has available many of the non-NASA publications cited in *STAR*. European requesters may purchase facsimile copy or microfiche of NASA and NASA-sponsored documents, those identified by both the symbols # and * from ESA — Information Retrieval Service European Space Agency, 8-10 rue Mario-Nikis, 75738 CEDEX 15, France.

STANDING ORDER SUBSCRIPTIONS

NASA SP-7037 supplements and annual index are available from the NASA Center for AeroSpace Information (CASI) on standing order subscription. Standing order subscriptions do not terminate at the end of a year, as do regular subscriptions, but continue indefinitely unless specifically terminated by the subscriber.

ADDRESSES OF ORGANIZATIONS

British Library Lending Division
Boston Spa, Wetherby, Yorkshire
England

National Technical Information Service
5285 Port Royal Road
Springfield, VA 22161

Commissioner of Patents and Trademarks
U.S. Patent and Trademark Office
Washington, DC 20231

Pendragon House, Inc.
899 Broadway Avenue
Redwood City, CA 94063

Department of Energy
Technical Information Center
P.O. Box 62
Oak Ridge, TN 37830

Superintendent of Documents
U.S. Government Printing Office
Washington, DC 20402

European Space Agency-
Information Retrieval Service ESRIN
Via Galileo Galilei
00044 Frascati (Rome) Italy

University Microfilms
A Xerox Company
300 North Zeeb Road
Ann Arbor, MI 48106

Engineering Sciences Data Unit International
P.O. Box 1633
Manassas, VA 22110

University Microfilms, Ltd.
Tylers Green
London, England

Engineering Sciences Data Unit
International, Ltd.
251-259 Regent Street
London, W1R 7AD, England

U.S. Geological Survey Library National Center
MS 950
12201 Sunrise Valley Drive
Reston, VA 22092

Fachinformationszentrum Karlsruhe
Gesellschaft für wissenschaftlich-technische
Information mbH
76344 Eggenstein-Leopoldshafen, Germany

U.S. Geological Survey Library
2255 North Gemini Drive
Flagstaff, AZ 86001

Her Majesty's Stationery Office
P.O. Box 569, S.E. 1
London, England

U.S. Geological Survey
345 Middlefield Road
Menlo Park, CA 94025

NASA Center for AeroSpace Information
800 Elkridge Landing Road
Linthicum Heights, MD 21090-2934

U.S. Geological Survey Library
Box 25046
Denver Federal Center, MS914
Denver, CO 80225

National Aeronautics and Space Administration
Scientific and Technical Information Office
(JT)
Washington, DC 20546-0001

Page Intentionally Left Blank

NASA CASI PRICE CODE TABLE

(Effective January 1, 1995)

CASI PRICE CODE	NORTH AMERICAN PRICE	FOREIGN PRICE
A01	\$ 6.00	\$ 12.00
A02	9.00	18.00
A03	17.50	35.00
A04-A05	19.50	39.00
A06-A09	27.00	54.00
A10-A13	36.50	73.00
A14-A17	44.50	89.00
A18-A21	52.00	104.00
A22-A25	61.00	122.00
A99	Call For Price	Call For Price

IMPORTANT NOTICE

For users not registered at the NASA CASI, prepayment is required. Additionally, a shipping and handling fee of \$1.00 per document for delivery within the United States and \$9.00 per document for delivery outside the United States is charged.

For users registered at the NASA CASI, document orders may be invoiced at the end of the month, charged against a deposit account, or paid by check or credit card. NASA CASI accepts American Express, Diners' Club, MasterCard, and VISA credit cards. There are no shipping and handling charges. To register at the NASA CASI, please request a registration form through the NASA Access Help Desk at the numbers or addresses below.

RETURN POLICY

Effective June 1, 1995, the NASA Center for AeroSpace Information will gladly replace or make full refund on items you have requested if we have made an error in your order, if the item is defective, or if it was received in damaged condition and you contact us within 30 days of your original request. Just contact our NASA Access Help Desk at the numbers or addresses listed below.

NASA Center for AeroSpace Information
800 Elkridge Landing Road
Linthicum Heights, MD 21090-2934
Telephone: (301) 621-0390
E-mail: help@sti.nasa.gov
Fax: (301) 621-0134

REPORT DOCUMENT PAGE

1. Report No. NASA SP-7037 (318)	2. Government Accession No.	3. Recipient's Catalog No.	
4. Title and Subtitle Aeronautical Engineering A Continuing Bibliography (Supplement 318)		5. Report Date June 1995	
		6. Performing Organization Code JT	
7. Author(s)		8. Performing Organization Report No.	
		10. Work Unit No.	
9. Performing Organization Name and Address NASA Scientific and Technical Information Office		11. Contract or Grant No.	
		13. Type of Report and Period Covered Special Publication	
12. Sponsoring Agency Name and Address National Aeronautics and Space Administration Washington, DC 20546-0001		14. Sponsoring Agency Code	
		15. Supplementary Notes	
16. Abstract This report lists 217 reports, articles and other documents recently announced in the NASA STI Database.			
17. Key Words (Suggested by Author(s)) Aeronautical Engineering Aeronautics Bibliographies		18. Distribution Statement Unclassified - Unlimited Subject Category - 01	
19. Security Classif. (of this report) Unclassified	20. Security Classif. (of this page) Unclassified	21. No. of Pages 98	22. Price A05/HC

FEDERAL REGIONAL DEPOSITORY LIBRARIES

ALABAMA

AUBURN UNIV. AT MONTGOMERY LIBRARY
Documents Dept.
7300 University Dr.
Montgomery, AL 36117-3596
(205) 244-3650 Fax: (205) 244-0678

UNIV. OF ALABAMA

Amelia Gayle Gorgas Library
Govt. Documents
P.O. Box 870266
Tuscaloosa, AL 35487-0266
(205) 348-6046 Fax: (205) 348-0760

ARIZONA

DEPT. OF LIBRARY, ARCHIVES, AND PUBLIC RECORDS
Research Division
Third Floor, State Capitol
1700 West Washington
Phoenix, AZ 85007
(602) 542-3701 Fax: (602) 542-4400

ARKANSAS

ARKANSAS STATE LIBRARY
State Library Service Section
Documents Service Section
One Capitol Mall
Little Rock, AR 72201-1014
(501) 682-2053 Fax: (501) 682-1529

CALIFORNIA

CALIFORNIA STATE LIBRARY
Govt. Publications Section
P.O. Box 942837 - 914 Capitol Mall
Sacramento, CA 94337-0091
(916) 654-0069 Fax: (916) 654-0241

COLORADO

UNIV. OF COLORADO - BOULDER
Libraries - Govt. Publications
Campus Box 184
Boulder, CO 80309-0184
(303) 492-8834 Fax: (303) 492-1881

DENVER PUBLIC LIBRARY

Govt. Publications Dept. BSG
1357 Broadway
Denver, CO 80203-2165
(303) 640-8846 Fax: (303) 640-8817

CONNECTICUT

CONNECTICUT STATE LIBRARY
231 Capitol Avenue
Hartford, CT 06106
(203) 566-4971 Fax: (203) 566-3322

FLORIDA

UNIV. OF FLORIDA LIBRARIES
Documents Dept.
240 Library West
Gainesville, FL 32611-2048
(904) 392-0366 Fax: (904) 392-7251

GEORGIA

UNIV. OF GEORGIA LIBRARIES
Govt. Documents Dept.
Jackson Street
Athens, GA 30602-1645
(706) 542-8949 Fax: (706) 542-4144

HAWAII

UNIV. OF HAWAII
Hamilton Library
Govt. Documents Collection
2550 The Mall
Honolulu, HI 96822
(808) 948-8230 Fax: (808) 956-5968

IDAHO

UNIV. OF IDAHO LIBRARY
Documents Section
Rayburn Street
Moscow, ID 83844-2353
(208) 885-6344 Fax: (208) 885-6817

ILLINOIS

ILLINOIS STATE LIBRARY
Federal Documents Dept.
300 South Second Street
Springfield, IL 62701-1796
(217) 782-7596 Fax: (217) 782-6437

INDIANA

INDIANA STATE LIBRARY
Serials/Documents Section
140 North Senate Avenue
Indianapolis, IN 46204-2296
(317) 232-3679 Fax: (317) 232-3728

IOWA

UNIV. OF IOWA LIBRARIES
Govt. Publications
Washington & Madison Streets
Iowa City, IA 52242-1166
(319) 335-5926 Fax: (319) 335-5900

KANSAS

UNIV. OF KANSAS
Govt. Documents & Maps Library
6001 Malott Hall
Lawrence, KS 66045-2800
(913) 864-4660 Fax: (913) 864-3855

KENTUCKY

UNIV. OF KENTUCKY
King Library South
Govt. Publications/Maps Dept.
Patterson Drive
Lexington, KY 40506-0039
(606) 257-3139 Fax: (606) 257-3139

LOUISIANA

LOUISIANA STATE UNIV.
Middleton Library
Govt. Documents Dept.
Baton Rouge, LA 70803-3312
(504) 388-2570 Fax: (504) 388-6992

LOUISIANA TECHNICAL UNIV.

Prescott Memorial Library
Govt. Documents Dept.
Ruston, LA 71272-0046
(318) 257-4962 Fax: (318) 257-2447

MAINE

UNIV. OF MAINE
Raymond H. Fogler Library
Govt. Documents Dept.
Orono, ME 04469-5729
(207) 581-1673 Fax: (207) 581-1653

MARYLAND

UNIV. OF MARYLAND - COLLEGE PARK
McKeldin Library
Govt. Documents/Maps Unit
College Park, MD 20742
(301) 405-9165 Fax: (301) 314-9416

MASSACHUSETTS

BOSTON PUBLIC LIBRARY
Govt. Documents
666 Boylston Street
Boston, MA 02117-0286
(617) 536-5400, ext. 226
Fax: (617) 536-7758

MICHIGAN

DETROIT PUBLIC LIBRARY
5201 Woodward Avenue
Detroit, MI 48202-4093
(313) 833-1025 Fax: (313) 833-0156

LIBRARY OF MICHIGAN

Govt. Documents Unit
P.O. Box 30007
717 West Allegan Street
Lansing, MI 48909
(517) 373-1300 Fax: (517) 373-3381

MINNESOTA

UNIV. OF MINNESOTA
Govt. Publications
409 Wilson Library
309 19th Avenue South
Minneapolis, MN 55455
(612) 624-5073 Fax: (612) 626-9355

MISSISSIPPI

UNIV. OF MISSISSIPPI
J.D. Williams Library
106 Old Gym Bldg.
University, MS 38677
(601) 232-5857 Fax: (601) 232-7465

MISSOURI

UNIV. OF MISSOURI - COLUMBIA
106B Ellis Library
Govt. Documents Sect.
Columbia, MO 65201-5149
(314) 882-6733 Fax: (314) 882-8044

MONTANA

UNIV. OF MONTANA
Mansfield Library
Documents Division
Missoula, MT 59812-1195
(406) 243-6700 Fax: (406) 243-2060

NEBRASKA

UNIV. OF NEBRASKA - LINCOLN
D.L. Love Memorial Library
Lincoln, NE 68588-0410
(402) 472-2562 Fax: (402) 472-5131

NEVADA

THE UNIV. OF NEVADA LIBRARIES
Business and Govt. Information Center
Reno, NV 89557-0044
(702) 784-6579 Fax: (702) 784-1751

NEW JERSEY

NEWARK PUBLIC LIBRARY
Science Div. - Public Access
P.O. Box 630
Five Washington Street
Newark, NJ 07101-7812
(201) 733-7782 Fax: (201) 733-5648

NEW MEXICO

UNIV. OF NEW MEXICO
General Library
Govt. Information Dept.
Albuquerque, NM 87131-1466
(505) 277-5441 Fax: (505) 277-6019

NEW MEXICO STATE LIBRARY

325 Don Gaspar Avenue
Santa Fe, NM 87503
(505) 827-3824 Fax: (505) 827-3888

NEW YORK

NEW YORK STATE LIBRARY
Cultural Education Center
Documents/Gift & Exchange Section
Empire State Plaza
Albany, NY 12230-0001
(518) 474-5355 Fax: (518) 474-5786

NORTH CAROLINA

UNIV. OF NORTH CAROLINA - CHAPEL HILL
Walter Royal Davis Library
CB 3912, Reference Dept.
Chapel Hill, NC 27514-8890
(919) 962-1151 Fax: (919) 962-4451

NORTH DAKOTA

NORTH DAKOTA STATE UNIV. LIB.
Documents
P.O. Box 5599
Fargo, ND 58105-5599
(701) 237-8886 Fax: (701) 237-7138

UNIV. OF NORTH DAKOTA

Chester Fritz Library
University Station
P.O. Box 9000 - Centennial and University Avenue
Grand Forks, ND 58202-9000
(701) 777-4632 Fax: (701) 777-3319

OHIO

STATE LIBRARY OF OHIO
Documents Dept.
65 South Front Street
Columbus, OH 43215-4163
(614) 644-7051 Fax: (614) 752-9178

OKLAHOMA

OKLAHOMA DEPT. OF LIBRARIES
U.S. Govt. Information Division
200 Northeast 18th Street
Oklahoma City, OK 73105-3298
(405) 521-2502, ext. 253
Fax: (405) 525-7804

OKLAHOMA STATE UNIV.

Edmon Low Library
Stillwater, OK 74078-0375
(405) 744-6546 Fax: (405) 744-5183

OREGON

PORTLAND STATE UNIV.
Branford P. Millar Library
934 Southwest Harrison
Portland, OR 97207-1151
(503) 725-4123 Fax: (503) 725-4524

PENNSYLVANIA

STATE LIBRARY OF PENN.
Govt. Publications Section
116 Walnut & Commonwealth Ave.
Harrisburg, PA 17105-1601
(717) 787-3752 Fax: (717) 783-2070

SOUTH CAROLINA

CLEMSON UNIV.
Robert Muldrow Cooper Library
Public Documents Unit
P.O. Box 343001
Clemson, SC 29634-3001
(803) 656-5174 Fax: (803) 656-3025

UNIV. OF SOUTH CAROLINA

Thomas Cooper Library
Green and Sumter Streets
Columbia, SC 29208
(803) 777-4841 Fax: (803) 777-9503

TENNESSEE

UNIV. OF MEMPHIS LIBRARIES
Govt. Publications Dept.
Memphis, TN 38152-0001
(901) 678-2206 Fax: (901) 678-2511

TEXAS

TEXAS STATE LIBRARY
United States Documents
P.O. Box 12927 - 1201 Brazos
Austin, TX 78701-0001
(512) 463-5455 Fax: (512) 463-5436

TEXAS TECH. UNIV. LIBRARIES

Documents Dept.
Lubbock, TX 79409-0002
(806) 742-2282 Fax: (806) 742-1920

UTAH

UTAH STATE UNIV.
Merrill Library Documents Dept.
Logan, UT 84322-3000
(801) 797-2678 Fax: (801) 797-2677

VIRGINIA

UNIV. OF VIRGINIA
Alderman Library
Govt. Documents
University Ave. & McCormick Rd.
Charlottesville, VA 22903-2498
(804) 824-3133 Fax: (804) 924-4337

WASHINGTON

WASHINGTON STATE LIBRARY
Govt. Publications
P.O. Box 42478
16th and Water Streets
Olympia, WA 98504-2478
(206) 753-4027 Fax: (206) 586-7575

WEST VIRGINIA

WEST VIRGINIA UNIV. LIBRARY
Govt. Documents Section
P.O. Box 6069 - 1549 University Ave.
Morgantown, WV 26506-6069
(304) 293-3051 Fax: (304) 293-6638

WISCONSIN

ST. HIST. SOC. OF WISCONSIN LIBRARY
Govt. Publication Section
816 State Street
Madison, WI 53706
(608) 264-6525 Fax: (608) 264-6520

MILWAUKEE PUBLIC LIBRARY

Documents Division
814 West Wisconsin Avenue
Milwaukee, WI 53233
(414) 286-3073 Fax: (414) 286-8074

National Aeronautics and
Space Administration
Code JTT
Washington, DC 20546-0001